Université Fédérale
Toulouse Midi-Pyrénées

THÈSE

En vue de l'obtention du

DOCTORAT DE L'UNIVERSITÉ DE TOULOUSE

Délivré par :

Université Toulouse 3 Paul Sabatier (UT3 Paul Sabatier)

Si vous êtes en cotutelle internationale, remplissez ce champs en notant : Cotutelle internationale avec "nom de l'établissement", sinon effacer ce texte pour qu'il n'apparaisse pas à l'impression

---

Présentée et soutenue par :
Fransky HANTELYS

le 20 février 2017

Titre :
Régulateurs traductionnels de l'expression génique lors de la différenciation et du stress cellulaire

---

École doctorale et discipline ou spécialité :
ED BSB : Physiopathologie

Unité de recherche :
INSERM U1048 - I2MC

Directeur/trice(s) de Thèse :
Dr. Anne-Catherine PRATS
Pr. Angelo PARINI

Jury :

Dr. Gilles PAGES	Directeur de recherche INSERM UMR 7284 de Nice	Rapporteur
Dr. Jean-Jacques DIAZ	Directeur de recherche INSERM UMR 1052 de Lyon	Rapporteur
Dr. Julia MORALES	Chargé de recherche CNRS UMR 8227 de Roscoff	Examinateur
Pr. Pierre-Emmanuel GLEIZES	Professeur Université Paul Sabatier Toulouse	Examinateur
Dr. Anne-Catherine Prats	Directeur de recherche U1048 Toulouse	Co-directeur de thèse
Pr. Angelo PARINI	PUPH/INSERM U1048 Toulouse	Co-directeur de thèse

RESUME

La cellule est susceptible de modifier l'expression de ces gènes en fonction de son environnement. Dans les cellules eucaryotes, la régulation de l'expression de ces gènes se présente dans plusieurs étapes. Cette régulation peut intervenir dès la transcription de l'ADN jusqu'au devenir des transcrits. La régulation post-transcriptionnelle tient un rôle déterminant dans la synthèse protéique. Elle regroupe l'ensemble des contrôles qui s'exercent sur les transcrits. Cette régulation est induite en réponse à différents stimuli comme la différenciation ou lors de stress cellulaires. En situation de stress, la traduction canonique dépendante de la coiffe est bloquée, à l'exception de certains ARNm essentiels pour assurer la survie des cellules. De ce fait, les cellules mettent en place un mécanisme alternatif afin de continuer la traduction. Un des mécanismes de traduction, implique le site d'entrée interne du ribosome ou IRES (Internal Ribosome Entry Site). L'IRES est une séquence en structure secondaire dans la partie 5' non-traduite de certains ARNm. Il existe des facteurs responsables de leur activation appelés ITAF ou IRES-transacting factor, permettant le recrutement des ribosomes pour initier la traduction. Les protéines pouvant se lier aux ARN sont les acteurs majeurs de l'activation des IRES.

Mon travail de thèse est d'étudier les régulateurs post-transcriptionnels en réponse à différents stimuli par le biais de la traduction IRES-dépendante.

Dans la première partie de mon projet, nous avons montré la régulation de la traduction via l'activation de l'IRES du FGF1 et ce de manière promoteur-dépendante au cours de la différenciation des myoblastes. Grâce à la technique de résonance plasmonique de surface (SPR) nous avons découvert deux protéines $p54^{nrb}$/NONO et hnRNPM en tant qu'ITAF capables de former un complexe pour activer l'IRES du FGF1 durant la différenciation des myoblastes.

Dans la deuxième partie de ma thèse, nous avons démontré l'existence de l'IRES du VEGFD durant un choc thermique dans les cellules cancéreuses. Nous avons aussi découvert que cette activation est médiée par un ITAF qui est la nucléoline, jamais démontrée auparavant comme ITAF de l'IRES du VEGFD. D'après nos résultats, le stress thermique induit la délocalisation de la nucléoline du noyau vers le cytoplasme pour changer la conformation de l'IRES du VEGFD afin de continuer sa traduction.

Dans la troisième partie de mon projet, j'ai étudié de manière générale la régulation des gènes angiogéniques et lymphangiogéniques. L'ensemble des données montre que ces gènes sont majoritairement régulés au niveau traductionnel dans les cardiomyocytes en condition hypoxique. En étudiant les IRES angiogéniques et lymphangiogéniques, nos résultats montrent l'activation de ces IRES à différents temps au cours de l'hypoxie précoce. Dans la même condition, nous avons découvert la protéine vasohibin-1 comme ITAF hypoxique et spécifique de l'IRES du FGF1 dans les cardiomyocytes.

En conclusion, nous avons découvert différents ITAF spécifiques à un IRES et en fonction du stress. $p54^{nrb}$/NONO, hnRNPM sont des ITAF de l'IRES du FGF1 durant la différenciation cellulaire et la vasohibine-1 en hypoxie dans les cardiomyocytes. La nucléoline permet d'activer un IRES du VEGFD en réponse au choc thermique.

SUMMARY

In cell, gene expression can be modified depending on the cellular microenvironment. Regulation of gene expression occurs at different levels, ranging from the transcription of the DNA to the mRNA. Among the post- transcriptional regulation, the control of translation plays a crucial role. In particular, the translational regulation occurs in response to different stimuli such as cell differentiation or cell stress. In stress condition, the canonical cap-dependent translation is blocked, excepted some mRNAs that are translated by alternative mechanisms. One of these mechanisms involves the structural elements of the mRNAs, the IRES (Internal Ribosome Entry Sites). The IRES activation involves some factors called ITAFs (IRES trans-acting factors), which allow the internal recruitement of ribosomes to initiate translation.
My thesis is to study the mechanisms of IRES-dependent translation regulation in response to different stimuli, and to identify ITAFs responsible for this regulation.
In the first part of my project, we have shown that the translation controlled by the FGF1 mRNA IRES is activated. This activation depends on its own promoter during the early phase of murine myoblast differentiation. Through biomolecular interaction analysis technology by surface plasmon resonance coupled to mass spectrometry (BIA/MS), we identified two proteins, $p54^{nrb}$/NONO and hnRNPM bound both to the IRES and the FGF1gene promoter. These two proteins are both ITAFs activators of IRES and activators of FGF1 promoter transcription, resulting in a coupling of transcription and translation responsible for the induction of the FGF1 expression during myoblast differentiation.
In the second part of this thesis, we demonstrated the existence of an IRES within the VEGFD mRNA. This IRES is activated by heat shock in mammary murine carcinoma. BIA/MS technology has enabled us to identify nucleolin as ITAF responsible for this activation. SHAPE experiments revealed the presence of two alternative structures of VEGFD IRES. According to our results, the heat shock induced the relocation of nucleolin from the nucleus to the cytoplasm, suggesting its binding to the mRNA in the cytoplasm could stabilize the conformation of the mRNA VEGFD IRES and activate its translation.
The third part of my thesis focused on translational regulation of lymphangiogenic and angiogenic genes into cardiomyocytes in hypoxic conditions. The data obtained by the semi-global approach Fluidigm indicate that only few genes are induced at the transcriptional level, while the majority of them, especially those which have the mRNA IRES, are activated at translational level in hypoxic cardiomyocytes. I have also shown that the mRNA IRES of factors (lymph)angiogenic VEGF and FGF are activated during early hypoxia. Through Technology BIA/MS, I identified a specific hypoxic ITAF of FGF1 IRES in cardiomyocytes: it is the vasohibin - 1 protein involved in angiogenesis and stress tolerance.

So, my thesis has enabled to make progress in understanding the mechanisms of IRES-dependent translation regulation. In addition, I have demonstrated that in cardiomyocytes during hypoxia the gene expression is surprisingly regulated at translational level. My work led to the identification of several molecular actors responsible for the regulation of mRNA (lymph)angiogenic factors translation, which could play a key role in ischemic pathologies and in cancer, and provide new targets therapeutic. .

Liste des abréviations

4EBP : eIF4E binding protein

4EHP : eIF4E homologous protein

ADAM : a disintegrin and metalloprotéinase

ADN : acide desoxynucléique

ALK : anaplastic lymphoma kinase

ANGPT : angiopoïetine

AP1 : activator protein 1

ARN : acide desoxyribonucléique

ARNm : ARN messager

ARNnc : ARN non codant

ARN pol II : ARN polymérase II

ARNr : ARN ribosomique

ARNt : ARN de transfert

ATF6 : activated transcription factor 6

AUG : codon initiateur (méthionine)

AVC : accident vasculaire cérébrale

BiP : binding immunoglobulin protein

BMP7 : bone morphogenetic protein 7

BRE : B recognition element

C/EBP-δ : CCAAT/enhancer-binding protein-δ

CCR4 : chemokine C-C motif receptor4

CDK9 : cyclin-dependent kinase 9

ChiP : chromatin immunoprecipitation

COUP-TF : COUP transcription factor 2

CrPV : cricket paralysis virus

CSFV : classical swine fever virus

CTD : C-terminal domain

CUG : codon initiateur (leucine)

Cyr 61 : cysteine-rich angiogenic protein 61

eEF : eukaryotic longation factor

EGFR : epidermal growth factor receptor

eIF : eukaryotic initiation factor

EMCV : encephalomyocarditis virus

ERAD : endoplasmic reticulum-associated protein degradation

eRF : eukaryotic releasing factor

ERK : extracellular signal-regulated kinases

FBXW7 : F-Box And WD repeat domain containing 7

FECH : ferrochelatase

FGF : fibroblast growth factor

FGFR : fibroblast growth factor receptor

FIFG : c-Fos induced growth factor

FMDV : foot-and-mouth disease virus

GBM-SCs : glioblastoma-stem cells

GCN : general control nonderepressible 2

GM-CSF : Granulocyte-macrophage colony-stimulating factor

GTP : guanosine triphosphate

HAV : hepatitis A virus

HCV: hepatitis C virus

HIF : hypoxia inducible factor

HMW : high mass weight

HNF-4α : hepatocyte nuclear factor 4 alpha

hnRNP : heterogeneous nuclear ribonucleoprotein

HR1 : hemin regulated inhibitor kinase

HRE : hypoxia response element

HSE : heat shock element

HSF : heat shock factor

HSPs : heat shock proteins

HuR : human antigen R

IGF : insulin-like growth factor

IGF1-R : insulin-like growth factor 1 receptor

INR : initiator element

IRE : iron responsive element

IRE1α : inositol requiring enzyme 1 a

IRES : internal ribosome entry site

IRP1 : iron responsive protein-1

ITAF : IRES-trans-acting factors

LEDGF : lens epithelium-derived growth factor

LPS : lipopolysacharide

m7GTP : 7-methylguanosine 5' triphosphate

MAPK : mitogen-activated protein kinase

miR : micro ARN

MNK1 : MAPK interacting kinase 1

mTOR : mammalian/mechanistic target of rapamycin

NGFB : nerve growth factor beta

NLS : nuclear localization signal

NOS2 : nitric oxyde synthase 2

ODDD : oxygen dependent degradation domain

OMS : organisation mondial de la santé

ORF : open reading frame

p53 : protein 53

p54nrb/NONO : Non-POU domain-containing octamer-binding protein

p75 : protein 75

PABP : polyA-binding protein

PAI-1 : plasminogen activator inhibitor-1

PCBP1 : poly (rC)-binding protein1

PDGF : platelet derived growth factor

PERK : protein kinase RNA (PKR)-like endoplasmic reticulm kinase

PHD : prolyl hydroxylase domain protein

PI3K : phosphoinositide 3-kinase

PIC : pre-inititation complex

PKR : protein kinase regulated

PSF : polypyrimidine tract-binding protein associated splicing factor

PTB : pyrimidine tract binding protein

RBD : RNA binding domain

RBM : RNA binding motif domain

RBP: RNA binding protein

RE : réticulum endoplasmique

RFX : regulatory factor X

SLC43A2 : solute carrier family 43 (amino acid system L transporter) member2

SNAT2 : system A amino acid transporter

snRNP : small nuclear ribonucleoprotein

SP1 : trans-acting transcription factor 1

SRE : serum response element

STAT3 : Signal transducer and activator of transcription 3

TAF : TBP-associated factors

TBP : TATA binding-protein

TEFb : positive transcription elongation factor

TFII : transcription factor for RNA polymérase II

TGFβ : transforming growth factor beta

TMEM79 : transmembrane Protein 79

UBN1 : ubinuclein 1

UPR : unfolded protein response

UTR : untranslated region

VEGF : vascular endothelial growth factor

VEGFR : vascular endothelial growth factor receptor

VHL : Von Hippel Lindau

XBP-1 : X-box binding protein 1

XIAP : X-linked inhibitor of apoptosis protein

Table des matières

Résumé 1

Abstract 2

Liste des abréviations 3

INTRODUCTION 12

I- Régulation de l'expression génique 12

I-1 Les différentes étapes de la régulation de l'expression génique.....13

I-1-1 La transcription 13

I-1-1-1 Le mécanisme d'initiation de la transcription 13

I-1-1-2 La régulation de la transcription 16

I-1-1-3 Le couplage de la transcription avec d'autres étapes 17

I-1-2- La traduction 21

I-1-2-1 Les différentes étapes de la traduction 21

I-1-2-2 Initiation de la traduction dépendante de la coiffe 21

I-1-2-3 Les régions régulatrices de la traduction : 3'UTR et 5'UTR 24

I-1-2-4 Un mécanisme de traduction alternatif : l'initiation dépendante des IRES 25

I-1-2-4-a) Les IRES, des éléments structuraux permettant l'entrée interne des ribosomes 25

I-1-2-4-b) Les gènes régulés par le mécanisme IRES-dépendant 28

- *FGF1*.....29
- *FGF2*.....30
- *VEGFA*.....31
- *VEGFC*.....32
- *VEGFD*.....33

I-1-2-4-c) Les facteurs régulateurs de l'activité des IRES : les ITAF 33

II- La régulation de l'expression génique par le stress et le microenvironnement 35

II-1- La réponse transcriptionnelle au stress 36

II-1-1 Hypoxie 36

II-1-2 Stress du réticulum endoplasmique 38

II-1-3 Choc thermique 39

II-2- La régulation de la traduction lors du stress 40

II-2-1 L'inhibition de la traduction dépendante de la coiffe 41

II-2-2 Les stress et stimuli capables d'activer la traduction IRES-dépendante 44

- Les IRES lors de l'hypoxie 44
- Les IRES lors du stress du réticulum 44
- Les IRES lors du choc thermique 45
- Déprivation en nutriment etcarence en acides aminés 45
- Activation des IRES en réponse à des stimuli physiologiques 45

III- Le stress dans les pathologies 47

- ♦ Impact de l'hypoxie dans le cancer 47
- ♦ Impact de l'hypoxie dans les pathologies ischémiques 49
- ♦ Les IRES, des outils biotechnologiques pour un transfert combiné de gènes thérapeutiques 51

III-1 Utilisation desvecteurs à IRES pour letraitement de l'ischémie du membre inférieur 52

III-2 Utilisation des vecteurs à IRES pour le traitement de l'ischémie cardiaque 55

IV- Objectifs de la thèse 56

RESULTATS 58

Chapitre 1 : Traduction promoteur-dépendante contrôlée par p54^{nrb}/NONO et hnRNPM durant la différenciation des myoblastes 58

Chapitre 2 : La nucléoline induit la traduction de VEGFD en réponse au choc thermique lors de la lymphangiogenèse tumorale 90

Chapitre 3 : Les IRES sont des régulons traductionnels qui gouvernent l'induction séquentielle des facteurs de croissance (lymph)angiogéniques dans les cardiomyocytes en hypoxie.....113

DISCUSSION 170

BIBLIOGRAPHIE 175

Liste des figures 206

ANNEXE 208

Introduction

INTRODUCTION

Régulation de l'expression génique :

L'information génétique portée par l'ADN est la même dans toutes les cellules. Elle est essentielle au développement et au fonctionnement de l'organisme. Cependant, chaque cellule a sa fonction et n'exprime donc pas les mêmes gènes. De ce fait, la régulation de l'expression des gènes est mise en place pour que chaque cellule mène à bien ses fonctions en adéquation avec son environnement. Cette régulation survient à toutes les étapes de l'expression génique, de l'ADN à la protéine. Celle-ci intervient donc au niveau de la transcription, la maturation, l'export, la stabilité et la traduction des ARNm, ainsi qu'au niveau post-traductionnel par la modification et la dégradation des protéines (**Figure 1**).

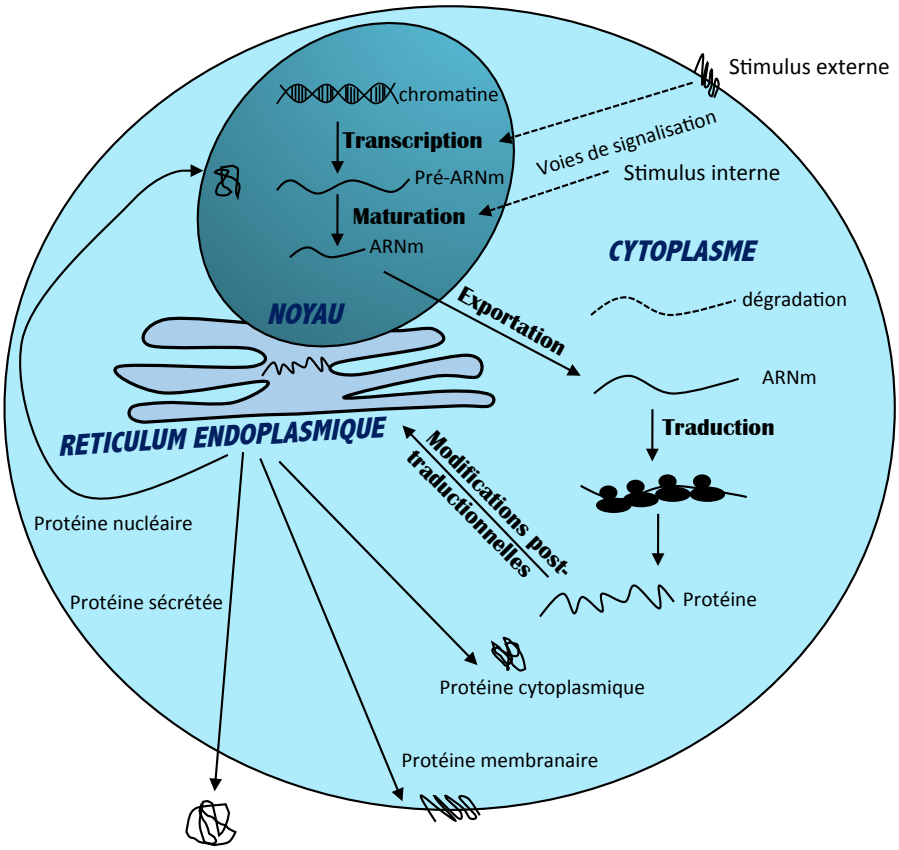

Figure 1 : Régulation de l'expression génique. La transcription et la maturation se font dans le noyau. L'ARN mature est transporté dans le cytoplasme où il sera traduit, dégradé ou stocké.

La protéine traduite va subir des modifications post-traductionnelles dans le réticulum endoplasmique avant d'atteindre une localisation précise pour fonctionner.

I-1 Les différentes étapes de la régulation de l'expression génique

Avant la transcription, l'ADN subit une première régulation, l'épigénétique qui module l'accessibilité de la double hélice à la machinerie transcriptionnelle. L'ADN peut être modifié directement par méthylation, ce qui inhibe la transcription, ou la modification peut se faire au niveau de la chromatine (association ADN et histones). En effet, l'ADN est associé à des protéines qui sont les histones, formant ainsi les nucléosomes. Les histones subissent des modifications post-traductionnelles (acétylations, méthylations, phosphorylations, ubiquitylations) qui influent sur la densité des nucléosomes, rendant ainsi une conformation relâchée (euchromatine) ou condensée (hétérochromatine) de la chromatine. L'euchromatine permet la transcription tandis que l'hétérochromatine réprime la transcription.

I-1-1 *La transcription*

La transcription est caractérisée par la synthèse d'ARN à partir d'une matrice d'ADN. Elle est catalysée par une ARN polymérase, qui synthétise l'ARN en lisant l'ADN de 5' en 3'. La transcription présente trois étapes : l'initiation, l'élongation et la terminaison. Le processus de la transcription est complexe mais l'étape cruciale est l'initiation de la transcription.

I-1-1-1- *Le mécanisme d'initiation de la transcription*

Chez les eucaryotes, il existe 3 types d'ARN polymérases. L'ARN polymérase I, la plus active, permet de synthétiser les ARN ribosomiques (ARNr) dans le nucléole, excepté l'ARN 5S. L'ARN polymérase II synthétise les précurseurs des ARNm dans le noyau ainsi qu'un grand nombre d'ARN non-codants (ARNnc) comme les petits ARNs nucléaires snRNA, les microARNs et les longs ARNnc. Quant à l'ARN polymérase III, elle synthétise les ARN de transfert (ARNt) ainsi que l'ARNr 5S dans le noyau.

Contrairement à ce qui se passe chez les procaryotes, chez les eucaryotes l'ARN polymérase II ne travaille pas seule mais elle est accompagnée de nombreux co-facteurs protéiques qui sont recrutés les uns les autres pour former le complexe d'initiation. Ces facteurs peuvent être généraux comme les TFII pour

« Transcription Factor for RNA polymerase II » qui se fixent au niveau de la région promotrice commune à plusieurs gènes de manière constitutive.

L'ARN polymérase II associée à des facteurs de transcription généraux forment le complexe de pré-initiation de la transcription (PIC), au niveau d'une séquence spécifique du promoteur (Thomas *et al* 2006). Chez les archées et les eucaryotes, les promoteurs contiennent une séquence conservée appelée la boîte TATA (Mathis *et al* 1981), nécessaire au recrutement des facteurs de transcription. Elle est située entre 25 et 35 paires de bases (pb) en amont du site de démarrage de la transcription. La boite TATA est reconnue par le facteur de transcription TFIID, complexe multiprotéique composé de la TATA Binding-Protein (TBP) associée aux TAF (TBP-associated factors). Cette liaison est stabilisée par TFIIA (Gill 2001). TFIIB se fixe à son tour sur TFIID en reconnaissant un motif BRE (B recognition element) en amont de la boîte TATA (Lagrange *et al* 1998). L'ensemble permet le recrutement de l'ARN polymérase II ainsi que le facteur TFIIF. Ensuite TFIIE est recruté au niveau du complexe, il a pour rôle de rendre accessible l'ADN. Puis TFIIH est recruté, il a une activité enzymatique facilitée par TFIIE. TFIIH phosphoryle l'ARN polymérase du côté C-terminal ce qui va déclencher la transcription. TFIIE et TFIIH, en plus de leur rôle dans la formation du PIC, jouent également un rôle dans la transition entre l'initiation et l'élongation de la transcription (Okamoto *et al* 1998). Toutefois, certains promoteurs ne disposent pas de TATA box mais présentent d'autres éléments comme l'initiateur INR. L'INR se trouve entre -3 et -5 du site d'initiation de la transcription et il est reconnu par TFIID. Ainsi, l'ARN polymérase II peut initier la transcription avec l'INR seul (**Figure 2**).

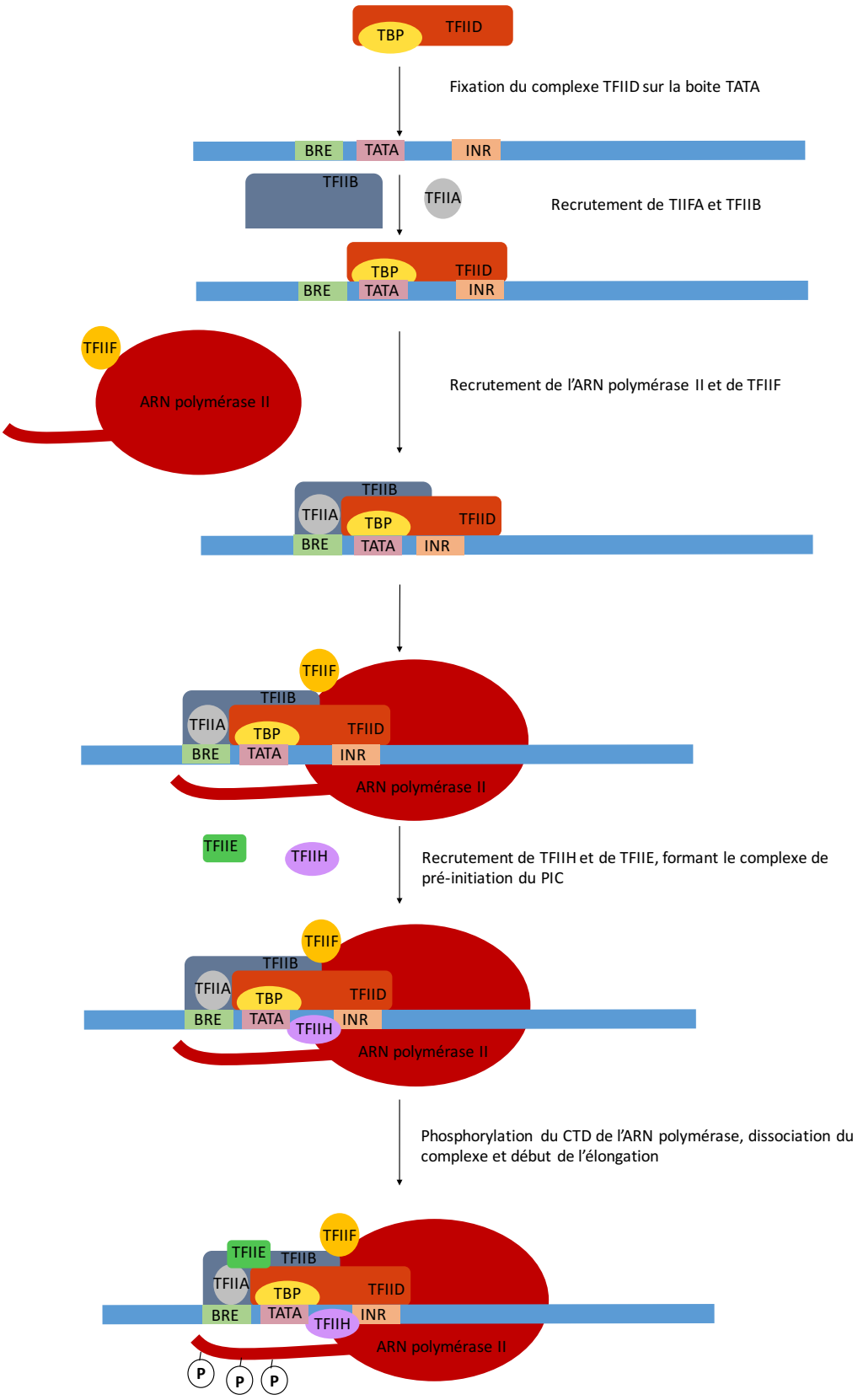

Figure 2 : Initiation de la transcription. La TBP (TATA binding protein) du complexe TFIID reconnaît la boite TATA. TFIIA et TFIIB se fixent sur TFIID. TFIIB reconnaît la séquence BRE. L'ARN polymérase II est recrutée avec TFIIF pour former le complexe de pré-initiation (PIC). TFIIE et TFIIH arrivent à leur tour. TFIIH phosphoryle le domaine CTD de l'ARN polymérase.

I-1-1-2 - *La régulation de la transcription*

La formation du complexe d'initiation de la transcription (ARN polymérase II associée à ses co-facteurs) qui aboutit à l'activation du promoteur est contrôlée par différents paramètres. En particulier le contrôle se fait via le remodelage de la chromatine et la fixation de facteurs spécifiques à des séquences distantes de la boîte TATA appelées "enhancers", ceci en réponse à divers stimuli extra- ou intracellulaires (Emerson 2002). La transcription est également régulée par des facteurs répresseurs.

L'amplificateur ou enhancer est une séquence sur laquelle se lie un ou plusieurs facteurs de transcription, qui n'est pas forcément proche du gène régulé. Cette séquence cis-régulatrice est située principalement en amont du gène concerné, parfois à des milliers de nucléotides du point d'initiation de la transcription. L'enhancer peut aussi se trouver en aval du site d'initiation de la transcription. Il recrute des facteurs trans-activateurs (**Figure 3**).

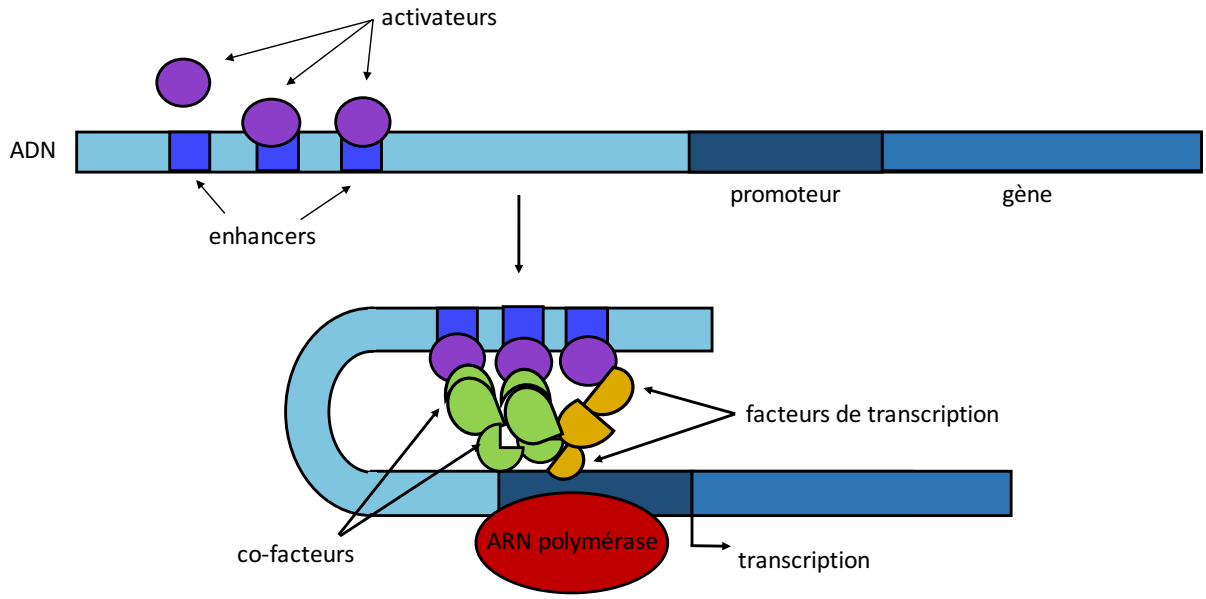

Figure 3 : Régulation de la transcription

Il existe aussi des séquences régulatrices en *cis* inhibant la transcription appelées silencers qui lient des régulateurs en *trans*, ce sont les répresseurs transcriptionnels. Ils peuvent agir de deux manières, soit en se liant directement au promoteur soit en se liant à l'enhancer pour bloquer la transcription.

Le domaine carboxy-terminal de l'ARN polymérase II dit CTD (C-terminal domain tient un rôle important dans la transcription. Il contient une séquence répétée et conservée de sept acides aminés : Tyr-Ser-Pro- Thr-Ser-Pro-Ser. Dans les années 1980, des formes phosphorylées et non-phosphorylées du CTD ont été établies *in-*

vivo et *in-vitro*. Les tests de co-immunoprécipitation de chromatine (ChIP) ont montré l'association de la forme phosphorylée avec le complexe de pré-initiation (Christmann *et al* 1981, Dahmus 1996).La phosphorylation se fait essentiellement sur les résidus Sérine2 et Sérine5. La transcription est associée à un cycle de phosphorylation et de déphosphorylation du CTD. Lors de la formation du complexe de pré-initiation, la forme non-phosphorylée s'associe au promoteur puis elle est phosphorylée par la kinase de TFIIH sur la Sérine5 permettant l'élongation de la transcription. La Sérine2 est alors phosphorylée au cours de l'élongation par P-TEFb ou CDK9 et la Sérine5 est déphosphorylée par les phosphatases (Hsin *et al* 2012).A la fin de la transcription du gène, les deux sérines sont déphosphorylées par des phosphatases. L'ARN polymérase et son CTD hypophosphorylé est recyclée pour assurer une nouvelle transcription.Le CTD de l'ARN polymérase II tient également un rôle crucial dans l'épissage (décrit dans la partie I-1-1-3).

I-1-1-3 *Le couplage de la transcription avec d'autres étapes*

Une fois la transcription terminée, le transcrit naissant est clivé et une queue PolyA est ajoutée à l'extrémité 3' (Proudfoot *et al* 2002). Chez les archées et les eucaryotes, le transcrit non-maturé, dit pré-ARNm subit un épissage. En effet, le pré-ARNm possède des séquences codantes, les exons, espacées par des régions non-codantes, les introns qui sont éliminées par un mécanisme appelé épissage. A ce stade, le transcrit devient l'ARNm. Jusqu'à cette étape, tout ces processus ont lieu dans le noyau mais pour être traduit, l'ARNm va être pris en charge par des protéines pour être exporté dans le cytoplasme.

De nombreuses études ont montré que toutes les étapes de la transcription à la traduction sont interconnectées, ce qui donne la notion de l'expression génique.

- ***Couplage transcription-épissage :***

Depuis plusieurs années, il est démontré que la transcription et l'épissage sont deux évènements liés dans le temps et l'espace. Le pré-ARNm est maturé de manière principalement co-transcriptionnelle : addition de la coiffe, épissage et polyadénylation.

L'épissage consiste à faire des coupures et ligations du pré-ARNm pour ne garder que les exons. Le pré-ARNm est pris en charge par un complexe ribonucléoprotéique appelé spliceosome. Le processus classique d'épissage est assuré par des facteurs qui sont des petites ribonucléoprotéines ou snRNP comportant de petits ARN U1, U2, U4/U6 et U5 associés à des protéines,

les facteurs d'épissage. Les introns présentent à leurs extrémités 5' et 3' des séquences spécifiques pour la délimitation entre intron/exon et pour être reconnus par le complexe spliceosome. Mise à part ces extrémités, l'intron présente également une séquence interne dite « boite de branchement » qui joue un rôle clé dans le mécanisme de l'épissage.

La snRNP U1 se lie au site 5' de l'épissage et U2 va se lier sur la boîte de branchement, ce qui va former le pré-spliceosome. Le complexe U4/U6 va permettre la jonction entre le 5'intron et la boîte de branchement. U5 s'associe au complexe à son tour et fait le rapprochement entre les 3' et 5' de l'exon à liguer. U4 et U5 quittent le complexe puis deux réactions chimiques vont se faire pour liguer les exons et éliminer l'intron sous forme de lasso (**Figure 4**). Le transcrit est dit alors mature : c'est l'ARNm.

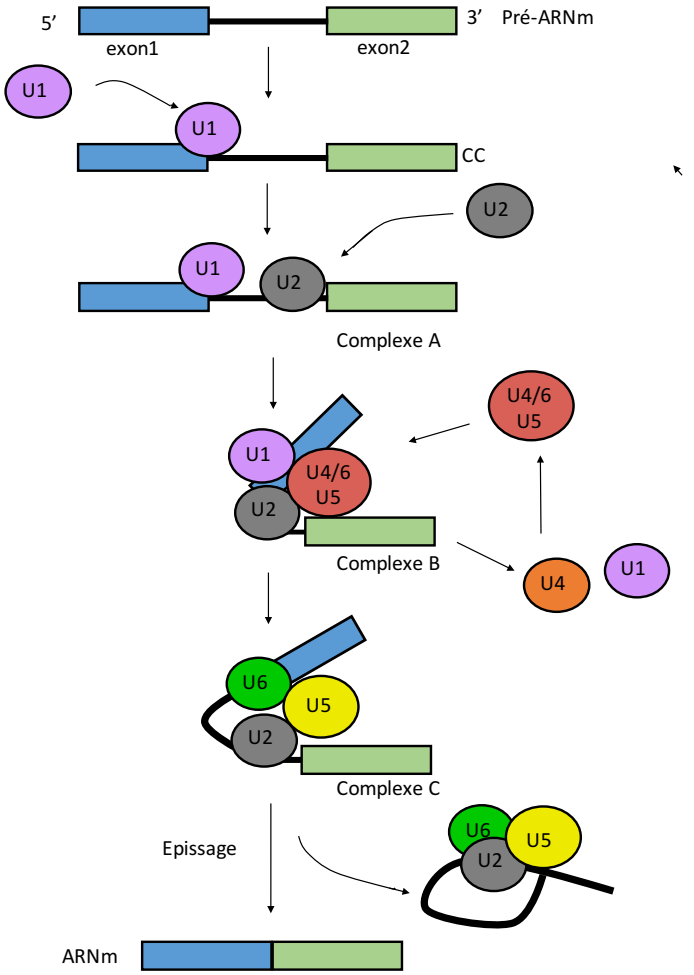

Figure 4 : Epissage. Les facteurs d'épissage sont recrutés au niveau du pré-ARNm pour former d'abord le complexe A (U1,U2) puis le complexeB (U1,U2,U4/U5/U6) ensuite le complexe C (U2,U5,U6), suivi d'un clivage de l'ARN formant ainsi l'ARNm.

La littérature a montré que la transcription peut influencer la maturation et inversement (Orphanides *et al* 2002, Braunschweig *et al* 2013). Certains facteurs peuvent être impliqués dans les deux évènements. Kwek et ses collègues ont démontré que le facteur principal de l'épissage snRNP U1 interagit avec le facteur de transcription général TFIIH et ils agissent de façon réciproque. U1 stimule l'initiation de la transcription et TFIIH favorise l'épissage de l'ARN (Kwek *et al* 2002). Les protéines PSF et $p54^{nrb}$/NONO se fixent sur le promoteur et sur le CTD. Elles activent la transcription et stimulent l'épissage des premiers introns (Rosonina *et al* 2005).

Le CTD de l'ARN polymérase II facilite également le recrutement des facteurs de la formation de la coiffe et de l'épissage. Peu après l'initiation de la transcription, le CTD phosphorylé recrute l'enzyme responsable de l'ajout de la coiffe en 5' de l'ARN naissant (Cho *et al* 1997, McCracken *et al* 1997). Le CTD phosphorylé permet également le recrutement du spliceosome par l'intermédiaire des protéines SR (protéines avec un domaine riche en résidus Sérine et Arginine) (Long *et al* 2009). Il est également associé aux facteurs de polyadénylation (Shi *et al* 2009) et de terminaison tel que PSF et $p54^{nrb}$/NONO (Hsin *et al* 2012). Plusieurs études *in-vitro* ont montré la stimulation de l'épissage par le CTD (Hirose *et al* 1999, David *et al* 2011) et permettant ainsi de définir l'exon (Zeng *et al* 2000). Le CTD servirait ainsi de plateforme d'assemblage pour faciliter la définition de l'exon et également la formation du complexe d'épissage (Braunschweig *et al* 2013). L'épissage se fait de manière essentiellement co-transcriptionnelle même si un processus post-transcriptionnel a également été décrit (**Figure 5**) (Braunschweig *et al* 2013).

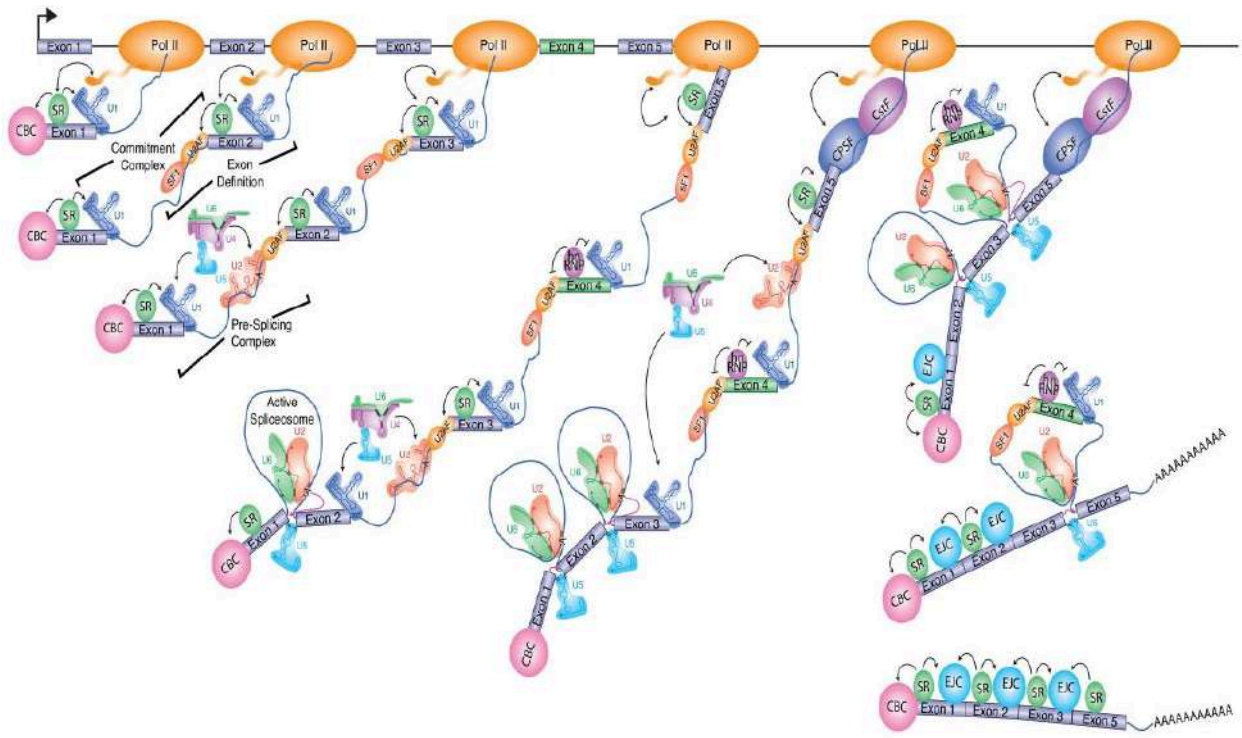

Figure 5 : Illustration du couplage entre transcription et épissage. L'épissage se fait de manière co-transcriptionnelle avec une étroite collaboration entre les facteurs d'épissage (protéines SR, snRNP), le CBP (cap binding protein complex) et le CTD de l'ARN polymérase II. Tiré de la publication (Braunschweig *et al* 2013).

- ***Couplage de la transcription et de la stabilité de l'ARN:***

La stabilité des ARNm tient un rôle important dans le contrôle de l'expression génique. Depuis plusieurs années, on sait que la coiffe inhibe la dégradation des ARN par les exoribonucléases 5' -> 3' (Furuichi *et al* 1977, LaGrandeur *et al* 1996). D'autres études ont également montré l'importance de la queue polyA dans la stabilité de l'ARNm.

Deux mécanismes majeurs sont décrits : la déadénylation et l'action de la PABP (PolyA-binding protein). La déadénylation ou le raccourcissement de la queue polyA est l'étape limitante de la dégradation des ARNm. Elle conduit à la dégradation de l'ARNm par deux mécanismes différents. Le premier est la dégradation 3'->5' par des exosomes cytoplasmiques et le second passe par l'élimination de la coiffe suivie de la dégradation par une exonucléase 5'->3'. En ce qui concerne la PABP, comme son nom l'indique, elle se lie avec une forte affinité par son domaine N-terminal à la queue polyA de l'ARNm. Par conséquent, l'extrémité 3' de l'ARNm est protégée de la déadénylation (Garneau *et al* 2007).Un couplage de la stabilité de l'ARN avec la transcription a été étudié chez la levure, les

facteurs transcriptionnels SWI5 et CLB2 régulent la stabilité de l'ARNm durant le cycle cellulaire (Trcek *et al* 2011).Rap1p stimule la transcription et la dégradation d'une population d'ARNm endogènes (Bregman *et al* 2011).

I-1-2- La traduction

La traduction est un événement cellulaire qui consiste à décoder l'ARN messager mature et synthétiser le produit du gène, c'est à dire la protéine, dans le cytoplasme chez les eucaryotes. Pour être traduit, l'ARNm doit contenir un cadre de lecture ouvert (ORF pour "open reading frame") correspondant à une phase ouverte entre un codon initiateur et un codon de terminaison. Depuis plusieurs années, de nombreuses études révèlent une absence de corrélation entre la quantité du transcrit et la quantité de protéines synthétisée, ce qui marque l'importance de la régulation traductionnelle dans le contrôle de l'expression génique (Gygi *et al* 1999).

I-1-2-1 *Les différentes étapes de la traduction*

De même que la transcription, la traduction présente trois phases distinctes : l'initiation, l'élongation et la terminaison. La régulation de la traduction peut intervenir au niveau de chaque phase mais survient surtout lors de la phase d'initiation qui comporte de multiples étapes. La sous-unité 40S du ribosome associée à l'ARN de transfert (ARNt), appelée complexe 43S, est un acteur majeur de l'initiation. Dans le mécanisme classique d'initiation, le ribosome 43S balaye le transcrit jusqu'à ce qu'il rencontre un codon initiateur à partir duquel commencera la synthèse protéique après assemblage du ribosome 80S. Plusieurs facteurs interviennent durant toutes ces phases : les facteurs d'initiation eIF (eukaryotic Initiation Factor), les facteurs d'élongation eEF (eukaryotic elongation factor) et les facteurs de terminaison eRF (eukaryotic releasing factor). Etant donné que ma thèse porte sur la régulation de l'initiation, seule cette étape sera approfondie ci-dessous.

I-1-2-2 *Initiation de la traduction dépendante de la coiffe*

Après sa maturation, l'ARNm contient à l'extrémité 5' une coiffe et à l'extrémité 3' une queue polyA. Il est exporté dans le cytoplasme pour être pris en charge par la machinerie traductionnelle.

Dans un premier temps, les deux sous-unités du ribosome sont dissociées dans le cytoplasme grâce aux facteurs eIF1A, eIF3 et eIF6. Les facteurs eIF1A et eIF3 sont liés à la sous-unité ribosomique 40S pour empêcher sa liaison avec la sous-unité 60S ; en revanche eIF6 se lie au ribosome 60S pour empêcher sa liaison avec le 40S.

L'initiation de la traduction classique dépendante de la coiffe fait intervenir de nombreuses protéines qui sont principalement les facteurs eIF ainsi que la PABP. Elle est assurée par l'association de deux complexes à l'ARNm : eIF4F et 43S, pour former le complexe d'initiation 48S. Le complexe eIF4F est composé de trois facteurs d'initiation : eIF4E, eIF4A, eIF4G.

L'initiation commence par le recrutement du facteur eIF4F sur la coiffe m7GTP de l'ARNm (Sonenberg *et al* 1978, Sonenberg *et al* 1979, Holcik *et al* 2005). Le facteur eIF4A est une hélicase à ARN qui dénature la structure secondaire de l'ARNm afin de faciliter l'accès du complexe à l'extrémité 5' non-traduite (5'UTR : 5' untranslated region). Son activité est stimulée par eIF4B et 4H (Rogers *et al* 2001). La protéine PABP est recrutée par eIF4G, partenaire du complexe 4F, ce qui permet le rapprochement physique entre l'extrémité 5'UTR et 3'UTR de l'ARNm. Ce complexe est appelé « modèle en boucle » (Kahvejian *et al* 2001) (**Figure 6**).

En parallèle se forme le complexe de pré-initiation 43S grâce à eIF2. Le facteur d'initiation eIF2 forme un complexe ternaire avec une molécule de GTP et le Met-ARNt_i^{Met}. Puis le complexe 43S ainsi que le facteur eIF1 se lient à la petite sous-unité ribosomique 40S à laquelle sont déjà associés eIF1A et eIF3, l'ensemble forme le complexe de pré-initiation 43S.

Le complexe eIF4F recrute le complexe de pré-initiation 43S via une interaction entre eIF3 et eIF4G pour former le complexe de pré-initiation 48S. Ces facteurs permettent de rendre accessible le site de liaison du ribosome à l'ARN (Passmore *et al* 2007).

Le complexe d'initiation 48S commence le balayage (scanning) de 5' vers 3' en explorant la région 5'UTR du messager jusqu'à la rencontre du codon initiateur AUG. Au niveau du site d'initiation, le GTP associé à eIF2 est hydrolysé par eIF5 ce qui va libérer les facteurs d'initiation et permettre l'association des deux sous-unités ribosomales 40S et 60S pour former le complexe 80S (**Figure 5**). Ainsi l'élongation peut commencer.

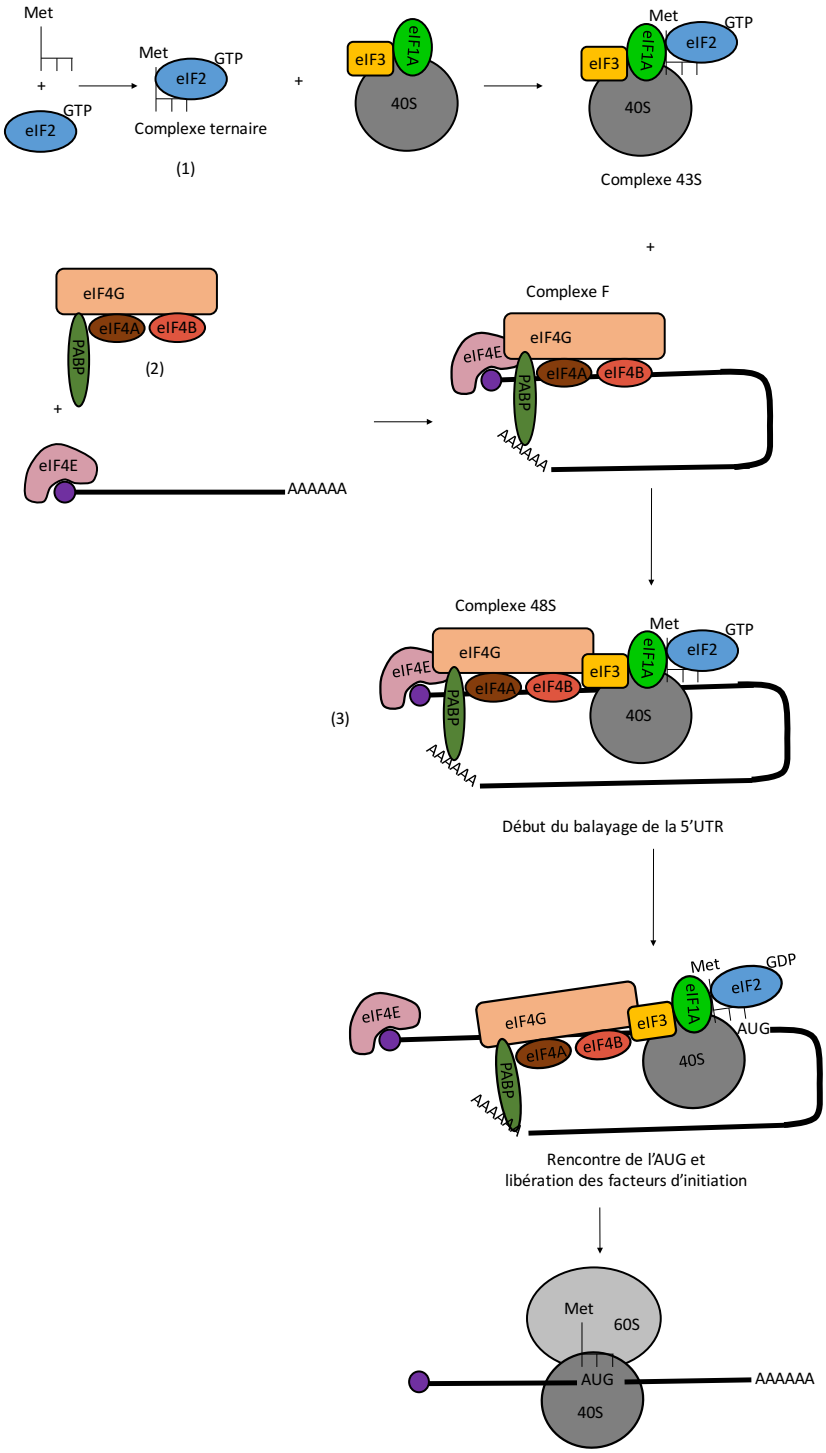

Figure 6 : Initiation de la traduction chez les eucaryotes. L'initiation commence par (1) la formation du complexe ternaire (association de l'ARNt$_i^{Met}$ et le facteur eIF2-GTP) associée à la sous-unité 40S liée aux facteurs eIF3 et eIF1A pour former le complexe 43S. (2) Elle est suivie du recrutement du complexe eIF4F et de la PABP sur la coiffe formant le «modèle en boucle». (3) Le complexe 43S est ensuite recruté, formant le complexe 48S, pour commencer le balayage de la région 5'UTR jusqu'à atteindre le codon AUG. Arrivés à l'AUG, les facteurs d'initiation sont relargués et la grande sous-unité ribosomique 60S est recrutée par la petite sous-unité 40S pour former le ribosome 80S.L'élongation de la traduction est alors engagée.

I-1-2-3 *Rôle des régions 3'UTR et 5'UTR dans la régulation de la traduction*

Les deux régions 3'UTR et 5'UTR coopèrent et interagissent de façon indirectepar l'intermédiaire des facteurs d'initiation généraux (eIF4G) et la PABP. La pseudo-circularisation de l'ARN le protège de la dégradation et facilite la ré-initiation de la traduction. Les régions non-traduites sont également les régions ciblées par des facteurs régulateurs de la traduction.

Le 5'UTR :

- La régulation par le 5'UTR met en jeu à la fois des structures spécifiques et des protéines régulatrices en réponse aux facteurs environnementaux. Par exemple en absence de fer, le répresseur IRP1 (iron responsive protein-1) se fixe sur la structure IRE (iron responsive element) située à 40 nucléotides de la coiffe de l'ARNm de la ferritine pour bloquer l'initiation de sa traduction (Rouault *et al* 1997). Par contre, la PABP régule elle-même sa propre synthèse en se fixant sur une séquence riche en A de son 5'UTR, en inhibant sa traduction lorsque la quantité d'ARNm baisse dans la cellule (Hornstein *et al* 1999).
- En amont du codon initiateur de l'ORF principal, il existe souvent des codons AUG appelés uAUG (upstream AUG), générant de petits cadres de lecture appelés uORF (upstream ORF).Deux cas peuvent se présenter : (i) lors du balayage, si le complexe d'initiation ne rencontre pas la séquence Kozak (A/GCCCATGG), l'initiation à partir de ce uAUG est abolie et l'initiation à partir du vrai AUG est établie ;(ii) soit la production de uORF se fait ce qui influencera la traduction de l'ORF principal.En effet, un uORF proche de l'ORF principal est souvent inhibiteur du fait que le complexe a peu de temps pour se réassembler (Kozak 1987). Dans les cellules neuronales, l'élimination des uORFs en 5'UTR de la protéine kinase Mζ (PKMζ) augmente la traduction du gène rapporteur in vitro et dans les cellules primaires (Bal *et al* 2016).Ce résultat, ainsi que de nombreuses études, montrent que les uORF sontdes répresseurs de la traduction.Comme chez la levure, en conditions de stress, la phosphorylation de eIF2α va inhiber la traduction initiée par les uORFs ce qui aboutit à la traduction de l'ORF principal de GCN4, un facteur transcriptionnel (Hinnebusch 1997).
- Le site d'entrée interne du ribosome ou IRES pour « internal ribosome entry site » est un élément structural en 5'UTR de certains ARNm permettant d'initier la traduction en réponse aux facteurs environnementaux.Les IRES feront l'objet d'une description détaillée dans la partie suivante (I-1-2-4).

Le 3'UTR :

La fixation des facteurs sur la région 3'UTR réprime souvent la traduction. Ce sont surtout les RBP (RNA Binding Proteins). Chez les mammifères, eIF4E2, un isoforme de eIF4E, réprime l'initiation de la traduction (Morita *et al* 2012) et son orthologue, chez la levure, 4EHP inhibe la traduction en se fixant sur la coiffe (Cho *et al* 2005). En revanche, eIF4E2 est un activateur de l'initiation de la traduction en hypoxie (Uniacke et al 2012). D'autres RBP agissent aussi au niveau de l'élongation de la traduction. HnRNP E1 interagit avec eEF-1A pour bloquer sa dissociation avec le ribosome, empêchant ainsi l'élongation (Hussey *et al* 2011). Puf se lie à la région 3'UTR empêchant la pseudo-circulation de l'ARN, inhibant l'initiation de la traduction et recrute le complexe de déadénylation CCR4/POP2/NOT (Miller *et al* 2011). La traduction est aussi régulée par la fixation de microARN à la région 3' non-traduite. Ce mécanisme de régulation par les ARN non codants a été décrit abondamment ces dernières années et concerne de nombreux ARNm (Mihailescu 2015).

Le 3'UTR régule aussi la traduction en jouant sur la stabilité de l'ARNm. La fixation du microARN sur cette région cible peut déstabiliser l'ARN. À l'inverse, la protéine HuR se fixe sur la séquence riche en AU dans la région 3'UTR (AU-rich element) de certains ARNm pour les stabiliser. Pour revue (Griseri *et al* 2014).

I-1-2-4 *Un mécanisme de traduction alternatif : l'initiation dépendante des IRES*

Certains messagers initient leur traduction malgré le blocage de la traduction dépendante de la coiffe, et ne nécessitent pas l'implication du facteur de liaison à la coiffe eIF4E.

I-1-2-4-a) Les IRES, des éléments structuraux permettant l'entrée interne des ribosomes:

L'IRES est une structure secondaire dans la région 5' UTR de certains messagers. Les IRES ont été découverts initialement chez les picornavirus. En effet, ces virussont capables d'initier la traduction de leur ARNm malgré l'absence de coiffe (Jang*et al* 1988, Pelletier*et al* 1988). Lors de l'infection, les picornavirus détournent la machinerie traductionnelle cellulaire à leur avantage en utilisant différentes stratégies pour bloquer la coiffe. Certains picornavirus comme l'encephalomyocarditis virus (EMCV) séquestrent le facteur eIF4E pour bloquer la traduction coiffe dépendante et induire la traduction IRES-dépendante (Canaani *et*

al 1976, Beretta *et al* 1996, Gingras *et al* 1996). En revanche, le rhinovirus clive le facteur eIF4G par sa protéase 2A pour inhiber la traduction initiée par la coiffe (Borman *et al* 1997). Le poliovirus utilise les deux mécanismes (Gingras *et al* 1996). Les IRES viraux sont classés par rapport à leur structure et leur fonction. Les IRES de type I (poliovirus) permettent un recrutement du ribosome dans la région 5' non traduite, au niveau d'un codon AUG qui n'est pas le codon initiateur. Le recrutement ribosomique par ces IRES est donc suivi d'un balayage afin d'atteindre le codon initiateur. Les IRES de type II (EMCV) permettent un recrutement du ribosome directement au niveau du codon initiateur sans balayage. Ce type d'IRES présente une fenêtre de recrutement assez petite, et si on déplace le codon initiateur par rapport à la structure de l'IRES, l'initiation de la traduction ne se fait plus. Les IRES de type III (HCV : Hepatitis C Virus) sont situés de part et d'autre du codon initiateur, ce qui veut dire qu'une partie de la séquence codante est requise pour leur activité. Quant aux IRES de type IV (Cricket Paralysis virus), ils permettent l'initiation de la traduction en l'absence de codon initiateur (Sarnow 2003, Kieft 2009). Les IRES de type I, II et III nécessitent les facteurs d'initiation classiques (sauf eIF4E) pour fonctionner. En revanche les IRES du type IV n'ont pas besoin de facteur d'initiation (**Figure 7**). Les IRES de type I et II ont leur activité régulée par des protéines cellulaires. C'est précisément le cas des premiers IRES découverts en 1988, ceux du poliovirus et d'EMCV : cette dépendance aux protéines cellulaires a suggéré que les ARNm cellulaires pourraient eux aussi être régulés par ce mécanisme (Jackson 1988).

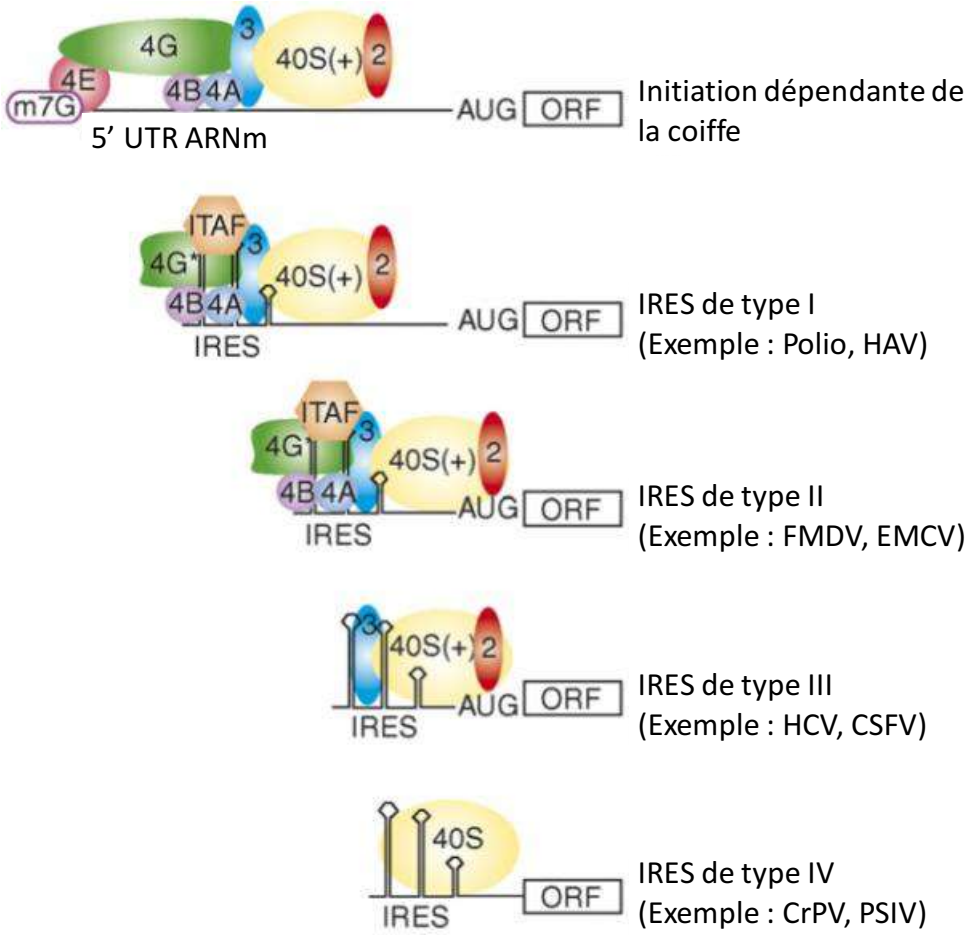

Figure 7 : Comparaison de la traduction dépendante de la coiffe et des 4 types d'IRES. La traduction dépendante des IRES de type I, II, III nécessite les facteurs d'initiation excepté eIF4E. Celle de l'IRES de type IV n'utilise pas de facteur d'initiation. Les IRES de type I et II ont besoin d'un facteur ITAF pour activer la traduction contrairement à ceux de type III et IV.Modifié d'après, Kieft, 2008 (Kieft 2008).

Le premier IRES dans un ARNm cellulaire a été découvert en 1991 dans l'ARNm codant pour la protéine chaperone des chaînes lourdes de l'immunoglobuline, BiP. En effet, cette protéine continue à être traduite malgré le blocage de la traduction dépendante de la coiffe dû à l'infection par le poliovirus (Macejak *et al* 1991). Cette première étude a été immédiatement suivie par d'autres publications démontrant la présence d'un IRES dans l'ARNm d'un facteur de transcription de drosophile, antennapedia, (Oh *et al* 1993) puis dans les ARNm de facteurs de croissance comme le FGF2 (Vagner *et al* 1995), le VEGFA (Huez *et al* 1998) ainsi que dans les ARNm de proto-oncogènes comme c-myc (Nanbru *et al* 1997). La présence d'IRES dans les ARNm de plusieurs gènes codant pour des protéines ayant une fonction de contrôle a suggéré un rôle pour l'initiation de la traduction dépendante des IRES. Ce mécanisme pourrait avoir pour but

decontrôler finement l'expression de messagers et permettre une réponse rapide à différents stimuli auxquels la cellule est confrontée, et ce dans des conditions dans lesquelles la traduction dépendante de la coiffe est bloquée, en particulier le stress.

Une recherche d'IRES par approche globale a montré qu'environ 3 à 5% des messagers cellulaires sont traduits indépendamment de la coiffe (Johannes *et al* 1999). Cette étude démontre que la majorité d'entre eux présente une région 5'UTR assez particulière. Leur 5'UTR présente une structure tridimensionnelle et ont la propriété de recruter directement le complexe ribosomal. Cette région a été appelée un IRES (Internal Ribosome Entry Site) ou site d'entrée interne du ribosome. La structure des IRESs cellulaires est souvent riche en GC et elle n'est pas conservée entre les IRES, contrairement à ce que l'on observe chez les picornavirus. En comparant les IRES cellulaires à des études de modèles structuraux basées sur des sondes chimiques et enzymatiques, la conclusion est que les IRES cellulaires n'ont pas de structure secondaire conservée, même entre deux gènes relativement proches à l'exemple de c-myc et L-myc (Le Quesne *et al* 2001, Bonnal *et al* 2003, Jopling *et al* 2004). En revanche pour plusieurs ARNm des éléments structuraux des IRES ont été décrits et sont conservés chez les mammifères, notamment pour FGF1 (Martineau *et al* 2004)etFGF2 (Bonnal *et al* 2003).

I-1-2-4-b) Les gènes régulés par le mécanisme IRES-dépendant :

Les états physiologiques et pathologiques cellulaires sont les principaux facteurs modulateurs de l'expression génique. L'IRES est un activateur traductionnel en *cis* présent dans certains ARNm. De plus, son activation n'est pas constitutive mais induite par des signaux intra-et extra-cellulaires. De façon surprenante, les ARNm contenant des IRES codent pour des protéines importantes pour la prolifération, différenciation et dans la régulation de l'apoptose (Holcik*et al* 2005). Parmi eux, des onco-protéines comme c-myc (Nanbru *et al* 1997, Stoneley *et al* 1998) et les VEGF (Stein *et al* 1998, Morfoisse *et al* 2014). De manière plus intéressante, plusieurs gènes angiogéniques impliqués dans les pathologies vasculaires et le cancer possèdent un IRES dans leur ARNm. C'est le cas du facteur de transcription HIF1α, (Lang *et al* 2002) et du facteur sécrété Cyr61 (Johannes *et al* 1999) ainsi que des facteurs de croissance VEGFA, VEGFC, VEGFD, FGF1 et FGF2 (Vagner *et al* 1995, Huez *et al* 1998, Martineau *et al* 2004, Morfoisse *et al* 2014).

Mon projet de thèse se focalise sur les facteurs de croissance des familles FGF et VEGF impliqués dans l'angiogenèse, dont les ARNm contiennent des IRES.

♦ FGF1

FGF1 est un des 23 gènes de la famille des FGF.Le gène du FGF1 possède quatre promoteurs A, B, C et D. Cependant, les quatres ARNm exprimés codent pour une seule isoforme de protéine de 16kDa. Ces promoteurs sont tissus spécifiques : le promoteur A est actif dans le muscle cardiaque et squelettique ainsi que le rein (Myers *et al* 1993, Conte *et al* 2009); le promoteur B fonctionne dans le cerveau (Myers *et al* 1993)et la rétine (Myers *et al* 1995). Quant aux promoteurs C et D, ils sont actifs majoritairement exprimés dans les cellules cancéreuses (prostate, sein, glioblastome) et sous certaines conditions dans les cellules musculaires lisses (Chotani *et al* 1995, Payson *et al* 1998).De plus, le FGF1 est le seul de la famille des FGF à avoir la capacité à lier et activer tous les récepteurs FGFR (FGFR1, FGFR2, FGFR3 et FGFR4) (Zhang *et al* 2006). Toutes ces propriétés lui confèrent une implication dans la régulation de la croissance cellulaire, la différenciation cellulaire, le développement, la myogenèse, la réparation tissulaire etsurtout l'**angiogenèse**.

L'angiogenèse est un mécanisme important dans certaines pathologies comme l'ischémie ou le cancer. *In vitro*, le FGF1 incubéavec des cellules endothéliales induit la formation de vaisseaux (Uriel *et al* 2006) mais il a également un rôle anti-apoptotique (Cuevas *et al* 1997). Plusieurs études ont aussi montré le rôle de FGF1 dans la cardio-protection (Htun *et al* 1998, Buehler *et al* 2002, Palmen *et al* 2004). Il a déjà fait l'objet d'un essai clinique en phase III pour induire la revascularisation de l'ischémie du membre inférieur (Nikol *et al* 2008). Qu'en est-il de sa régulation ?

Au niveau transcriptionnel, en plus des promoteurs tissu-spécifiques, de nombreusesétudes ont montré que la régulation de ces promoteurs passe par des facteurs de transcription. Le transcrit B, issu du promoteur B, est régulé par le facteur de transcription RFX dans les cellules souches de glioblastomes (GBM-SCs) (Hsu *et al* 2010), le transcrit D par Ets2 (Chotani *et al* 2000), les transcrits C et D par TGFβ (Alam *et al* 1996, Chotani *et al* 1997) et le transcrit D par Ras, Rac1 via son motif SRE (Serum Response Element) (Chotani *et al* 2000).

Au niveau traductionnel, mon équipe a montré la présence d'un IRES dans les transcrits A et C (Martineau *et al* 2004). Cela confirme les résultats de plusieurs études sur l'expression du FGF1 au niveau protéique en réponse à des stress. L'expression de FGF1 est fortement induite lorsque la cellule est soumise à différents types de stress comme l'hypoxie (Mouta Carreira *et al* 2001), la privation de sérum (Shin *et al* 1996, Matsunaga *et al* 2006) et le choc thermique (Jackson *et al* 1992, Mouta Carreira *et al* 1998).Mon équipe a donc étudié la régulation de l'IRES présent dans le transcrit A du FGF1. Nous avons montré une augmentation de

l'expression protéique de FGF1 avec l'activation de son IRES durant la différenciation myoblastique et durant la régénération du muscle chez la souris (Conte *et al* 2009). De plus, cette activation est corrélée avec l'activité du promoteur A, suggérant un couplage transcription-traduction lors de la régulation de l'expression de FGF1 (Conte *et al* 2009).

♦ FGF2

FGF2, connu comme un facteur angiogénique majeur, est un facteur de croissance pléiotropique qui possède donc par définition plusieurs fonctions biologiques. Il stimule l'hématopoièse (Allouche *et al* 1995) et joue un rôle important dans la différenciation (McAvoy *et al* 1991). De plus, grâce à sa propriété angiogénique, FGF2 stimule *in vivo* et *in vitro* non seulement la croissance des cellules endothéliales, mais aussi la croissance des cellules musculaires lisses, la réparation tissulaire et la cicatrisation (Basilico *et al* 1992, Schwartz *et al* 1993).FGF2 présente aussi un rôle neutrophique (Mudo *et al* 2009).

Quatre transcrits du FGF2 ont été identifiés, synthétisés à partir d'un seul promoteur, dont les tailles s'étalent entre 1,5kb et 7kb. Ces transcrits se caractérisent par des 3'UTR plus au moins longs résultant de l'utilisation de sites de polyadénylation alternatifs présents au nombre de 7 (Sternfeld *et al* 1988). le transcrit du FGF2 possède des éléments régulateurs dans son 3'UTR situé entre le 1er et le 2nd site de polyadénylation où se trouve des séquences de déstabilisation de l'ARNm (Touriol *et al* 1999), ainsi qu'une séquence activatrice de la traduction en amont du 7ème site de polyadénylation (Touriol *et al* 2000). Quant à la région 5', elle est riche en GC et très structurée, cce qui confère la présence d'éléments régulateurs en *cis* contrôlant l'initiation alternative de la traduction (Prats *et al* 1992). En effet, FGF2 possède 5 codons initiateurs différents : un codon canonique AUG et quatre non-canoniques CUG (Prats *et al* 1989, Arnaud *et al* 1999). Ces différents codons initiateurs engendrent la synthèse de 5 isoformes protéiques de FGF2 chez l'homme : 18, 22, 22.5, 24 et 34kDa. FGF2 a une forte affinité pour les récepteurs FGFR1 et FGFR2. La petite isoforme de 18kDa est issue de la traduction dépendante de la coiffe et localisée dans le cytoplasme, tandis que les grandes isoformes ou HMW (High Mass Weight) de FGF2 sont traduites par le mécanisme alternatif IRES-dépendant et sont majoritairement nucléaires (Renko *et al* 1990, Quarto *et al* 1991). En ce qui concerne leur fonction, la petite forme de 18kDa est impliquée dans la prolifération et la migration cellulaire alors que le FGF2 HMW est impliqué dans la prolifération cellulaire mais pas dans la migration (Quarto *et al* 1991). L'IRES de l'ARNm FGF2 est situé en amont du premier codon CUG (Vagner *et al* 1995). Plusieurs études sur l'activation de l'IRES du FGF2 ont démontré une spécificité tissulaire (Creancier *et al* 2000) mais également une

régulation par différents stress comme l'hyperglycémie (Teshima-Kondo *et al* 2004), le stress oxydatif ou le choc thermique (Vagner *et al* 1996). Le premier facteur régulateur responsable de l'activation de l'IRES du FGF2 est la protéine HNRNPA1 (Bonnal *et al* 2005).

FGF2 joue un rôle crucial dans l'angiogenèse en agissant de façon autocrine en synergie avec le facteur angiogénique VEGFA (Vascular Endothélial Growth Factor A) dans les cellules endothéliales (Seghezzi *et al* 1998). D'autre part, le FGF2 induit la prolifération et la migration des cellules endothéliales en formant de nouveaux vaisseaux (Kroon *et al* 2000, Cross *et al* 2001).

♦ VEGFA

VEFGA a un pouvoir mitogène stimulateur de la prolifération des cellules endothéliales via l'activation de VEGFR2 (Meadows *et al* 2001, Zachary *et al* 2001). Cependant, VEGFA se lie à trois récepteurs : VEGFR1 et VEGFR2 en homo- ou hétérodimère, ainsi qu'à VEGFR3 hétérodimérisé à VEGFR2. Il se lie également aux co-récepteurs neuropilines présents sur la surface des cellules endothéliales vasculaires pour induire la transduction du signal. VEGFR2 est le principal récepteur impliqué dans l'activation de l'angiogenèse. Outre ses fonctions dans l'angiogenèse, VEGFA est également un facteur lymphangiogénique (Nagy *et al* 2002, Gerhardt *et al* 2005, Wuest *et al* 2010, Dellinger *et al* 2013). Les voies de signalisation impliquées sont les PI3K et ERK1/2 stimulant la migration et la prolifération des cellules endothéliales lymphatiques (Dellinger *et al* 2011). De plus l'activation de VEGFA sur l'hétérodimérisation VEGFR2/VEGFR3 permet l'activation des voies de signalisation impliquées dans la lymphangiogenèse. Cursiefen et ses collègues ont aussi montré que VEGFA induit indirectement la lymphangiogenèse via le récepteur VEGFR1 en activant la synthèse les facteurs lymphangiogéniques VEGFC et VEGFD par les macrophages (Cursiefen *et al* 2004).

En raison de multiples épissages alternatifs, VEGFA présente neuf isoformes : $VEGF_{111}$, $VEGFA_{121}$, $VEGFA_{145}$, $VEGFA_{148}$, $VEGFA_{162}$, $VEGFA_{165}$, $VEGFA_{183}$, $VEGFA_{189}$ et $VEGFA_{206}$ (Arcondeguy *et al* 2013). L'expression de VEGFA est extrêmement contrôlée pour répondre précisément à un stimulus extracellulaire. La régulation de l'expression de VEGFA est importante au vu de son rôle sur le plan physiologique et pathologique. Son expression est régulée à différents niveaux. La plus connue est l'activation de sa transcription par le facteur de transcriptions HIF (Germain *et al* 2010) dans certains états physiologiques comme la cicatrisation, le développement embryonnaire mais également dans certaines pathologies comme le cancer. En effet, la région promotrice de VEGFA contient une séquence HRE (Hypoxia response element) (Forsythe *et al* 1996). Par

ailleurs, la transcription de VEGFA est également induite par d'autres facteurs comme SP1 (Milanini *et al* 1998), STAT3 et AP1 (Minet *et al* 2001) ; (Gerald *et al* 2004). En réponse à l'hypoxie, l'ARNm de VEGFA est stabilisé par la protéine HuR qui se fixe sur sa région 3'UTR (Levy *et al* 1998).

Du côté de la régulation traductionnelle, la région 5' non traduite de VEGFA est longue et très structurée et possède deux IRES (Huez *et al* 1998). Des études *in vivo* révèlent l'activité des IRES A et B du VEGFA dans le muscle en condition d'ischémie (Bornes *et al* 2007). Il existe des régulateurs négatifs inhibant l'activation des deux IRES en présence d'oxygène : le miR-16 (Karaa *et al* 2009, Dejean *et al* 2011) et l'hélicase DEAD-box (Casanova *et al* 2012).

♦ VEGFC

VEGFC est un facteur lymphangiogénique majeur et tient un rôle dans la survie et la migration des cellules endothéliales lymphatiques (Karkkainen *et al* 2004) (Ferrara *et al* 1997). La liaison de VEGFC à son récepteur VEGFR3, active plusieurs voies de signalisation indispensables aux cellules endothéliales lymphatiques : la voie Ras/GTP en activant la voie MAPK/ERK est essentielle à la prolifération (Ichise *et al* 2010) ; la voie PI3K/Akt active mTOR pour la survie et la migration (Makinen *et al* 2001). En effet, il est bien connu que dans les tumeurs solides, l'activation de VEGFC/VEGFR3 stimule la mobilité des cellules cancéreuses vers la métastase et en induisant la lymphangiogenèse (Karpanen *et al* 2001, Skobe *et al* 2001).VEGFC est exprimé non seulement par les cellules endothéliales mais aussi par les cellules cancéreuses (Su *et al* 2007).

La transcription de l'ARNm du VEGFC est contrôlée par des facteurs transcriptionnels en fonction du stress, en se fixant sur des sites spécifiques sur la région promotrice de VEGFC: NF-κB lors de l'inflammation (Du *et al* 2014), C/EBP-δ (CCAAT/enhancer-binding protein-δ) dans le cancer du poumon (Min *et al* 2011) et LEDGF/p75 (lens epithelium-derived growth factor) en réponse au stress thermique et oxydatif (Cohen *et al* 2009). Cependant le promoteur du VEGFC ne possède pas de site HRE reconnu par HIF (Morfoisse *et al* 2014).

Récemment, une étude de la régulation de VEGFC en hypoxie a démontré la présence d'un IRES sur la région 5' non traduite de son ARNm. Ces résultats montrent l'activation de la traduction de VEGFC par le mécanisme IRES-dépendant dans plusieurs lignées tumorales *in vitro* et *in vivo* (Morfoisse *et al* 2014).

♦ VEGFD

VEGFD est aussi appelé FIGF (c-fos induced growth factor). Comme VEGFC, c'est un facteur lymphangiogénique majeur et il se lie au récepteur VEGFR3. La fixation de VEGFD sur son récepteur VEGFR3 induit les mêmes voies de signalisation que VEGFC à savoir MAPK/ERK et PI3K/Akt. L'administration de VEGFD à des animaux déficients du réseau lymphatique permet de rétablir la lymphangiogenèse (Haiko *et al* 2008).

En terme de régulation, la région promotrice du gène VEGFD contient un site de liaison au facteur de transcription AP-1 permettant sa transcription (Debinski*et al* 2001). Des études sur le cancer ont montré la régulation de son expression au niveau transcriptionnel par STAT3, HNF-4α et COUP-TF1/2 (Schafer *et al* 2008, Deng *et al* 2014). La régulation de la traduction de VEGFD est régulée par l'interleukine7 dans le cancer du poumon (Ming *et al* 2009). La régulation traductionnelle de VEGFD par le mécanisme IRES-dépendant fait partie de mon projet de thèse et sera abordé dans la partie résultats.

I-1-2-4-c) Les facteurs régulateurs de l'activité des IRES : les ITAF

L'activation des IRES est induite sous certaines conditions en réponse à des stimuli environnementaux de la cellule. Mis à part certains facteurs d'initiation, les IRES sont activés par des facteurs spécifiques. Une étude sur les IRES viraux de type II montre la nécessité d'un ajout d'extrait cellulaire pour initier la traduction via les IRES (Belsham *et al* 1996). Il en découle que la traduction IRES dépendante peut être stimulée par des facteurs en *trans* appelés ITAF (IRES-trans-acting factors), qui sont essentiellement des protéines cellulaires.

Le mécanisme des ITAF sur l'activation de l'IRES n'est pas encore complètement élucidé. Le principal mécanisme décrit indique que lesITAF agissent comme des chaperonnes de l'ARN en modifiant et stabilisant la conformation de l'IRES pour faciliter le recrutement de la sous unité 40S du ribosome (Stoneley *et al* 2004). La majorité des ITAF découverts à ce jour possède des domaines de liaison à l'ARN (RBD : RNA-Binding Domain), comme les hnRNP (hnRNPI surtout connu sous le nom de PTB (pyrimidine tract binding protein) pour les IRES de EMCV (Pestova *et al* 1996), de Apaf-1 (Mitchell *et al* 2001), de IGF1-R (Giraud *et al* 2001) et deP53 (Ray *et al* 2006) ; hnRNPA1 pour les IRES de c-myc (Evans *et al* 2003) et de FGF2 (Bonnal *et al* 2005) ou $p54^{nrb}$/NONO pour l'IRES de c-myc (Cobbold *et al* 2008). Ce rôle de chaperonne à ARN des ITAF a déjà été démontré

par quelques études. En 2003, l'équipe de Anne Willis a montré que l'IRES de Apaf-1 nécessite la fixation de Unr pour ouvrir la structure secondaire et permettre la fixation de deux molécules de PTB (Mitchell *et al* 2003). Ces molécules de PTB vont à leur tour défaire la structure secondaire pour que la sous-unité 40S du ribosome puisse s'y fixer. Il en est de même pour l'IRES de Bag-1, qui a besoin de deux ITAF, PCBP1 (poly (rC)-binding protein1) et PTB (polypyrimidine-tract-binding protein). PCBP1 va se fixer sur le domaine II de l'IRES et ouvre la structure secondaire du domaine III pour que la PTB s'y fixe. La PTB à son tour modifie la structure de l'IRES pour rendre accessible la fixation du ribosome (Pickering *et al* 2004) (**Figure 8**).

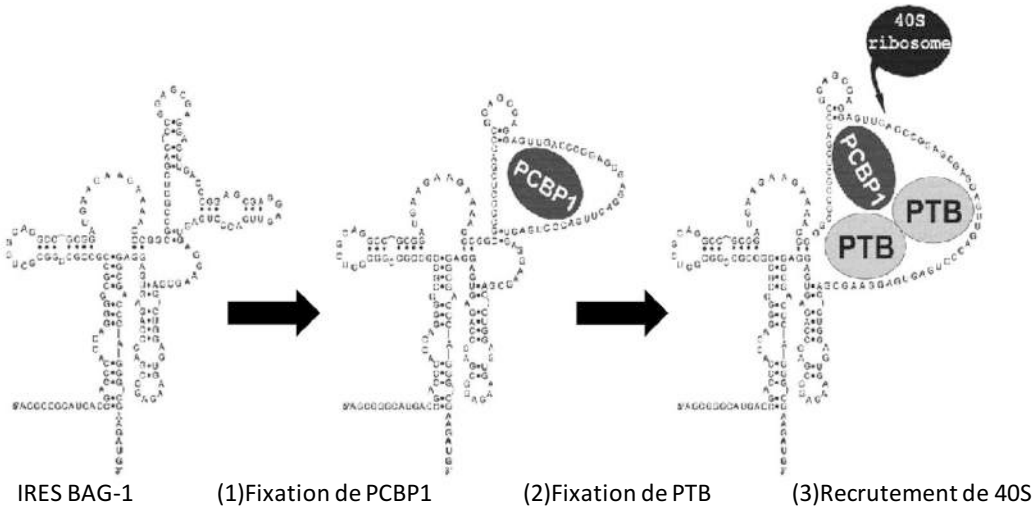

Figure 8 : Activation de l'IRES Bag-1 par les ITAF PCBP1 et PTB. PCBP1 se fixe sur le domaine II de l'IRES BAG-1 rendant accessible le domaine III pour la fixation des deux PTB. Ces derniers jouent à leur tour leur rôle de chaperonnes pour donner l'accès à la sous unité ribosomale 40S. Modifié d'après (Pickering *et al* 2004, King *et al* 2010).

L'activité des IRES est très variable en fonction du type cellulaire suggérant que la concentration des ITAFs est donc différente selon le type cellulaire (Ye *et al* 1997, Stoneley *et al* 2000).

La disponibilité et la spécificité des ITAF constituent des paramètres importants pour répondre finement aux stimuli via la traduction dépendante des IRES. Le principal stress cellulaire au coursduquel des ITAF ont été identifiés est l'apoptose (Holcik *et al* 2005). Pour les autres stress comme l'hypoxie et le choc thermique, aucune étude n'a identifié d'ITAF outre mon travail de thèse qui sera présenté ci-après.

II-La régulation de l'expression génique par le stress et le microenvironnement

A chaque étape de sa vie, durant la croissance, la différenciation ou en réponse à un stimulus, la cellule doit réguler de façon précise l'expression génique. Les états physiologiques et pathologiques sont les principaux facteurs de la régulation de l'expression génique. Pour répondre efficacement et rapidement au microenvironnement, la cellule met en place plusieurs mécanismes de contrôle. Ces régulations s'opèrent à toutes les étapes de l'expression génique, dès la conformation de la chromatine jusqu'au produit final, la protéine. Plus concrètement, ces facteurs environnementaux peuvent agir à plusieurs niveaux : la transcription, la maturation de l'ARNm, la traduction, et après la traduction par des modifications post-traductionnelles (**Figure 9**).

En terme d'énergie, la traduction consomme 90% de l'énergie cellulaire tandis que la transcription en consomme moins de 10% (Buttgereit *et al* 1995, Schwanhausser *et al* 2011). En réponse au stress environnemental, la cellule induit la transcription de certains gènes et bloque la traduction globale dépendante de la coiffe (**Figure 9**).

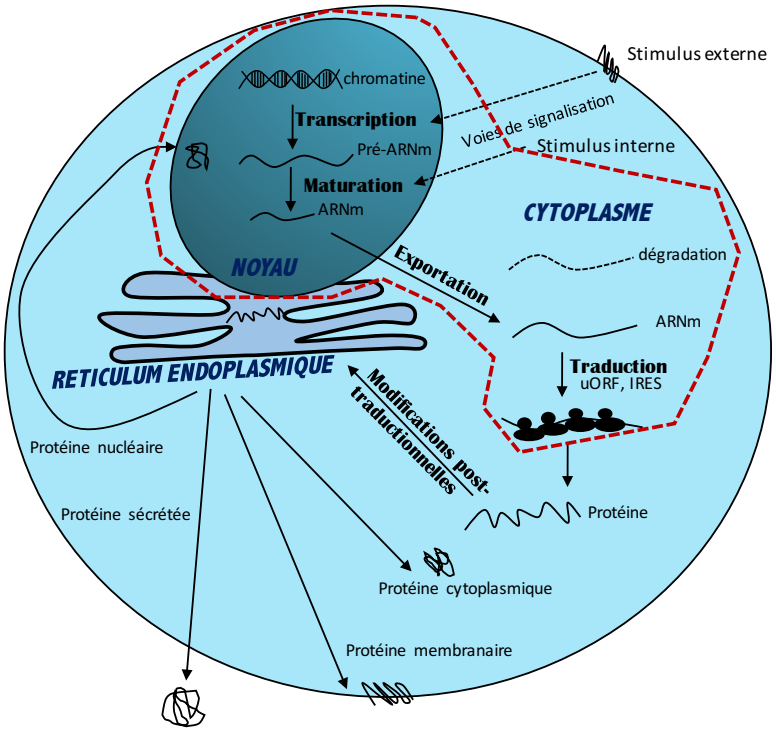

Figure 9 : Les principales étapes de la régulation de l'expression génique en réponse à des stimuli externes et internes. Les tirets (----) indiquent les étapes de régulation transcriptionnelle ou post-transcriptionnelle au niveau de l'ARNm.

II-1- La réponse transcriptionnelle au stress

La régulation de la transcription par le stress a pour résultat d'induire ou de réprimer des gènes spécifiques. Une cascade de signalisation va se mettre en place pour induire l'expression des gènes spécifiques afin de répondre finement au stress. Plusieurs stress peuvent intervenir dans une pathologie comme dans le cas de l'ischémie, où les cellules non irriguées sont en hypoxie mais sont également soumises au stress du réticulum endoplasmique aussi connu sous le nom de réponse UPR (unfolded protein response). Dans d'autres situations comme lors de l'inflammation, le stress peut être un choc thermique. L'hypoxie et le choc thermique seront détaillés ci-dessous étant donné qu'ils ont fait l'objet de mon travail de thèse.

II-1-1- *Hypoxie*

L'hypoxie est caractérisée par le manque d'oxygène au sein de la cellule. Elle peut être physiologique comme par exemple durant l'embryogenèse (Yin *et al* 2002) mais également pathologique comme dans les ischémies et les cancers (Brahimi-Horn *et al* 2007, Brahimi-Horn *et al* 2007, Martinez-Sanchez *et al* 2007). L'hypoxie cellulaire va induire la mort des cellules ou la survie des cellules plus résistantes. Dans les deux cas il y a induction de gènes spécifiques (exemple : gènes angiogéniques en vue de générer une reperfusion du tissu ischémique et permettre la survie cellulaire).

Le principal acteur moléculaire connu en réponse à l'hypoxie est le facteur de transcription HIF (hypoxia inducible factor). La découverte de HIF en 1992 a fait l'objet de plusieurs études. Ces études ont mis en évidence l'implication de HIF dans différentes situations physiopathologiques de la cellule. Ainsi elles ont montré que le facteur HIF régule une multitude de gènes impliqués dans l'**angiogenèse** (Ferrara 2005), la **survie** ou la **mort cellulaire** (Brahimi-Horn *et al* 2005, Gordan *et al* 2007), le **métabolisme** (Masson *et al* 2014), la régulation du pH (Shimoda *et al* 2006)et dans les **métastases** (Chan *et al* 2007, Sullivan *et al* 2007).

Du point de vue mécanistique, les facteurs HIF correspondent à un hétérodimère composé de deux sous-unités : l'une extrêmement labile HIF1α, HIF2α ou HIF3α et l'autre extrêmement stable HIF1β (ou ARNT1 : aryl hydrocarbon receptor nuclear translocator). L'expression de la sous-unité HIF1α est régulée à différents niveaux (transcription, stabilité de l'ARN, traduction), mais cette régulation est surtout post-traductionnelle car la protéine est dégradée en

présence d'oxygène et stabilisée en hypoxie. En revanche, la sous-unité HIF1β est exprimée constitutivement dans la cellule (Jewell *et al* 2001). Un domaine ODDD (oxygen dependent degradation domain) est présent dans la sous-unité HIF1α, la rendant sensible à la présence d'oxygène. En normoxie (présence d'oxygène), les prolines 402 et 564 du domaine ODDD de HIF1α sont hydroxylées par les protéines PHD 1-3 (Prolyl hydroxylase domain protein). Ces hydroxylations vont recruter la protéine Pvhl (Von Hippel Lindau) et conduire à la dégradation de HIF1α par le protéasome 26S (Salceda *et al* 1997). Ainsi en hypoxie, l'absence d'oxygène va inhiber l'hydroxylation de HIF1α par PHD, empêchant sa dégradation. Il est à noter que la protéine HIF1α possède une séquence NLS (Nuclear Localization Signal). Une fois HIF1α stabilisée, elle sera transportée dans le noyau pour se lier à la sous-unité HIF1β (protéine nucléaire), ce qui va rendre actif le facteur de transcription HIF et induire l'initiation de la transcription des gènes possédant un motif HRE (hypoxia response element) dans leur région promotrice (Pollenz *et al* 1994, Eguchi *et al* 1997) (**Figure 10**).

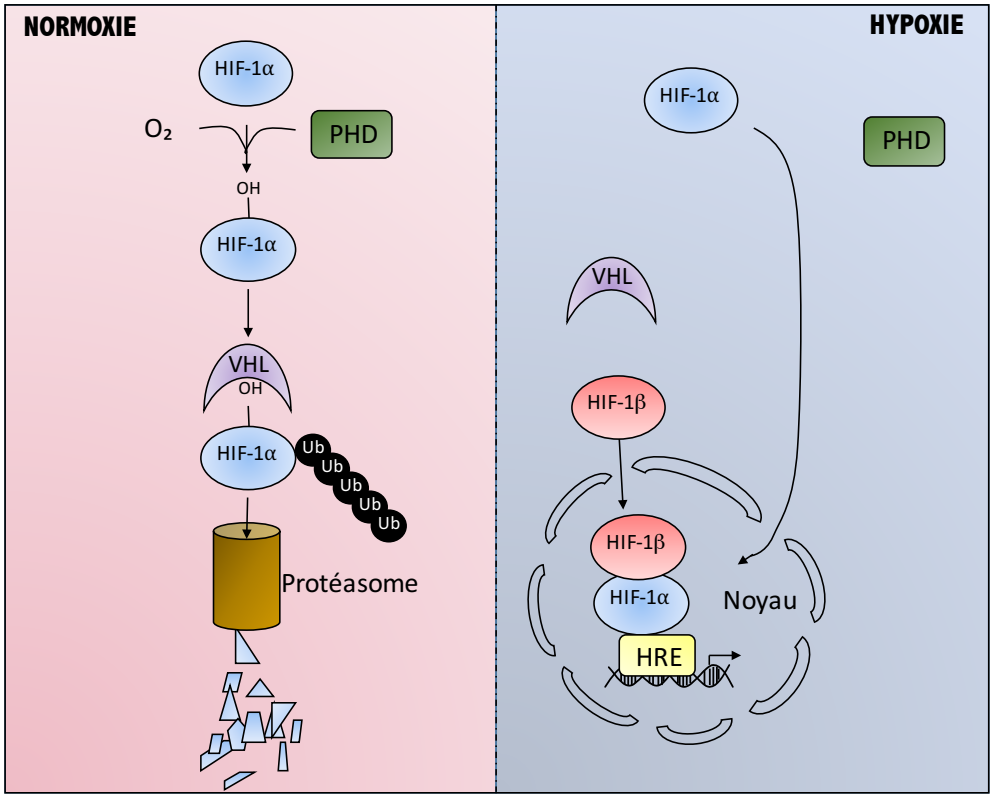

Figure 10 : Schéma de la régulation de HIF par la concentration en oxygène. La présence d'oxygène va hydroxyler HIF1α et recruter la protéine VHL pour aboutir à la dégradation de HIF1α par le protéasome. En hypoxie, HIF1α échappe à la dégradation et entre dans le noyaupour s'hétérodimériser avec HIF1βpour former le facteur HIF1 qui se fixera sur la séquence HRE des gènes sensibles à l'hypoxie et induira leur transcription.

Au départ le facteur de transcription HIF1 a été décrit comme régulateur de l'expression des gènes EPO en hypoxie (Semenza *et al* 1991) mais son expression dans tous les types cellulaires a suscité des études sur la région promotrice des gènes connus pour être sensibles à l'hypoxie. Parmi eux, le facteur de croissance VEGFA qui présente un site fonctionnel HRE dans son promoteur et dont l'expression induit l'angiogenèse au cours de processus physiologiques ou physiopathologiques. HIF a un rôle clé dans l'induction transcriptionnelle des gènes angiogéniques: en plus du VEGFA il induit notamment les gènes PAI-1 (plasminogen activator inhibitor1), VEGFR1, TGFβ (transforming growth factor β), IGF2 (Insulin-like growth factor2), NOS2 (nitric oxyde synthase 2) et angiopoietine-2 (Ferrara *et al* 2005).

La sous-unité HIF1α est la plus connue et la plus étudiée, cependant la sous-unité HIF2α régule également l'expression de certains gènes comme l'angiopoïetine-1 (Park *et al* 2016).

II-1-2 *Stress du réticulum endoplasmique*

Le stress du réticulum endoplasmique a un rôle physiologique dans l'adaptation des cellules à des changements environnementaux. Il a également un rôle physiopathologique dans de nombreuses maladies comme le diabète, l'athérosclérose, l'ischémie cardiaque, les maladies neurodégénératives et le cancer. L'origine du stress du réticulum endoplasmique provient d'une accumulation de protéines de conformation incorrecte. Face à ce stress, la cellule s'adapte en activant les voies de signalisation UPR. Elle a été caractérisée dans les années 1990 chez la levure *Saccharomyces cerevisae*. L'UPR permet la restauration de la fonction du réticulum endoplasmique ainsi que l'homéostasie cellulaire. Il existe trois voies de signalisation impliquant trois protéines transmembranaires : IRE1α (Inositol Requiring Enzyme 1α), la protéine kinase PERK (Protein kinase RNA (PKR)-like Endoplasmic Reticulum Kinase) et le facteur de transcription ATF6 (Activated Transcription Factor 6). En condition normale, les trois récepteurs sont liés à la protéine chaperonne BiP. Lors d'un stress BiP se dissocie pour se lier aux protéines mal conformées, ce qui entraine la libération et l'activation des récepteurs transmembranaires qui vont à leur tour activer des régulations transcriptionnelles et traductionnelles (Pour revue, (Zhang *et al* 2004)). Cette régulation agit à plusieurs niveaux : (i) elle active la transcription des gènes essentiels au bon repliement des protéines, sous le contrôle des facteurs de transcription ATF6 et XBP-1 (Okada *et*

al 2002, Lee *et al* 2003) (ii) l'expression de XBP-1 est elle-même activée par un processus d'épissage suite au déclenchement de l'activité endoribonucléasique de IRE1 (pour revue, (Barouki 2002)) (iii) elle bloque la traduction globale, sous le contrôle de PERK qui phosphoryle eIF2α (Lu *et al* 2004) (iv) elle active l'expression desprotéines de dégradation du système ERAD (Endoplasmic-reticulum-associated protein degradation) (Werner *et al* 1996) (v) elle induit l'activation des gènes apoptotiques quand le stress est plus intense (Nakagawa *et al* 2000).

II-1-3 *Choc thermique :*

Le choc thermique peut survenir au cours de certains états physiopathologiques (cancer ou infection). La réponse au choc thermique a été décrite par Ritossa en 1962. Quelques années après, cette réponse a été corrélée à l'expression d'un petit nombre de nouvelles protéines, les HSP (heat shock proteins). Les HSPs sont des protéines chaperonnes. Elles ont été initialement purifiées chez la drosophile (Tissieres *et al* 1974), mais leur conservation a été confirmée dans tous les organismes allant de la bactérie jusqu'à l'homme. Chez les mammifères, six familles ont été identifiées : HSP110, HSP90, HSP70, HSP60, HSP40 et les petites HSP (HSP25 et HSP30) (les nombres correspondent à leur taille en kDa). La majorité des HSP sont exprimées de manière constitutive pour maintenir l'homéostasie cellulaire (Tanguay *et al* 1993, Wickner *et al* 1999). La famille des HSP70 (HSP70 et HSP72) est induite en réponse au choc thermique, ce qui fait d'elle le « marqueur de la réponse au choc thermique ». L'induction des HSP70 se fait au niveau transcriptionnel grâce au facteur HSF (heat shock factor) qui reconnaît le motif HSE (heat shock element) dans la région promotrice des gènes HSP70 (Wu 1995). Le gène hsp70 ne possédant pas d'intron permet une transcription et une synthèse rapide de la protéine en réponse au stress intracellulaire (Yost *et al* 1986, Forsdyke 1994). L'expression des HSP est également induite en réponse à d'autres stress physiques ou chimiques à l'exemple d'une infection virale et en présence d'éthanol.

Le stress thermique est rencontré dans différentes pathologies comme dans les maladies vasculaires ou le cancer, en particulier suite à l'inflammation (Sevin *et al* 2015). Il se manifeste par la dilatation des vaisseaux. Par exemple dans le contexte inflammatoire tumoral, les vaisseaux lymphatiques sont dilatés (**Figure 11**).

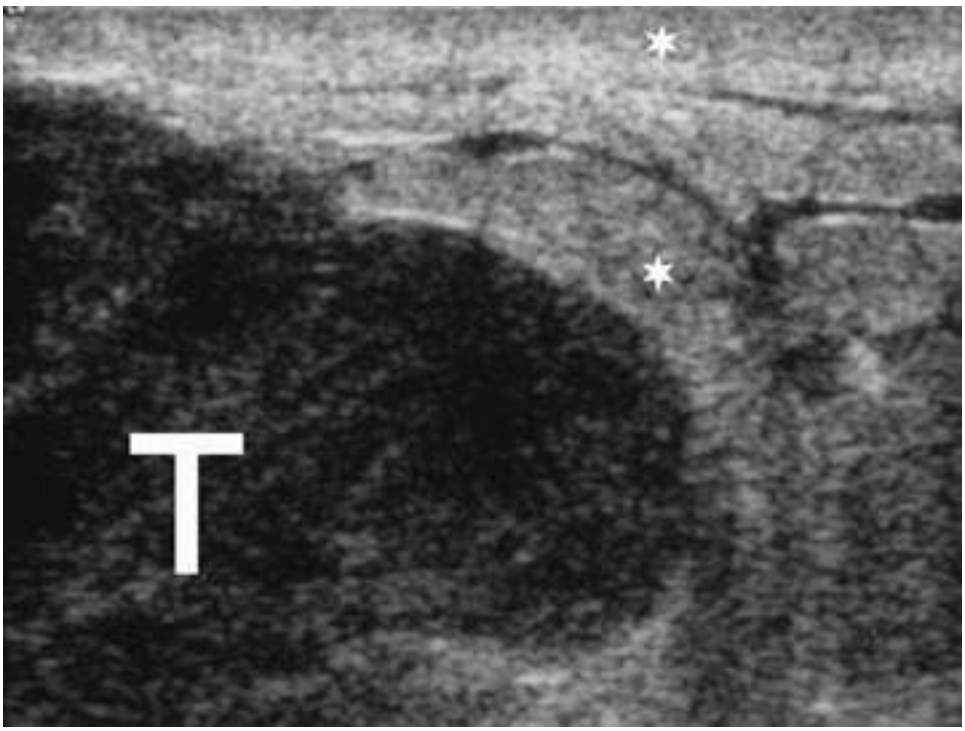

Figure 11 : Tumeur mammaire durant une inflammation

Biopsie avec de multiples emboles lymphatiques. Observation d'une dilatation des voies lymphatiques en contact de la tumeur. Les étoiles représentent le derme et l'hypoderme présentant un important œdème

Source http://www.em-consulte.com/en/article/121291#JR-05-2002-83-5-0221-0363-101019-ART3-FIG17

II-2- La régulation de la traduction lors du stress

Pour s'adapter et survivre à des conditions de stress, les cellules mettent en place différentes stratégies. Comme je l'ai mentionné précédemment, elles modulent l'expression des gènes à plusieurs niveaux. La traduction est un processus complexe et énergivore, or la cellule doit économiser de l'énergie et répondre rapidement et efficacement au stress. Pour cela, la cellule bloque la traduction canonique dépendante de la coiffe.

II-2-1 *L'inhibition de la traduction dépendante de la coiffe :*

L'inhibition de la traduction dépendante de la coiffe s'opère essentiellement à l'étape de l'initiation. Les deux cibles principales de ce blocage sont les facteurs d'initiation eIF4E et eIF2α.

eIF4E:

a) Hypo- (ou dé-)phosphorylation d'eIF4E

Le facteur eIF4E est le facteur qui reconnait la coiffe pour initier la traduction. EIF4E est phosphorylé par des kinases. Sa phosphorylation se fait sur la Sérine 209 par la kinase C *in vivo* ou par la kinase effectrice MNK1 (Flynn *et al* 1996, Sonenberg 1996, Morley 1997) résultant de l'activation de la voie MAPK. La partie C-terminale d'eIF4G se lie à MNK1 pour phosphoryler eIF4E (Pyronnet *et al* 1999). Cette phosphorylation favorise l'interaction avec le complexe de pré-initiation 43S et correspond à une augmentation de la traduction dépendante de la coiffe, en particulier des ARNm dont les régions 5'UTR sont structurées et inhibitrices de la traduction du fait qu'elles sont dépendantes d'eIF4E (Pelletier *et al* 1987, Joshi-Barve *et al* 1990, Koromilas *et al* 1992). Elle est corrélée à une augmentation de la traduction des proto-oncogènes (Furic *et al* 2010).

Chez les souris *nude,* la surexpression d'eIF4E induit la formation de tumeurs (Sonenberg *et al* 1998). De même, dans les lignées cellulaires transformées obtenues à partir des tumeurs, eIF4E est fortement exprimé (Miyagi *et al* 1995).

La traduction est augmentée avec la phosphorylation d'eIF4E durant la maturation des ovocytes de xénope (Morley *et al* 1995), d'étoile de mer (Xu *et al* 1993) et de souris (Gavin *et al* 1997).

Cependant, en fonction du stress eIF4E peut être phosphorylé ou déphosphorylé. Durant une infection bactérienne le lipopolysaccharide (LPS) induit une phosphorylation d'eIF4G alors que le choc thermique peut le déphosphoryler. La phosphorylation d'eIF4E en condition de stress n'est pas encore très bien établie (Pour revue, (Sonenberg *et al* 1998)).

b) Séquestration d'eIF4E par 4E-BP :

En condition normale, le facteur eIF4E se lie au facteur eIF4G pour former le complexe eIF4F. En conditions de stress, eIF4E est séquestré par la protéine 4E-BP (eIF4E-binding protein) empêchant ainsi la formation du complexe eIF4F, ce

qui aboutit à l'inhibition de la traduction. Plus précisément, l'état de phosphorylation de 4E-BP en est l'origine car il détermine son interaction avec eIF4E. 4E-BP présente quatre sites de phosphorylation très conservés (Ser65, Thr37, Thr46 et Thr70). En l'absence de stress, la phosphorylation de 4E-BP sur ces sites libère le facteur eIF4E, permettant l'assemblage du complexe eIF4F et donc l'initiation de la traduction (Bah *et al* 2015). Cette phosphorylation résulte de l'activité de la voie mTOR (mammalian ou mechanistic Target Of Rapamycin) (Brunn *et al* 1997). En revanche, dans des conditions de stress, 4E-BP est hypophosphorylé et se lie à eIF4E, ce qui inhibe l'initiation de la traduction coiffe-dépendante (**Figure 12**).

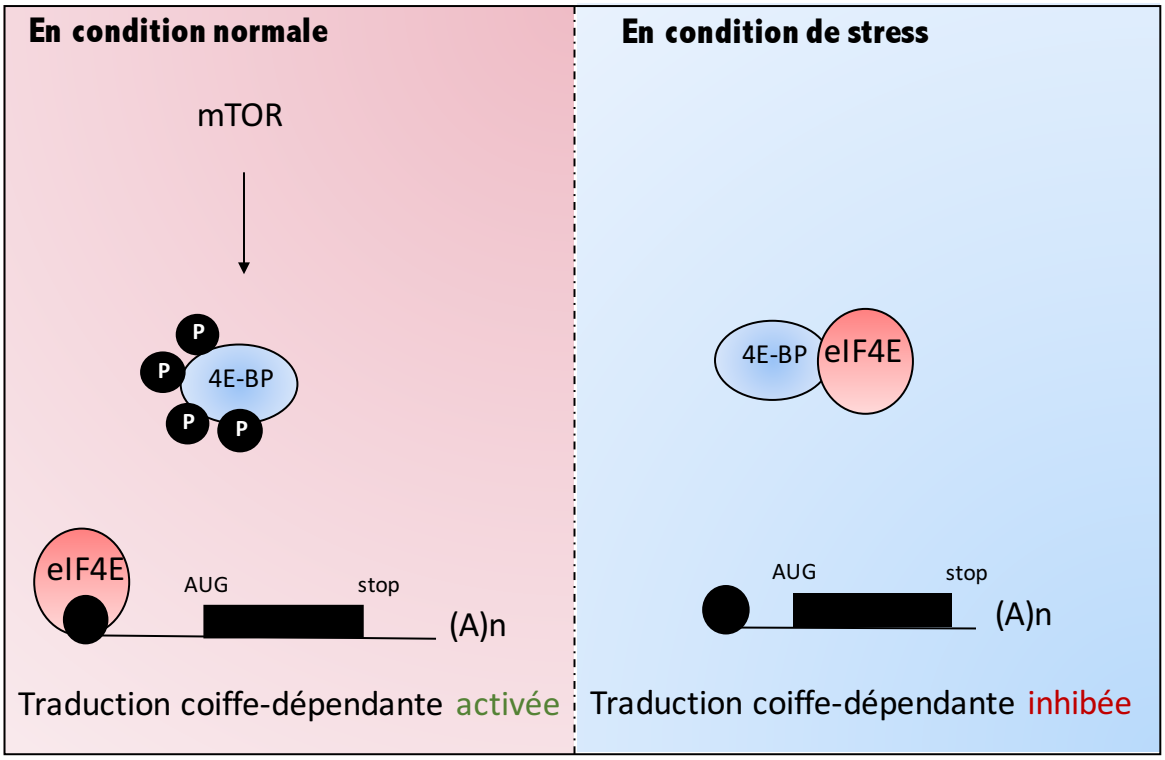

Figure 12 : Mécanisme de régulation de la traduction par 4E-BP. En condition normale, 4E-BP est hyperphosphorylé par mTOR, libérant eIF4E pour initier la traduction. Lors d'un stress, 4E-BP est hypophosphorylé et séquestre eIF4E, inhibant la traduction.

Chez les mammifères, il existe trois isoformes de 4E-BP (4E-BP1, 4E-BP2, 4E-BP3) qui sont toutes capables de lier eIF4E mais qui sont tissu-spécifiques (Joshi *et al* 2004). L'expression de 4E-BP1 est plus forte dans le muscle squelettique, le tissu adipeux et le pancréas (Hu *et al* 1994, Tsukiyama-Kohara *et al* 1996). 4E-BP2 est exprimé dans les cellules cérébrales et 4E-BP3 dans les cellules coliques et cardiaques (Poulin *et al* 1998, Tsukiyama-Kohara *et al* 2001).

eIF2α :

EIF2 est nécessaire à la formation du complexe ternaire pour initier la traduction. Ce facteur est composé de trois sous-unités : α, β et ϒ. La sous-unité eIF2α présente un site de phosphorylation sur la sérine (Ser 51). Le facteur eIF2β est capable de se lier à l'ARNm et eIF2ϒ possède deux sites de liaison : GTP et Met- $ARNt_i^{Met}$. Les sous-unités eIF2β et eIF2ϒ interagissent avec le facteur d'échange de guanine eIF2B et le facteur activateur de GTPase eIF5. Lors d'un stress, eIF2α est phosphorylé et empêche l'activité d'eIF2B en le séquestrant (Rowlands *et al* 1988, Dholakia *et al* 1989, Kimball *et al* 1998). Ainsi, l'échange d'eIF2-GDP en eIF2-GTP n'est pas établi, ce qui empêche la formation du complexe ternaire et inhibe l'initiation de la traduction (Merrick 1992) (**Figure 13**).

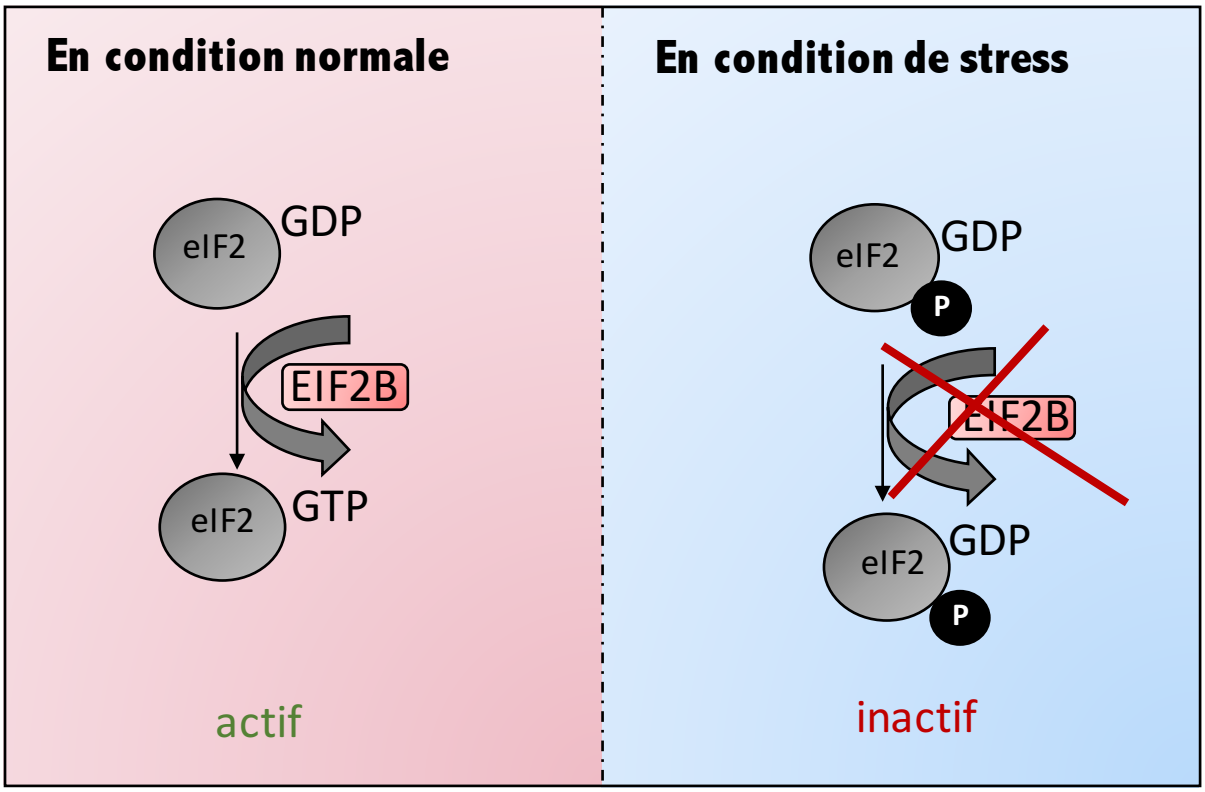

Figure 13 : Régulation de l'initiation de la traduction par phosphorylation d'eIF2α. En condition normale, eIF2B hydrolyse le GDP en GTP chargé sur eIF2 pour activer l'initiation de la traduction. En condition de stress eIF2 est phosphorylé empêchant l'action de eIF2B, la traduction est inhibée.

Quatre protéines kinases sont responsables de la phosphorylation d'eIF2α:

- HR1 (Hemin Regulated Inhibitor Kinase) en réponse à une carence en hème dans les réticulocytes (M. J. Clemens 1996)
- GCN2 (General Control Nonderepressible 2) en réponse à une carence en acide aminé induisant la présence d'ARNt non chargé (Sood *et al* 2000).

- PKR (Protein Kinase Regulated) en réponse à la présence d'ARN double brin (M. J. Clemens 1996).
- PERK (PKR-like Endoplasmic Reticulum Kinase) en réponse au stress du réticulum endoplasmique.

II-2-2 *Les stress et stimuli capables d'activer la traduction IRES-dépendante :*

La présence d'une structure IRES peut permettre l'initiation de la traduction en réponse à un stress car l'IRES rend la traduction indépendante d'eIF4E. Il existe de nombreux stress ou stimuli physiopathologiques pouvant activer la traduction IRES-dépendante.

Les IRES lors de l'hypoxie :

Il a été montré que le stress hypoxique active les IRES des facteurs FGF2 (Conte *et al* 2008), VEGFA (Bornes *et al* 2004), (Philippe *et al* 2016), PDGF (Sella *et al* 1999) et VEGFC (Morfoisse *et al* 2014). L'IRES du facteur régulateur post-transcriptionnel Staufen1 (Stau1) est également activé en hypoxie (Bonnet-Magnaval *et al* 2016). Je parlerai davantage de cette régulation dans le contexte pathologique dans la partie III.

Dans le cas du cancer, l'initiation de la traduction de ces gènes angiogéniques est en faveur de la tumeur. Cette induction traductionnelle favorise la progression tumorale et la dissémination métastatique. Dans le cas de l'ischémie, cela permettra une revascularisation en vue de la survie des cellules.

Il est à noter que dans au moins deux cas, ceux du FGF2 et du VEGFC, l'induction se fait de manière HIF-indépendante, ce qui suggère que la voie dépendante des IRES est un mécanisme d'induction par l'hypoxie qui se distingue de la voie HIF.

Les IRES lors du stress du réticulum endoplasmique :

Quelques études ont mis en évidence l'activation de certains IRES en réponse à ce stress, notamment ceux de Stau1 (Bonnet-Magnaval *et al* 2016) de c-

myc dans les cellules de myélome (Shi *et al* 2016)et de certains facteurs angiogéniques (Philippe *et al* 2016). Comme décrit précédemment, le stress du réticulum endoplasmique soutenu peut déclencher l'apoptose. Des études ont montré l'expression protéique de certains ARNm liés à l'apoptose dépend du mécanisme lié à l'IRES tels que XIAP (X-linked inhibitor of apoptosis protein) (Holcik *et al* 1999) et Apaf-1 (Coldwell *et al* 2000).

Les IRES lors du choc thermique :

Le choc thermique induit le blocage de la traduction classique par plusieurs stratégies décrites précédemment, permettant la traduction spécifique de certains ARNm contenant un IRES. Lors du choc thermique, quand la traduction cap-dépendante est bloquée, la traduction de BAG-1 est maintenue grâce à l'activité de son IRES (Coldwell *et al* 2001). Dans les cellules cancéreuses soumises au choc thermique, l'expression de BiP est induite non seulement au niveau de la transcription mais également de la traduction. Grâce au vecteur bicistronique, il a été mis en évidence l'activation de l'IRES BiP en réponse à un choc thermique soutenu (15h) (Kim *et al* 2002).

Déprivation en nutriment ou carence en acide aminé :

Contrairement aux autres molécules, le stockage d'acides aminés n'existe pas dans la cellule. L'homéostasie cellulaire se fait par un équilibre entre les acides aminés entrants et sortants. De ce fait les transporteurs sont les principaux gènes régulés face à une carence en acide aminé. A titre d'exemple, le gène cat-1 (cationic amino acid transporter) codant pour un transporteur Arg/Lys essentiel à la survie des cellules en réponse à une carence en nutriment, est régulépar un IRES ainsi que par un uORF (Fernandez *et al* 2005). Un autre transporteur responsable de l'activité du système de transport A comme cat-1, SNAT2 : la quantité de son ARNm est augmentée ainsi que celle de sa protéine. Il a été démontré que la traduction de l'ARNm SNAT2 en réponse à une carence en acide aminé passe par le mécanisme IRES-dépendant (Gaccioli *et al* 2006).

Activation des IRES en réponse à des stimuli physiologiques :

Certains états physiologiques des cellules nécessitent une modification de l'expression génique notamment la différenciation cellulaire. En 1996, Bernstein et

ses collègues ont montré l'activation de l'IRES de l'ARNm du PDGF lors de la différenciation des mégakaryocytes (Bernstein *et al* 1997). Une étude sur la spermatogenèse a démontré l'activation de l'IRES de FGF2 par la testostérone (Gonzalez-Herrera *et al* 2006).

L'activité de l'IRES du FGF2 s'est avérée être extrêmement forte dans les neurones. Notamment, elle est fortement activée lors de la formation du réseau synaptique (Audigier *et al* 2008).

Des résultats de l'équipe montrent aussi que la traduction IRES-dépendante permet d'induire le FGF1 lors de la différenciation myogénique. L'IRES du FGF1 est activé de manière couplée avec celle de son promoteur, révélant un mécanisme de couplage transcription-traduction (Conte *et al* 2009). Ce mécanisme sera développé dans le chapitre 1 de ma thèse.

III- Le stress dans les pathologies

Impact de l'hypoxie dans le cancer

Durant le développement tumoral, les cellules cancéreuses prolifèrent et forment par la suite une masse cellulaire avascularisée. Ainsi les apports en oxygène et en nutriment au centre de cette masse ne sont pas assurés. Les cellules cancéreuses sont alors en hypoxie, on parle d'hypoxie tumorale. L'hypoxie tumorale tient un rôle important dans l'agressivité de la tumeur. Elle permet sa progression, son invasion et sa dissémination métastatique. De plus, la tumeur devient résistante aux traitements de radio- et chimiothérapies, du fait de la perte de perfusion causée par l'hypoxie. Ce stress hypoxique va déclencher plusieurs cascades de signalisation permettant l'expression des facteurs pro-angiogéniques aboutissant à l'angiogenèse tumorale (Carmeliet *et al* 2000). Le développement et la progression tumorale sont caractérisés par la formation de nouveaux vaisseaux au sein de la tumeur. Le vaisseau tumoral formé permet de restaurer le flux sanguin mais de manière transitoire. On observe des cycles d'arrêts transitoires de la perfusion suivis de ré-oxygénation. Cela est dû à l'inadéquation entre la croissance des cellules tumorales et l'angiogenèse. En effet, la croissance tumorale est plus rapide que l'angiogenèse. L'autre système vasculaire est le système lymphatique qui joue également un rôle crucial dans la dissémination métastatique. L'étude de la lymphangiogenèse dans le contexte tumoral montre que l'hypoxie au centre de la tumeur induit la sécrétion du facteur lymphangiogénique VEGFC, stimulateur de la lymphangiogenèse (Morfoisse *et al* 2014). Les cellules tumorales utilisent les vaisseaux lymphatiques qui sont très perméables, pour atteindre les ganglions lymphatiques puis d'autres organes. A la base, les vaisseaux lymphatiques ont pour rôle de drainer les fluides interstitiels à partir des tissus afin de les renvoyer dans la circulation sanguine. La tumeur utilise cette voie pour se disséminer.

Comme je l'ai décrit dans la partie II, HIF est le principal facteur de la régulation transcriptionnelle en réponse à l'hypoxie. Il a été décrit que l'hypoxie active l'expression de plusieurs facteurs pro-angiogéniques qui sont les cibles de HIF1α du fait de la présence d'un élément HRE dans leur promoteur. C'est le cas du facteur VEGF-A, dont l'ARNm s'accumule dans les cellules endothéliales en réponse à l'hypoxie (Liu *et al* 1995). Dans le cancer du pancréas, l'expression de VEGF-A est régulée par HIF1α (Buchler *et al* 2003, Pages *et al* 2005). Et la transcription du facteur TGFβ (transforming growth factor) est également régulée

par HIF1α (Saed *et al* 2002, Jiang *et al* 2007). De plus, l'hypoxie induit la lymphangiogenèse par l'induction de l'expression de VEGFC par un mécanisme IRES-dépendant, indépendant de HIF1 dans les tumeurs mammaires (Morfoisse *et al* 2014). HIF2α est moins étudiéque HIF1α mais peut également réguler l'expression de certains gènes en hypoxie. Le récepteur EGFR (Epidermal growth factor receptor) est induit en hypoxie par HIF2α dans le carcinome épidermoïde (Wang *et al* 2010). De même l'ARN non codant NEAT1 est induit dans les tumeurs mammaires par un mécanisme dépendant de HIF2 (Choudhry *et al* 2015).

Ainsi, l'hypoxie tumorale module l'expression des gènes angiogéniques au niveau transcriptionnel grâce au facteur HIF mais elle peut également réguler la synthèse protéique par le mécanisme alternatif IRES-dépendant.

Face à l'hypoxie, la cellule réduit sa production de protéines en bloquant la cascade de signalisation mTOR. La phosphorylation de mTOR va bloquer l'initiation de la traduction dépendante de la coiffe en agissant sur les facteurs d'initiation de la traduction (partie II-2). Cette baisse de la synthèse protéique permet une économie d'énergie et l'activation de la traduction des gènes spécifiques suite à ce stress, par le mécanisme dépendant des IRES ou celui des uORF.

Le facteur hypoxique HIF, qui a un fort pouvoir angiogénique, possède justement un IRES dans son ARNm, permettant de maintenir, la synthèse de la protéine HIF en condition hypoxique (Lang *et al* 2002). Dans le cancer du sein, l'hypoxie inhibe la traduction dépendante de la coiffe par une hypophosphorylation de 4E-BP1 engendrant la séquestration du facteur eIF4E. Une étude dans des cellules de neuroblastome humain montre une augmentation de l'expression du facteur EGFR (Epidermal growth factor receptor) en condition hypoxique. Ce travail a démontré la présence et l'activation d'un IRES dans le 5'UTR de l'ARNm EGFR (Webb *et al* 2015).

Durant la croissance tumorale, les cellules cancéreuses rencontrent plusieurs stress : l'hypoxie, la carence en nutriment et l'acidose. Lorsque ces derniers persistent, ils déclenchent le stress du réticulum endoplasmique qui active la voie UPR pour la survie des cellules. A plus long terme, le stress du réticulum endoplasmique induit la mort cellulaire. Dans un modèle de transplantation de la tumeur chez la souris, il a été montré que la voie IRE1-XBP1 (X-box binding protein1) favorise la croissance tumorale (Romero-Ramirez *et al* 2004). XBP1 est un régulateur transcriptionnel activé par la voie UPR Son invalidation dans des tumeurs injectées en sous-cutané chez la souris induit la mort cellulaire par la réponse au stress du RE, conduisant à une réduction de la croissance tumorale. Ce résultat suggère que XBP1 est essentiel à la croissance tumorale durant le stress du réticulum

endoplasmique. En plus du stress du RE, l'hypoxie tumorale peut aussi induire les protéines du choc thermique. Le choc thermique est caractérisé par l'expression des protéines HSP. Ces protéines HSP ont un fort pouvoir anti-apoptotique par conséquent les cellules cancéreuses les expriment pour empêcher leur mort cellulaire (Lanneau *et al* 2008). Les cellules tumorales utilisent les HSP pour résister aux chimiothérapies (Jego *et al* 2013). D'ailleurs, plusieurs inhibiteurs de HSP90 et HSP27 on fait l'objet d'essais cliniques (Wang *et al* 2014).

Impact de l'hypoxie dans les pathologies ischémiques :

D'après le rapport de l'organisation mondiale de la santé (OMS), les maladies cardio-vasculaires sont les premières causes de mortalité mondiale. Les chiffres de 2012 estiment à 17,5 millions de nombre de décès, ce qui représente 31% de la mortalité mondiale. Les maladies cardiovasculaires causant le plus de décès sont l'infarctus du myocarde et l'accident vasculaire cérébral (AVC). En France, selon la santé publique, le nombre de décès pour ces deux pathologies s'élève à 44 971 dont 37% sont dus à l'infarctus du myocarde et 63% à l'AVC. En 2013, elles concernent plus de 900 000 patients. En dépit des traitements existants, l'ischémie du membre inférieur et l'ischémie cardiaque restent un problème majeur de la santé publique.

L'ischémie est principalement causée par l'athérosclérose qui est une lésion de l'intima due à une accumulation de lipoprotéines athérogènes modifiées dans l'espace sous-endothélial (Carew *et al* 1984, Boren *et al* 2000). Cette lésion va induire une réponse inflammatoire mobilisant les cellules inflammatoires (macrophages et lymphocytes T) suivie d'une prolifération cellulaire pour la cicatrisation (Buschmann *et al* 1999). Ces évènements conduisent à la formation de la plaque d'athérome. Si la cicatrisation n'est pas stabilisée, elle peut avoir des conséquences dramatiques. A terme, la rupture de la plaque provoque la formation d'un thrombus (ou caillot) obstruant les artères ; à titre d'exemple de pathologie avancée : l'infarctus myocardique ou cérébral (Virmani *et al* 2000) (**Figure 14**).

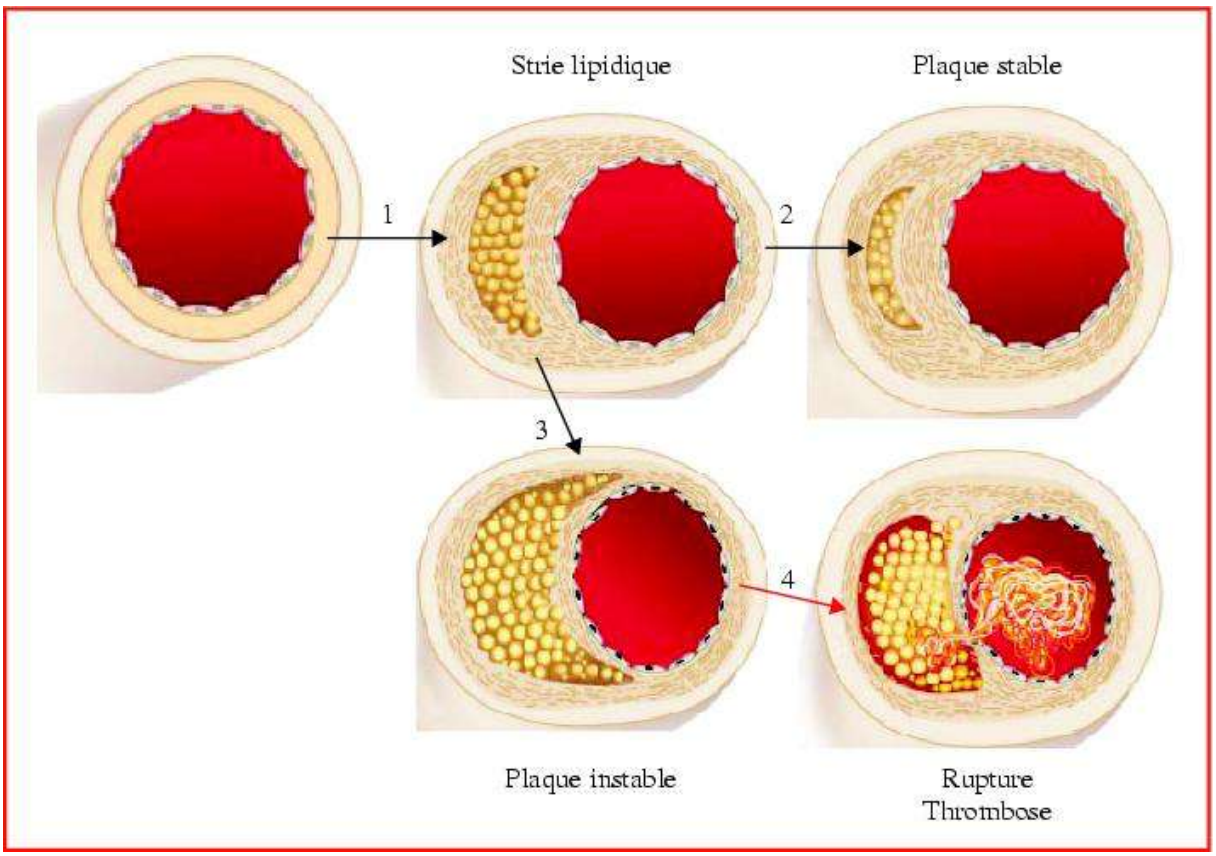

Figure 14 : Illustration de la formation de l'atherosclérose. D'après Gourdy, Bayard et Arnal, Sang Thrombose Vaisseaux 2005 (Pierre Gourdy 2005)

L'occlusion des artères provoque une ischémie dans la zone en aval de l'obstruction. L'ischémie est caractérisée par une diminution d'apport en oxygène par le sang ce qui déclenche une hypoxie des cellules non irriguées.

En réponse à l'hypoxie, les cellules vont mettre en place différents processus de revascularisation post-ischémique. Un de ces processus est l'angiogenèse qui est définie par la formation d'une extension vasculaire à partir des vaisseaux préexistants. Pour y parvenir les cellules régulent l'expression de leurs gènes face à ce stress hypoxique.

Le facteur hypoxique HIF tient un rôle important dans la revascularisation post-ischémique. La sous unité HIF1 est communément connue comme régulateur transcriptionnel de nombreux gènes angiogéniques comme VEGF, PLGF (placental growth factor), angiopoïetine 1 (ANGPT1), et ANGPT2 (Bosch-Marce *et al* 2007). Du côté de la sous-unité HIF2, l'invalidation du facteur eIF3E dans les cellules musculaires murines et humaines post-ischémiques montre une stabilisation de HIF2αcorrélée à une surexpression de FGF2 et de PDGF (platelet-derived growth factor) (Hashimoto *et al* 2016). Dans un modèle murin, l'inhibition du PHD

permet une surexpression des facteurs HIF qui est corrélée à l'augmentation de l'expression de VEGFA et TGF-β. Cela résulte en une réduction du niveau d'athérosclérose (Heim *et al* 2016). *In vivo*, VEGFA protège le cœur après ischémie chez le rat (Luo *et al* 1997). L'invalidation de ADAM17 (A disintegrin and metalloproteinase 17) dans les cardiomyocytes primaires inhibe la transcription de VEGFR2. ADAM17 est essentiel pour stimuler l'angiogenèse (Fan *et al* 2015).

Des études par analyse transcriptomique à haut débit ont été faites sur l'ischémie cérébrale, focalisées sur l'expression génique dans les neutrophiles et les monocytes (Moore *et al* 2005, Tang *et al* 2006). Tang et ses collègues ont publié une signature des gènes régulés par l'inflammation. Tandis que Moore et ses collègues ont trouvé différentes classes de gènes régulés. Parmi eux, un groupe de gènes liés à l'hypoxie comme l'adrénomédulline et le cytochrome b-245.

Smih et son équipe ont fait une étude pour rechercher un biomarqueur de l'insuffisance cardiaque systolique. Le transcriptome à grande échelle sur les globules blancs dans le sang a permis d'identifier sept gènes marqueurs de l'insuffisance cardiaque : ALK, SLC43A2, NGFB, FBXW7, TMEM79, UBN1 et FECH (Smih *et al* 2011).

L'élément structural IRES présent dans certains ARNm joue un rôle crucial dans la régulation traductionnelle survenant lors de l'ischémie. Dans l'ischémie du membre inférieur, la quantité d'ARNm de FGF2 baisse, en revanche l'expression de la protéine est augmentée (Conte *et al* 2008). L'IRES du FGF2 est activé en réponse à l'hypoxie dans cette pathologie en corrélation avec une meilleure vascularisation. Durant le stress ischémique, la traduction de l'ARNm VEGFA est induite par l'activation de ses IRES A et B (Bornes *et al* 2007). L'équipe a démontré que l'IRES A initie la traduction au codon attendu AUG tandis que l'IRES B permet l'initiation à un codon CUG situé en amont. L'année suivante, la même équipe montre *in vitro* la régulation de l'expression de l'isoforme prédominante de VEGFA (VEGF 121) par l'IRES A (Bastide *et al* 2008).

Les IRES, des outils biotechnologiques pour un transfert combiné de gènes thérapeutiques :

Il existe des traitements chirurgicaux comme l'angioplastie et le pontage. L'angioplastie consiste à dilater l'artère pur rétablir le flux sanguin. Le pontage permet de rétablir le flux sanguin en contournant l'endroit obstrué par greffe d'une

artère. Malgré l'avancée de ces chirurgies, ces techniques ont des limites. Déjà dans un premier temps, certains patients sont inéligibles à ces chirurgies. Deuxièmement, malgré le recours à l'angioplastie, la sténose réapparaît chez certains patients au bout de quelques mois. Face à ces difficultés, des stratégies alternatives de traitements comme la thérapie cellulaire et la thérapie génique offrent des perspectives prometteuses. Je me focaliserai ici sur la thérapie génique.

La thérapie génique consiste à apporter un gène fonctionnel pour rétablir une fonction lésée dans la cellule. Ainsi pour traiter les pathologies ischémiques, l'apport en gènes angiogéniques va faciliter la néo-vascularisation. L'approche thérapeutique retenue dans la plupart des études est l'angiogenèse thérapeutique. Le but est de faciliter le développement collatéral pour contourner l'occlusion en apportant des facteurs angiogéniques comme les VEGF ou les FGF à l'aide d'un vecteur (Rubanyi 2013).

III-1-1- *Utilisation des vecteurs à IRES pour le traitement de l'ischémie du membre inférieur*

Les différents essais cliniques publiés à ce jour utilisent un seul facteur angiogénique comme VEGFA (Isner *et al* 1996)ou FGF1 (Nikol *et al* 2008). Cependant ces essais dont les bénéfices thérapeutiques étaient encourageants en phase II, se sont soldés par un échec en phase III. Parmi les causes possibles de ces échecs, il y a le type de vecteur utilisé (plasmide ou adénovirus qui donnent une expression transitoire du transgène) ou le fait que l'utilisation d'un seul gène thérapeutique ne suffise pas. En effet, de fortes doses d'un seul facteur angiogénique peuvent générer des vaisseaux non fonctionnels. Ainsi il a été montré que la surexpression de VEGF génère des vaisseaux trop perméables (Baumgartner *et al* 1998). Effectivement il est apparu que la thérapie combinée utilisant plusieurs facteurs angiogéniques engendre une meilleure efficacité thérapeutique sur des modèles animaux (pour revue (Renaud-Gabardos *et al.* 2015)). Dans l'ischémie des membres, la combinaison de FGF2 et PDGF induit synergiquement le réseau vasculaire dans des modèles animaux de rat et de lapin (Cao *et al* 2003). Après ligature de l'artère fémorale, la surexpression de PDGF et de FGF2 augmente la vascularisation et améliore le flux sanguin. D'autres études combinant FGF2 et GM-CSF, VEGFA et FGF2 ou VEGFA et angiopoétine ont démontré le bénéfice d'une association de deux facteurs angiogéniques par rapport à l'effet de chaque

facteur de croissance pris isolément (Chae *et al* 2000, Lee *et al* 2007, Layman *et al* 2009).

Il existe plusieurs moyens de co-exprimer deux gènes (ou plus) mais qui présentent des inconvénients. Il est possible d'utiliser deux vecteurs séparés pour chaque gène, mais dans ce cas on n'a pas la certitude que les deux vecteurs se maintiennent avec la même stabilité à long terme et il est possible que l'expression de l'un des deux gènes disparaisse (notamment s'il est contre-sélectionné parce qu'il a une activité toxique ou inhibitrice de la prolifération cellulaire) (Allera-Moreau *et al* 2007). De même, si les deux gènes sont clonés dans le même vecteur mais sous contrôle de deux promoteurs, il y a un risque d'extinction de l'un des deux car il peut y avoir une compétition entre ces deux promoteurs (Allera-Moreau *et al* 2006, Lee *et al* 2007). L'expression d'une protéine de fusion a aussi ses limites. La fusion des protéines peut inhiber la localisation où la protéine exerce sa fonction. La localisation d'une protéine peut déterminer sa fonction. Par conséquent, une mauvaise localisation de la protéine de fusion rend la protéine non fonctionnelle (de Felipe *et al* 2006). Le problème de la protéine de fusion peut aussi être d'altérer la conformation de la protéine essentielle à sa fonction.

Ainsi, il est apparu que les IRES constituent un outil essentiel pour la co-expression des transgènes. En effet un vecteur à IRES peut produire plusieurs protéines différentes à partir d'un seul transcrit, grâce au mécanisme d'entrée interne des ribosomes (**Figure 15**).

Le vecteur à IRES présente plusieurs avantages par rapport aux autres systèmes de co-expression : (i) l'IRES permet de s'affranchir de la compétition entre deux promoteurs (ii) il permet de maintenir un ratio stable des protéines exprimées dans le temps (Allera-Moreau *et al* 2006) (iii) l'IRES peut être tissu-spécifique, c'est notamment le cas de certains IRES d'ARNm cellulaires, ce qui peut limiter les effets indésirables suite à la surexpression de facteurs à distance du site d'intérêt (Creancier *et al* 2000, Creancier *et al* 2001) (iv) certains IRES sont activés en condition de stress, permettant une synthèse protéique contrôlée (Bornes *et al* 2007, Conte *et al* 2008).

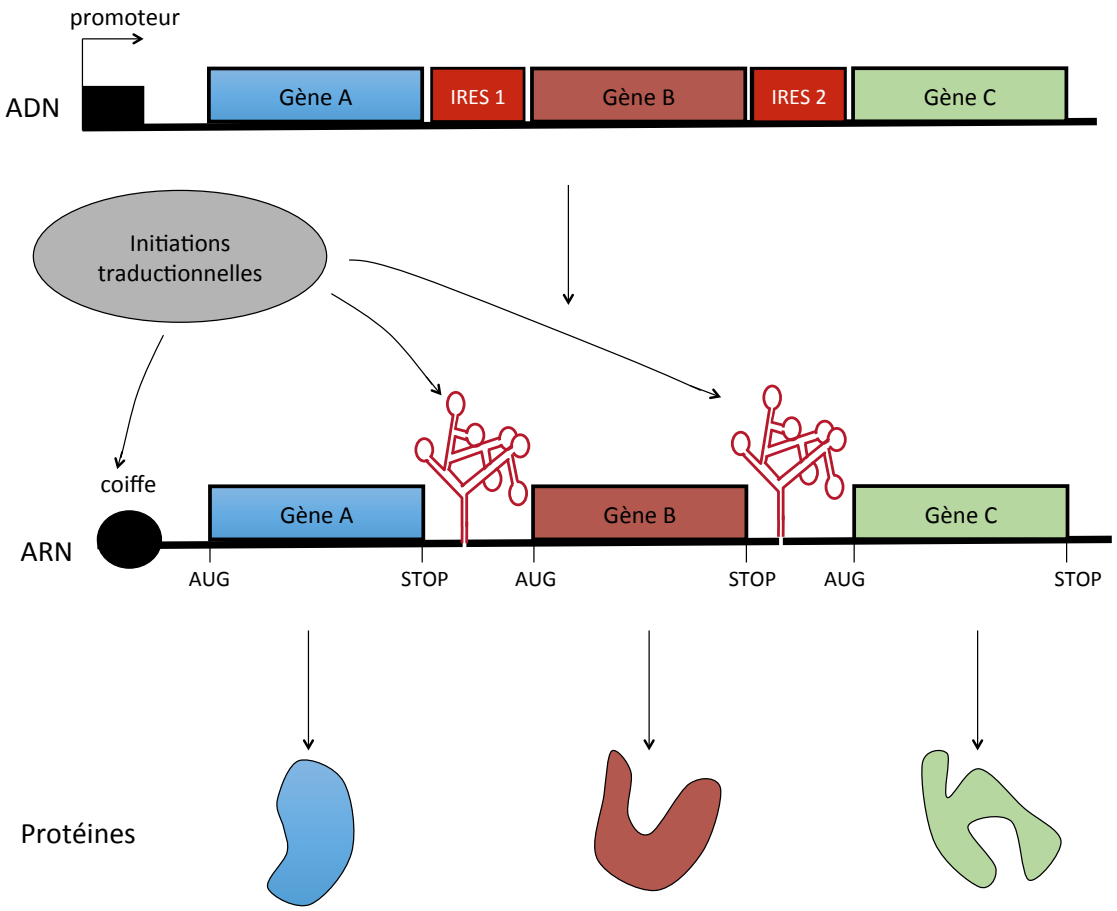

Figure 15 : Le concept du vecteur multicistronique basé sur les IRES.

D'après Renaud-Gabardos *et al*, (Renaud-Gabardos *et al* 2015)

Comme les pathologies ischémiques induisent différents stress et que certains IRES sont actifs dans ces conditions, la traduction IRES-dépendante permet de maintenir l'homéostasie cellulaire en induisant spécifiquement la traduction de certains gènes. Le choix de l'IRES est alors crucial.

Ce concept a déjà fait l'objet de plusieurs études dans la revascularisation après l'ischémie du membre. Notre laboratoire a validé le concept du vecteur bicistronique basé sur l'IRES en combinant FGF2 et Cyr-61 pour induire la vascularisation dans le traitement de l'ischémie du membre inférieur chez la souris (Rayssac *et al* 2009). Ce travail a démontré que le vecteur bicistronique permet un effet synergique des deux molécules thérapeutiques avec une meilleure efficacité thérapeutique à de plus faibles doses de molécules. Ceci permet aussi d'éviter des effets indésirables sur l'angiogenèse tumorale contrairement à ce qui a été observé avec un vecteur monocistronique qui exprime de fortes doses de Cyr61 (Rayssac *et al* 2009). D'autres études vont dans le mêmesens. Chez le lapin, la combinaison des gènes VEGFA et BMP7 (bone morphogenetic protein) séparés par l'IRES

d'EMCV stimule l'angiogenèse et la régénération osseuse (Zhang *et al* 2010). Plus récemment, une équipe a montré l'effet de la combinaison des facteurs VEGFA et FGF4 avec l'IRES EMCV sur la vascularisation du membre chez la souris (Jazwa *et al* 2013).

III-2*Utilisation des vecteurs à IRES pour le traitement de l'ischémie cardiaque :*

La co-administration de transgènes a démontré un bénéfice thérapeutique ces vingt dernières années surtout dans des études essentiellement pré-cliniques dans des pathologies telles que le cancer et l'ischémie du membre inférieur. Peu d'études ont été réalisées sur l'ischémie cardiaque. Cependant, une équipe a combiné VEGFA et PDGFB et a obtenu avec deux vecteurs AAV exprimant chaque facteur de croissance un meilleur bénéfice thérapeutique à la fois dans l'ischémie du membre et dans l'ischémie cardiaque (Kupatt *et al* 2010). Récemment, chez le rat, la combinaison de Gata4, Mef2C et Tbx5 a donné de bons résultats pour la transdifférenciation de fibroblastes cardiaques en cardiomyocytes en utilisant le système du peptide 2A (Mathison *et al* 2014).

Des travaux récents de l'équipe combinant dans un lentivecteur trois gènes thérapeutiques, l'apeline (facteur cardioprotecteur), le FGF2 (angiogène) et SERCA2a (pompe à calcium restaurateur de la fonction contractile) séparés de l'IRES de FGF1 ont permis de montrer que l'apeline et le FGF2 ont un effet coopératif sur l'angiogenèse, et que la coopération des trois protéines permet d'améliorer les paramètres de la fonction cardiaque, l'hypertrophie et la fibrose dans des souris en insuffisance cardiaque (Renaud-Gabardos *et al*, soumis, thèse de doctorat Renaud-Gabardos Décembre 2016).

Afin de réguler finement l'expression traductionnelle d'un gène, l'étude de la régulation des IRES d'ARNm cellulaires s'avère essentielle pour développer des systèmes optimisés de transfert combiné de plusieurs gènes thérapeutiques pour la thérapie génique de différentes pathologies, notamment celles liées à l'angiogenèse. Ainsi je me suis penchée durant ce travail de thèse sur l'identification des mécanismes moléculaires permettant la régulation de l'activité des IRES lors du stress hypoxique.

IV- Objectifs de la thèse :

Cette introduction m'a permis de souligner l'importance de la régulation traductionnelle, complémentaire à la régulation transcriptionnelle afin de répondre finement en temps et en heure aux stimuli perçus par la cellule pour le bon fonctionnement de l'organisme. Parmi elle, les IRES tiennent une place importante du fait de leur spécificité en fonction du signal.

Cependant, une meilleure compréhension des mécanismes traductionnels dépendants des IRES en réponse à un stimulus spécifique est nécessaire. Cette question amène à mon travail de thèse qui a eu pour objectif d'identifier les mécanismes de régulation de la traduction dépendante de l'IRES en réponse à différents stimuli du microenvironnement cellulaire.

Tout au long de ma thèse je me suis focalisée sur l'identification des acteurs moléculaires responsables de la régulation de la traduction IRES-dépendante dans trois situations physiologiques et/ou pathologiques cellulaires qui sont : la différenciation myogénique, le stress thermique et l'hypoxie.

Le premier chapitre de ma thèse portera sur la régulation de la traduction dépendante du promoteur FGF1 par les facteurs $p54^{nrb}$/NONO et hnRNPM durant la différenciation myoblastique.

Dans le deuxième chapitre, je décrirai l'identification d'un nouvel IRES, celui du VEGF-D, et son mécanisme de régulation par le stress thermique.

Finalement, un troisième chapitre qui a été le cœur de ma thèse, portera sur la régulation de l'activité IRES des ARNm des facteurs angiogéniques lors de l'hypoxie dans les cardiomyocytes, qui m'a amenée à l'identification d'un nouvel ITAF.

Résultats

Chapitre 1

Traduction promoteur-dépendante de l'IRES de FGF1 contrôlée par p54nrb et hnRNPM au cours de la différenciation des myoblastes

Le facteur de croissance FGF1 est impliqué dans la différenciation des myoblastes. Il est régulé au niveau de sa transcription et de sa traduction. La notion de couplage entre ces deux étapes de régulation a été abordée dans l'introduction. En effet, le gène FGF1 possède quatre promoteurs (A, B, C, D) qui sont tissu-spécifiques. Tous les transcrits expriment la même protéine. En revanche, chacun d'entre eux présente un 5'UTR différent suite à un épissage alternatif qui varie selon le promoteur utilisé. Les transcrits issus des promoteurs A et C possèdent un IRES.

Durant la différenciation myoblastique, le promoteur A est activé conjointement à l'IRES du transcrit A. Dans ce premier chapitre de ma thèse, je me suis focalisée sur l'identification des acteurs moléculaires responsables de l'activation de l'IRES couplée à celle du promoteur. Ainsi, nous avons cherché à identifier, par la technologie de bioanalyse moléculaire par résonance plasmonique de surface couplée à la spectrométrie de masse (BIA-MS), les protéines liées au promoteur et à l'IRES du FGF1. Nous avons identifié deux protéines, $p54^{nrb}$/NONO et hnRNPM, capables de se lier à la fois au promoteur et à l'IRES. Des expériences d'invalidation et de surexpression indiquent que ces deux protéines sont à la fois des activateurs transcriptionnels du promoteur et des ITAF capables d'activer l'IRES durant la différenciation myoblastique. De manière surprenante, nos travaux démontrent qu'un événement nucléaire est requis pour l'activation de l'IRES par ces deux ITAF, et que la présence du promoteur du FGF1 accroît significativement leur rôle d'activateurs traductionnels.

Ainsi notre étude a démontré que la régulation de la traduction de l'ARNm FGF1 par les régulateurs $p54^{nrb}$/NONO et hnRNPM durant la différenciation des myoblastes est dépendante de son promoteur. Ces résultats nous amènent à faire l'hypothèse que les deux ITAF sont recrutés de manière co-transcriptionnelle pour former "l'IRESome" sur l'ARNm naissant, et que ce complexe sera ensuite exporté vers le cytoplasme où l'ARNm sera alors traduit par le mécanisme IRES-dépendant.

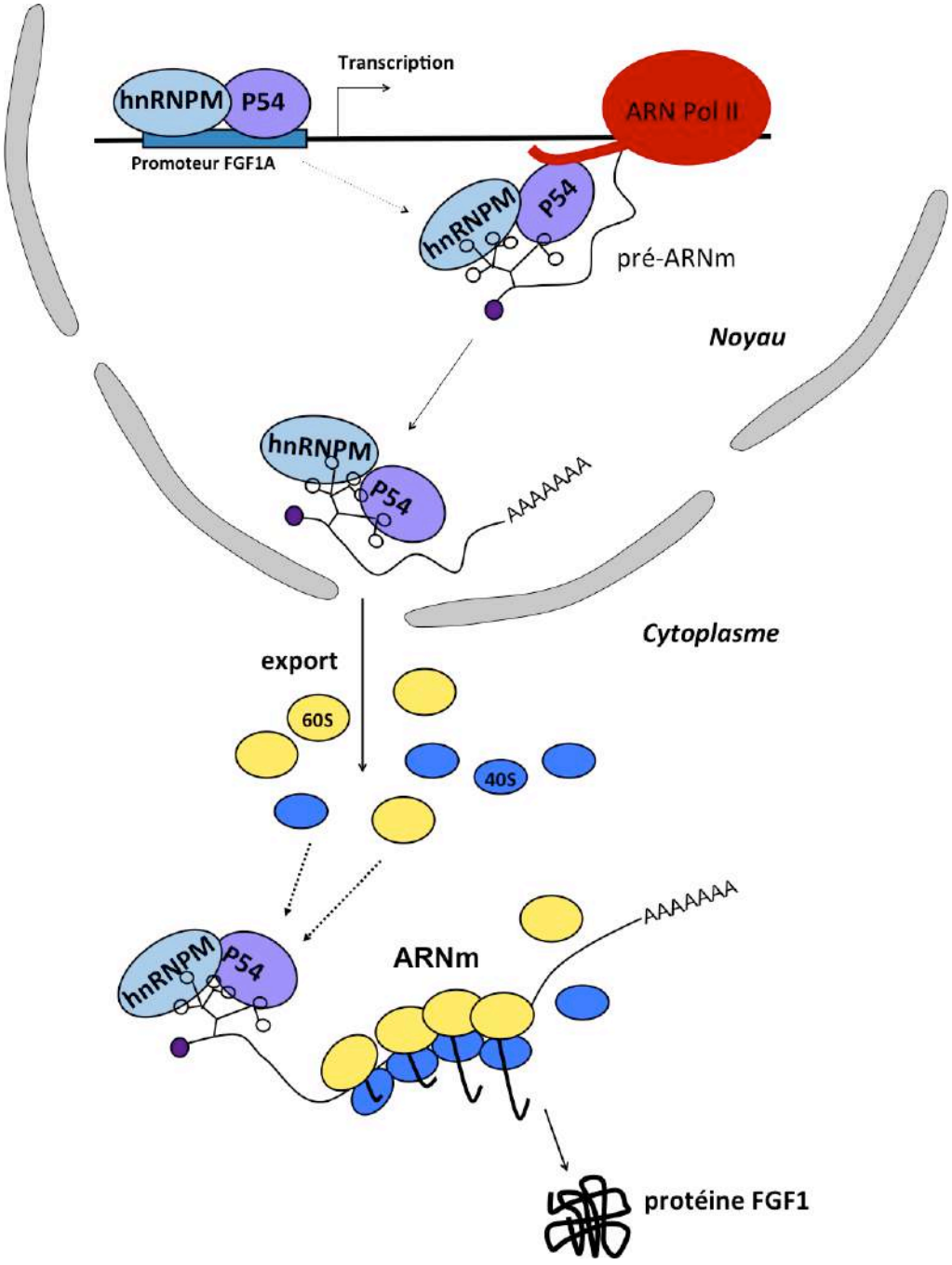

Figure 16 : Modèle du mécanisme d'expression de FGF1 par les facteurs p54^{nrb}/NONO et hnRNPM durant la différenciation des myoblastes. P54nrb/NONO et hnRNPM se fixent sur le promoteur de FGF1 en induisant sa transcription. Ils se fixent ensuite sur le pré-ARNm naissant en se liant au CTD de l'ARN PolII (non publié). Les ITAF p54^{nrb}/NONO et et hnRNPM liés sur l'IRES de FGF1 vont être exportés dans le cytoplasme en activant l'IRES pour synthétiser la protéine FGF1.

PLOS ONE

RESEARCH ARTICLE

Promoter-Dependent Translation Controlled by p54^{nrb} and hnRNPM during Myoblast Differentiation

Nadera Ainaoui[1☯], Fransky Hantelys[1☯], Edith Renaud-Gabardos[1☯], Morgane Bunel[1], Frédéric Lopez[2], Françoise Pujol[1], Remi Planes[3], Elmostafa Bahraoui[3], Carole Pichereaux[4], Odile Burlet-Schiltz[4], Angelo Parini[5], Barbara Garmy-Susini[5], Anne-Catherine Prats[1]*

1 TRADGENE, UPS (EA4554), Toulouse, France, **2** UMR U1037-CRCT, Inserm, UPS, Toulouse, France, **3** UMR U1043-CPTP, Inserm, UPS, Toulouse, France, **4** UMR U5282-IPBS, CNRS, UPS, Toulouse, France, **5** UMR U1048-I2MC, Inserm, UPS, Toulouse, France

☯ These authors contributed equally to this work.
* Anne-Catherine.Prats@inserm.fr

OPEN ACCESS

Citation: Ainaoui N, Hantelys F, Renaud-Gabardos E, Bunel M, Lopez F, Pujol F, et al. (2015) Promoter-Dependent Translation Controlled by p54^{nrb} and hnRNPM during Myoblast Differentiation. PLoS ONE 10(9): e0136466. doi:10.1371/journal.pone.0136466

Editor: Yoon Ki Kim, Korea University, REPUBLIC OF KOREA

Received: April 17, 2015

Accepted: August 4, 2015

Published: September 2, 2015

Data Availability Statement: All relevant data are within the paper and its Supporting Information files.

Funding: This work has been funded by Association Française contre les Myopathies (grant 16966), Association pour la Recherche sur le Cancer (grant PJA-20131200230), Ligue pour la Recherche Contre le Cancer, Cancéropole Grand Sud-Ouest, Institut National du Cancer (grant RIBCCAN no. 2008-039), Fondation de l'Avenir (grant ET0-583), Région Midi-Pyrénées (grant 11052677), Fonds Européen du Développement Régional (grant REFBIO-VEMT). There was no commercial funder. The funders had no

Abstract

Fibroblast growth factor 1 (FGF1) is induced during myoblast differentiation at both transcriptional and translational levels. Here, we identify hnRNPM and p54^{nrb}/NONO present in protein complexes bound to the FGF1 promoter and to the mRNA internal ribosome entry site (IRES). Knockdown or overexpression of these proteins indicate that they cooperate in activating IRES-dependent translation during myoblast differentiation, in a promoter-dependent manner. Importantly, mRNA transfection and promoter deletion experiments clearly demonstrate the impact of the FGF1 promoter on the activation of IRES-dependent translation via p54^{nrb} and hnRNPM. Accordingly, knockdown of either p54 or hnRNPM also blocks endogenous FGF1 induction and myotube formation, demonstrating the physiological relevance of this mechanism and the role of these two proteins in myogenesis. Our study demonstrates the cooperative function of hnRNPM and p54^{nrb} as regulators of IRES-dependent translation and indicates the involvement of a promoter-dependent mechanism.

Introduction

Gene expression in eukaryotes is regulated at multiple levels. Transcription, as well as post-transcriptional processes such as mRNA splicing, polyadenylation, degradation and translation, require a wide range of multi-component cellular machines in order to finely control protein production. For a long time, these steps have been considered to be a simple linear assembly line. Then, it has become apparent that gene expression, including steps such as transcription, capping, splicing, polyadenylation, RNA export and degradation, is coordinated in a complex and extensively coupled network [1, 2]. However, coordination resulting from the co-transcriptional loading of mRNA processing proteins by the C-terminal domain of RNA polymerase II seemed to exclude translational regulatory complexes [3].

role in study design, data collection and analysis, decision to publish, or preparation of the manuscript.

Competing Interests: The authors have declared that no competing interests exist.

The fibroblast growth factor 1 (FGF1) gene provides an attractive system to decipher a mechanism of coupling between transcription and translation. Indeed, we have shown that this growth factor is induced by a transcription-translation coupling mechanism during myoblast differentiation [4]. The FGF1 gene structure has been well documented in human. Transcription occurs from four promoters A, B, C and D, which are either tissue specific or inducible [5, 6]. Promoters A, B and C are conserved in mouse [5]. The promoter A is active in heart, skeletal muscle and kidney while the promoter B is brain specific [4, 7]. Promoters C and D are inducible and considered as markers of cell proliferation [8–10]. The only FGF1 promoter to be activated during myoblast differentiation is the promoter A whereas the other promoters remain silent [4].

Transcription from each promoter generates alternative splicing of exon 1, leading to four mRNAs with distinct 5' untranslated regions (5'UTR), each of them expressing the same protein, FGF1. Two of these 5' UTRs contain internal ribosome entry sites (IRES) [11]. IRESs have been described in several mRNAs containing long structured 5' UTRs. Most of these mRNAs code for proteins involved in the control of gene expression [12]. IRES structures have been determined in several mRNAs by chemical and enzymatic methods, allowing identification of stem loops responsible for the IRES activity [11, 13, 14]. As regards the FGF1 IRES, the IRES structural domain is conserved in mammals [11]. However this IRES structure is different from the IRES structures found in other mRNAs. In particular, it clearly differs from the IRES structure of another member of the FGF family, FGF2, suggesting distinct regulations of these growth factors by the IRES-dependent mechanism [13]. IRES-mediated translation is involved in the major translational process in conditions when the classical mechanism of cap-dependent translation is blocked [14–16]. We have previously shown that FGF1 is translationally induced via the IRES present in the promoter A transcribed mRNA, while cap-dependent translation is blocked during the first steps of myoblast differentiation [4]. FGF1 IRES-mediated translation is concomitant with transcriptional activation at promoter A. Furthermore IRES activity is drastically enhanced when transcription is controlled by promoter A, compared to the cytomegalovirus (CMV) promoter [4].

The concept of a nuclear event governing formation of the "IRESome", the ribonucleoprotein complex responsible for activation of IRES-dependent translation, has been reported in the literature for c-myc and Smad1 IRESs, although the cell factors responsible for this process have not been identified [17, 18]. Furthermore, most ITAFs are nuclear proteins primarily identified as splicing regulators. The first to be identified, pyrimidine tract binding protein (PTB), was described as an intron-binding protein before being characterized as an ITAF of encephalomyocarditis virus (EMCV) IRES [19, 20]. Several years after being identified as an ITAF for EMCV IRES, PTB has been shown to control several cellular IRESs such as APAF-1, BAG-1 or Bip [21–23]. Other splicing regulators, such as hnRNPK, hnRNPC1/2, hnRNPA1 or RBM4, have been identified as ITAFs [24–28]. HnRNPA1 has been described as an ITAF of several IRESs including FGF2, XIAP and c-myc IRESs [24, 29, 30]. It has been recently shown that this ITAF couples nuclear export and translation of several IRES-containing mRNAs [31].

Although the FGF1 IRES A has been reported to be stimulated during myoblast differentiation and muscle regeneration, nothing was known about ITAFs responsible for such regulation [4]. Biomolecular interaction analysis (BIA) uses a surface plasmon resonance phenomenon to characterize macromolecular interactions and has been recently optimized to enable the recovery and identification of interacting molecules by coupling BIA with mass spectrometry (MS) [32]. BIA-MS has proven successful in the identification of the partners in protein-protein interactions as it provides a high sensitivity compared to classical affinity chromatography approaches and permits identification from small quantities of bound ligands. A very reproducible "microelution" is now possible with the BIACORE 3000 instruments. This novel

technology was selected in the present study to search for proteins bound to the FGF1 promoter A and IRES A during myoblast differentiation to find candidate ITAFs and transcription factors involved in the transcription-translation coupling mechanism.

In the present report, we identified hnRNPM and $p54^{nrb}$/NONO bound (directly or indirectly) to FGF1 promoter A and IRES A in differentiating myoblasts (C2C12). Knockdown and overexpression approaches revealed that $p54^{nrb}$ and hnRNPM are required to activate the IRES-dependent translation in a promoter-dependent manner. Furthermore, $p54^{nrb}$ and/or hnRNPM knockdown inhibited myotube formation. Altogether, this study identifies a novel regulation of FGF1 gene expression, implying a cooperation between promoter and translational regulators to promote the time controlled process of myoblast differentiation.

Materials and Methods

Plasmids

The bicistronic plasmids with the CMV promoter and FGF1 IRES A (pCRF1AL2) or EMCV IRES (pCREL2), with the FGF1 promoter A and IRES A (pP1ARF1AL2) were previously described [4]. Human hnRNPM4 and $p54^{nrb}$ cDNAs were the gifts of M. Swanson and A. Krainer, respectively. cDNAs were PCR-amplified and introduced into the pTRIP-DU3-MCS vector (pTRIP-p54 and pTRIP-HM) [33–35]. The bicistronic vector pTRIP-p54iHM contains the two cDNAs separated by the FGF1 IRES. Plasmid construction details are available upon request.

Cell culture and transfection

C2C12 myoblasts (European Collection of Cell Culture ECACC No 91031101) were maintained in Dulbecco's modified Eagle's medium (DMEM) with 20% fetal calf serum in 100-mm diameter dishes at 37°C with 5% CO2. For differentiation, cells were changed into fusion medium (DMEM with 5% horse serum). Transient transfections were performed in 6-well dishes using 1 μg plasmid with FuGene-6 (Biochemichals) and OptiMEM (Gibco-BRL, Invitrogen).

Small interference RNAs were from Thermoscientific ONE TARGET plus SMARTpool targeting hnRNP M (siM) cat L-013452-01 lot 100508 or p54 cat L-007756-01 lot 100809 (sip54) or siGENOME non-targeting siRNA (sic). Only in S3 File, different siRNAs were used: siM-2 (5'-CAUUGGAAUGGGAAACCUATT-3') and sip54-2 (5'-GCUGAAUUUGCUCCAAAU ATT-3') (Sigma). C2C12 cells were transfected with 50nM siRNA with Hyperfect transfection reagent (Qiagen). mRNA transfection, were performed using Lipofectamine 2000 (Invitrogen) according to the manufacter's recommendations, with 2μg of each bicistronic mRNA. Cells were incubated at 37°C for 12h before harvesting and analysis.

Cell fractionation

C2C12 cells on 14 cm culture dishes were rinsed twice in cold phosphate-buffered saline (PBS 1X). Cells were scraped with a rubber policeman in 1 ml PBS 1X and pelleted by centrifugation at 2500 g for 10 min at 4°C. The pellet was resuspended in the 400 μl buffer A (10 mM HEPES pH7.9; 10 mM KCl; 0,1 mM EGTA; 1 mM DTT; 1X proteases inhibitors). The cells were allowed to swell on ice for 15 min. 25 μl the buffer B (100 mM HEPES; 100 mM KCL2; 10 mM EGTA; 500 mM MgCL2; 10% NP40) was added and the tube was vigorously vortexed for 10 sec. The homogenate was centrifuged for 30 sec; the supernatant containing cytoplasmic extract was recovered. The nuclear pellet was resuspended in 50 μl the ice-cold buffer C (20 mM HEPES, 400 mM NaCl; 1mM EGTA; 1 mM DTT; 1% proteases inhibitors) and vigorously rocked at 4°C

for 15 min on a shaking platform. The nuclear extract was centrifuged for 5 min at 4°C and the supernatant recovered.

Preparation of biotinylated RNA and DNA, and of capped and polyadenylated mRNA

The FGF1 5'UTR cDNA containing the IRES A sequence obtained by PCR was cloned in the pCR 4Blunt-TOPO plasmid (Invitrogen) downstream the T3 sequence [11]. The IRES T3 promoter fragment was cut with NcoI and transcription was performed with the MEGAscript T3 (Ambion), as per the manufacturer's protocol, in the presence of UTP-16-biotin (Roche Diagnostics GmbH), and the newly synthesized RNA was purified using an RNeasy column (Qiagen). The FGF1 promoter A was amplified from the bicistronic plasmid pP1AF1AL2 with the 5' biotin primers purchased from Invitrogen [4]: primer 5'biotin forward: 5'agcttaggtgaggagccttttcca-3', reverse: 5'accctgaaaggcagatgtgg-3'.

The purification PCR products were performed by the Nucleospin Extract II kit (Macherey-Nagel).

Capped and polyadenylated bicistronic mRNAs containing the FGF-1 IRES-A or the EMCV IRES were obtained using as templates PCR fragments amplified from bicistronic plasmids pCRF1AL2 and pCREL2, respectively, using primers (oligo(dt) included in the 3' primer) purchased from Sigma [4]. Transcription in vitro was performed with mMessage mMachine T3 Ultra kit (Ambion) according to the manufacter's recommendations.

BIA-MS experiments

SPR experiments were performed on a Proteon XPR36 (Biorad) and BIAcore 3000 (GE Healthcare) apparatus. The biotinylated targets RNA and DNA were immobilized on NLC sensorchip (Biorad) or carboxymethylated dextran sensor chips coated with streptavidin (SA sensorchip BIAcore) prepared according to the manufacturer's instructions. All RNA and DNA samples were prepared in HBS-EP buffer (0.01 M HEPES, pH 7.4; 15 M NaCl; 3 mM EDTA; 0.005% 20 surfactant). The proteins were injected at 20 μl/min at 20°C, at 500 μg/mL concentration across the sensor surface in this buffer. The regeneration of the RNA or DNA coated surface was achieved at 90 sec with a solution (20mM TEA; 0.5 M Urea).

Eluted protein samples (6 μL) were digested by the addition of 10μL of a solution of modified trypsin in 25 mM NH_4HCO_3 (20 ng/μL, sequence grade, Promega) at 37°C for 4h. The peptides mixtures were analyzed by nanoLC-MS/MS using a nanochromatography system (Ulmitate, Dionex) coupled to a Q-Star (Applied Biosystems, Altringham, USA) or an LTQ-Orbitrap (Thermo Fisher Scientific) mass spectrometer. Five microliters of each sample were loaded on a C18 precolumn (300 μm inner diameter x5 mm; Dionex) at 20 μL/min in 5% acetonitrile, 0.05% trifluoroacetic acid. After 5 min of desalting, the precolumn was switched on line with the analytical C18 column (75-μm inner diameter x 15 cm; PepMap C18, Dionex) equilibrated in 95% solvent A (5% acetonitrile, 0.2% formic acid) and 5% solvent B (80% acetonitrile, 0.2% formic acid). Peptides were eluted using a 5–50% gradient of solvent B during 80 min at a 300 nl/min flow rate. The mass spectrometer was operated in data-dependent acquisition mode. MS spectra were acquired on the 300–2000 m/z range and the three most intense ions were then selected for CID fragmentation. Dynamic exclusion was used within 60 s to prevent repetitive selection of the same peptide.

Database search and data analysis

The Mascot Daemon software (version 2.3.2, Matrix Science, London, UK) was used to perform database searches in batch mode with all the raw files acquired on each sample. Data

were searched against all entries in the SwissProt Human Mouse_20090127 protein database (36322 sequences; 19974433 residues). Oxidation of methionine was set as a variable modification for all Mascot searches. Specificity of trypsin digestion was set for cleavage after Lys or Arg except before Pro, and one missed trypsin cleavage site was allowed. The mass tolerances in MS and MS/MS were set to 5 ppm and 0.6 Da, respectively. Mascot results were parsed with the in-house developed software Mascot File Parsing and Quantification (MFPaQ) version 4.0 and protein hits were automatically validated if they satisfied a false discovery rate (FDR) of 1% with peptides of a minimal length of 8 amino acids [36].

ChIP

C2C12 cells on 14 cm culture dishes (10 millions cells per dish) were treated 10 min at 25°C with cross-linking buffer (buffer A, ChIP Diagenode kit) at a final concentration of 1% formaldehyde. The cross-linking reaction was quenched by addition of glycine at 0.125 M (5 min at 25°C) and the cross-linked cells were washed with the ice-cold PBS and treated with 500μl of lysis buffer (buffer B, Diagenode kit). Lysates were centrifuged for 5 min at 4°C, pellets were resuspended in 50 μL of buffer C containing protease inhibitors and incubated for 10 min at 4°C with gentle mixing. DNA was adjusted at a concentration of 10ng/μL as recommended by the supplier. The chromatin samples were sonicated for 15 cycles of 30 sec "ON"/30 sec "OFF" using the Bioruptor from Diagenode, then subjected to immunoprecipitation using antibodies anti-hnRNPM (1/D8) (Santa Cruz Biotechnologies), or anti-p54^{nrb}/NONO (BD Bio-sciences), or without antibody for the "mock" control. The immunoprecipitates or the input without immunoprecipitation were qPCR-amplified using according to the manufacturer's instructions. The TBP (TATA binding protein) gene was used as a reference gene.

RNA immunoprecipitation (RIP)

RNA-binding protein immunoprecipitation (RIP) is the RNA analog of the more well-known ChIP application and used to identify specific RNA molecules (of many types) associated with specific nuclear or cytoplasmic binding proteins. C2C12 cells on 14 cm culture dishes were treated for 10 min at 25°C with cross-linking buffer containing formaldehyde at 1% final concentration (buffer A, Magna RIP kit from Millipore). The cross-linking reaction was quenched for 5 min at 25°C with addition of glycine to 0.125 M. The cross-linked cells were rinsed twice in cold phosphate-buffered saline (PBS 1X). Cells were scraped with a rubber policeman in 10 mL PBS 1X and pelleted by centrifugation at 1500g for 5 min at 4°C. Pellets were resuspended in 500 μL of RIP lysis buffer (1% NP40, 10 mM HEPES, 100 mM KCl, 5 mM $MgCl_2$, protease inhibitor cocktail 1x, RNases inhibitors, Magna RIP kit, Millipore).

50 μL of magnetic beads protein A/G was washed four times in 500μL of RIP wash buffer (0.05M Tris, 0.15M NaCl, pH 7.5) then incubated for 30 min at room temperature with 10μg of antibody anti-hnRNPM (1D8 Santa Cruz Biotechnologies), anti-p54^{nrb}/NONO (BD Bio-sciences) or anti-IgG. The beads-antibody complex was washed twelve times in 500 μL of RIP wash buffer before adding 900 μL of immunoprecipitation buffer (RIP wash buffer: 0.5 M EDTA, 5 μL RNase inhibitor). The cell lysate was centrifuged at 14000 rpm for 10 min at 4°C, 100 μL of the supernatant was added to each sample of beads-antibody complex and incubated at 4°C overnight. Immunoprecipitates were washed six times before protein and RNA recovery. Proteins were recovered with 50 μl of SDS-PAGE loading buffer and analyzed by Western Blot. RNA was recovered by incubation of the immunoprecipitate for 30 min at 55°C in 150 μl of proteinase K buffer containing 117 μL of RIP wash buffer, 15 μL of SDS 10% and 18 μL of proteinase K at 10 mg/mL. The immunoprecipitates were analyzed by RT-PCR using the High

Capacity cDNA Reverse Transcription kit from Applied Biosystems and qPCR-amplified according to the manufacturer's instructions.

Immunoprecipitation

C2C12 cells were harvested in 1 mL PBS (1X), pelleted and resuspended in 100μl of lysis buffer (RIPA). 100 μL Protein G-plus or Protein A was precoated with mouse anti-hnRNPM (1D8 Santa Cruz Biotechnologies) or anti-p54 antibody (BD Biosciences), and was incubated with 70 μL of the cell lysate. After 5 times washing with IP buffer plus 0.5% BSA, proteins were eluted in 100 μL elution buffer and 50μL was loaded on SDS-PAGE gel for Western analysis using rabbit antibodies against hnRNPM (Sigma AV40620), p54 (Sigma N8789). Mock experiments were performed similarly but without primary antibody.

Western blotting

C2C12 were harvested in lysis buffer (50 mM Tris-HCL pH8, 150mM NaCl, 1mM EDTA, 1% NP40, 20 μL protease inhibitor mixture (Roche) and clarified by centrifugation at 13000 rpm for 10 min at 4°C. Proteins supernatant were quantified using the Bradford method (Biorad).

Primary antibodies were mouse monoclonal antibodies against hnRNPM (Santa Cruz Biotechnologies, 1/400), p54nrb (BD Bio-sciences, 1/400), myogenin (Santa Cruz Biotechnologies 1/400), Glyceraldehyde 3-phosphate deshydrogenase (GAPDH, Santa Cruz biotechnologies 1/10000) and the rabbit polyclonal FGF1 (F5521, sigma, 1/400). Secondary antibodies were peroxidase-conjugated-AffiniPure Donkey Anti-Rabbit IgG and AffiniPure Donkey Anti-Mouse IgG (Jackson ImmunoResearch, 1/10000).

Protein detection was carried out using Supersignal West Pico Cheluminescent Substrat and ECL western blotting substrate (ThermoScientific).

RNA extraction and real time RT-qPCR

Total RNA was isolated from C2C12 cells using Nucleospin RNA II kit (Macherey-Nagel). After DNase I treatment (DNase I Amplification Grade, Invitrogen), reverse transcription was performed with the High capacity cDNA Archive Kit (Applied Biosystems, Foster City, CA). As an internal control, ribosomal 18S (m18S) RNA was used.

Quantitative PCR was performed on a Stepone sequence detection system (Applied Biosystems) using Sybr Green PCR Master Mix (Applied Biosystems) for detection of LucF, LucR, FGF1 and 18S transcripts.

Primer sequences are available upon request.

Reporter activity assay

Protein from C2C12 cells were extracted with reporter Passive Lysis buffer (Promega) and protein concentration was quantified by Bradford Standard Assay. Quantification of bioluminescence was performed with a luminometer (Centro LB960, Berthold) using the Dual-Luciferase Reporter Assay (Promega France).

Ethics statements

Experiments have been conducted with the genetically modified organisms agreement n°496 from the French Technologies High Committee.

Authors comply with best practices in publication ethics, specifically regarding authorship, dual publication, plagiarism, figure manipulation, and competing interests.

Results

BIA-MS identification of p54^{nrb} and hnRNPM bound to the FGF1 promoter and IRES

BIA-MS technology was used to identify proteins bound to the FGF1 promoter A and IRES A. Biotinylated promoter DNA and IRES RNA were (separately) immobilized on biacore streptavidin sensorchips (Fig 1A). This method is not denaturing and allows identification of proteins present in the complex bound to DNA or RNA. Binding to nucleic acids may be direct or indirect. Total or nuclear cell extracts, from proliferating or differentiating C2C12 cells (day 2), were injected into the BIACORE 3000 apparatus to obtain the association phase (Fig 1B). Interestingly, a significant association was obtained with extracts of differentiating cells, but not with proliferating cell extracts. Using nuclear extracts an important binding activity was obtained with both FGF1 IRES RNA and promoter DNA. Bound proteins were recovered and identified by nanoLC-MS/MS after tryptic digestion (Fig 1C and S1 File). Proteins from total extracts bound to the IRES included: 1) ribosomal proteins and elongation factor eEF1A1, expected to be involved in translation and 2) nuclear proteins including several histones, nucleophosmin, and the splicing protein hnRNPM (Fig 1C, Table A in S1 File) [37–39]. Using nuclear extracts, we identified IRES interactions with the splicing proteins hnRNPA3, U2AF2, SFR2 and U5 snRNP component S1 as well as p54^{nrb}, a protein involved in both splicing and transcription (Fig 1C, Table B in S1 File) [27, 28]. Interestingly, none of these proteins bound the EMCV IRES, used as a control (Table C in S1 File). Several DNA binding proteins were identified as interacting (directly or indirectly) with the FGF1 promoter: Poly(ADP-ribose) polymerase (PARP), transcriptional activator Purβ, ATP-dependent DNA helicases KU70 and KU86 and p54^{nrb}, which was also bound to the IRES (Fig 1C, Table D in S1 File). The dual presence of p54^{nrb} promoted it as the most interesting candidate. Furthermore, its interaction with hnRNPM and co-localization within defined nuclear structures incited us to focus on the role of these two proteins in the control of FGF1 expression during myoblast differentiation [40].

P54^{nrb} and hnRNPM bind to FGF1 promoter and IRES in differentiating, but not in proliferating myoblasts

Interaction of hnRNPM and p54^{nrb} with the promoter was analyzed by chromatin immunoprecipitation (ChIP), using DNA extracts either from proliferating or differentiating myoblasts (Fig 2A). We checked by immunoprecipitation that the two proteins are expressed in proliferating as well as in differentiating cells (Fig 2B). However no interaction was detected with either of the two proteins in proliferating cells, whereas significant interaction was observed with both proteins in differentiating myoblasts (Fig 2A). RNA immunoprecipitation (RIP) was also performed using anti-hnRNPM or anti-p54 antibodies revealing that the two proteins interact with the FGF1 IRES RNA in differentiating, but not in proliferating, myoblasts (Fig 2C). These data demonstrated that hnRNPM and p54^{nrb} interact (directly or indirectly) with FGF1 promoter A and IRES A only in differentiating myoblasts. In contrast the two proteins very poorly interact with the FGF2 IRES, and such interaction did not increase during differentiation (Fig 2D).

Thus, hnRNPM and p54^{nrb} binding to FGF1 promoter and IRES correlates with the previously shown induction during differentiation [4]. Binding and activity are very weak during proliferation and induced by day 2 of differentiation. This suggests that these proteins may be involved in the specific activation of FGF1 mRNA accumulation and IRES-mediated translation.

A

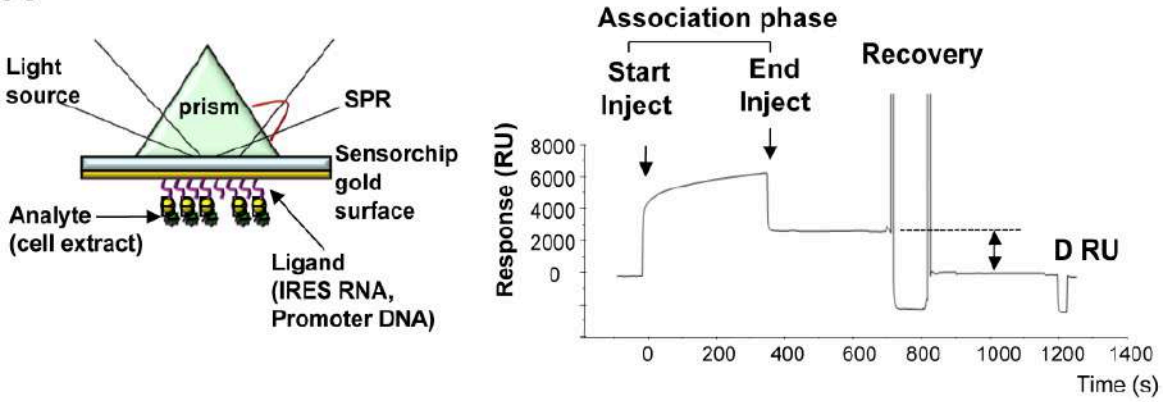

B

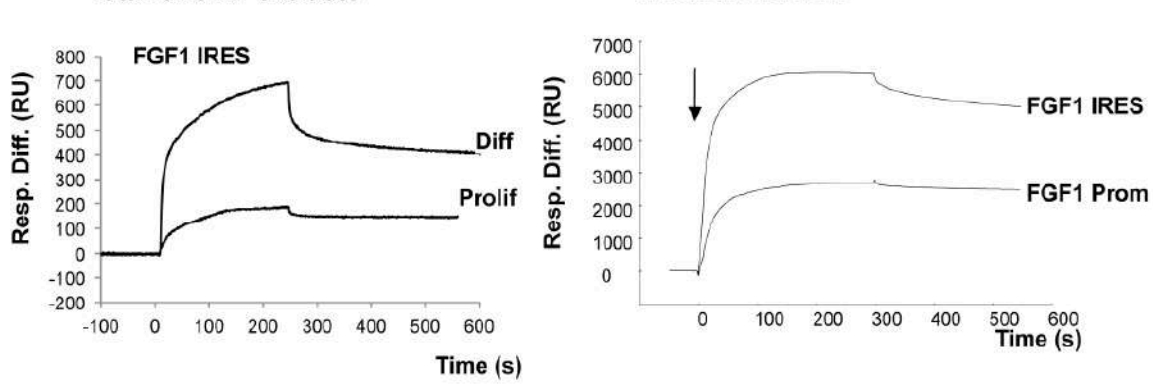

C

Candidate proteins identified by mass spectrometry in differentiating C2C12

	Total cell extracts	Nuclear extracts	
Probe:	**FGF1 IRES RNA**	**FGF1 IRES RNA**	**FGF1 Promoter DNA**
	Elongation factor 1-a1	HnRNP A3	**P54^{nrb}/NonO Non-POU**
	Histone H1.3	**P54^{nrb}/NonO Non-POU**	Poly (ADP-ribose) polymerase
	Histone H1.4	RNPS1	Transcriptional activator Purb
	Histone H1.5	SmD1	ATP-dep DNA helicase KU70
	Histone H1t	Splicing factor SFR2	ATP-dep DNA helicase KU86
	Histone H2B type1-B	Splicing factor U2AF2	
	Histone H4	SRRM1	
	HnRNP M	U5 snRNP component 1	
	Nucleophosmine NPM1		

Fig 1. Identification of RNA and DNA binding proteins by BIA-MS. (A) BIACORE 3000 analysis using surface plasmon resonance. Left: the ligand corresponding to biotinylated RNA or DNA is immobilized by streptavidin coupled to the sensorchip gold surface. On the other side of the sensorchip, a light source is directed to the sensorchip through a prism and is reflected in all angles except one at which it is absorbed into the gold surface in the form of an evanescent wave. The binding of the analyte corresponding to RNA or DNA binding proteins to the ligand results in a change in the index of refraction proportional to the number of bound molecules. This generates a shift in the absorption angle that is recorded by the detector and appears on a sensogram. Right: Sensogram generated during a binding cycle followed by protein recovery. The response appears in resonance units (RU). The association phase lasts from the start to the end of analyte injection (400 s). Protein recovery is achieved at 800 s and the ΔRU indicates the efficiency of dissociation of the bound proteins. (B) C2C12 myoblast protein binding and recovery. Total extracts of proliferating or differentiating C2C12 myoblasts (left) or nuclear extracts of differentiating C2C12 (right) were injected as analytes in several BIACORE 3000 channels after immobilization of ligands corresponding to FGF1 IRES A RNA (nt 1 to 442) or promoter A DNA (distal part nt 1 to 391). Bound proteins were recovered as described in Mat. & Meth. (C) Mass spectrometry analysis of proteins recovered from the BIACORE 3000 experiments. For each BIA-MS experiment, 6 recovery cycles were pooled to obtain a sufficient RU quantity (about 2000 RU). The mass spectrometry analysis was performed as described in Mat. & Meth. The most significant proteins (RNA and DNA binding proteins) are listed here, whereas the complete list is provided in S1 File. hnRNPM and p54^{nrb} have been selected as the most interesting candidates.

doi:10.1371/journal.pone.0136466.g001

p54^{nrb} and hnRNPM knockdown silences the FGF1 promoter-dependent accumulation of mRNA during myoblast differentiation

The role of p54^{nrb} and hnRNPM on FGF1 expression was studied by a knockdown approach using siRNA smartpools targeting either p54^{nrb} (sip54) or hnRNPM (siM) (S2 File). Myoblasts were co-transfected with bicistronic vectors containing the FGF1 IRES and siRNAs. The bicistronic cassette, coding for *renilla* luciferase (LucR) and firefly luciferase (LucF) separated by the FGF1 IRES, was under the control of either the CMV promoter or the FGF1 promoter A (Fig 3). Endogenous FGF1 mRNA was quantified by RT qPCR, and expression of the bicistronic mRNA under the control of either the CMV or FGF1 promoter was compared.

RT qPCR quantification of endogenous FGF1 mRNA clearly showed, as we have previously reported, a strong induction of FGF1 mRNA accumulation at day 2 of differentiation [4]. This induction was abolished upon transfection with siRNA against either hnRNPM or p54^{nrb} (Fig 3A and S2 File).

Bicistronic mRNA levels produced from the CMV or FGF1 promoter were quantified with LucF and LucR couples of primers. No variation of mRNA amount was observed with the CMV promoter in response to siRNA knockdown of hnRNPM or p54^{nrb} (Fig 3B). In contrast, the level of bicistronic mRNA transcribed from the FGF1 promoter was strongly downregulated by hnRNPM or p54^{nrb} knockdown in differentiating myoblasts (Fig 3C). In addition, the two cistrons LucR and LucF were present in equal amounts in all experiments, ruling out any effect of hnRNPM or p54^{nrb} on a putative cryptic splicing site or promoter in the IRES (Fig 3B and 3C).

These data showed, together with the ChIP data (Fig 2A), that hnRNPM and p54^{nrb}/NONO binding to the FGF1 promoter A is responsible for FGF1 mRNA accumulation during myoblast differentiation, suggesting an effect of these proteins on the FGF1 mRNA transcription or stability.

p54^{nrb} and hnRNPM knockdown silences the FGF1 IRES during myoblast differentiation

The knockdown approach was also used to evaluate the effect of hnRNPM and p54^{nrb} on translation mediated by the FGF1 IRES A. In the bicistronic construct, LucR activity reflects the mRNA level and cap-dependent translation while LucF reflects the IRES activity. Luciferase activities were measured in myoblasts co-transfected with bicistronic vectors and siRNAs targeting hnRNPM and/or p54^{nrb} (see above, and S2 File). Under the CMV promoter, FGF1 IRES activity decreased by 5.6 or 7 fold following knockdown of hnRNPM or p54^{nrb}, respectively (Fig 4A, left panel). A double knockdown resulted in a 13.5 fold inhibition (Fig 4A, right panel). These effects were observed in differentiating but not proliferating myoblasts. When the bicistronic cassette was under the control of the FGF1 promoter A, the IRES activity was 39

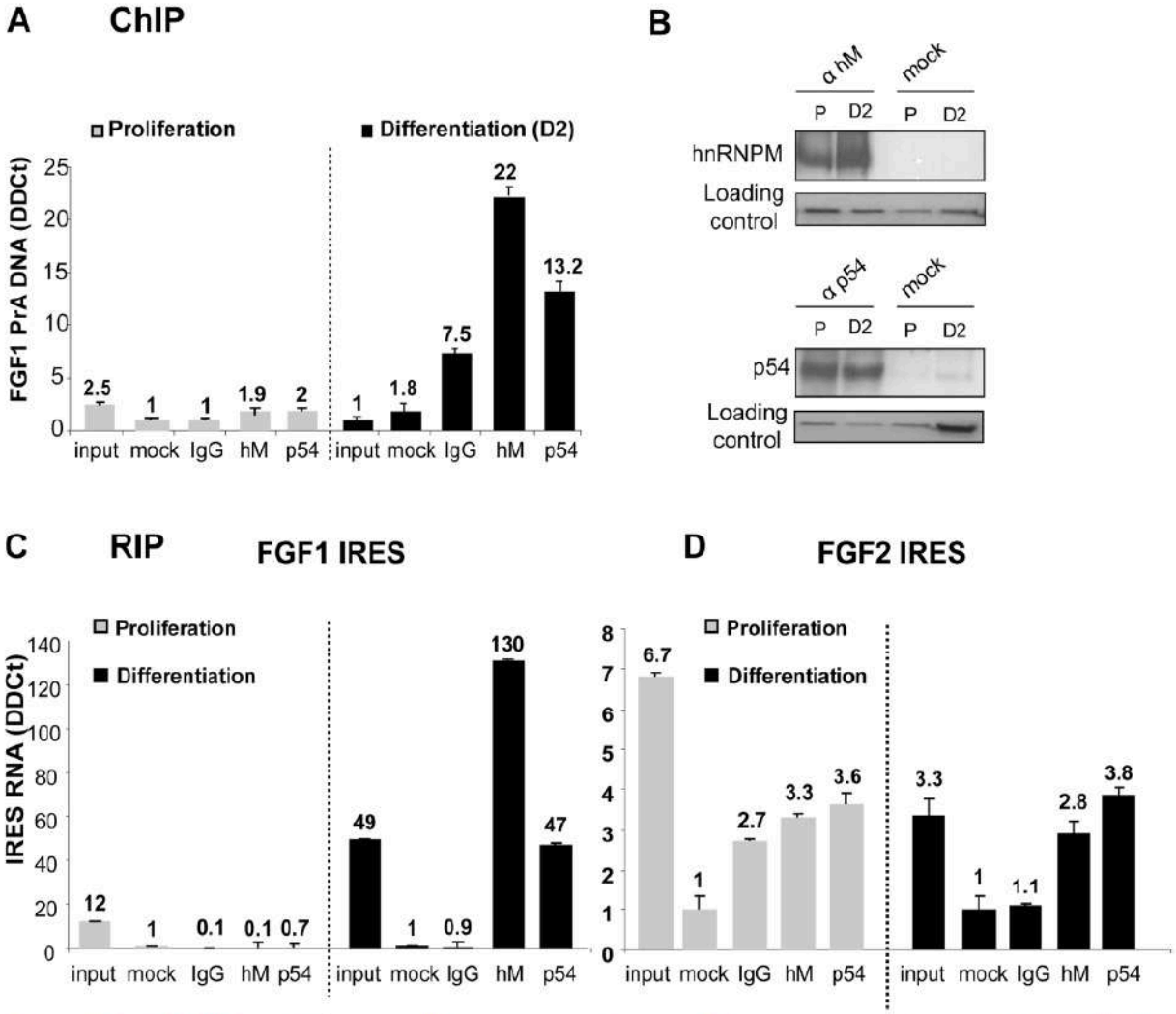

Fig 2. Interaction of hnRNPM and p54^{nrb} proteins with FGF1 promoter and IRES. (A) ChIP assays were performed as described in Mat. & Meth. with genomic DNA purified and fragmented from C2C12 extracts in proliferation (left panel) or differentiation 2 days after serum-starvation treatment (right panel). Immunoprecipitation experiments were performed with anti-hnRNPM (1/D8), anti-p54^{nrb} antibodies, control IgG provided by the manufacturer (IgG) or without antibodies (mock), respectively. qPCR quantification was achieved with primers specific to the 1–391 FGF1-A promoter fragment or with primers specific to the TBP gene used as the reference gene. The values are expressed relatively to the reference gene. Experiments were performed in biological triplicates and repeated three times. A representative experiment is shown (mean +- standard deviation). (B) HnRNPM and p54^{nrb} protein levels were analyzed by immunoprecipitation followed by Western blotting in proliferating (P) or differentiating (day 2 after serum-starvation, D2) C2C12 cell lysates, using anti-hnRNPM or antip54 antibodies. The loading control was checked by Ponceau Red staining. (C, D) RIP assays were performed as described in Mat. & Meth. with cell lysates from proliferating or differentiating myoblasts. Immunoprecipitation was achieved as in (A). RNAs present in the immunoprecipitated complexes were quantified by RT qPCR using primers specific to the FGF1 (C) or FGF2 IRES (D). The reference gene was 18S RNA, reflecting non specific RNA binding. The values are expressed relatively to the control (mock) without antibody. Experiments were performed in biological triplicates and repeated three times. A representative experiment is shown (mean +- standard deviation).

doi:10.1371/journal.pone.0136466.g002

fold higher than with the CMV promoter (as published previously) and more strongly affected by hnRNPM or p54^{nrb} knockdown (8 and 11 fold, respectively, Fig 4B, left panel) [4]. In addition, the double knockdown drastically inhibited the IRES activity 54 fold (Fig 4B, right panel). Additional siRNAs targeting p54^{nrb} or hnRNPM, but not contained in the smartpools, were

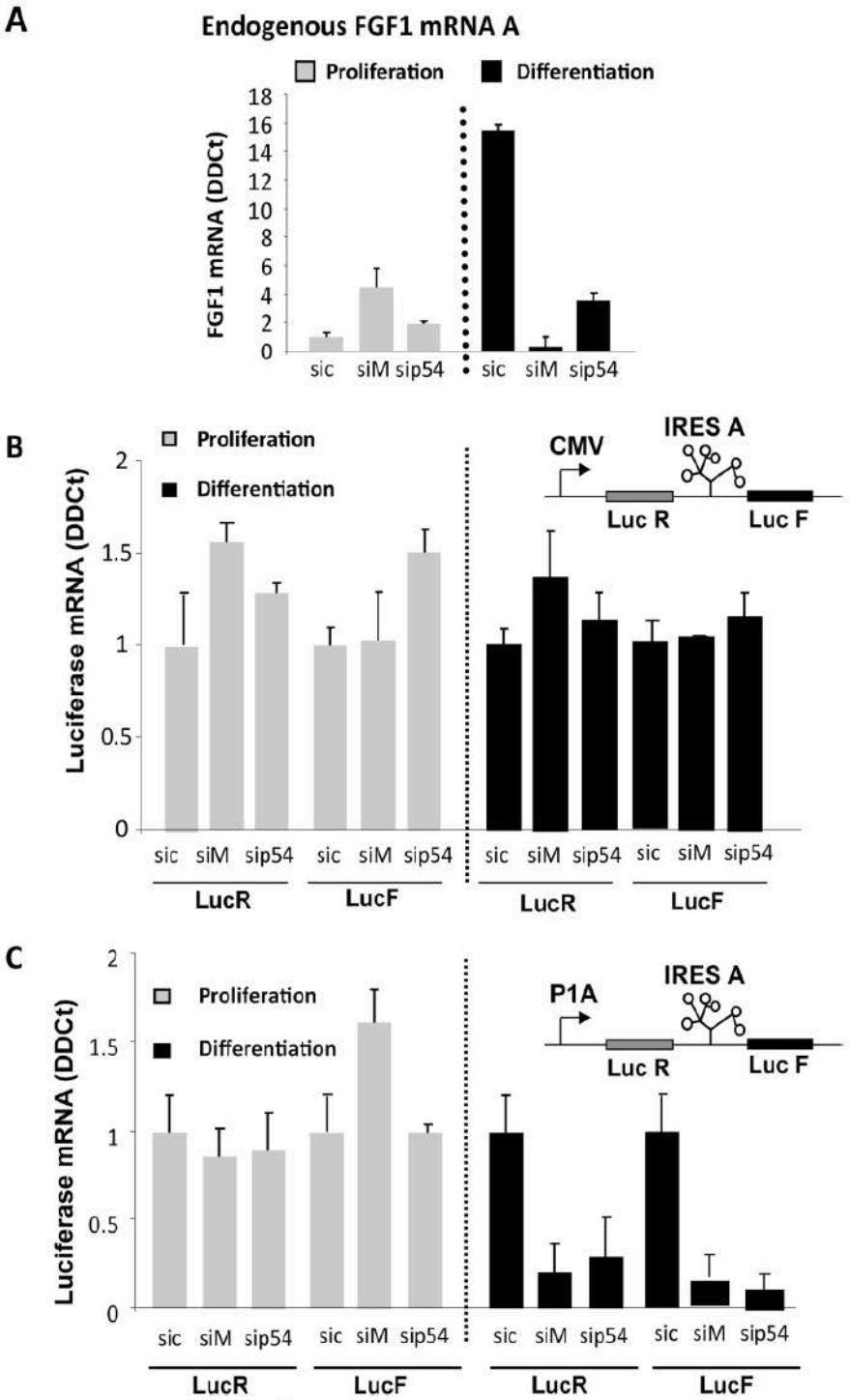

Fig 3. Effect of hnRNPM and p54^{nrb} knockdown on expression of endogenous FGF1 mRNA and bicistronic mRNAs during myoblast differentiation. (A) RT qPCR quantification of endogenous FGF1 mRNA A was performed as described in Mat. & Meth. during C2C12 myoblast proliferation or day 2 differentiation after transfection with siRNA ONE TARGET PLUS smartpool against hnRNPM (siM), p54^{nrb} (sip54) or siRNA control (sic). mRNA

quantification was standardized with RNA 18S. Experiments were performed in biological triplicates and repeated three times. A representative experiment is shown (mean +- standard deviation). The knockdown efficiency, analyzed by Western blot, is shown in S2 File and was also checked by RT qPCR (not shown). (B, C) C2C12 cells co-transfected with bicistronic plasmids and 48h later with siRNA siM, sip54 or sic as above. *Renilla* luciferase (LucR, left) and firefly luciferase (LucF, right) mRNA levels were quantified by RT qPCR during C2C12 myoblast proliferation (grey histograms) and differentiation (black histograms), standardized to 18S RNA. The bicistronic cassette contains either the CMV promoter (B) or the FGF1 promoter A (C). For each experiment, values are shown relatively to the siRNA control. Experiments were performed in biological triplicates and repeated at least three times. A representative experiment is shown (mean +- standard deviation).

doi:10.1371/journal.pone.0136466.g003

assessed, confirming that the effect of p54 or hnRNPM knockdown on FGF1 IRES activity is specific to these targets (S3 File).

To check the specificity of FGF1 IRES regulation by hnRNPM and p54^{nrb}, knockdown was performed as above using bicistronic contructs with the EMCV or FGF2 IRES. Results showed that the activities of the EMCV and FGF2 IRESs remained completely unaffected by either knockdown (Fig 4C and 4D).

These data suggested that hnRNPM and p54^{nrb} participate in the IRESome complex responsible for FGF1 IRES A activation during myoblast differentiation, but are unable to activate EMCV or FGF2 IRESs. In addition, the presence of the FGF1 promoter A stimulated the IRES activating function of the two proteins, suggesting that the recruitment of hnRNPM and p54^{nrb} on the promoter by a direct or indirect interaction might enhance their recruitment in the IRESome.

P54^{nrb} is sufficient to stimulate the FGF1 promoter whereas it cooperates with hnRNPM to activate the FGF1 IRES

To evaluate the double activity of p54^{nrb} and hnRNPM on FGF1 promoter and IRES, C2C12 myoblasts were co-transfected by the bicistronic FGF1 IRES-containing dual luciferase plasmid and by plasmids coding either p54^{nrb} or hnRNPM, or both proteins (Fig 5A and 5B). Measurement of the LucR activity showed significant mRNA accumulation in response to p54^{nrb} overexpression (Fig 5C). The IRES activity reflected by the ratio LucF/LucR was enhanced by p54^{nrb} alone, but more strongly with the combination of p54^{nrb} and hnRNPM (Fig 5D and 5E). Surprisingly, overexpression of hnRNPM alone inhibited both mRNA accumulation and IRES activities, suggesting that the ratio of the two proteins may be important for hnRNPM function (Fig 5C–5E). The effects of protein overexpression were stronger in proliferating myoblasts, which could be expected, because promoter and IRES are in a basal inactive state in proliferating cells, while they are activated by the endogenous p54^{nrb} and hnRNPM in differentiating cells. These results suggested that p54^{nrb} is sufficient to enhance mRNA accumulation, whereas it cooperates with hnRNPM to stimulate the IRES. Such a cooperative effect confirmed the data of the knockdown experiments (Figs 3 and 4).

Regulation of IRES activity by hnRNPM and p54^{nrb} is promoter-dependent

To analyse the impact of the promoter on activation of IRES-dependent translation by hnRNPM and p54^{nrb}, C2C12 cells were transfected with either bicistronic plasmid DNAs or in vitro transcribed capped and polyadenylated bicistronic mRNAs (Fig 6). DNA transfection resulted (as already shown in Fig 4) in a high FGF1 IRES activity, strongly induced by C2C12 differentiation, and downregulated by the knockdown of hnRNPM or p54^{nrb} (Fig 6A and S4 File). In contrast, basal FGF1 IRES activity was 500 times lower following RNA transfection, and no induction by either hnRNPM or p54 was observed (Fig 6B and S4 File). These features were not observed with the EMCV IRES, whose activity was low after DNA or RNA transfection and was not affected by hnRNPM or p54 knockdown (Fig 6C and 6D). As a negative

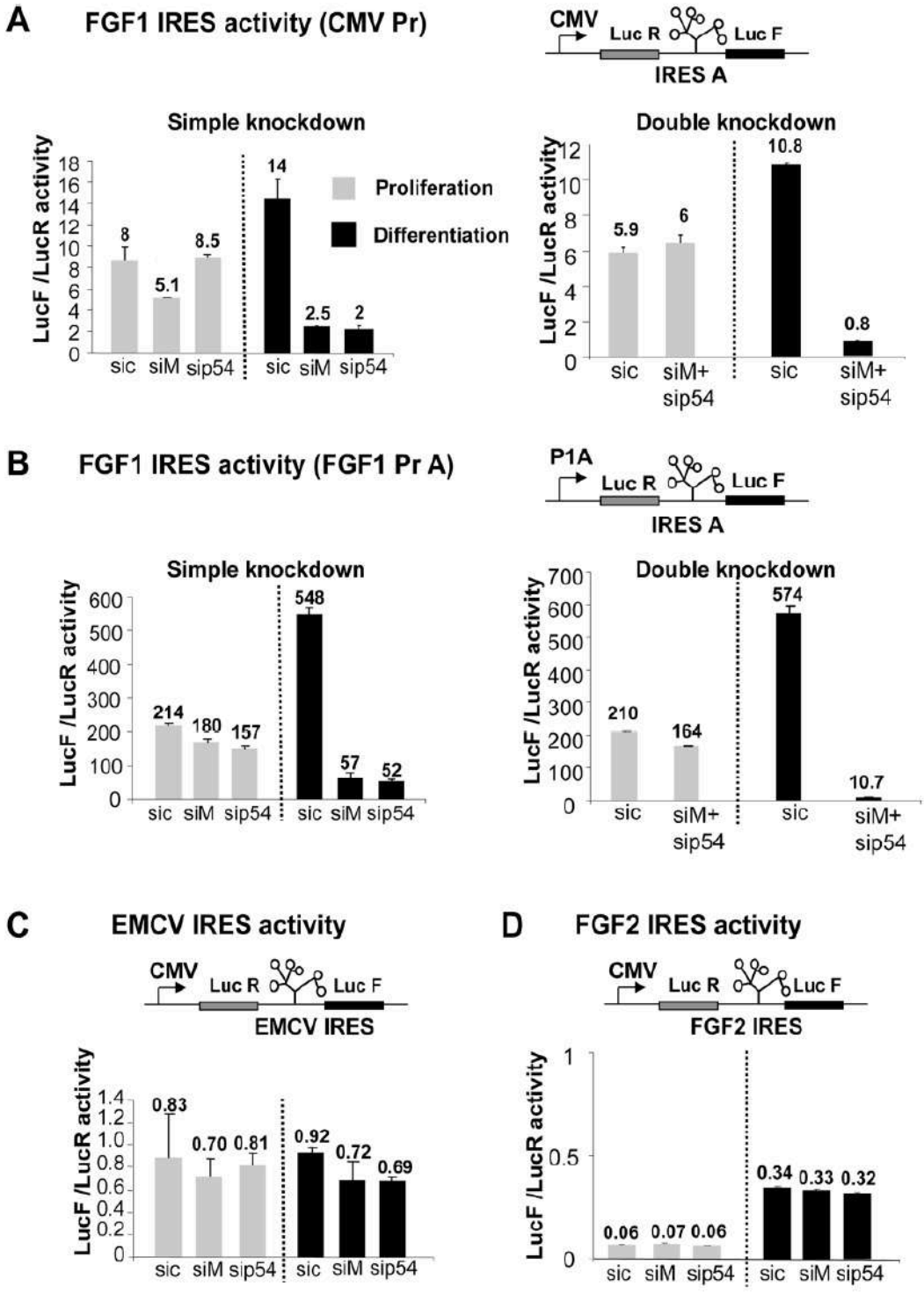
A
FGF1 IRES activity (CMV Pr)
CMV
Luc R
Luc F
IRES A
Simple knockdown
LucF /LucR activity
Proliferation
Differentiation
8
5.1
8.5
14
2.5
2
sic
siM
sip54
Double knockdown
5.9
6
10.8
0.8
siM+ sip54
B
FGF1 IRES activity (FGF1 Pr A)
P1A
214
180
157
548
57
52
210
164
574
10.7
C
EMCV IRES activity
EMCV IRES
0.83
0.70
0.81
0.92
0.72
0.69
D
FGF2 IRES activity
FGF2 IRES
0.06
0.07
0.06
0.34
0.33
0.32

Fig 4. Effect of hnRNPM and/or p54^{nrb} knockdown on the regulation of FGF1 IRES A activity during myoblast differentiation. C2C12 cells were first transfected with bicistronic plasmids and 48h later with siRNAs targeting hnRNPM (siM), p54^{nrb} (sip54) or control (sic), (see Fig 3). Luciferase activities were measured as described in Mat. & Meth two days after siRNA transfection, from C2C12 myoblasts maintained in proliferation (grey histogram) or serum-starved to induce differentiation (day 2, black histogram). The bicistronic cassette contains LucR and LucF reporter genes, separated by different IRESs (FGF1, FGF2 or EMCV). LucR and LucF activities reflect the cap-dependent and IRES dependent translation, respectively [4]. The knockdown efficiency was checked by Western blot (S2 File). (A, B) FGF1 IRES activities were measured in C2C12 myoblasts in proliferation (grey histogram) and differentiation two days after serum-starvation treatment (black histogram). The bicistronic constructs are schematized. The bicistronic cassette is under the control of either the CMV promoter (A) or the FGF1 promoter A (B). Single and double knockdowns are shown in left and right panels, respectively. IRES activities are represented as LucF/LucR ratios. (C, D). Absence of effect of hnRNPM and/or p54^{nrb} knockdown on the regulation of EMCV and FGF2 IRESs during myoblast differentiation. Activities of EMCV (C) and FGF2 (D) IRESs were measured as above. For all panels, experiments were performed in biological triplicates and repeated at least three times. A representative experiment is shown (mean +- standard deviation).

doi:10.1371/journal.pone.0136466.g004

control, we used a construct containing a hairpin between the two cistrons instead of an IRES. The LucF/LucR ratios in the absence of an IRES were very low for both DNA and RNA transfections and were not affected by hnRNPM or p54 knockdown (Fig 6E and 6F). These results suggested that a nuclear step may be a prerequisite to IRES induction by the hnRNPM and p54^{nrb}.

To go further with this hypothesis, we transfected C2C12 with a construct containing a deleted form of promoter F1A, P1AΔ1–391 (Fig 7). Measurements of LucR activity showed that this promoter is about ten times less efficient than the wild type promoter, whereas it was still sensitive to hnRNPM and p54 knockdown (Fig 7A). In contrast, in the presence of the deleted form of the promoter, IRES activity was no longer induced and was very mildly altered by the knockdown of hnRNPM or p54^{nrb} (Fig 7B).

These two sets of data showed that FGF1 IRES induction by hnRNPM and p54^{nrb} depends on a sequence present in the promoter and involves multifunctional roles of these proteins.

p54^{nrb} and hnRNPM are required for FGF1 induction and myotube formation

To determine whether p54^{nrb} and hnRNPM are responsible for endogenous FGF1 induction during differentiation and if these proteins exhibit a physiological role in the development of muscle fiber, simple and double knockdowns of hnRNPM and/or p54^{nrb} were performed (Fig 8A). Expression of FGF1, analyzed by Western Blot, was strongly inhibited by the simple or double knockdown (Fig 8A and data not shown). Furthermore, formation of myotubes was drastically affected by knockdown of p54^{nrb} or hnRNPM, and even more strongly inhibited by the double knockdown (Fig 8B). Decrease of endogenous FGF1 expression upon treatment with siRNA against p54^{nrb} and/or hnRNPM confirmed that these two proteins are involved in the control of FGF1 expression and consequently in its induction during differentiation. In addition, these data also revealed that p54^{nrb} and hnRNPM are required for differentiation of myoblasts into myotubes, revealing the important role of these proteins in myogenesis.

Discussion

The present data reveal that FGF1 IRES activity is promoter-dependent and that this process is governed by two multifunctional trans-acting factors, p54^{nrb} and hnRNPM. P54^{nrb} and hnRNPM also appear as crucial actors of myoblast differentiation, demonstrating the physiological relevance of this new mechanism.

Nuclear formation of the IRESome

The present data suggest that IRESome formation occurs in the nuclear compartment. The regulating features of p54^{nrb} and hnRNPM on both promoter and IRES activities are not

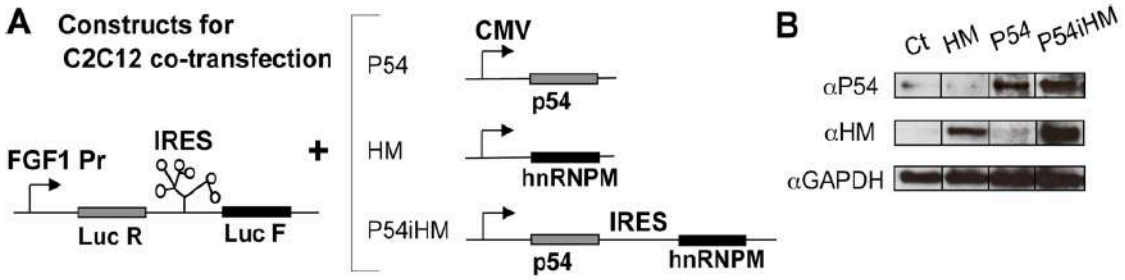
A
Constructs for C2C12 co-transfection
FGF1 Pr
IRES
Luc R
Luc F
+
P54
CMV
p54
HM
hnRNPM
P54iHM
IRES
p54
hnRNPM
B
Ct HM P54 P54iHM
αP54
αHM
αGAPDH

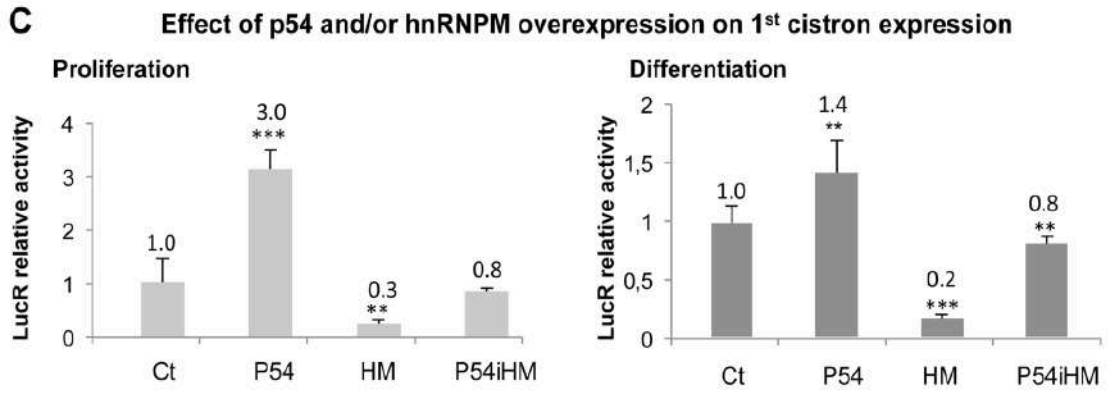
C
Effect of p54 and/or hnRNPM overexpression on 1st cistron expression
Proliferation
LucR relative activity
1.0
3.0
***
0.3
**
0.8
Ct
P54
HM
P54iHM
Differentiation
LucR relative activity
1.0
1.4
**
0.2
***
0.8
**
Ct
P54
HM
P54iHM

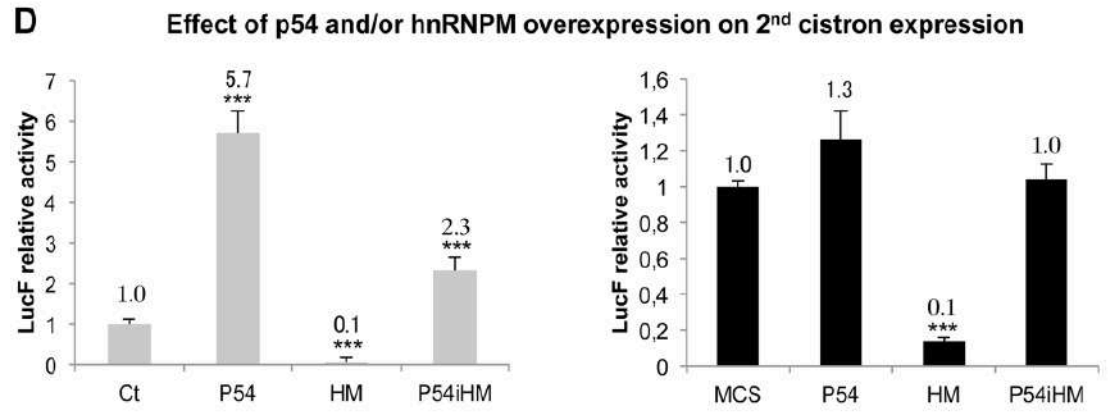
D
Effect of p54 and/or hnRNPM overexpression on 2nd cistron expression
LucF relative activity
1.0
5.7
***
0.1
***
2.3
***
Ct
P54
HM
P54iHM
LucF relative activity
1.0
1.3
0.1
***
1.0
MCS
P54
HM
P54iHM

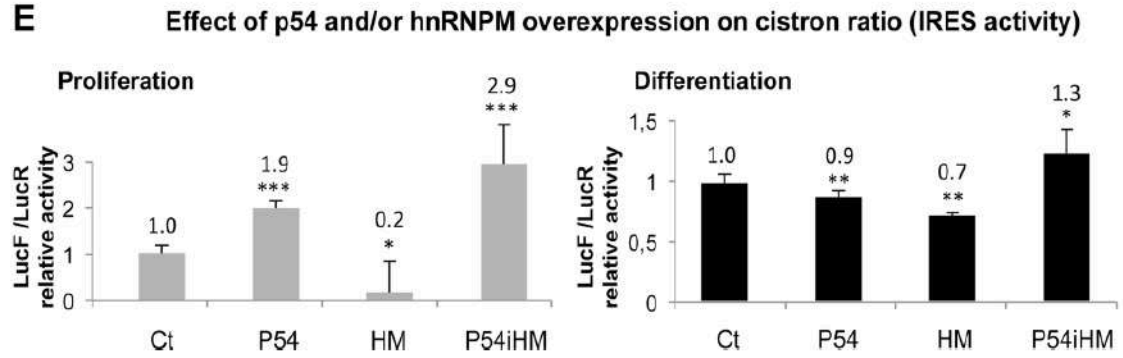
E
Effect of p54 and/or hnRNPM overexpression on cistron ratio (IRES activity)
Proliferation
LucF /LucR relative activity
1.0
1.9
***
0.2
*
2.9
***
Ct
P54
HM
P54iHM
Differentiation
LucF /LucR relative activity
1.0
0.9
**
0.7
**
1.3
*
Ct
P54
HM
P54iHM

Fig 5. Cooperative effect of p54^{nrb} and hnRNPM on FGF1 IRES activation. (A) Schema of the constructs used for C2C12 cell co-transfection. The target plasmid is the bicistronic dual luciferase vector with the FGF1 promoter and IRES. The effector plasmids express p54^{nrb} (p54) or hnRNPM (HM), or co-express p54^{nrb} and hnRNPM. The latter plasmid is a bicistronic contruct containing the FGF1 IRES. (B) Western blots of transfected proliferating C2C12 cell extracts using antibodies against p54(αHM), hnRNPM (αHM) of GAPDH as a control (αGAPDH). (C-E) Luciferase activities measurement of co-transfected proliferating or differentiating C2C12 cell extracts. LucR activity reflects the FGF1 mRNA promoter activity (as cap-dependent translation does not significantly vary, as shown by RNA transfection, see Table B in S4 File) (C). LucF reflects IRES-dependent translation but is also dependent on mRNA amount (D). LucF/LucR ratio reflects the IRES activity normalized to mRNA amount, expressed relatively to the control (co-transfection with empty vector) (E). Experiments were performed in biological triplicates and repeated three times. The statistical test used is the Student test. (mean +- standard deviation, *p<0.05, **p<0.01, ***<0.001).

doi:10.1371/journal.pone.0136466.g005

independent events, as these two translational regulators do not work when the promoter is absent (RNA transfection) or inactivated (promoter mutation).

The importance of ITAF subcellular localization in the regulation of their activity appeared a few years ago, with the first observation that a nuclear event is required in the control of c-myc IRES activity [18]. Later, it has been shown that shuttling of ITAFs, such as hnRNP A1, RBM4, PTB and PCBP1, between the nucleus and the cytoplasm influences their activity [24, 27, 30, 41]. Two different mechanisms have been proposed [42]: 1) the nuclear localized ITAFs may associate with their target in this compartment, resulting in the sequestration of the mRNA in the nucleus until an appropriate signal occurs, allowing cytoplasmic export and translation, 2) the ITAFs may be primarily located in the nucleus to keep them separate from their target IRESs and await a signal that warrants their accumulation in the cytoplasm. These two models could apply to cellular and viral IRESs, respectively, as explained by Semler & Waterman who argue that nuclear versus cytoplasmic synthesis of IRES-containing mRNAs is a major determinant in assembling different RNA–protein complexes [43]. The synthesis of uncapped picornaviral mRNAs occurs in the cytoplasm, in contrast to cellular mRNAs, which are transcribed in the nucleus and then exported to the cytoplasm. Our study not only reinforces the hypothesis that the IRESome is constituted in the nucleus, but further elaborates this model by showing that its formation is influenced by the promoter activity.

HnRNPM and p54^{nrb} cooperate in activation of IRES-dependent translation

The IRES-regulating function of hnRNPM discovered in our study represents a novel finding, as well as its cooperative activity with p54^{nrb}. Interestingly, nuclear interaction of hnRNPM and p54^{nrb} has been previously reported [40]. Like other hnRNPs, hnRNPM has been first identified as a splicing regulatory protein, associated with early spliceosomes where it modulates the alternative splicing pattern of specific mRNAs including the FGF receptor [39, 40]. Interestingly, hnRNPM has also been reported to influence the localization of *nanos* mRNA by binding to its 3' UTR [44]. The additional function of hnRNPM shown in our study confirms that hnRNPs are multifunctional, depending on their interacting partners.

p54^{nrb}/NONO is also a multifunctional protein. It has been previously shown to associate with 5' splicing sites in large transcription-splicing complexes, providing a direct role for this protein in linking transcription to splicing [3, 45]. P54^{nrb} also behaves as a specific transcriptional activator, binding to the intracisternal A particle proximal enhancer element, and as an RNA binding protein, preferentially binding to the sequence UAGGGA/U identified by SELEX [37]. In addition, p54^{nrb} has been identified as an ITAF of the myc family IRESs (c-, L- and N-myc), and has also been shown to stimulate the APAF-1 IRES [46]. Here we demonstrate that p54^{nrb} is able to cooperate with hnRNPM, suggesting that the two proteins may activate the FGF1 IRES as a complex. Unexpectedly, hnRNPM overexpression is inhibitory, whereas knockdown experiments clearly showed it is required for both IRES and promoter activation. We hypothesize that excess of hnRNPM might inhibit p54^{nrb} functions on FGF1 gene

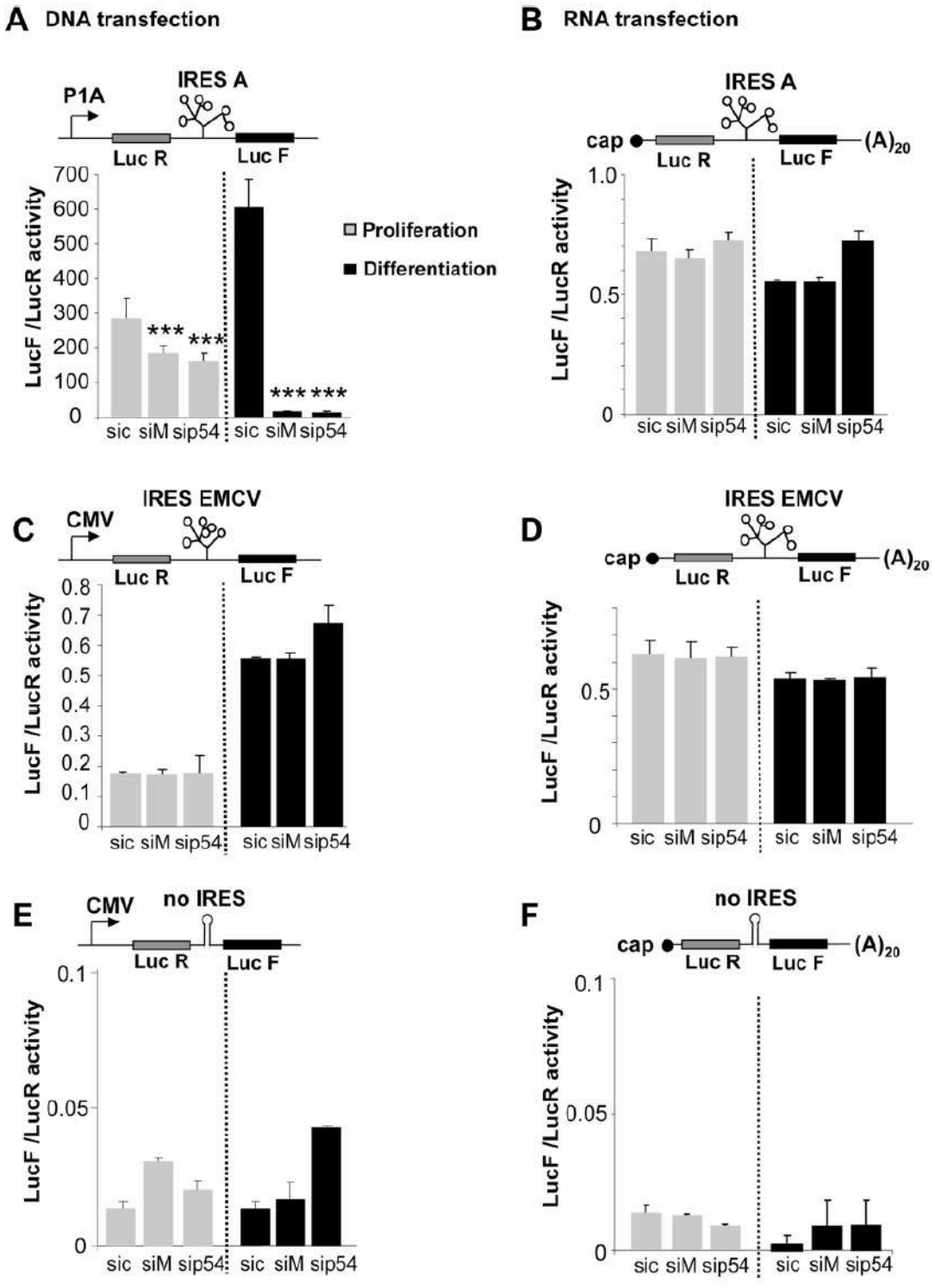
A DNA transfection
P1A
IRES A
Luc R
Luc F
LucF /LucR activity
700
600
500
400
300
200
100
0
***
***
***
***
sic siM sip54
sic siM sip54
Proliferation
Differentiation
B RNA transfection
IRES A
cap
Luc R
Luc F
(A)20
LucF /LucR activity
1.0
0.5
0
sic siM sip54
sic siM sip54
C
CMV
IRES EMCV
Luc R
Luc F
LucF /LucR activity
0.8
0.7
0.6
0.5
0.4
0.3
0.2
0.1
0
sic siM sip54
sic siM sip54
D
IRES EMCV
cap
Luc R
Luc F
(A)20
LucF /LucR activity
0.5
0
sic siM sip54
sic siM sip54
E
CMV
no IRES
Luc R
Luc F
LucF /LucR activity
0.1
0.05
0
sic siM sip54
sic siM sip54
F
no IRES
cap
Luc R
Luc F
(A)20
LucF /LucR activity
0.1
0.05
0
sic siM sip54
sic siM sip54

Fig 6. Comparison of IRES activities following DNA or RNA transfection. (A, C, E) C2C12 cells were transfected with bicistronic plasmids containing either the FGF1 IRES, or EMCV IRES or a hairpin (control without IRES) and with siRNA siM, sip54 or sic, and IRES activities measured as in Fig 4B, 4D and 4F C2C12 cells were transfected with siRNA siM, sip54 or sic and 24h later with bicistronic mRNAs containing either the FGF1 IRES, or the EMCV IRES, or a hairpin as above. mRNAs were transcribed in vitro, capped and polyadenylated, as described in Mat. & Meth. The LucF/LucR activity ratio was measured 12h post-transfection. Experiments were performed in biological triplicates and repeated three times. The Student test was used. A representative experiment is shown (mean +- standard deviation, *p<0.05, **p<0.01, ***<0.001). For A and B, the Luc R and Luc F values are shown in S4 File.

doi:10.1371/journal.pone.0136466.g006

expression, presumably by preventing $p54^{nrb}$ binding to FGF1 DNA and RNA due to an inadequate stoechiometry of the two proteins.

Although the proteins are expressed in proliferating cells, they are not found in the complex with the IRES or the promoter A. This suggests that the proteins might carry different post-translational modifications. Alternatively these proteins could join the complex through the interaction with another protein, which is absent in the proliferating cells and remains to be discovered. This could also explain that overexpressed hnRNPM is not functional.

Very few proteins were bound to the EMCV IRES, which may be explained by the low efficiency of the EMCV IRES in myoblasts. However, we were also surprised that no transcription factor was bound to promoter DNA. This indicates that BIA-MS does not provide an exhaustive view of all proteins bound to RNA or DNA and that one can miss important proteins. This also explains that we have missed hnRNPM present in the promoter-bound complex.

Although the direct interaction of $p54^{nrb}$ and hnRNPM with RNA has not been demonstrated, the present study strongly suggest that the two proteins are ITAFs involved in FGF1 IRES activation. However The BIA-MS data provides a list of additional proteins bound to the FGF1 IRES, including histones and splicing factors. These proteins may participate in the IRESome ribonucleoprotein.

Promoter-dependent activation of the FGF1 IRES may involve transcription or mRNA stabilization

Promoter-dependent translation controlled by hnRNPM and $p54^{nrb}$ asks the question of how a promoter is able to impact on translation, which is in principle cytoplasmic.

One among several possible models, one can propose transcription/translation coupling: hnRNPM and $p54^{nrb}$ might be first recruited to the promoter, where they would contribute to transcription activation. This process would also facilitate hnRNPM and $p54^{nrb}$ binding onto mRNA IRES and subsequently activate IRES-dependent translation. A recent study supports the hypothesis of a co-transcriptional ITAF binding, by showing that the translation elongation factor eEF1A1 couples transcription to translation during heat shock response [47]. These authors have demonstrated that eEF1A1 activates HSP70 transcription, then associates with RNA polymerase II, binds the mRNA 3'UTR, stabilizes it and facilitates its nuclear export to active ribosomes. hnRNPM and $p54^{nrb}$ may well have a similar mode of action, except that they bind to the mRNA 5'UTR and directly activate IRES-dependent translation by their ITAF function.

Other hnRNPs have been previously described for their involvement in transcription: hnRNPK, reported as a transcription factor interacting with the RNA polymerase II machinery in the c-myc promoter, and hnRNP A1, involved in the transcription of the KRAS proto-oncogene [48, 49]. More recently, hnRNPC has been shown to regulate transcription in osteoblasts [50]. Interestingly, hnRNP A1 and-K also exhibit an ITAF function, although no coupling between transcriptional and translational functions has been mentioned [24, 25, 30].

An alternative model to explain promoter-dependent regulation of translation by hnRNPM and $p54^{nrb}$ might be their effect on mRNA stability. Binding of these proteins to the FGF1 promoter would not have an effect on transcription but would facilitate their binding to the

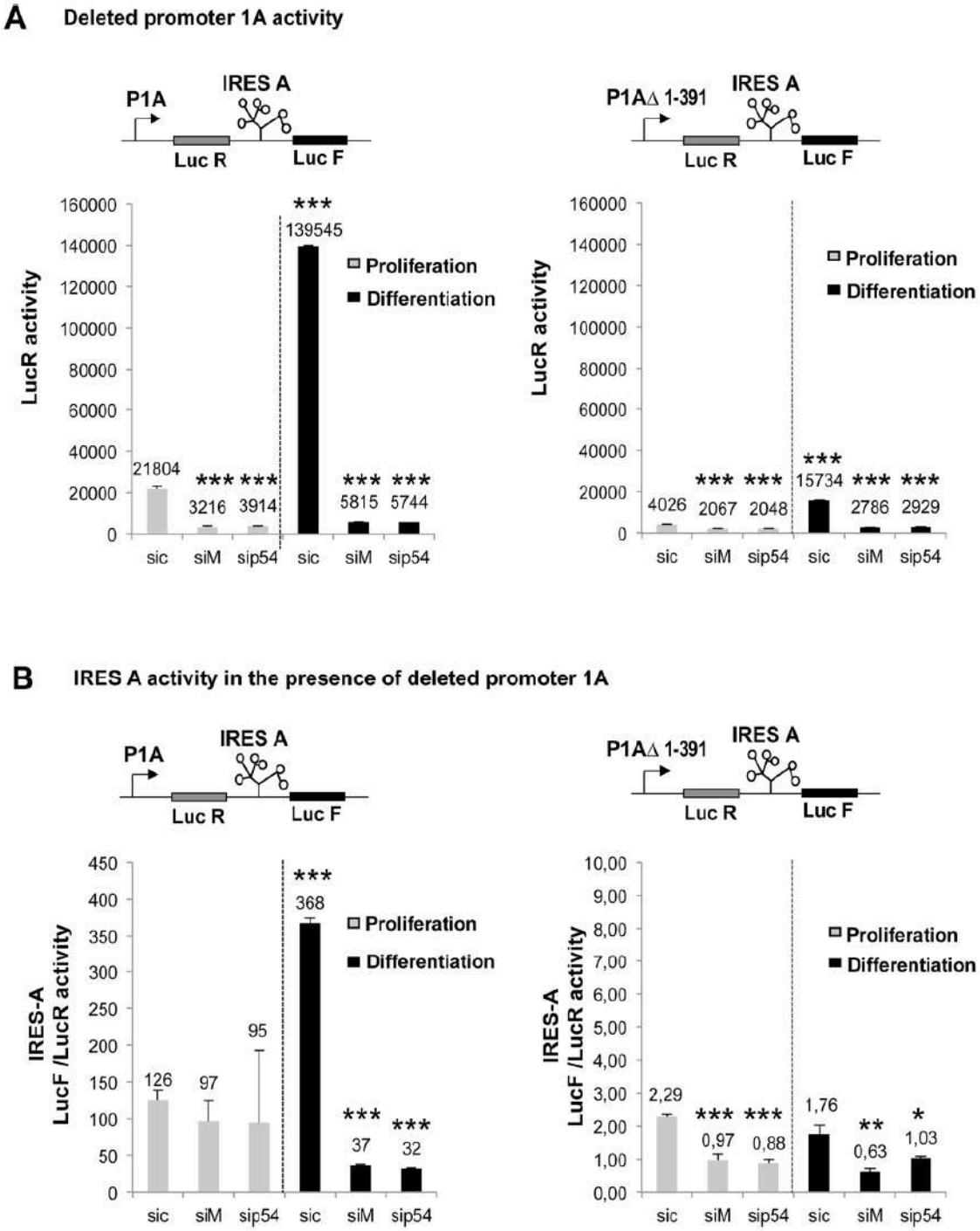

Fig 7. Influence of transcription level on the activity of the FGF1 IRES A. C2C12 cells were transfected with bicistronic plasmids containing either the complete promoter 1A or a deleted promoter lacking nucleotides 1 to 391. Transfected cells were treated 24h later with siRNA siM, sip54 or sic, and luciferase activities were measured as in Fig 6. (A) mRNA expression in the presence of promoter 1A and 1AΔ1–391 reflected by the LucR activities. (B) Activity of FGF1 IRES A in the presence of promoter 1A and 1AΔ1–391, reflected by the LucF/LucR ratio as above. Experiments were performed in biological triplicates and repeated three times. The statistical test used is the Student test. (mean +- standard deviation, *p<0.05, **p<0.01, ***<0.001).

doi:10.1371/journal.pone.0136466.g007

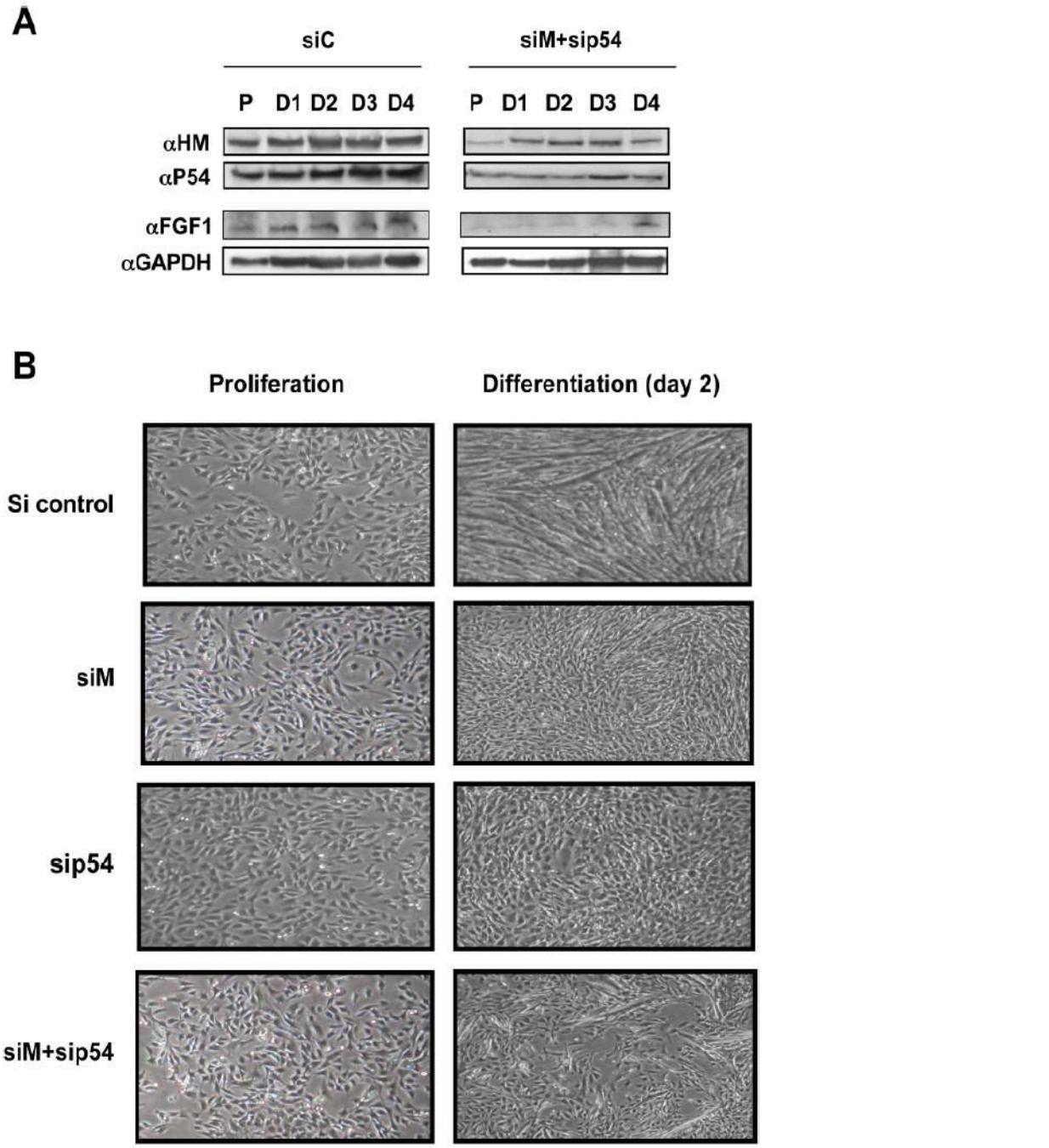

Fig 8. Role of hnRNPM and p54^{nrb} in myoblast differentiation. (A) Effect of hnRNPM and p54^{nrb} knockdown on expression of endogenous FGF1. C2C12 cells were transfected with siRNA, siM+sip54 or sic. Western blot was performed as above using cell extracts of proliferating (P) and differentiating myoblasts (D1 to D4). GAPDH was used as a normalization control. These data correspond to a representative experiment (repeated at least three times). (B) Effect of hnRNPM and/or p54^{nrb} knockdown on myotube formation. C2C12 cells were transfected with siRNA siM, sip54, siM+sip54 or sic and myotube formation was followed by phase contrast microscopy. Data are shown for day 2 cells compared to proliferative cells.

doi:10.1371/journal.pone.0136466.g008

nascent mRNA, resulting in mRNA stabilization, as has been shown for the yeast protein Dbf2P [51]. These authors demonstrate that Dbf2p is recruited to the SW15 and CBL2 promoters, and co-transcriptionally deposited onto the SW15 and CLB2 mRNAs. Once they are exported into the cytoplasm, the two mRNAs are protected from degradation by Dbf2p. According to this model, hnRNPM and $p54^{nrb}$ binding to mRNA might have the double effect of stabilizing the FGF1 mRNA and activating the IRES. Anyway, further investigation is needed to determine whether the promoter-dependent function of hnRNPM and $p54^{nrb}$ involves transcription enhancement or RNA stabilization.

Promoter-dependent translation, a physiologically relevant mechanism during myogenesis

An important feature of our study is the physiological relevance of $p54^{nrb}$ and hnRNPM function in myoblast differentiation. It clearly appears that $p54^{nrb}$ and hnRNPM are important for myotube formation and such a role is novel for these two proteins. We have previously shown that FGF1 is required for myoblast differentiation [4]. Thus the effect of hnRNPM and/or p54 knockdown on myoblast differentiation may be a direct consequence of FGF1 downregulation. Alternatively, hnRNPM and $p54^{nrb}$ may act on the expression of additional IRES-containing genes, including Smad5 and utrophin A IRESs whose activites have been reported in myoblasts [17, 52, 53]. It will be of great interest to investigate the possible role of hnRNPM and $p54^{nrb}$ in the promoter-dependent regulation of such IRESs during muscle development.

As seen with the coordination of transcription and mRNA processing, such as splicing, whose regulators often exhibit the additional function of ITAFs (i.e. hnRNPs), one can expect that the promoter-dependent translation mechanism described in our study will extend to other IRES-containing mRNAs. Such a mechanism becomes more significant for genes that are induced in response to conditions that block cap-dependent translation, such as stress. Coupling of IRES activation with the promoter guarantees that the induction of a given gene in response to a specific stimulus will result in the synthesis of that gene product.

Supporting Information

S1 File. Identification of RNA and DNA binding proteins by BIA-MS. Total or nuclear extracts of differentiating C2C12 myoblasts were injected (see Fig 1) as analytes in several BIACORE 3000 channels after immobilization of ligands corresponding to FGF1 IRES A, EMCV IRES, FGF1 promoter A or CMV promoter. Bound proteins were recovered as described in Mat. & Meth. and identified by mass spectrometry. For each BIA-MS experiment, 6 recovery cycles were pooled to obtain a sufficient RU quantity (about 2000 RU). Mass spectrometry analysis was performed as described in Mat. & Meth. Bound proteins (RNA and DNA binding proteins) are listed here. (Table A) FGF1 IRES RNA, C2C12 total extracts, (Table B) FGF1 IRES RNA, C2C12 nuclear extracts, (Table C) EMCV IRES RNA, C2C12 total extracts, (Table D) FGF1 promoter A DNA, C2C12 nuclearFGF1 extracts.
(DOC)

S2 File. Knockdown of hnRNPM and/or $p54^{nrb}$. C2C12 cells were first transfected with bicistronic plasmids and 48h later with siRNAs targeting hnRNPM (siM), $p54^{nrb}$ (sip54) or control (sic). RNA levels and luciferase activities are presented in Figs 3 and 4, respectively, from C2C12 myoblasts maintained in proliferation or at day 2 of differentiation. $p54^{nrb}$ and hnRNPM expression was analysed by Western blot following single knockdown with siRNA siM (Fig A) or sip54 (Fig B) or double knockdown with the two siRNAs together (Fig C).
(TIF)

S3 File. Effect of hnRNPM and/or p54^{nrb} knockdown on the regulation of FGF1 IRES A using siRNAs different from the smartpool. C2C12 cells co-transfected with bicistronic plasmids and 48h later with a siRNA against hnRNPM (siM), p54^{nrb} (sip54) or siRNA control (sic). SiM and siP54 corresponded to sequences different from that of the siRNA smartpools used in Fig 4. (Fig A) Ratio of the luciferase activities measured as in Fig 4, two days after siRNA transfection, from differentiating C2C12 myoblasts (day 2). (Fig B) The knockdown was checked by Western blot as in S2 File.
(TIF)

S4 File. Effect of hnRNPM and p54 knockdown on FGF1 IRES activity after DNA or RNA transfection. (Table A) C2C12 cells were transfected with bicistronic plasmids containing the FGF1 promoter and IRES (see Fig 6) and with siRNA siM, sip54 or sic. (Table B) C2C12 cells were transfected with siRNA siM, sip54 or sic and 24h later with bicistronic mRNA containing the FGF1 IRES (see Fig 6). mRNAs were transcribed in vitro, capped and polyadenylated, as described in Mat. & Meth. For Tables A and B, firefly and *renilla* luciferase activities were measured. Values are presented as well as the LucF/LucR (F/R) ratio representing the IRES activity. Experiments were performed in biological triplicates and repeated three times. The Student test was used (mean +- standard deviation).
(DOC)

Acknowledgments

We thank J.J. Maoret (Genotoul quantitative transcriptomics facility), B. Montsarrat (Genoutoul Proteomics facility), P. Billon, N. Fenie, J.B. Mauroux, J. Mermet and M. Serrero for technical assistance. This work was supported by Association Française contre les Myopathies (AFM), Association pour la Recherche sur le Cancer, Ligue pour la Recherche Contre le Cancer, Cancéropole GSO, INCA, Fondation de l'Avenir, Région Midi-Pyrénées, European funding (FEDER). N.A. and E.R.G. had a fellowship from AFM, F.H. from the Région Midi-Pyrénées.

Author Contributions

Conceived and designed the experiments: EB AP BGS ACP. Performed the experiments: NA FH ERG MB FL FP RP CP. Analyzed the data: NA FH ERG MB RP EB CP OBS BGS ACP. Contributed reagents/materials/analysis tools: ACP. Wrote the paper: NA FH ERG AP BGS ACP.

References

1. Braunschweig U, Gueroussov S, Plocik AM, Graveley BR, Blencowe BJ. Dynamic integration of splicing within gene regulatory pathways. Cell. 2013 Mar 14; 152(6):1252–69. PMID: 23498935. Pubmed Central PMCID: 3642998. Epub 2013/03/19. eng. doi: 10.1016/j.cell.2013.02.034
2. Maniatis T, Reed R. An extensive network of coupling among gene expression machines. Nature. 2002 Apr 4; 416(6880):499–506. PMID: 11932736.
3. Pandit S, Wang D, Fu XD. Functional integration of transcriptional and RNA processing machineries. Curr Opin Cell Biol. 2008 Jun; 20(3):260–5. PMID: 18436438. doi: 10.1016/j.ceb.2008.03.001
4. Conte C, Ainaoui N, Delluc-Clavieres A, Khoury MP, Azar R, Pujol F, et al. Fibroblast growth factor 1 induced during myogenesis by a transcription-translation coupling mechanism. Nucleic Acids Res. 2009 Sep; 37(16):5267–78. PMID: 19561198. doi: 10.1093/nar/gkp550
5. Madiai F, Hackshaw KV, Chiu IM. Characterization of the entire transcription unit of the mouse fibroblast growth factor 1 (FGF-1) gene. Tissue-specific expression of the FGF-1.A mRNA. J Biol Chem. 1999 Apr 23; 274(17):11937–44. PMID: 10207015.

6. Myers RL, Chedid M, Tronick SR, Chiu IM. Different fibroblast growth factor 1 (FGF-1) transcripts in neural tissues, glioblastomas and kidney carcinoma cell lines. Oncogene. 1995 Aug 17; 11(4):785–9. PMID: 7544453.
7. Myers RL, Payson RA, Chotani MA, Deaven LL, Chiu IM. Gene structure and differential expression of acidic fibroblast growth factor mRNA: identification and distribution of four different transcripts. Oncogene. 1993 Feb; 8(2):341–9. PMID: 7678925.
8. Chotani MA, Chiu IM. Differential regulation of human fibroblast growth factor 1 transcripts provides a distinct mechanism of cell-specific growth factor expression. Cell Growth Differ. 1997 Sep; 8(9):999–1013. PMID: 9300182.
9. Chotani MA, Payson RA, Winkles JA, Chiu IM. Human fibroblast growth factor 1 gene expression in vascular smooth muscle cells is modulated via an alternate promoter in response to serum and phorbol ester. Nucleic Acids Res. 1995 Feb 11; 23(3):434–41. PMID: 7533902. Pubmed Central PMCID: 306694. Epub 1995/02/11. eng.
10. Payson RA, Chotani MA, Chiu IM. Regulation of a promoter of the fibroblast growth factor 1 gene in prostate and breast cancer cells. The Journal of steroid biochemistry and molecular biology. 1998 Aug; 66(3):93–103. PMID: 9719443. Epub 1998/08/27. eng.
11. Martineau Y, Le Bec C, Monbrun L, Allo V, Chiu IM, Danos O, et al. Internal ribosome entry site structural motifs conserved among mammalian fibroblast growth factor 1 alternatively spliced mRNAs. Mol Cell Biol. 2004 Sep; 24(17):7622–35. PMID: 15314170.
12. Baird SD, Lewis SM, Turcotte M, Holcik M. A search for structurally similar cellular internal ribosome entry sites. Nucleic Acids Res. 2007; 35(14):4664–77. PMID: 17591613.
13. Bonnal S, Schaeffer C, Creancier L, Clamens S, Moine H, Prats AC, et al. A single internal ribosome entry site containing a G quartet RNA structure drives fibroblast growth factor 2 gene expression at four alternative translation initiation codons. J Biol Chem. 2003 Oct 10; 278(41):39330–6. PMID: 12857733.
14. Morfoisse F, Kuchnio A, Frainay C, Gomez-Brouchet A, Delisle MB, Marzi S, et al. Hypoxia induces VEGF-C expression in metastatic tumor cells via a HIF-1alpha-independent translation-mediated mechanism. Cell reports. 2014 Jan 16; 6(1):155–67. PMID: 24388748. Epub 2014/01/07. eng. doi: 10.1016/j.celrep.2013.12.011
15. Braunstein S, Karpisheva K, Pola C, Goldberg J, Hochman T, Yee H, et al. A hypoxia-controlled cap-dependent to cap-independent translation switch in breast cancer. Mol Cell. 2007 Nov 9; 28(3):501–12. PMID: 17996713.
16. Holcik M, Sonenberg N. Translational control in stress and apoptosis. Nat Rev Mol Cell Biol. 2005 Apr; 6(4):318–27. PMID: 15803138.
17. Shiroki K, Ohsawa C, Sugi N, Wakiyama M, Miura K, Watanabe M, et al. Internal ribosome entry site-mediated translation of Smad5 in vivo: requirement for a nuclear event. Nucleic Acids Res. 2002 Jul 1; 30(13):2851–61. PMID: 12087169. Pubmed Central PMCID: 117063. Epub 2002/06/28. eng.
18. Stoneley M, Subkhankulova T, Le Quesne JP, Coldwell MJ, Jopling CL, Belsham GJ, et al. Analysis of the c-myc IRES; a potential role for cell-type specific trans-acting factors and the nuclear compartment. Nucleic Acids Res. 2000 Feb 1; 28(3):687–94. PMID: 10637319.
19. Garcia-Blanco MA, Jamison SF, Sharp PA. Identification and purification of a 62,000-dalton protein that binds specifically to the polypyrimidine tract of introns. Genes Dev. 1989 Dec; 3(12A):1874–86. PMID: 2533575.
20. Jang SK, Wimmer E. Cap-independent translation of encephalomyocarditis virus RNA: structural elements of the internal ribosomal entry site and involvement of a cellular 57-kD RNA-binding protein. Genes Dev. 1990 Sep; 4(9):1560–72. PMID: 2174810.
21. Kim YK, Hahm B, Jang SK. Polypyrimidine tract-binding protein inhibits translation of bip mRNA. J Mol Biol. 2000 Nov 24; 304(2):119–33. PMID: 11080450.
22. Mitchell SA, Spriggs KA, Coldwell MJ, Jackson RJ, Willis AE. The Apaf-1 internal ribosome entry segment attains the correct structural conformation for function via interactions with PTB and unr. Mol Cell. 2003 Mar; 11(3):757–71. PMID: 12667457.
23. Pickering BM, Mitchell SA, Evans JR, Willis AE. Polypyrimidine tract binding protein and poly r(C) binding protein 1 interact with the BAG-1 IRES and stimulate its activity in vitro and in vivo. Nucleic Acids Res. 2003 Jan 15; 31(2):639–46. PMID: 12527772.
24. Bonnal S, Pileur F, Orsini C, Parker F, Pujol F, Prats AC, et al. Heterogeneous nuclear ribonucleoprotein A1 is a novel internal ribosome entry site trans-acting factor that modulates alternative initiation of translation of the fibroblast growth factor 2 mRNA. J Biol Chem. 2005 Feb 11; 280(6):4144–53. PMID: 15525641.

25. Evans JR, Mitchell SA, Spriggs KA, Ostrowski J, Bomsztyk K, Ostarek D, et al. Members of the poly (rC) binding protein family stimulate the activity of the c-myc internal ribosome entry segment in vitro and in vivo. Oncogene. 2003 Sep 11; 22(39):8012–20. PMID: 12970749.

26. Holcik M, Gordon BW, Korneluk RG. The internal ribosome entry site-mediated translation of antiapoptotic protein XIAP is modulated by the heterogeneous nuclear ribonucleoproteins C1 and C2. Mol Cell Biol. 2003 Jan; 23(1):280–8. PMID: 12482981.

27. Lin JC, Hsu M, Tarn WY. Cell stress modulates the function of splicing regulatory protein RBM4 in translation control. Proc Natl Acad Sci U S A. 2007 Feb 13; 104(7):2235–40. PMID: 17284590.

28. Spriggs KA, Bushell M, Mitchell SA, Willis AE. Internal ribosome entry segment-mediated translation during apoptosis: the role of IRES-trans-acting factors. Cell Death Differ. 2005 Jun; 12(6):585–91. PMID: 15900315.

29. Jo OD, Martin J, Bernath A, Masri J, Lichtenstein A, Gera J. Heterogeneous nuclear ribonucleoprotein A1 regulates cyclin D1 and c-myc internal ribosome entry site function through Akt signaling. J Biol Chem. 2008 Aug 22; 283(34):23274–87. PMID: 18562319. Pubmed Central PMCID: 2516998. Epub 2008/06/20. eng. doi: 10.1074/jbc.M801185200

30. Lewis SM, Veyrier A, Hosszu Ungureanu N, Bonnal S, Vagner S, Holcik M. Subcellular relocalization of a trans-acting factor regulates XIAP IRES-dependent translation. Mol Biol Cell. 2007 Apr; 18(4):1302–11. PMID: 17287399.

31. Roy R, Durie D, Li H, Liu BQ, Skehel JM, Mauri F, et al. hnRNPA1 couples nuclear export and translation of specific mRNAs downstream of FGF-2/S6K2 signalling. Nucleic Acids Res. 2014 Nov 10; 42 (20):12483–97. PMID: 25324306. Pubmed Central PMCID: 4227786. Epub 2014/10/18. eng. doi: 10.1093/nar/gku953

32. Lopez F, Pichereaux C, Burlet-Schiltz O, Pradayrol L, Monsarrat B, Esteve JP. Improved sensitivity of biomolecular interaction analysis mass spectrometry for the identification of interacting molecules. Proteomics. 2003 Apr; 3(4):402–12. PMID: 12687608.

33. Datar KV, Dreyfuss G, Swanson MS. The human hnRNP M proteins: identification of a methionine/arginine-rich repeat motif in ribonucleoproteins. Nucleic Acids Res. 1993 Feb 11; 21(3):439–46. PMID: 8441656.

34. Dong B, Horowitz DS, Kobayashi R, Krainer AR. Purification and cDNA cloning of HeLa cell p54nrb, a nuclear protein with two RNA recognition motifs and extensive homology to human splicing factor PSF and Drosophila NONA/BJ6. Nucleic Acids Res. 1993 Aug 25; 21(17):4085–92. PMID: 8371983. Pubmed Central PMCID: 310009. Epub 1993/08/25. eng.

35. Prats AC, Van den Berghe L, Rayssac A, Ainaoui N, Morfoisse F, Pujol F, et al. CXCL4L1-fibstatin cooperation inhibits tumor angiogenesis, lymphangiogenesis and metastasis. Microvascular research. 2013 Jun 4. PMID: 23747987. Epub 2013/06/12. Eng.

36. Bouyssie D, Gonzalez de Peredo A, Mouton E, Albigot R, Roussel L, Ortega N, et al. Mascot file parsing and quantification (MFPaQ), a new software to parse, validate, and quantify proteomics data generated by ICAT and SILAC mass spectrometric analyses: application to the proteomics study of membrane proteins from primary human endothelial cells. Molecular & cellular proteomics: MCP. 2007 Sep; 6(9):1621–37. PMID: 17533220. Epub 2007/05/30. eng.

37. Basu A, Dong B, Krainer AR, Howe CC. The intracisternal A-particle proximal enhancer-binding protein activates transcription and is identical to the RNA- and DNA-binding protein p54nrb/NonO. Mol Cell Biol. 1997 Feb; 17(2):677–86. PMID: 9001221.

38. Emili A, Shales M, McCracken S, Xie W, Tucker PW, Kobayashi R, et al. Splicing and transcription-associated proteins PSF and p54nrb/nonO bind to the RNA polymerase II CTD. Rna. 2002 Sep; 8 (9):1102–11. PMID: 12358429.

39. Hovhannisyan RH, Carstens RP. Heterogeneous ribonucleoprotein m is a splicing regulatory protein that can enhance or silence splicing of alternatively spliced exons. J Biol Chem. 2007 Dec 14; 282 (50):36265–74. PMID: 17959601.

40. Marko M, Leichter M, Patrinou-Georgoula M, Guialis A. hnRNP M interacts with PSF and p54(nrb) and co-localizes within defined nuclear structures. Exp Cell Res. 2010 Feb 1; 316(3):390–400. PMID: 19874820. doi: 10.1016/j.yexcr.2009.10.021

41. Dobbyn HC, Hill K, Hamilton TL, Spriggs KA, Pickering BM, Coldwell MJ, et al. Regulation of BAG-1 IRES-mediated translation following chemotoxic stress. Oncogene. 2008 Feb 14; 27(8):1167–74. PMID: 17700523.

42. Lewis SM, Holcik M. For IRES trans-acting factors, it is all about location. Oncogene. 2008 Feb 14; 27 (8):1033–5. PMID: 17767196.

43. Semler BL, Waterman ML. IRES-mediated pathways to polysomes: nuclear versus cytoplasmic routes. Trends Microbiol. 2008 Jan; 16(1):1–5. PMID: 18083033.

44. Jain RA, Gavis ER. The Drosophila hnRNP M homolog Rumpelstiltskin regulates nanos mRNA localization. Development. 2008 Mar; 135(5):973–82. PMID: 18234721. doi: 10.1242/dev.015438

45. Kameoka S, Duque P, Konarska MM. p54(nrb) associates with the 5' splice site within large transcription/splicing complexes. Embo J. 2004 Apr 21; 23(8):1782–91. PMID: 15057275.

46. Cobbold LC, Spriggs KA, Haines SJ, Dobbyn HC, Hayes C, de Moor CH, et al. Identification of internal ribosome entry segment (IRES)-trans-acting factors for the Myc family of IRESs. Mol Cell Biol. 2008 Jan; 28(1):40–9. PMID: 17967896.

47. Vera M, Pani B, Griffiths LA, Muchardt C, Abbott CM, Singer RH, et al. The translation elongation factor eEF1A1 couples transcription to translation during heat shock response. eLife. 2014; 3:e03164. PMID: 25233275. Pubmed Central PMCID: 4164936. Epub 2014/09/19. eng. doi: 10.7554/eLife.03164

48. Michelotti EF, Michelotti GA, Aronsohn AI, Levens D. Heterogeneous nuclear ribonucleoprotein K is a transcription factor. Mol Cell Biol. 1996 May; 16(5):2350–60. PMID: 8628302.

49. Xodo L, Paramasivam M, Membrino A, Cogoi S. Protein hnRNPA1 binds to a critical G-rich element of KRAS and unwinds G-quadruplex structures: implications in transcription. Nucleic Acids Symp Ser (Oxf). 2008 (52:):159–60. PMID: 18776302.

50. Lisse TS, Vadivel K, Bajaj SP, Chun RF, Hewison M, Adams JS. The heterodimeric structure of heterogeneous nuclear ribonucleoprotein C1/C2 dictates 1,25-dihydroxyvitamin D-directed transcriptional events in osteoblasts. Bone research. 2014; 2. PMID: 25506471. Pubmed Central PMCID: 4261231. Epub 2014/12/17. Eng.

51. Trcek T, Larson DR, Moldon A, Query CC, Singer RH. Single-molecule mRNA decay measurements reveal promoter- regulated mRNA stability in yeast. Cell. 2011 Dec 23; 147(7):1484–97. PMID: 22196726. Pubmed Central PMCID: 3286490. Epub 2011/12/27. eng. doi: 10.1016/j.cell.2011.11.051

52. Miura P, Coriati A, Belanger G, De Repentigny Y, Lee J, Kothary R, et al. The utrophin A 5'-UTR drives cap-independent translation exclusively in skeletal muscles of transgenic mice and interacts with eEF1A2. Hum Mol Genet. 2010 Apr 1; 19(7):1211–20. PMID: 20053670. doi: 10.1093/hmg/ddp591

53. Miura P, Thompson J, Chakkalakal JV, Holcik M, Jasmin BJ. The utrophin A 5'-untranslated region confers internal ribosome entry site-mediated translational control during regeneration of skeletal muscle fibers. J Biol Chem. 2005 Sep 23; 280(38):32997–3005. PMID: 16061482.

Ainaoui et al, S1 file.

A: BIA-MS data: total C2C12 extract proteins bound to the FGF1 IRES A RNA.

AC	ID	Description	MW	pI	Score	Peptides	Protein Coverage (%)
P20152	VIME_MOUSE	Vimentin	53655.06	5.06	400.67	27	52.4
P62737	ACTA_MOUSE	Actin. aortic smooth muscle	41981.81	5.23	270.48	15	10.1
P60710	ACTB_MOUSE	Actin. cytoplasmic 1	41709.73	5.29	258.1	15	10.2
P99024	TBB5_MOUSE	Tubulin beta-5 chain	49638.97	4.78	120.76	5	2.9
P62908	RS3_MOUSE	40S ribosomal protein S3	26657.41	9.68	112.42	6	11.4
P62264	RS14_MOUSE	40S ribosomal protein S14	16262.53	10.07	88.8	2	10.5
P31001	DESM_MOUSE	Desmin	53465.04	5.21	87.77	5	1.8
P43277	H13_MOUSE	Histone H1.3	22086.13	11.03	85.81	6	4.7
P43274	H14_MOUSE	Histone H1.4	21964.02	11.1	84.73	5	21.9
Q8BFZ3	ACTBL_MOUSE	Beta-actin-like protein 2	41976.99	5.3	76.41	8	20.5
Q9D0E1	HNRPM_MOUSE	Heterogeneous nuclear ribonucleoprotein M	77597.38	8.8	72.2	15	17
P10126	EF1A1_MOUSE	Elongation factor 1-alpha 1	50082.1	9.1	72.14	6	2.4
P62751	RL23A_MOUSE	60S ribosomal protein L23a	17684.13	10.44	70.52	1	5.3
P99027	RLA2_MOUSE	60S acidic ribosomal protein P2	11643.83	4.42	69.92	5	60
P62852	RS25_MOUSE	40S ribosomal protein S25	13733.7	10.12	65.11	4	22.4
P15331	PERI_MOUSE	Peripherin	54234.59	5.4	63.83	3	1.1
Q922F4	TBB6_MOUSE	Tubulin beta-6 chain	50058.13	4.8	60.29	3	6.7
P10107	ANXA1_MOUSE	Annexin A1	38709.97	6.97	57.9	3	10.7
P16858	G3P_MOUSE	Glyceraldehyde-3-phosphate dehydrogenase	35787.21	8.44	57.42	9	22.5
P62918	RL8_MOUSE	60S ribosomal protein L8	28007.29	11.03	56.28	3	5.1
P17182	ENOA_MOUSE	Alpha-enolase	47111.21	6.37	53.17	6	11.5
Q07133	H1T_MOUSE	Histone H1t	21527.15	11.71	52.28	3	13.5
P47963	RL13_MOUSE	60S ribosomal protein L13	24290.5	11.54	49.61	2	10.9
P61255	RL26_MOUSE	60S ribosomal protein L26	17247.53	10.55	42.74	2	4.9
P11499	HS90B_MOUSE	Heat shock protein HSP 90-beta	83273.12	4.97	42.71	3	4.8
P43276	H15_MOUSE	Histone H1.5	22562.44	10.91	42.06	4	7.8
Q61937	NPM_MOUSE	Nucleophosmin	32539.81	4.62	41.88	6	18.2
Q9CQN1	TRAP1_MOUSE	Heat shock protein 75 kDa, mitochondrial	80158.53	6.25	41.74	1	0.3
Q64475	H2B1B_MOUSE	Histone H2B type 1-B	13943.56	10.31	40.93	3	23
P61358	RL27_MOUSE	60S ribosomal protein L27	15787.75	10.56	37.85	2	9.2
P62900	RL31_MOUSE	60S ribosomal protein L31	14453.93	10.54	36.02	3	12.2
P62806	H4_MOUSE	Histone H4	11360.38	11.36	35.55	2	18.8
P35700	PRDX1_MOUSE	Peroxiredoxin-1	22162.35	8.26	31.21	3	15.1
O08807	PRDX4_MOUSE	Peroxiredoxin-4	31033.14	6.67	31.21	2	2.6
P68369	TBA1A_MOUSE	Tubulin alpha-1A chain	50103.61	4.94	25.46	5	2.5

B: BIA-MS data: nuclear C2C12 extract proteins bound to the FGF1 IRES A RNA.

AC	ID	Description	MW	pI	Score	Peptides	Protein Coverage (%)
P60710	ACTB_MOUSE	Actin, cytoplasmic 1	41709.73	5.29	1487.66	20	15.2
P68033	ACTC_MOUSE	Actin, alpha cardiac muscle 1	41991.88	5.23	1216.7	19	14.8
Q62093	SFRS2_MOUSE	Splicing factor. arginine/serine-rich 2	25461.18	11.86	709.72	7	13.1
Q8BFZ3	ACTBL_MOUSE	Beta-actin-like protein 2	41976.99	5.3	591.13	11	30.6
P56480	ATPB_MOUSE	ATP synthase subunit beta, mitochondrial	56265.47	5.19	561.29	16	47.1
Q99M28	RNPS1_MOUSE	RNA-binding protein with serine-rich domain 1	34187.7	11.85	337.96	5	7.6
Q03265	ATPA_MOUSE	ATP synthase subunit alpha. mitochondrial	59715.59	9.22	230.42	9	21.7
P63038	CH60_MOUSE	60 kDa heat shock protein, mitochondrial	60917.39	5.91	221.49	6	20.1
P24369	PPIB_MOUSE	Peptidyl-prolyl cis-trans isomerase B	23698.56	9.56	209.89	10	44.4
Q569Z6	TR150_MOUSE	Thyroid hormone receptor-associated protein 3	108113.69	10.17	142.45	8	10.8
P19324	SERPH_MOUSE	Serpin H1	46560.2	8.9	111.84	5	17.5
Q52KI8	SRRM1_MOUSE	Serine/arginine repetitive matrix protein 1	106828.46	11.87	86.78	6	7.9
P62315	SMD1_MOUSE	Small nuclear ribonucleoprotein Sm D1	13273.36	11.56	84.79	1	14.1
Q8BG05	ROA3_MOUSE	Heterogeneous nuclear ribonucleoprotein A3	39627.61	9.1	72.53	4	3.4
Q6PDM2	SFRS1_MOUSE	Splicing factor, arginine/serine-rich 1	27727.81	10.37	71.53	9	16.6
P26369	U2AF2_MOUSE	Splicing factor U2AF 65 kDa subunit	53483.22	9.19	60.31	1	1.1
Q99K48	NONO_MOUSE	p54^{nrb}/NONO Non-POU domain-containing octamer-binding protein	54506.42	9.01	56.11	2	1.3
P67984	RL22_MOUSE	60S ribosomal protein L22	14749.77	9.21	55.76	2	17.1
O08810	U5S1_MOUSE	116 kDa U5 small nuclear ribonucleoprotein component EFTUD2	109291.3	4.86	43.05	1	0.2

C: BIA-MS data: total C2C12 extract proteins bound to the EMCV IRES RNA.

AC	ID	Description	MW	pI	Score	Peptides	Protein Coverage (%)
P645534	ACTA2_MOUSE	Actin alpha 2 smooth muscle	16748,18	5,31	76,71	2	13,9
P8603	ACTA-MOUSE	Actin alpha smooth muscle	41981,81	5,23	76,33	3	7,4
P27547	DCD_MOUSE	dermcidin	11276,83	6,08	60,65	1	10

D: BIA-MS data: nuclear C2C12 extract proteins bound to the FGF1 promoter A DNA.

AC	ID	Description	MW	pI	Score	Peptides	Protein Coverage (%)
P03995	GFAP_MOUSE	Glial fibrillary acidic protein	49869.5	5.27	995.36	5	9.5
P60710	ACTB_MOUSE	Actin. cytoplasmic 1	41709.7	5.29	247.21	9	6.9
P63038	CH60_MOUSE	60 kDa heat shock protein, mitochondrial	60917.4	5.91	209.39	5	1.8
P68033	ACTC_MOUSE	Actin. alpha cardiac muscle 1	41991.9	5.23	195.65	9	6.8
P56480	ATPB_MOUSE	ATP synthase subunit beta, mitochondrial	56265.5	5.19	192.06	6	20
P11103	PARP1_MOUSE	Poly [ADP-ribose] polymerase 1	113028	9.05	100.2	2	0.3
O35295	PURB_MOUSE	Transcriptional activator protein Pur-beta	33880.8	5.35	76.87	4	9.6
P19324	SERPH_MOUSE	Serpin H1	46560.2	8.9	69.96	2	9.4
P23475	KU70_MOUSE	ATP-dependent DNA helicase 2 subunit 1	69440.9	6.35	66.58	2	5.3
P50543	S10AB_MOUSE	Protein S100-A11	11075.5	5.28	64.81	1	15.5
P27641	KU86_MOUSE	ATP-dependent DNA helicase 2 subunit 2	83004	5.04	59.15	3	6.7
Q99K48	NONO_MOUSE	p54^{nrb}/NONO Non-POU domain-containing octamer-binding protein	54506.4	9.01	57.77	1	1
Q03265	ATPA_MOUSE	ATP synthase subunit alpha, mitochondrial	59715.6	9.22	55.43	2	6.5
Q569Z6	TR150_MOUSE	Thyroid hormone receptor-associated protein 3	108114	10.17	49.81	5	5.6

E: BIA-MS data: total C2C12 extract proteins bound to the CMV promoter DNA.

AC	ID	Description	MW	pI	Score	Peptides	Protein Coverage (%)
P21428	ACTA_MOUSE	Actin alpha skeletal muscle	42023.9	5.23	266.7	14	38.7
P3476	ATP-MOUSE	ATP5B ATP synthetase subunit beta mitochandrial	41981.81	5.23	270.48	15	10.1
P29744	SSBP1_MOUSE	Single-stranded DNA-binding protein, mitochondrial	17249	9.59	204.56	5	32.5
P479743	POTEE_MOUSE	Isoform 1 of POTE ankyrin domain family membre E	121286	5.83	182.01	7	8
P784154	HSPD1_MOUSE	Heat shock protein, mitochondrial	26657.41	9.68	112.42	6	11.4
P7047	S100-A8_MOUSE	S100A8 protein S100-A8	10827.7	6.51	167.34	3	6.8
P3269	ACTBL2_MOUSE	Beta actin-like protein 2	41976	5.39	148.72	6	16.8
P14230	C1QBP_MOUSE	Complement composent 1 Q subcomponent-binding protein mitochondrial	31342.6	19.9	143.06	2	19.9
P27462	S100-A9_MOUSE	S100A9 protein	13233.5	5.71	139.28	6	43
P3935	HT2H2BE_MOUSE	Histone H2B type 2-E	13911.6	10.31	66.47	4	33.3
P7188	SLC25A5_MOUSE	ADP/ATP translocase2	32874.2	9.7	48.84	3	9.7
P291467	SLC25A6_MOUSE	ADP/ATP translocase3	32845.2	9.76	48.84	3	9.7
P440493	ATP5A1_MOUSE	ATP5A1 ATP synthase subunit alpha mitochondrial	59713.6	9.16	47.52	4	9.4
P26272	HT H2A_MOUSE	Histone H2A type 1-B/E	14127	11.05	43.44	1	22.3

Chapitre 2

La nucleoline induit la traduction de VEGFD en réponse au choc thermique lors de la lymphangiogenèse tumorale

Le système lymphatique est utilisé par les tumeurs comme une voie de dissémination métastatique. De plus, la tumeur induit plusieurs stress successifs (hypoxie, choc thermique, stress du réticulum, ...). Notre équipe a montré précédemment que le facteur lymphangiogénique majeur VEGFC est induit par l'hypoxie, et que cette induction est liée à l'activation d'un IRES identifié dans son ARN messager. J'ai d'ailleurs contribué à ce travail qui a fait l'objet d'un article dans Cell Report, joint en annexe. Cette étude suggère que d'autres facteurs lymphangiogéniques pourraient être induit par le stress au niveau traductionnel.

Dans ce deuxième volet de ma thèse, qui a donné lieu à l'article ci-après, nous nous sommes intéressés à la régulation de l'expression de l'autre facteur lymphangiogénique majeur, le VEGFD, lors de la progression tumorale. Le VEGFD induit non seulement la lymphangiogenèse mais aussi la dilatation des vaisseaux lymphatiques, ce qui les rend plus perméables à la dissémination métastatique. Nous avons mis en évidence une régulation traductionnelle de l'expression du facteur VEGFD dans des tumeurs mammaires de souris. Cette activation a lieu en dépit de la surexpression et la déphosphorylation de 4E-BP1 qui inactive la traduction dépendante de la coiffe. Nous avons caractérisé la présence d'un IRES dans la région 5' non traduite du transcrit VEGFD. En soumettant les cellules tumorales à différents stress il est apparu que le stress qui active l'IRES du VEGFD dans ces cellules est le choc thermique. De manière plus intéressante encore, nous avons identifié un ITAF qui contrôle l'activité de cet IRES: il s'agit de la nucléoline. Cette protéine a été identifiée en utilisant à nouveau la technologie de BIA-MS validée dans le chapitre 1. Nous montrons que cette protéine, majoritairement nucléolaire, est relocalisée dans le cytoplasme en réponse au choc thermique. L'invalidation de la nucléoline par un siARN ou par un agent anti-inflammatoire inhibe la traduction de l'ARNm VEGFD tout en induisant une vasoconstriction au niveau des vaisseaux lymphatiques.

Cette étude fournit la première évidence que la régulation traductionnelle IRES-dépendante contrôlée par la nucléoline a un impact sur la dilatation des vaisseaux lymphatiques, qui est un événement majeur lors de la progression tumorale métastatique.

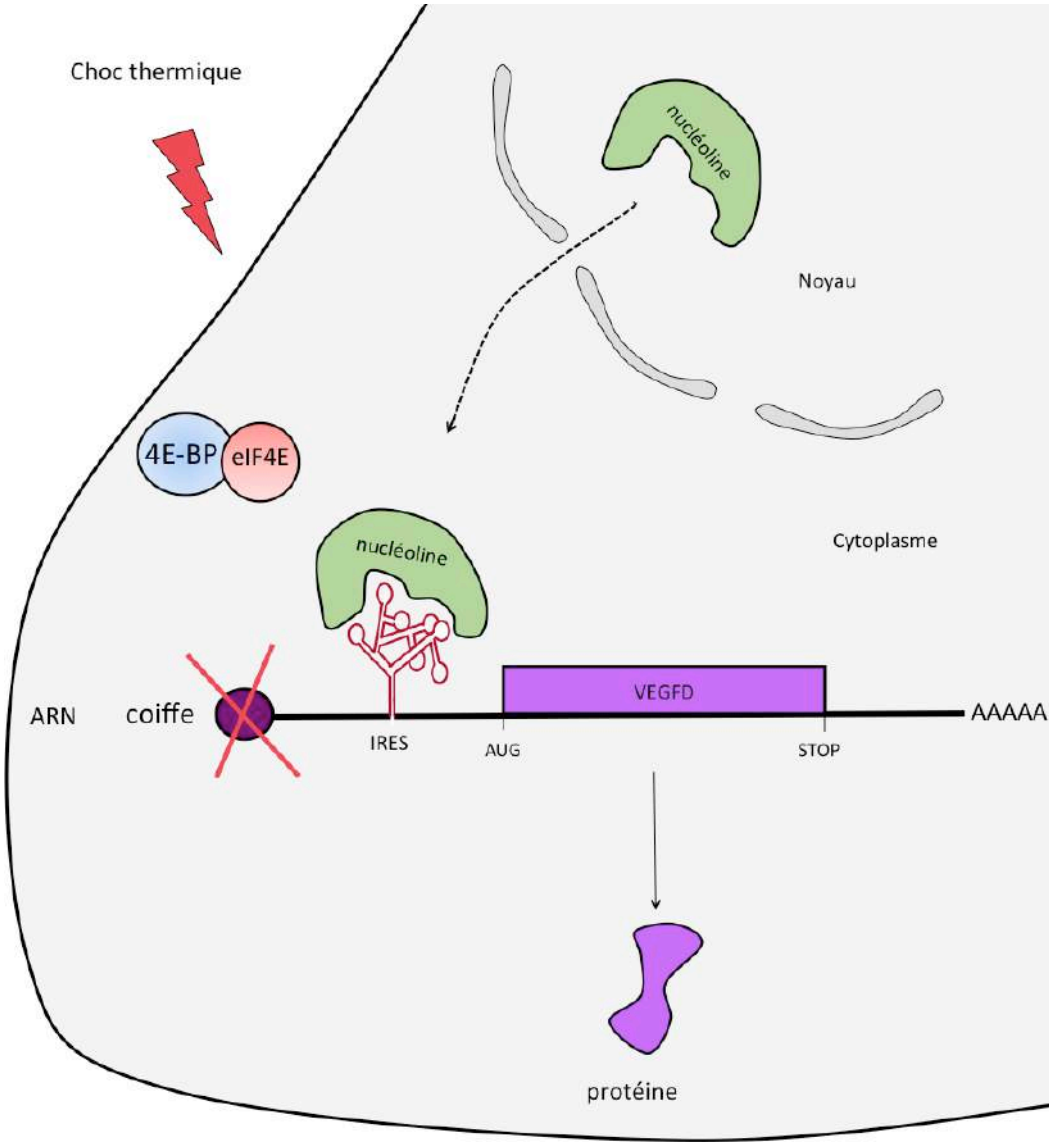

<u>Figure 15</u> : Modèle d'activation de l'IRES de VEGF-D par la nucléoline lors du choc thermique. Lors du choc thermique, 4^{E}-BP séquestre eIF4E inhibant la traduction dépendante de la coiffe. En réponse à ce même stress, la nucléoline se délocalise dans le cytoplasme pour activer l'IRES de l'ARNm VEGF-D et induire au niveau traductionnel l'expression de ce facteur de croissance.

Molecular and Cellular Pathobiology

Cancer Research

Nucleolin Promotes Heat Shock–Associated Translation of VEGF-D to Promote Tumor Lymphangiogenesis

Florent Morfoisse[1], Florence Tatin[1], Fransky Hantelys[1], Aurelien Adoue[1], Anne-Catherine Helfer[2], Stephanie Cassant-Sourdy[3], Françoise Pujol[1], Anne Gomez-Brouchet[4,5], Laetitia Ligat[6], Frederic Lopez[6], Stephane Pyronnet[3], Jose Courty[7], Julie Guillermet-Guibert[3], Stefano Marzi[2], Robert J. Schneider[8], Anne-Catherine Prats[1], and Barbara H. Garmy-Susini[1]

Abstract

The vascular endothelial growth factor VEGF-D promotes metastasis by inducing lymphangiogenesis and dilatation of the lymphatic vasculature, facilitating tumor cell extravasion. Here we report a novel level of control for VEGF-D expression at the level of protein translation. In human tumor cells, VEGF-D colocalized with eIF4GI and 4E-BP1, which can program increased initiation at IRES motifs on mRNA by the translational initiation complex. In murine tumors, the steady-state level of VEGF-D protein was increased despite the overexpression and dephosphorylation of 4E-BP1, which downregulates protein synthesis, suggesting the presence of an internal ribosome entry site (IRES) in the 5′ UTR of VEGF-D mRNA. We found that nucleolin, a nucleolar protein involved in ribosomal maturation, bound directly to the 5′UTR of VEGF-D mRNA, thereby improving its translation following heat shock stress via IRES activation. Nucleolin blockade by RNAi-mediated silencing or pharmacologic inhibition reduced VEGF-D translation along with a subsequent constriction of lymphatic vessels in tumors. Our results identify nucleolin as a key regulator of VEGF-D expression, deepening understanding of lymphangiogenesis control during tumor formation. *Cancer Res; 76(15); 4394–405. ©2016 AACR.*

Introduction

Lymphatic vessels encircle tumors and enhance metastasis by improving the capillary high permeability and the collecting vessels' dilatation (1). Nonetheless, very little is known regarding the molecular mechanisms governing cancer invasion into the lymphatic system.

VEGF-C and VEGF-D are the chief inducers of lymphangiogenesis (2). Their activity is regulated by protein processing that occurs mainly in the extracellular environment to generate peptides with high affinity for their receptor, VEGFR-3 (3, 4). Our group recently identified regulation of VEGF-C at the translational initiation step induced by hypoxic stress (5). The stress-induced VEGF production in pathologic conditions has been largely described in the literature (6, 7). In this study, we sought to identify whether VEGF-D activity responds to cellular stress.

VEGF-D was first described to promote tumor metastasis through the lymphatic system (8, 9). This observation was extended to many solid tumors such as pancreatic cancer and endometrial cancer (10, 11). More recently, Karnezis and colleagues have demonstrated that the prometastatic effect of VEGF-D was associated with a lymphatic collecting vessel dilatation by regulating the prostaglandin pathway (1). The effect of VEGF-D on vessel enlargement was also observed in dermal initial lymphatics (12). Here, we found an original mechanism underlying regulation of VEGF-D translation that is induced by increased temperature.

Translational control plays a critical role in the regulation of gene expression during tumor development (13). In fact, the majority of cellular stresses lead to strong inhibition of mRNA translation by the classical cap-dependent scanning mechanism (5, 14). Several mRNAs, however, are translated by an eIF4E-independent mechanism, mediated by internal ribosome entry site (IRES) that are mRNA structures located in IRESs were previously described for VEGF-A and VEGF-C mRNA (15, 16). Here, we demonstrated that the 5′UTR of VEGF-D mRNA harbors an IRES trans-acting factor, which drives VEGF-D translation under heat shock stress.

IRES-dependent translation initiation is controlled by IRES trans-acting factors (ITAF), which participate in the recruitment of the small ribosome subunit (17). ITAFs seemingly stabilize the IRES active conformation (18) to allow efficient expression of key regulators in tumor growth and spreading (16). The activity of

[1]UMR 1048-I12MC, Université de Toulouse, Inserm, UPS, Toulouse, France. [2]IBMC-CNRS, Université de Strasbourg, Strasbourg, France. [3]UMR 1037-CRCT, Inserm, UPS, Toulouse, France. [4]UMR 5089-IPBS, CNRS, UPS, Toulouse, France. [5]Department of Pathology, IUCT-Oncopole, Toulouse, France. [6]Pôle Technologique du CRCT - INSERM-UMR1037, Toulouse, France. [7]Laboratoire CRRET Laboratory, Université Paris EST Créteil, Créteil, France. [8]NYU School of Medicine, New York, New York.

Note: Supplementary data for this article are available at Cancer Research Online (http://cancerres.aacrjournals.org/).

Corresponding Author: Barbara H. Garmy-Susini, INSERM, 1 av J. poulhes Eq15, BP84225, Toulouse 31432, France. Phone: 3356-1312-24087; Fax: 335-6132-3841; E-mail: barbara.garmy-susini@inserm.fr

doi: 10.1158/0008-5472.CAN-15-3140

AACR

ITAFs is dependent on their subcellular localization. They are nuclear proteins that are exported to the cytoplasm to participate in mRNA translation initiation (19). ITAFs bind the mRNA 5′ untranslated region to recruit the ribosome, thereby promoting protein synthesis under stress conditions. Here, we found that nucleolin, a multifunctional nucleolar protein involved in ribosome maturation, is an ITAF of the VEGF-D mRNA. Specifically, our data showed that cytoplasmic accumulation of nucleolin in cells enduring heat shock improved VEGF-D mRNA translation by binding of ITAF to the VEGF-D 5′ UTR.

Nucleolin was first described to be an ITAF for viral 5′UTR mRNAs such as rhinovirus (20). Recently, nucleolin was shown to participate in IRES-dependent translation of cellular mRNAs. It associated with hnRNP proteins to promote translation of long interspersed element one (LINE-1; ref. 21). Moreover, recent reports confirmed the ITAF activity of nucleolin during tumorigenesis and demonstrated that it is a key regulator of specificity protein 1 (Sp1) protein accumulation via induction of its IRES-dependent translation initiation (22).

In the current study, we demonstrate a link between the translational control of VEGF-D expression and lymphatic dilatation. We show that RNA-binding protein nucleolin specifically and directly binds to the 5′UTR of VEGF-D and functions to induce VEGF-D mRNA translation in cells. Our results advocate that nucleolin contributes to the maintenance of lymphatic vessel plasticity under heat shock stress conditions by controlling VEGF-D expression.

Of interest, inhibition of nucleolin synthesis by NSAIDs specifically repressed VEGF-D translation, suggesting a putative protein synthesis control using NSAIDs that could interfere with a physiologic function such as lymphatic dilatation.

Altogether, our results suggest that nucleolin contributes to the maintenance of lymphatic functioning network by controlling the expression of VEGF-D.

Materials and Methods

Tissue specimens

In total, 15 primary human breast cancer specimens and their associated lymph nodes were collected. Samples were obtained from archival paraffin blocks of breast cancer from patients treated at the Rangueil hospital (Toulouse, France) between 2002 and 2008. Samples were selected as coded specimens under a protocol approved by the INSERM Institutional Review Board (DC-2008-463) and Research State Department (Ministère de la recherche, ARS, CPP2, authorization AC-2008-820) and included tumor specimens identified as invasive ductal carcinoma. Each series included as controls normal breast tissue from the same patient.

Tumor studies

Animal experiments were conducted in accordance with recommendations of the European Convention for the Protection of Vertebrate Animals used for experimentation. All animal experiments were performed according to the INSERM Institutional Animal Care and Use Committee guidelines for laboratory animals' husbandry and have been approved by the local branch INSERM Rangueil-Purpan of the Midi-Pyrénées ethics committee (protocol n° 091037615).

In total, 5×10^5 cells of murine Lewis Lung Carcinoma (LLC1; ATCC CRL-1642; obtained in 2011) and human pancreatic adenocarcinoma (Capan-1, ATCC HTB79; obtained in 2009) cell lines were injected subcutaneously into wild type (WT, $n = 8–10$) mice on a C57Bl6 or NMRI Nu/Nu background, respectively ($n = 8–10$). Animals were sacrificed 2 or 3 weeks later when tumors and inguinal lymph nodes were excised and embedded into optimal cutting temperature (OCT) compound (Tissue-Tek; Sakura Finetek). To study the orthotopic model of breast carcinoma, 5×10^4 syngeneic Balb/c 4T1 and 67NR (ATCC CRL-2539, obtained in 2007) cells were injected into Balb/c the fourth mammary fat pad ($n = 8–10$). Animals were sacrificed 1 or 2 weeks later when tumor and inguinal lymph nodes were excised and embedded into OCT compound.

Bicistronic lentivector construction and transduction

The cDNAs coding human VEGF-D 5′UTR and EMCV 5′UTR were subcloned between the *Renilla* (LucR) and firefly (LucF) genes under the control of the CMV promoter into the lentivector pTRIP-DU3-CMV-MCS as described previously (5). Bicistronic lentivectors were produced using the tri-transfection procedure using the plasmids pLvPack and pLvVSVg (Sigma-Aldrich), and were evaluated for their ability to transduce the cell lines as described previously (5).

Reporter gene assay

To obtain stable vector expression in cells, the bicistronic cassette with the VEGFD 5′UTRs between the two luciferase genes was introduced into lentivectors. Bicistronic lentivectors with the viral EMCV IRES and the hairpin were used as negative and positive controls. The principle of the bicistronic vector is that the first cistron, *Renilla* luciferase (LucR), is translated by the cap-dependent mechanism, whereas the second cistron, firefly luciferase (LucF), is translated under the control of the IRES. *In vitro* or *ex vivo* luciferase assays were performed on lysed cells or tissues as described previously (5).

Reagents

Rat anti-mouse VEGFD (SC101585) was from Santa Cruz Biotechnology (TebuBio). Rabbit-anti human 4E-BP1 (9644) was from Ozyme. Rabbit anti-mouse -1 antibody (RDI-103PA50) was from Research Diagnostics Incorporated. Rat anti-mouse CD31 (MEC 13.3) was from BD Biosciences. Goat anti-PAN cytokeratin, donkey anti-rabbit, and rat IgGs conjugated with Dylights Fluors 488, 568 were from TebuBio. Anti-podoplanin was from Santa Cruz Biotechnology. Anti-luciferase Firefly was from Promega. Hypoxyprobe was from Euromedex. Anti-GAPDH was from Sigma Aldrich.

Immunohistochemistry

Tumors and lymph nodes were embedded into OCT compound and 5-μm tissue sections were immunostained with specific antibodies. The mean number of lymphatic vessels (±SEM for each treatment group) were quantified in 5–10 microscopic fields per cryosection using automated pixel density determination. The vessel diameters were quantified using 5 measures per vessel as described in Supplementary Fig. S1. In total, 3 sections/tumor were analyzed (8–10 tumors per group), 5 microscopic fields/section leading to 100–150 fields/condition. The mean number of mice with lymph node metastases was determined by immunostaining with 10 μg/mL of anti-pancytokeratin and quantified in 5–10 microscopic fields per cryosection using

automated pixel density determination as the mean number of pixels ± SEM for each group.

Quantitative real-time RT-PCR

Total cellular RNA was isolated from mouse 4T1, 67NR, Capan-1, and LLC tumors using a tissue lyser (Ultrathurax) in TRIzol solution as described previously (5).

Primers. The following primers were used: LucF forward (F): 5′-TCCTATGATTATGTCCGGTTATGTAAA-3′; LucF reverse (R): 5′-TGTAGCCATCCATCCTTGTCAA-3′; LucR (F): 5′- ATGGGCAAAT-CAGGCAAA-3′; LucR (R): 5′- CGCAATATCTTCTTCAATATCAGG-3′; VEGF-D (F): 5′- CCTATTGACATGCTGTGGGAT-3′; VEGF-D (R): 5′-GTGGGTTCCTGGAGGTAAGAG-3′

siRNA and cell transfection

A pool of siRNAs synthesized by Dharmacon with the following sequences: siRNA-1: 5′-GCAAAUUCCUAUACAUCUA-3′, siRNA-2: 5′-UGUCAGAGGUCCAGUUUAA-3′, siRNA-3: 5′-UGG-CAAACCUAAAGGGUAU-3′, siRNA-4: 5′-UGGGAAAAGUAAA-GGGAUU-3′ were used. Nontargeting siRNA (siGENOME Non-Targeting Smartpool; Dharmacon) was used as control. To examine the effect of the siRNAs on nucleolin protein expression, 4T1 cells were plated onto 6-well plates in antibiotic-free RPMI1640 medium supplemented with FBS (10%) before being transfected with 20 nmol/L siRNA as described previously (5). Vehicle control and nontargeting siRNA were applied to cell culture replicates. Cells were incubated for 1 day before changing the culture medium and incubating them for 72 hours before the 30-minute heat shock. Efficacy of downregulation was analyzed by immunoblotting.

N6L inhibitor treatment

N6L, a synthetic ligand of nucleolin that exerts antitumor activity in mouse xenograft model (23), was provided by J. Courty's laboratory (Laboratoire CRRET Laboratory, Université Paris EST Créteil, Créteil, France). Stock solution of N6L (2 mmol/L) was diluted in mannitol to a final concentration of 50 μmol/L. Heat shock was applied for 30 minutes at 42°C.

In vitro stress-induced IRES activity

Stress stimulation assays were performed *in vitro* on 4T1-transduced cells. Reticulum stress was promoted using 12 nmol/L dithiothreitol (DTT; Sigma-Aldrich) during 4 and 8 hours. Deprivation stress was performed in RPMI without serum during 8 hours at 37°C. Inflammatory stress was performed in the presence of 1 μg/mL lipopolysaccharid (LPS; Sigma-Aldrich Chemie GmbH) during 4 and 8 hours. Heat shock was applied during 5, 10, 20, and 30 minutes at 37°C.

In vivo sc-236 treatment

NSAID treatment was performed by injecting 1 μg of anti-COX-2 inhibitor sc-236 (Sigma-Aldrich Chimie GmbH) every 2 days during 12 days. Tumor-bearing mice were sacrificed after 2 weeks.

RNA structure determination in solution chemical and enzymatic probing

RNA preparation, RNA structure probing, and RNA primer extension analysis were performed as described previously (5).

Primers.. The following primer sequences were used:

VEGF-D_3: ATTCCCCATTCTCCATACATTTTGAATATTTTAAA-TGTCTACCG

VEGF-D_4: TAATACGACTCACTATAGGAAGATATGACCACC-TCC

VEGF-D_5: GAATATTTTAAATGTCTACCG

BIA-MS assays

Biomolecular analysis coupled to mass spectrometry (BIA-MS) was performed on a BIAcore T200 optical biosensor instrument (GE Healthcare). Immobilization of biotinylated VEGF-D and EMCV IRES RNAs was performed on a streptavidin-coated (SA) sensorchip in HBS-EP buffer (10 mmol/L HEPES, pH 7.4, 150 mmol/L NaCl, 3 mmol/L EDTA, 0.005% surfactant P20; GE Healthcare). All immobilization steps were performed at a flow rate of 2 μL/minute with a final concentration of 100 μg/mL. Total amount of immobilized VEGF-D and EMCV IRES RNAs was 552 RU and 650 RU, respectively.

Binding analyses were performed with cell protein extracts at 100 μg/mL over the immobilized VEGF-D and EMCV IRES RNA surface at 37°C and 42°C for 7 minutes at a flow rate of 30 μL/minute. The channel (Fc1) was used as a reference surface for nonspecific binding measurements. The recovery wizard was used to recover selected proteins from cell protein extracts at 37°C and 42°C. This step was carried out with 0.1% SDS. Five recovery procedures were performed to get enough amounts of proteins for MS identification. LC/MS-MS analyses were performed on Bruker Amazon ETD mass spectrometer.

Polysome profiling. 4T1 cell line were incubated with cycloheximide (100 μg/mL) 15 minutes at 37°C before preparing extracts in hypotonic lysis buffer (5 mmol/L Tris-HCl, pH7.5; 2.5 mmol/L MgCl2; 1.5 mmol/L KCl). Cell extracts were layered onto 10%–50% sucrose gradient and sedimented via centrifugation at 39,000 rpm for 2 hours at 4°C in a Beckman ultracentrifuge. Fractions were collected (24 fractions of 12 drops each) using a Foxy JR ISCO collector and UV optical unit type 11.

Statistical analysis

All statistical analyses were performed using a two-tailed Student *t* test or one-way ANOVA. All experiments were performed three times, with one exception, where the incidence of metastasis is reported as the average ± SEM of three separate animal experiments. All data presented are from a single representative experiment.

Results

VEGF-D synthesis is modulated by a cap-independent initiation of mRNA translation

VEGF-D level was examined in invasive ductal breast carcinoma biopsies and compared with normal breast epithelium (Fig. 1A). VEGF-D is overexpressed in breast tumors and is associated with an upregulation of eIF4GI and 4E-BP1 expressions, suggesting a cap-independent VEGF-D synthesis.

To study the expression of VEGF-D, we performed RT-qPCR and Western blot analysis showing that VEGF-D is ubiquitously expressed in organs containing lymphatic vessels (lymph nodes, mammary gland, etc.), whereas no VEGF-D was found in organs containing no (brain) or low level (muscle) of lymphatic vessels (Supplementary Fig. S2).

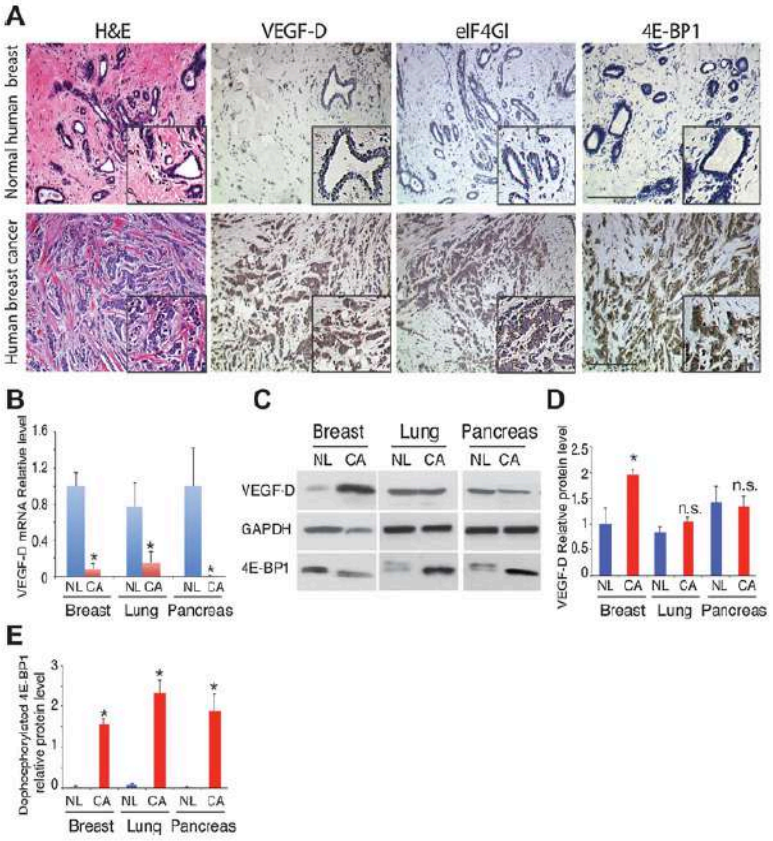

Figure 1.
VEGF-D overexpression correlates with the upregulation of eIF4GI and 4E-BP1. **A,** immunohistochemical staining of representative breast cancer tumors ($n = 15$) and normal breast epithelium ($n = 15$) for VEGF-D, eIF4GI, and 4E-BP1. Scale bar, 100 μm. **B,** quantitative RT-PCR for breast, lung, and pancreatic tumors (CA) compared with normal tissue (NL; *, $P < 0.001$). **C–E,** immunoblot analysis of VEGF-D and 4E-BP1 in mouse breast, lung, and pancreatic tumors. **D,** quantification by densitometry of VEGF-D signal normalized to GAPDH (*, $P < 0.01$). **E,** quantification by densitometry of dephosphorylated 4E-BP1 normalized to GAPDH (*, $P < 0.001$). n.s., nonsignificant.

To study the effect of the microenvironment on lymphatic vessel development *in vivo*, we used mouse tumor models, which we previously showed to early induce lymphangiogenesis: an orthotopic syngeneic mouse model of highly metastatic breast cancer (4T1); a syngeneic subcutaneous model of Lewis lung carcinoma (LLC); and a xenograft model of pancreatic adenocarcinoma (Capan-1; Fig. 1B). We studied the expression of VEGF-D and surprisingly found that VEGF-D mRNA levels strongly decreased in tumors compared with normal tissues (Fig. 1B). Despite the decrease in VEGF-D mRNA amounts, VEGF-D protein level increased during breast tumor development, but not in lung and pancreas (Fig. 1C and D), confirming a posttranscriptional regulation of VEGF-D expression.

In parallel, we analyzed regulation of translation initiation in mice tumors by studying the phosphorylation status of 4E-BP1, which is known to inhibit cap-dependent translation by binding to eIF4E in its hypophosphorylated state (Fig. 1C–E).

As expected, VEGF-D protein synthesis was not stimulated in lung and pancreatic tumors containing hypophosphorylated 4E-BP1 compared with normal tissue (Fig. 1C–E). In contrast, despite an accumulation of hypophosphorylated 4E-BP1 indicating a blockade of cap-dependent translation in breast cancer compared with normal breast, we observed an increase in VEGF-D expression in the tumors *in vivo* (Fig. 1C–E). These data suggest that VEGF-D expression is promoted by a posttranscriptional mechanism in breast cancer.

VEGF-D mRNA 5′UTR contains an IRES activated by increased temperature

To demonstrate the presence of an IRES activity in VEGF-D mRNA 5′UTR, we used the double luciferase bicistronic vector strategy validated in previous studies (Fig. 2A; ref. 5). Considering that the EMCV IRES is not activated in the current tumor models (5), we used bicistronic lentivectors with the EMCV IRES and hairpin as controls to transduce 4T1 and 67NR with the bicistronic lentivectors (Fig. 2A). To verify the presence of a single mRNA that generates the two different proteins, the relative amounts of LucR and LucF mRNAs were measured by quantitative RT-PCR (Fig. 2B). Amplification values revealed an equal amount of LucF and LucR RNA sequences, indicating the absence of any cryptic promoter or splicing event that would have increased the presence of one of the cistrons compared with the other (24).

IRES elements have been discovered in several viral and cellular RNA elements and are preferentially used to initiate translation of specific mRNAs during cellular stress when overall global translation is compromised (25–27). Recent observations in tumor models show a VEGF-D–driven lymphogenous spread by

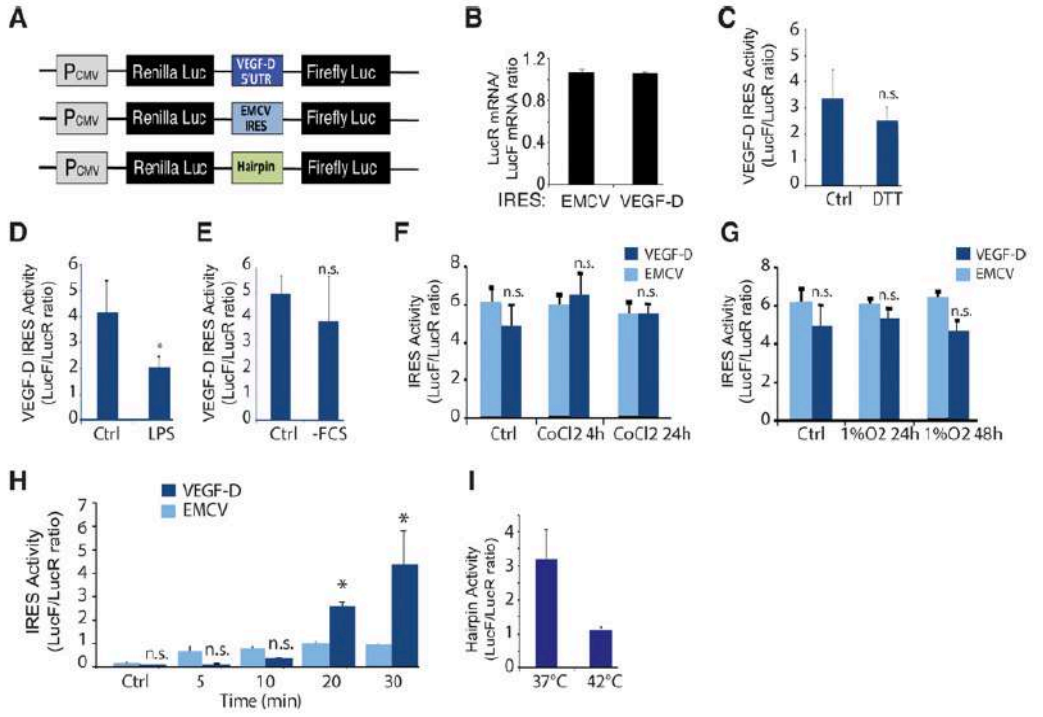

Figure 2.

VEGF-D mRNA contains an IRES element. **A,** schematics of the bicistronic expression cassettes subcloned into lentivectors. **B,** ratio of quantitative RT-PCR relative values for LucR versus LucF, separated by VEGF-D 5′UTR. **C–G,** *in vitro* VEGF-D IRES activity in 4T1 cell lines submitted to DTT-induced endoplasmic reticulum stress (**C**), lipopolysaccharide (LPS) inflammatory stress (**D**), nutriment deprivation (-FCS) stress (**E**), and hypoxic stresses (**F** and **G**). **H** and **I,** *in vitro* VEGF-D and EMCV IRES (**H**) activities in 4T1 cell lines submitted to heat shock stress (**I**). *In vitro* hairpin activity in 4T1 cell lines submitted to heat shock stress. n.s., nonsignificant.

increasing lymph flow through vessel dilation (28). Vessel dilatation is mainly observed during inflammation and is promoted by an activation of the endothelial prostaglandin pathways (29). Therefore, we submitted 4T1 transduced cell lines to physiologic stresses associated with a local vasodilatation to identify which stimulus is associated with IRES activation (Fig. 2C–I). VEGF-D IRES activity was not affected by endoplasmic reticulum stress (Fig. 2C), lipopolysaccharides (Fig. 2D), serum deprivation (Fig. 2E), or hypoxia (Fig. 2F and G). In contrast, VEGF-D IRES activity was significantly activated *in vitro* after 20-minute heat shock (Fig. 2H), whereas no activation was found for EMCV control IRES (Fig. 2H) or hairpin (Fig. 2I).

VEGF-D synthesis promotes lymphatic vessel dilatation and metastasis

The role of overexpressed VEGF-D was examined in mice breast tumor models. We compared lymphatic-mediated metastasis in 4T1 tumors to orthotopic syngeneic 67NR low metastatic breast tumors. Despite similar level of VEGF-D mRNA in 4T1 and 67NR cell lines (Fig. 3A), we found that 67NR poorly expressed VEGF-D compared with 4T1 (Fig. 3B and C). Surprisingly, this difference in VEGF-D expression had no effect on tumor growth (Fig. 3D). To investigate the role of VEGF-D in breast tumors lymphatic vessels, we performed immunostaining using antibodies directed against lymphatic vessel endothelial receptor (LYVE-1; ref. 30) and podoplanin (Fig. 3E and Supplementary Fig. S3; ref. 31).

In these models, VEGF-D expression has no effect on tumor lymphangiogenesis (Fig. 3E and F). In parallel, we found that the tumor expressing a high level of VEGF-D (4T1) exhibited dilated tumor lymphatic vessels compared to tumor with low level of VEGF-D (67NR; Fig. 3G and H). As expected, the lymphatic vessel dilatation is associated with an increase of tumor metastasis (Fig. 3I and J), but has no effect on draining lymph nodes lymphangiogenesis (Supplementary Fig. S4).

To identify *in vivo* VEGF-D IRES activity, bicistronic lentivector–transduced 4T1 and 67NR cell lines were injected in mice mammary fat pad (Fig. 3K–N). IRES activity in tumors was observed using immunodetection of firefly luciferase and quantified by measuring luciferase activities after 7 and 14 days (Fig. 3K–N and Supplementary Fig. S4). We checked that the transduction of the reporter genes did not affect tumor growth (Supplementary Fig. S4). Interestingly, VEGF-D IRES activity strongly increased in 4T1 tumors (Fig. 3K) compared with EMCV IRES (Fig. 3L), but not in 67NR tumors (Fig. 3M), which exhibit low VEGF-D protein levels. As expected, the EMCV viral IRES, which is not involved in angiogenesis or lymphangiogenesis stimulation, was poorly (4T1) or not (67NR) activated during tumorigenesis (Fig. 2L and N).

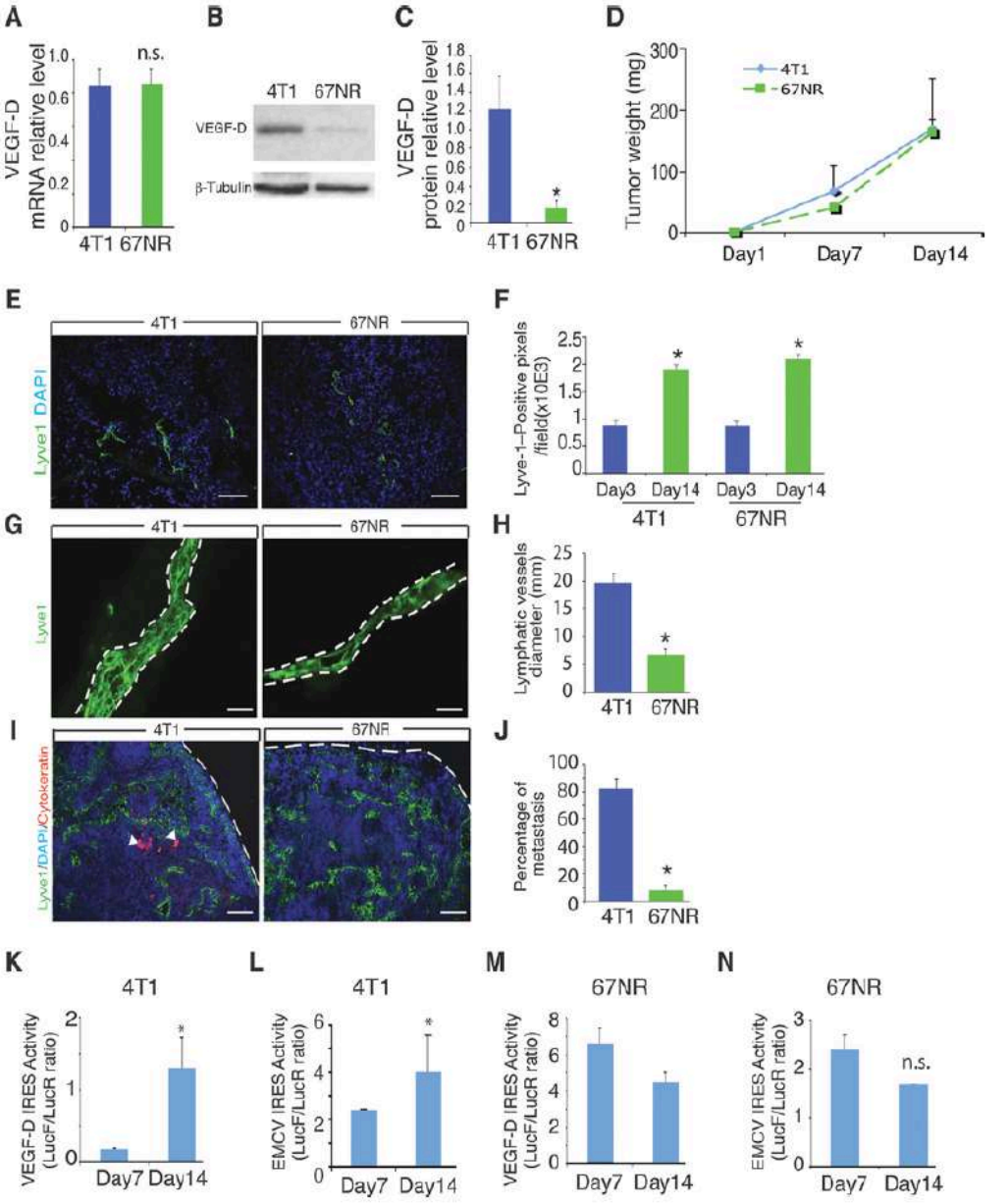

Figure 3.

Tumor posttranscriptional induction of VEGF-D *in vivo* promotes lymphatic vessel dilatation. **A,** quantitative RT-PCR in 4T1 and 67NR mice breast cancer cell lines. **B,** immunoblot analysis of VEGF-D in 4T1 and 67NR cell lines. **C,** quantification of VEGF-D relative levels (*, $P < 0.001$). **D,** 4T1 and 67NR tumor growth analysis. **E** and **F,** staining for Lyve-1 (green) and DAPI (blue) demonstrated VEGF-D–independent lymphangiogenesis during breast carcinoma development (*, $P < 0.001$). Scale bar, 50 μm. **G** and **H,** staining for −1 (green) and DAPI (blue) demonstrated a significant decrease of lymphatic vessel dilatation in tumor lacking VEGF-D (*, $P < 0.001$). Scale bar, 25 μm. **I** and **J,** staining for −1 (green), cytokeratin (red), and DAPI (blue) demonstrated a significant decrease in lymph node metastasis (*, $P < 0.001$). Scale bar, 50 μm. **K–N,** *in vivo* VEGF-D IRES activity exhibits a significant increase in 4T1 (**K**) compared with EMCV (**L**), whereas no activity was promoted in 67NR for both IRESs (**M** and **N**). n.s., nonsignificant.

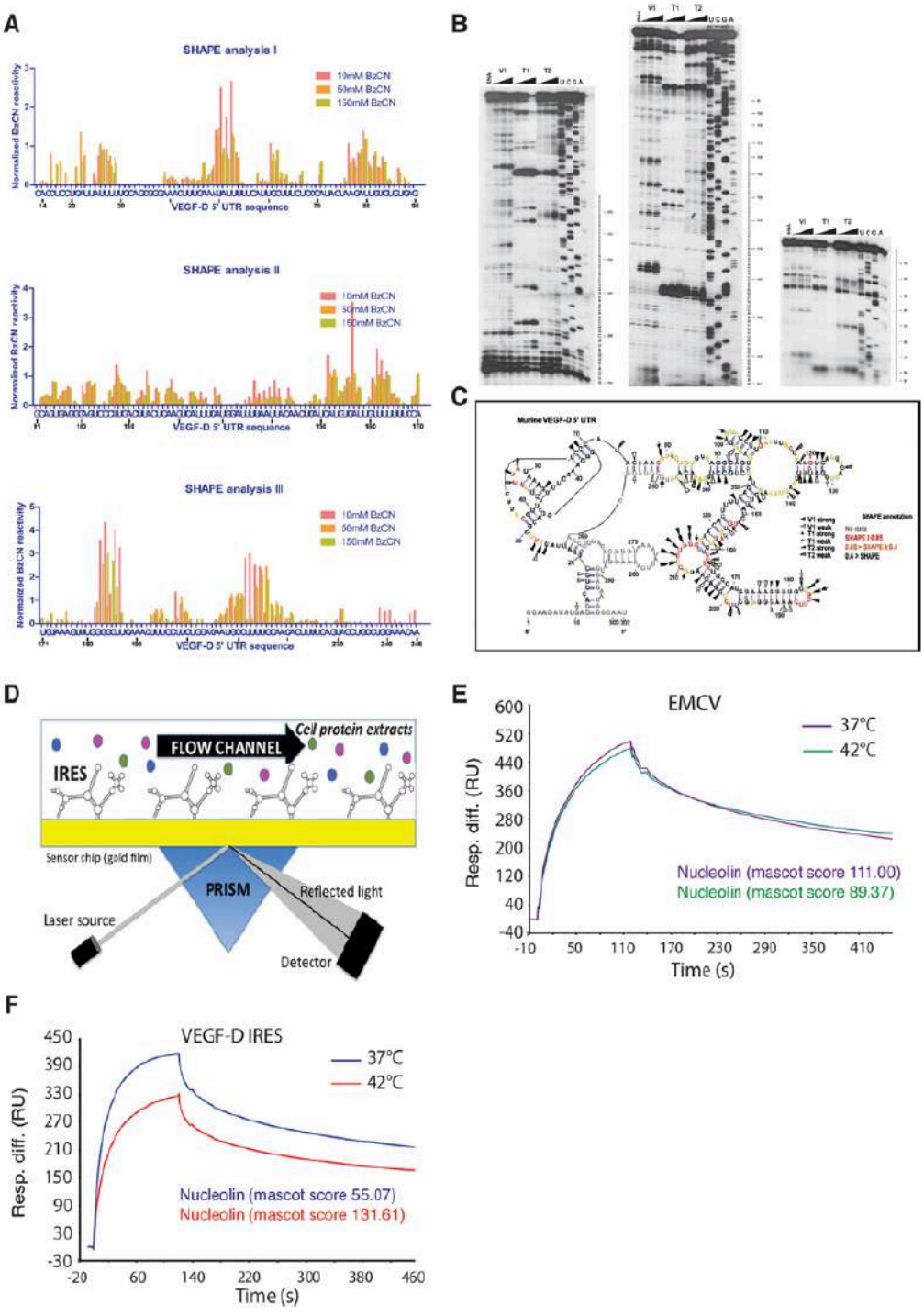
A
SHAPE analysis I
10mM BzCN
50mM BzCN
150mM BzCN
Normalized BzCN reactivity
VEGF-D 5' UTR sequence
SHAPE analysis II
SHAPE analysis III
B
C
Murine VEGF-D 5' UTR
D
FLOW CHANNEL
Cell protein extracts
IRES
Sensor chip (gold film)
PRISM
Reflected light
Laser source
Detector
E
EMCV
37°C
42°C
Resp. diff. (RU)
Nucleolin (mascot score 111.00)
Nucleolin (mascot score 89.37)
Time (s)
F
VEGF-D IRES
37°C
42°C
Resp. diff. (RU)
Nucleolin (mascot score 55.07)
Nucleolin (mascot score 131.61)
Time (s)

These data demonstrate that the VEGF-D mRNA contains an IRES that is activated during tumor growth in correlation with the high levels of VEGF-D protein expression.

Altogether, our data suggest a cap-independent regulation of VEGF-D translation that is not related with lymphangiogenesis, but directly correlated with lymphatic vessels dilatation and metastasis formation.

VEGF-D IRES exhibits two alternative structures stabilized by an ITAF: nucleolin

RNA structure plays important roles in every level of gene regulation including translation initiation. Predicting how mRNA 5′UTRs fold into secondary structures is an essential step in understanding the IRES activity. We then performed the shape analysis method for probing of VEGF-D mRNA 5′UTR structure (Fig. 4A–C and Supplementary Fig. S5). The pattern of benzoyl-cyanide modifications suggested that VEGF-D 5′ UTR is highly structured. Our structure prediction revealed the presence of a pseudoknot (nucleotides 30–70) and several stable helices. Nevertheless, enzymatic probing data (Fig. 4A and Supplementary Fig. S5) showed a region (nucleotides 225–229) with double reactivity toward both double strand (V1) and single-strand probes (T2), and a native gel analysis confirmed the presence of two alternative structures (Fig. 4B). On the basis of shape analysis, we identified a predictive folding of VEGF-D IRES as shown in Fig. 4C.

The presence of alternative conformations at equilibrium has been previously observed also for the VEGF-C IRES (5) and could be an indication that the active structure might necessitate a cofactor (18), that is, an ITAF or a specific eIF, to fold correctly.

IRES activation requires binding of canonical initiation factors to initiate translation, but also other proteins called IRES trans-acting factors (ITAF) that facilitate ribosome recruitment to the IRES (32). ITAFs are RNA-binding proteins involved in other aspects of RNA metabolism that are important in carcinogenesis such as mRNA splicing, export and stability, and represent potential targeted therapy in certain types of cancer.

To identify VEGF-D ITAFs, we used an analytic method coupling surface plasmon resonance and mass spectrometry (BIA-MS; Fig. 4D–G), a technology recently validated for ITAF identification (33). Biotinylated VEGF-D and EMCV IRES RNAs were immobilized on a BIACORE streptavidin sensorchip (Fig. 4D). Control (37°C) or heat shock (42°C) total cell protein extracts were injected into the BIACORE T200 apparatus to obtain the association phase (Fig. 4E and F). Bound proteins were recovered and identified by nano-LC/MS-MS after tryptic digestion. Interestingly, proteins bound the VEGF-D IRES with a lower affinity at 42°C compared with 37°C, whereas no difference was observed for EMCV IRES (Fig. 4E and F). Mass spectrometry analysis allowed identification of a few proteins bound to the VEGF-D IRES, including an RNA-binding protein, nucleolin (Fig. 4E and F and Supplementary Fig. S5). As nucleolin has previously been described to be an ITAF for viral IRESs (20, 21), and plays a role in RNA stability of cellular oncogenes such as Bcl2 (34), we investigated its effect on VEGF-D IRES activity.

Nucleolin ITAF activity is mediated by its subcellular location

To study whether nucleolin participates in VEGF-D translational initiation during heat shock stress, we first analyzed protein expression in breast cancer cell lines (Fig. 5). Surprisingly, no difference in nucleolin protein synthesis was observed in cells submitted to an increased temperature (42°C; Fig. 5A). Interestingly, we found a delocalization of nucleolin from the nucleus to the cell cytoplasm under heat shock (Fig. 5B and C). The protein export is in accordance with previous studies showing that ITAF activity depends on its subcellular location (19).

To determine the role of nucleolin in VEGF-D IRES activity under heat shock stress, we designed siRNAs against nucleolin (Fig. 5D–J). Nucleolin protein synthesis is inhibited by siRNA, but is not affected by control si scramble (Fig. 5D and E). To decipher whether the nucleolin knock down could modulate VEGFD synthesis, the VEGFD mRNA relative level and protein expression were analyzed under heat shock condition after knocking down the nucleolin. Despite a downregulation of mRNA level, VEGF-D protein level is maintained, suggesting a posttranscriptional regulation (Fig. 5F and G). In that context, the knockdown of nucleolin induces a downregulation of protein expression confirming its role as an ITAF (Fig. 5G). To investigate the effect of nucleolin on VEGF-D translation, polysome profiling has been performed comparing VEGF-D expression under stressed condition in polysomal fraction from cells transfected with nucleolin siRNA (Supplementary Fig. S6 and Fig. 5H). We observed a strong downregulation of translated VEGFD in the absence of nucleolin at 42°C compared with 37°C, suggesting that the downregulation of the ITAF directly affects the association of the mRNA with the polysomes (Fig. 5H). As expected, in the absence of nucleolin, VEGF-D IRES activity was strongly decreased, whereas no effect was observed for EMCV IRES activity (Fig. 5I). In this context, VEGF-D IRES was affected by nucleolin knockdown, demonstrating the role of nucleolin as an ITAF under heat stress condition. To decipher whether transcription and cap-dependent translation is regulated by heat shock stress, we performed transcription and translation analysis on a gene involved in vascular biology that does not contain an IRES: platelet growth factor 4 (PF4). We show that PF4 is not regulated at the transcriptional level under heat shock condition (Supplementary Fig. S6). As expected, we observed a downregulation of PF4 mRNA under stressed condition in polysomal fraction (Supplementary Fig. S6).

Figure 4.

VEGF-D 5′UTR exhibits the presence of highly stable structures compatible with an IRES-driven mechanism of translation. **A,** quantification and normalization of the SHAPE analysis obtained by the QuSHAPE software. The 302 nucleotides long sequence of VEGF-D 5′UTR has been split into three graphs representing the 5′ (graph I, top), graph II (middle), and 3′ (graph III, bottom) regions. **B,** autoradiograms of RNA enzymatic probing experiments followed by primer extension showing the localization of the enzymatic cleavages obtained with RNase V1 (V1), RNase T1 (T1), and RNase T2 (T2). (i) RNA, control RNA without enzymes; (ii) V1, T1 and T2: three different increasing concentrations of the three RNAses; (iii) RNA sequencing ladders were run in parallel (U,C,G,A lanes on each gel). **C,** putative secondary structure of the murine 5′ UTR of VEGF-D mRNA. **D,** schematic representation of the BIACORE T200 analysis using surface plasmon resonance. **E** and **F,** sensogram analysis for EMCV IRES (**E**) and VEGF-D IRES (**F**) coupled to mass spectrometry reveals the binding of a nuclear protein: nucleolin.

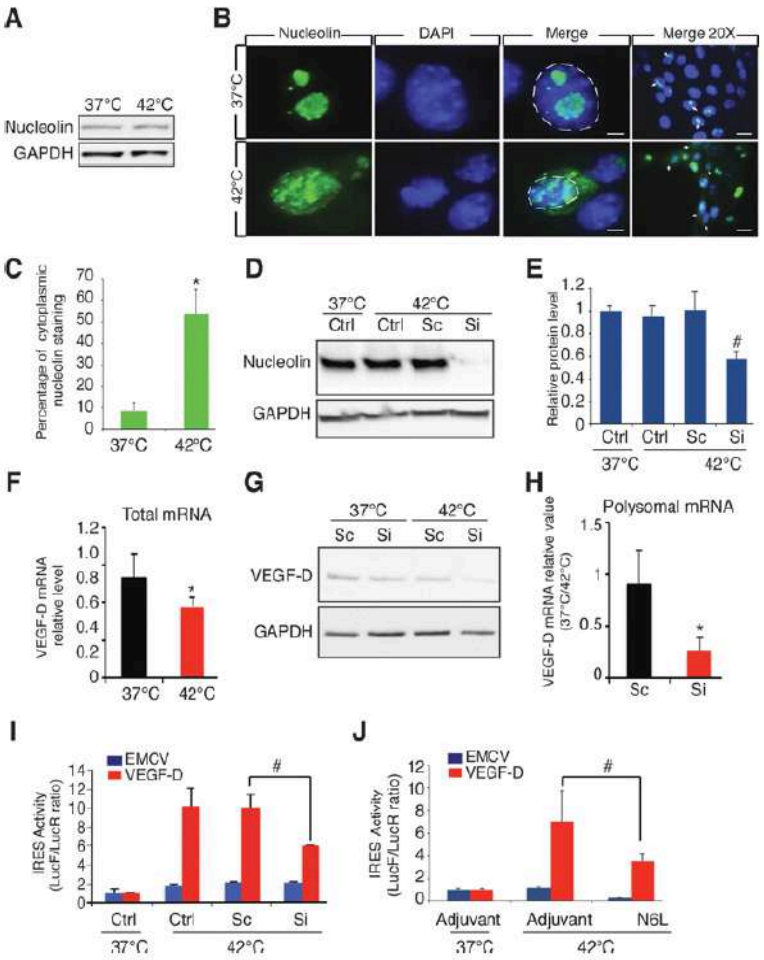

Figure 5.
VEGF-D IRES activity is regulated by nucleolin. **A,** immunoblot of nucleolin in mouse cell lines. **B,** staining for nucleolin (green) and DAPI (blue) in 4T1 submitted to heat shock; scale bar, 5 μm (left); scale bar, 25 μm (right). **C,** quantification of the percentage of 4T1 cell lines, which exhibits a cytoplasm staining of nucleolin under increased temperature (*, $P < 0.001$). **D,** immunoblot of nucleolin in lysates of 4T1 cells incubated in physiologic (37°C) or heated (42°C) temperature and treated with or without siRNA against nucleolin (Si) or a scrambled (Sc) siRNA control. **E,** densitometric quantification of the immunoblot (#, $P < 0.05$). **F,** quantitative VEGF-D RT-PCR on total mRNA from 4T1 cells incubated in physiologic (37°C) or heated (42°C) temperature. **G,** immunoblot of VEGF-D in lysates of 4T1 cells incubated in physiologic(37°C) or heated (42°C) temperature and treated with or without siRNA against nucleolin (Si) or a scrambled (Sc) siRNA control. **H,** comparison of VEGF-D mRNA relative levels in polysomal mRNA from 4T1 cells incubated in physiologic (37°C) or heated (42°C) temperature and treated with or without siRNA against nucleolin (Si) or a scrambled (Sc) siRNA control (*, $P < 0.01$). **I,** VEGF-D IRES activity in 4T1 cells incubated in physiologic (37°C) or heated (42°C) temperature and treated with or without siRNA against nucleolin (Si) or a scrambled (Sc) siRNA control (#, $P < 0.05$). **J,** VEGF-D IRES activity in 4T1 cells incubated in physiologic (37°C) or heated (42°C) temperature and treated with adjuvant (mannitol) or nucleolin inhibitor (N6L; #, $P < 0.05$).

To confirm the effect of nucleolin, we then used a pharmacologic inhibitor, a synthetic ligand of nucleolin: N6L (23). As expected, we observed a decrease of VEGF-D IRES activity in the presence of nucleolin inhibitor (Fig. 5J).

COX-2 inhibitors abolish VEGF-D stress response by modulating nucleolin expression

Recent studies have demonstrated that VEGF-D regulates the tumor-draining collecting lymphatic vessels dilatation through a prostaglandin (PG)-dependent mechanism, consistent with the elevated levels of inflammatory mediators, such as PGs (28, 35). VEGF-D modulates COX-2–derived PGE2 to promote tumor progression and metastasis leading to a chemoprotective effect of COX-2 inhibitors (NSAIDs) by reducing PGE2 levels. To determine the role of COX-2 inhibitors on molecular regulations of VEGF-D expression, we evaluated the effect of sc236 *in vitro* (Fig. 6A–E). As shown in Fig. 5, the increased temperature has no effect on nucleolin synthesis (Fig. 6A). Surprisingly, we observed a COX-2 inhibitor downregulation of nucleolin synthesis at both 37°C and 42°C (Fig. 6A), suggesting that the drug interferes with VEGF-D translational initiation by modulating its ITAF synthesis. Using immunocytodetection, we found that cytoplasmic nucleolin was hardly detected upon sc236 treatment in 4T1 cell lines under heat shock conditions (Fig. 6B and C). In parallel, COX-2 inhibitor abolished heat shock–induced VEGF-D IRES activity in 4T1 cells (Fig. 6D), but had no effect on 67NR cell lines (Fig. 6E). To investigate whether COX-2 inhibitor could modulate VEGF-D translation initiation *in vivo*, tumor-bearing mice were treated every 2 days during 10 days by intraperitoneal injection of COX-2 inhibitor (Fig. 6F–J). As expected, we found a downregulation of nucleolin expression in tumors (Fig. 6F). IRES activities were studied *in vivo* at day 7 (1–2 mm diameter, well vascularized, nonmetastatic) and day 14 (4–8 mm diameter, necrotic, metastatic) to compare low-stressed to high-stressed condition (Fig. 6G). As expected, the EMCV viral IRES is not affected by the COX-2 inhibition. The VEGF-D IRES is activated at day 14, and this effect is abolished by COX-2 inhibitor (Fig. 6G), whereas no difference was observed in tumor growth (Supplementary

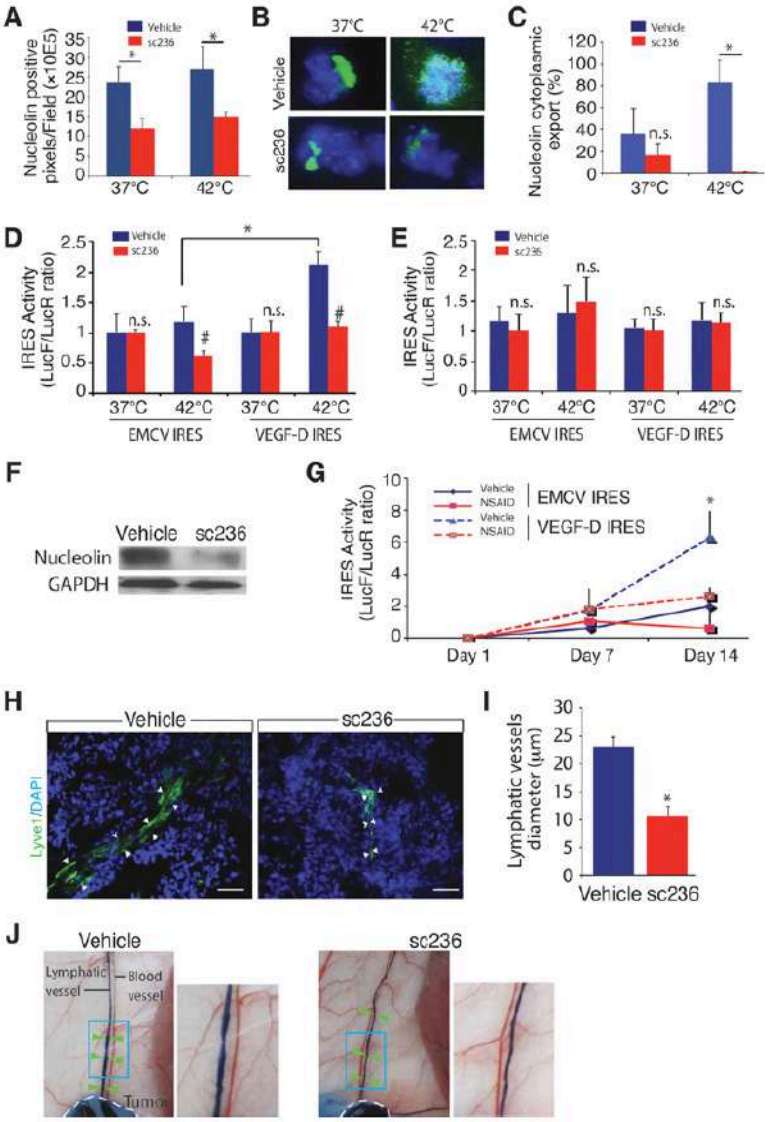

Figure 6.
VEGF-D IRES activity is modulated by COX-2 inhibitor. **A,** quantification of nucleolin-positive pixels in 4T1 cells submitted to heat shock (*, $P < 0.01$). **B,** staining for nucleolin (green) and (blue) in heated 4T1 cell lines incubated with COX-2 inhibitor (sc236). **C,** quantification of the percentage of 4T1 cell lines incubated with sc236, which exhibit a cytoplasm staining of nucleolin under increased temperature (*, $P < 0.001$). **D,** stimulation of VEGF-D and EMCV IRES activity in 4T1 cell line (#, $P < 0.05$). **E,** stimulation of VEGF-D and EMCV IRES activity in 67NR cell line (#, $P < 0.05$). **F,** immunoblot of nucleolin in 4T1-bearing mice treated with mouse sc236. **G,** stimulation of 4T1 VEGF-D IRES activity *in vivo* is inhibited by sc236. **H,** staining for LYVE-1 (green) and (blue) demonstrated a significant decrease of lymphatic vessel dilatation in sc236-treated 4T1 tumors. **I,** quantification of lymphatic vessel diameters *in vivo* in sc236-treated 4T1 tumors (*, $P < 0.01$). **J,** Evans blue perfusion of the 4T1 draining lymphatics exhibits a vessel dilatation that is abolished after sc236 treatment. n.s., nonsignificant.

Fig. S7). In parallel, we observed a strong decrease of lymphatic vessel diameter in tumors (Fig. 6H and I) associated with a vasoconstriction of the tumor-draining collecting vessels in COX-2 inhibitor–treated mice (Fig. 6J). These data demonstrated for the first time that an anti-inflammatory drug can modulate growth factor synthesis under stress condition by controlling an ITAF subcellular location and synthesis.

Discussion

Tumor metastases are a leading cause of cancer-related mortality and can be promoted by both intrinsic and extrinsic factors in tumor cells. This study has identified an original translational regulation mechanism of VEGF-D expression under stress conditions in primary tumors promoting lymphatic vessel increased diameter that can be reversed by NSAIDs acting on ITAF expression. Translational initiation is promoted by eIF4E initiation factor binding to the mRNA. Under stress condition, eIF4E is targeted by the translational inhibitor 4E-Binding Protein 1 (4E-BP1) in its hypophosphorylated form, which leads to inhibition of cap-dependent, but not cap-independent, translation (36). Also, translation reprograming was previously reported in inflammatory breast cancer due to an overexpression of eIF4GI and overexpression/dephosphorylation of 4E-BP1 (37, 38).

We found a colocalization of these two markers with VEGF-D in human breast carcinoma, suggesting a cap-independent translation initiation of VEGF-D mRNA. Moreover, we show that VEGF-D transcript levels are reduced in mice tumors, whereas VEGF-D protein levels are increased due to a switch from cap-dependent to IRES-dependent VEGF-D translation. Notably, this regulation seems to depend on an increased temperature, but is not regulated by hypoxia as it has been previously described for other (lymph)angiogenic growth factors, such as VEGF-A and VEGF-C, two related and homologous members of the VEGF family (5). This feature distinguishes VEGF-D from the other hypoxia-induced (lymph) angiogenic growth factors. Importantly, we found two alternative structures for VEGF-D 5′UTR, suggesting an equilibrium between basal and stressed conditions to facilitate the ITAF binding. Switching from cap-dependent to IRES-dependent translation of VEGF-D in tumor cells required adapter protein called ITAFs. The VEGF-D IRES might be regulated by distinct ITAFs, which would be activated during heat shock (and in inflammation), but not during hypoxia. Our findings reveal that nucleolin, a nucleolar protein involved in the control of transcription of ribosomal RNA, is translocated to the cytoplasm in response to heat shock and controls VEGF-D mRNA translation after binding to the IRES region. Nucleolin has been previously described as an ITAF for virus IRESs such as poliovirus (20). Recently, it has been found to enhance cellular IRES-dependent translation of specificity protein-1 (Sp1), a transcription factor involved in tumor cells proliferation (22, 39). These results are in accordance with findings showing that IRES-dependent translation initiation is regulated by ITAFs subcellular location (19).

Tumor cells spread to distant organs via lymphatic using two mechanisms: lymphangiogenesis and lymphatic dilatation. Here, we demonstrated that breast tumors lacking VEGF-D expression do not exhibit a defect in primary tumor or lymph nodes lymphangiogenesis, but have a reduced amount of dilated lymphatic vessels associated with an inhibition of metastasis. Our findings suggested that this process is restricted to breast cancer, in agreement with previous studies showing a correlation between metastases and dilated lymphatic vessels in breast cancer patients (40).

We know for decades that inflammation is a major inducer of prostaglandin-induced vasodilatation (29). Previous studies reported that expression of VEGF-D by cancer cells promoted tumor lymphatic vessels dilatation and metastasis by regulating prostaglandins produced by the collecting lymphatic endothelium (1). COX-2 inhibitors, the most common NSAIDs, reduce VEGF-D–driven metastasis by reversing the morphologic changes in collecting lymphatic vessels. In this study, we demonstrated that COX-2 inhibitor–induced lymphatic vessel constriction is in part due to a downregulation of VEGF-D IRES translation initiation. We observed that the VEGF-D IRES activity is abolished by NSAIDs during tumor development. Notably, vessel diameters were reduced in COX-2 inhibitor–treated mice. These data indicate that lymphatic vessels plasticity is controlled by a regulatory loop involving VEGF-D protein synthesis and prostaglandin signaling (Supplementary Fig. S8).

Our study may be relevant to provide the first evidence of a translational initiation control of the lymphatic vessels dilatation, a major pathophysiologic event in tumor metastasis.

A key finding of our study is that increased temperature mediates lymphangiogenic growth factor responses, through the suppression of cap-dependent and an increase of IRES-mediated mRNA translation. Collectively, our data allow us to propose the existence of two VEGF-D translational control pathways involved in cancer dissemination that depends on stresses associated with inflammation. A nucleolar protein, the nucleolin, which can provide a novel therapeutic target for lymphatic vessel plasticity during tumor inflammation, controls this mechanism.

Disclosure of Potential Conflicts of Interest

No potential conflicts of interest were disclosed.

Authors' Contributions

Conception and design: F. Morfoisse, A. Adoue, S. Pyronnet, J. Guillermet-Guibert, A.-C. Prats, B.H. Garmy-Susini

Development of methodology: F. Morfoisse, A. Adoue, F. Pujol, R.J. Schneider, A.-C. Prats, B.H. Garmy-Susini

Acquisition of data (provided animals, acquired and managed patients, provided facilities, etc.): F. Tatin, F. Hantelys, A. Adoue, A.-C. Helfer, S. Cassant-Sourdy, L. Ligat, F. Lopez, S. Marzi, B.H. Garmy-Susini

Analysis and interpretation of data (e.g., statistical analysis, biostatistics, computational analysis): F. Morfoisse, F. Tatin, A. Adoue, A.-C. Helfer, L. Ligat, F. Lopez, J. Guillermet-Guibert, S. Marzi, R.J. Schneider, A.-C. Prats, B.H. Garmy-Susini

Writing, review, and/or revision of the manuscript: S. Pyronnet, J. Guillermet-Guibert, S. Marzi, R.J. Schneider, A.-C. Prats, B.H. Garmy-Susini

Administrative, technical, or material support (i.e., reporting or organizing data, constructing databases): F. Lopez, B.H. Garmy-Susini

Study supervision: F. Morfoisse, B.H. Garmy-Susini

Other (supplier of an antagonist of nucleolin): J. Courty

Acknowledgments

We thank J.J. Maoret for his technical support and Y. Barreira from the platform Anexplo Genotoul (Inserm US006, Toulouse, France) for their outstanding technical assistance, M. Khatib from the imaging platform of 12MC for her scientific and technical support, and A. Henras (LBME-CNRS UMR 5100, Toulouse, France) for his scientific and technical support in ribosome profiling. We thank Dr. P. Romby (IBMC-CNRS) and D. Arvanitis for their scientific support.

Grant Support

This work has been supported by the Ligue Régionale Contre le Cancer, the foundation ARC pour la Recherche sur le Cancer, the foundation Lefoulon Delalande, Cancéropôle Grand Sud-Ouest GSO, IDEX Paul Sabatier Federal University, AFM-Telethon, Région Midi-Pyrénées.

The costs of publication of this article were defrayed in part by the payment of page charges. This article must therefore be hereby marked *advertisement* in accordance with 18 U.S.C. Section 1734 solely to indicate this fact.

Received November 23, 2015; revised May 11, 2016; accepted May 24, 2016; published OnlineFirst June 8, 2016.

References

1. Kamezis T, Shayan R, Caesar C, Roufail S, Harris NC, Ardipradja K, et al. VEGF-D promotes tumor metastasis by regulating prostaglandins produced by the collecting lymphatic endothelium. Cancer Cell 2012;21:181–95.

2. Zheng W, Aspelund A, Alitalo K. Lymphangiogenic factors, mechanisms, and applications. J Clin Invest 2014;124:878–87.
3. Joukov V, Sorsa T, Kumar V, Jeltsch M, Claesson-Welsh L, Cao Y, et al. Proteolytic processing regulates receptor specificity and activity of VEGF-C. EMBO J 1997;16:3898–911.
4. Stacker SA, Stenvers K, Caesar C, Vitali A, Domagala T, Nice E, et al. Biosynthesis of vascular endothelial growth factor-D involves proteolytic processing which generates non-covalent homodimers. J Biol Chem 1999;274:32127–36.
5. Morfoisse F, Kuchnio A, Frainay C, Gomez-Brouchet A, Delisle MB, Marzi S, et al. Hypoxia induces VEGF-C expression in metastatic tumor cells via a HIF-1alpha-independent translation-mediated mechanism. Cell Rep 2014;6:155–67.
6. Lambrechts D, Carmeliet P. Genetics in zebrafish, mice, and humans to dissect congenital heart disease: insights in the role of VEGF. Curr Top Dev Biol 2004;62:189–224.
7. Hoier B, Hellsten Y. Exercise-induced capillary growth in human skeletal muscle and the dynamics of VEGF. Microcirculation 2014;21:301–14.
8. Stacker SA, Caesar C, Baldwin ME, Thornton GE, Williams RA, Prevo R, et al. VEGF-D promotes the metastatic spread of tumor cells via the lymphatics. Nat Med 2001;7:186–91.
9. Stacker SA, Achen MG, Jussila L, Baldwin ME, Alitalo K. Lymphangiogenesis and cancer metastasis. Nat Rev Cancer 2002;2:573–83.
10. Kopfstein L, Veikkola T, Djonov VG, Baeriswyl V, Schomber T, Strittmatter K, et al. Distinct roles of vascular endothelial growth factor-D in lymphangiogenesis and metastasis. Am J Pathol 2007;170:1348–61.
11. Girling JE, Donoghue JF, Lederman FL, Cann LM, Achen MG, Stacker SA, et al. Vascular endothelial growth factor-D over-expressing tumor cells induce differential effects on uterine vasculature in a mouse model of endometrial cancer. Reprod Biol Endocrinol 2010;8:84.
12. Paquet-Fifield S, Levy SM, Sato T, Shayan R, Kamezis T, Davydova N, et al. Vascular endothelial growth factor-d modulates caliber and function of initial lymphatics in the dermis. J Invest Dermatol 2013;133:2074–84.
13. Sonenberg N, Hinnebusch AG. New modes of translational control in development, behavior, and disease. Mol Cell 2007;28:721–9.
14. Holcik M, Sonenberg N. Translational control in stress and apoptosis. Nat Rev Mol Cell Biol 2005;6:318–27.
15. Miller DL, Dibbens JA, Damert A, Risau W, Vadas MA, Goodall GJ. The vascular endothelial growth factor mRNA contains an internal ribosome entry site. FEBS Lett 1998;434:417–20.
16. Morfoisse F, Renaud E, Hantelys F, Prats AC, Garmy-Susini B. [Lymphangiogenic gene expression adaptation in tumor hypoxic environment]. Med Sci 2014;30:506–8.
17. Lewis SM, Veyrier A, Hosszu Ungureanu N, Bonnal S, Vagner S, Holcik M. Subcellular relocalization of a trans-acting factor regulates XIAP IRES-dependent translation. Mol Biol Cell 2007;18:1302–11.
18. Sonenberg N, Hinnebusch AG. Regulation of translation initiation in eukaryotes: mechanisms and biological targets. Cell 2009;136:731–45.
19. Lewis SM, Holcik M. For IRES trans-acting factors, it is all about location. Oncogene 2008;27:1033–5.
20. Izumi RE, Valdez B, Banerjee R, Srivastava M, Dasgupta A. Nucleolin stimulates viral internal ribosome entry site-mediated translation. Virus Res 2001;76:17–29.
21. Peddigari S, Li PW, Rabe JL, Martin SL. hnRNPL and nucleolin bind LINE-1 RNA and function as host factors to modulate retrotransposition. Nucleic Acids Res 2013;41:575–85.
22. Hung CY, Yang WB, Wang SA, Hsu TI, Chang WC, Hung JJ. Nucleolin enhances internal ribosomal entry site (IRES)-mediated translation of Sp1 in tumorigenesis. Biochim Biophys Acta 2014;1843:2843–54.
23. Destouches D, Page N, Hamma-Kourbali Y, Machi V, Chaloin O, Frechault S, et al. A simple approach to cancer therapy afforded by multivalent pseudopeptides that target cell-surface nucleoproteins. Cancer Res 2011;71:3296–305.
24. Martineau Y, Le Bec C, Monbrun L, Allo V, Chiu IM, Danos O, et al. Internal ribosome entry site structural motifs conserved among mammalian fibroblast growth factor 1 alternatively spliced mRNAs. Mol Cell Biol 2004;24:7622–35.
25. Pestova TV, Kolupaeva VG, Lomakin IB, Pilipenko EV, Shatsky IN, Agol VI, et al. Molecular mechanisms of translation initiation in eukaryotes. Proc Natl Acad Sci U S A 2001;98:7029–36.
26. Sachs AB. Cell cycle-dependent translation initiation: IRES elements prevail. Cell 2000;101:243–5.
27. Vagner S, Galy B, Pyronnet S. Irresistible IRES. Attracting the translation machinery to internal ribosome entry sites. EMBO Rep 2001;2:893–8.
28. Karnezis T, Shayan R, Fox S, Achen MG, Stacker SA. The connection between lymphangiogenic signalling and prostaglandin biology: a missing link in the metastatic pathway. Oncotarget 2012;3:893–906.
29. Williams TJ, Peck MJ. Role of prostaglandin-mediated vasodilatation in inflammation. Nature 1977;270:530–2.
30. Banerji S, Ni J, Wang SX, Clasper S, Su J, Tammi R, et al. LYVE-1, a new homologue of the CD44 glycoprotein, is a lymph-specific receptor for hyaluronan. J Cell Biol 1999;144:789–801.
31. Breiteneder-Geleff S, Soleiman A, Horvat R, Amann G, Kowalski H, Kerjaschki D. [Podoplanin–a specific marker for lymphatic endothelium expressed in angiosarcoma]. Verh Dtsch Ges Pathol 1999;83:270–5.
32. Faye MD, Holcik M. The role of IRES trans-acting factors in carcinogenesis. Biochim Biophys Acta 2015;1849:887–97.
33. Ainaoui N, Hantelys F, Renaud-Gabardos E, Bunel M, Lopez F, Pujol F, et al. Promoter-dependent translation controlled by p54nrb and hnRNPM during myoblast differentiation. PLoS One 2015;10:e0136466.
34. Willimott S, Wagner SD. Post-transcriptional and post-translational regulation of Bcl2. Biochem Soc Trans 2010;38:1571–5.
35. Stacker SA, Williams SP, Karnezis T, Shayan R, Fox SB, Achen MG. Lymphangiogenesis and lymphatic vessel remodelling in cancer. Nat Rev Cancer 2014;14:159–72.
36. Whalen SG, Gingras AC, Amankwa L, Mader S, Branton PE, Aebersold R, et al. Phosphorylation of eIF-4E on serine 209 by protein kinase C is inhibited by the translational repressors, 4E-binding proteins. J Biol Chem 1996;271:11831–7.
37. Silvera D, Arju R, Darvishian F, Levine PH, Zolfaghari L, Goldberg J, et al. Essential role for eIF4GI overexpression in the pathogenesis of inflammatory breast cancer. Nat Cell Biol 2009;11:903–8.
38. Avdulov S, Li S, Michalek V, Burrichter D, Peterson M, Perlman DM, et al. Activation of translation complex eIF4F is essential for the genesis and maintenance of the malignant phenotype in human mammary epithelial cells. Cancer Cell 2004;5:553–63.
39. Luo J, Wang X, Xia Z, Yang L, Ding Z, Chen S, et al. Transcriptional factor specificity protein 1 (SP1) promotes the proliferation of glioma cells by upregulating midkine (MDK). Mol Biol Cell 2015;26:430–9.
40. Lu Q, Hua J, Kassir MM, Delproposto Z, Dai Y, Sun J, et al. Imaging lymphatic system in breast cancer patients with magnetic resonance lymphangiography. PLoS One 2013;8:e69701.

Figure S1

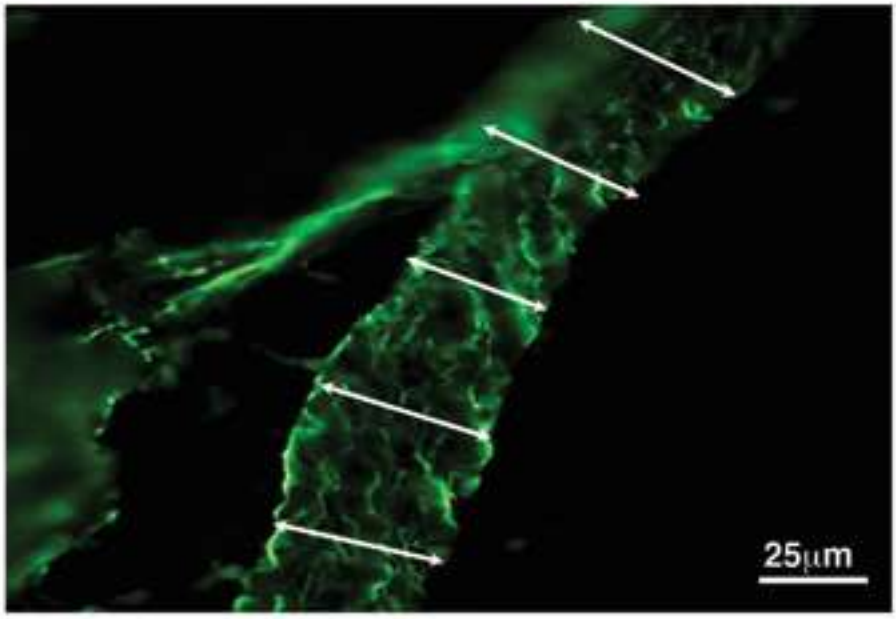

Figure S2

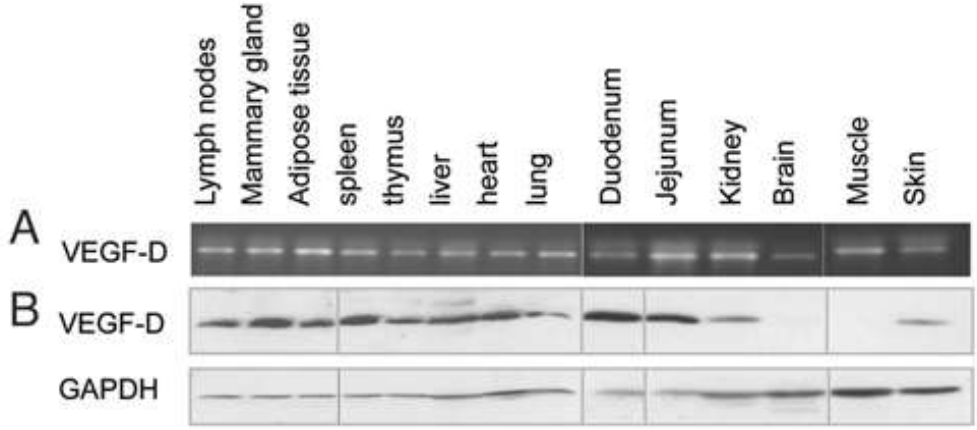

Figure S3

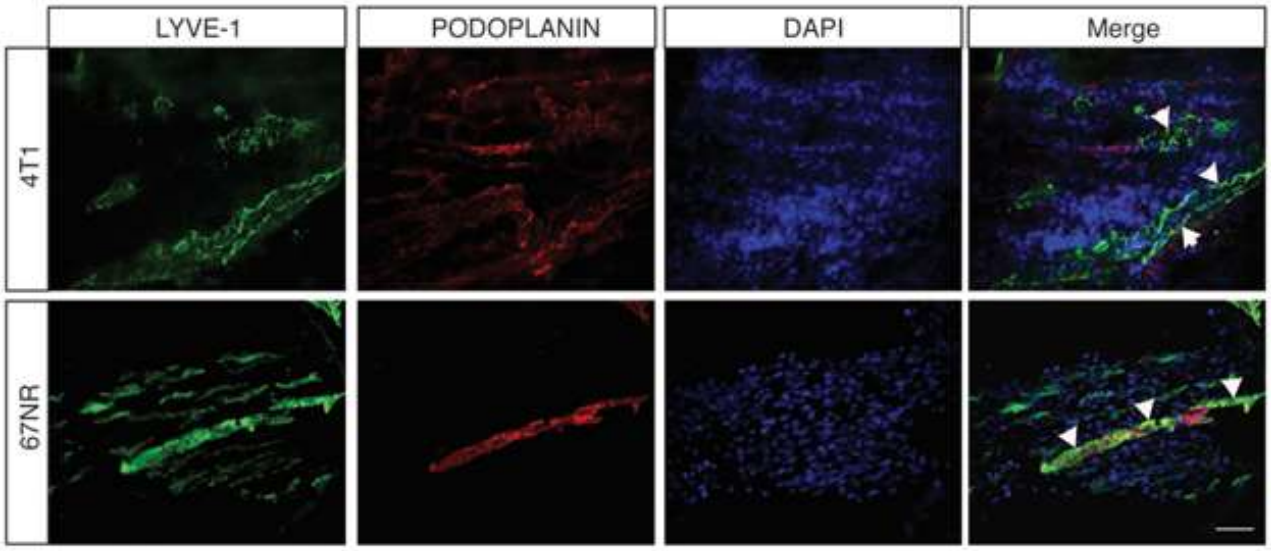

Figure S4

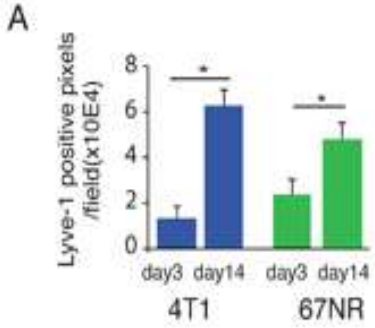

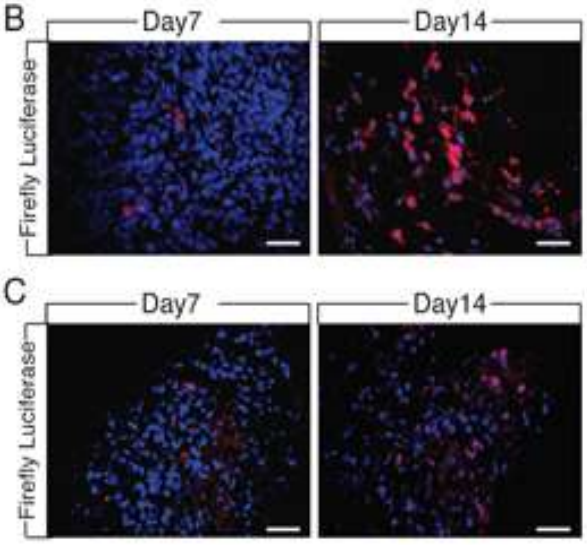

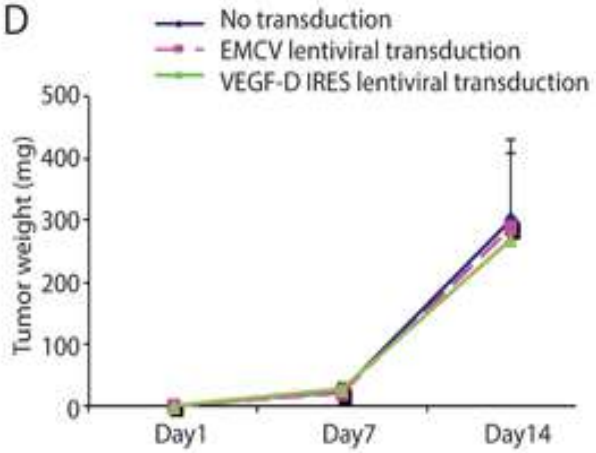

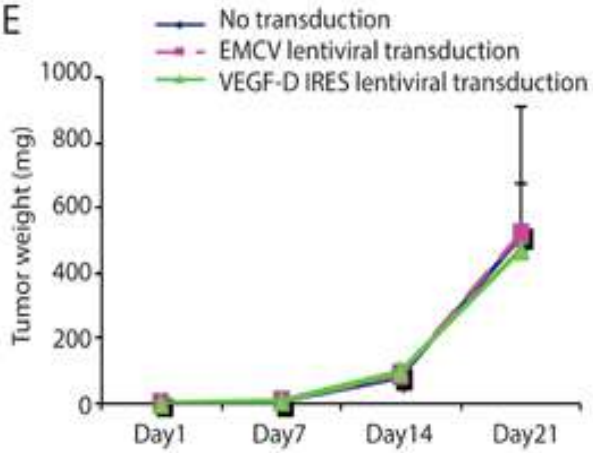

Figure S5

A

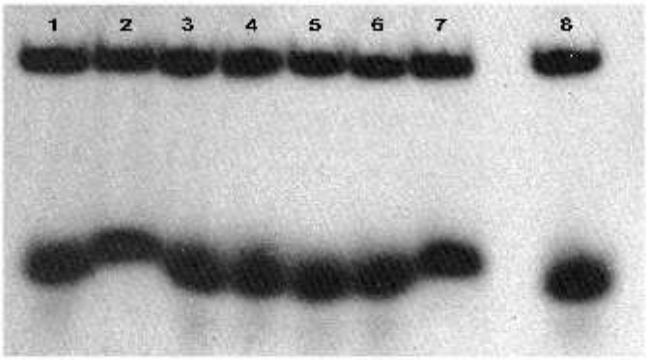

B

VEGF-D 37°C					
Accession	Name	MW (kDa)	pI	Mascot Score	Peptides
FIBB	Fibrinogen beta chain - Mus musculus	54.72	8.83	98.13	6
FIBG	Fibrinogen gamma chain - Mus musculus	49.36	5.47	143.13	8
NUCL	**Nucleolin - Mus musculus**	**78.68**	**4.53**	**55.07**	**1**
K1C10	Keratin, type I cytosqueletal 10 - Mus musculus	57.74	4.9	192.52	4
K2C8	Keratin, type II cytosqueletal 8 - Mus musculus	54.53	5.59	90.65	2
K2C79	Keratin, type II cytosqueletal 79 - Mus musculus	57.52	8.62	112.09	2

VEGF-D 42°C					
Accession	Name	MW (kDa)	pI	Mascot Score	Peptides
FIBB	Fibrinogen beta chain - Mus musculus	54.72	6.83	170.56	7
ROAA	Heterogeneous nuclear ribonucleoprotein A/B - Mus musculus	30.81	8.74	85.4	3
CERU	Ceruloplasmin - Mus musculus	121.07	5.47	48.35	2
NUCL	**Nucleolin - Mus musculus**	**76.68**	**4.53**	**131.61**	**3**
K1C10	Keratin, type I cytosqueletal 10 - Mus musculus	57.74	4.90	231.86	6
K2C79	Keratin, type II cytosqueletal 79 - Mus musculus	57.52	8.62	97.41	3
K2C8	Keratin, type II cytosqueletal 8 - Mus musculus	54.53	5.59	132.68	5
EMCV 37°C					
Accession	Name	MW (kDa)	pI	Mascot Score	Peptides
FIBB	Fibrinogen beta chain - Mus musculus	54.72	6.83	188.41	7
FIBG	Fibrinogen gamma chain - Mus musculus	49.36	5.47	171.7	4
NUCL	**Nucleolin - Mus musculus**	**76.78**	**4.53**	**111.0**	**3**
K1C10	Keratin, type I cytosqueletal 10 - Mus musculus	57.74	4.90	222.94	5
K2C79	Keratin, type II cytosqueletal 79 - Mus musculus	57.52	8.62	74.48	2
PA2G4	Proliferation-associated protein 2G4 - mus musculus	43.67	6.44	312.55	7
EMCV 42°C					
Accession	Name	MW (kDa)	pI	Mascot Score	Peptides
FIBB	Fibrinogen beta chain - Mus musculus	54.72	6.83	129.68	5
FIBG	Fibrinogen gamma chain - Mus musculus	49.36	5.47	190.82	8
NUCL	**Nucleolin - Mus musculus**	**76.68**	**4.53**	**89.37**	**2**
K1C16	Keratin, type I cytosqueletal 16 - Mus musculus	51.57	4.98	48.87	1
K2C8	Keratin, type II cytosqueletal 8 - Mus musculus	54.53	5.59	89.08	6
K22E	Keratin, type II cytosqueletal 2 epidermal - Mus musculus	70.88	9.07	128.27	2
K1C10	Keratin, type I cytosqueletal 10 - Mus musculus	57.74	4.90	217.37	5
K2C79	Keratin, type II cytosqueletal 79 - Mus musculus	57.52	8.62	90.1	2

Figure S6

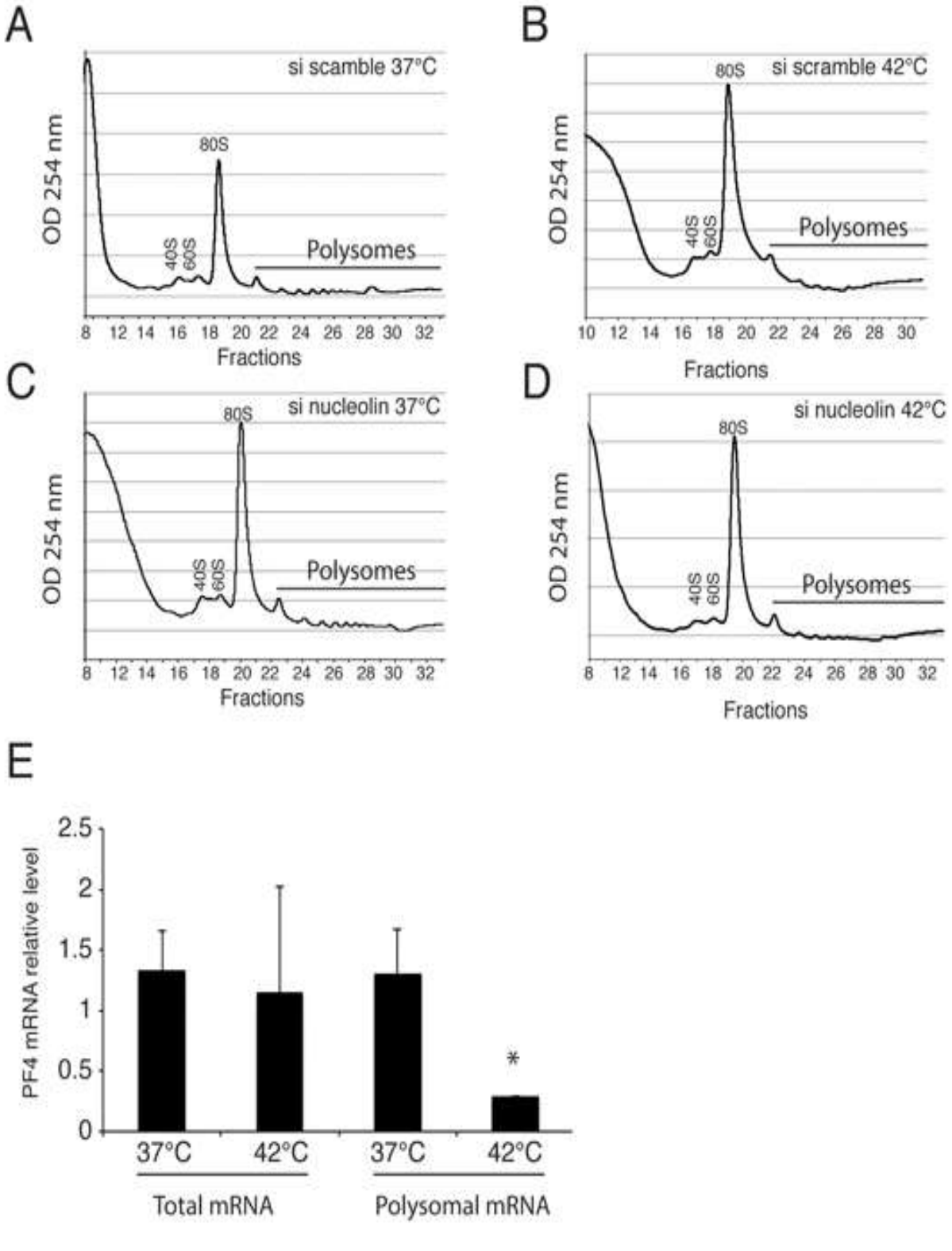
A
si scamble 37°C
OD 254 nm
80S
40S
60S
Polysomes
8 12 14 16 18 20 22 24 26 28 30 32
Fractions
B
si scramble 42°C
80S
OD 254 nm
40S
60S
Polysomes
10 12 14 16 18 20 22 24 26 28 30
Fractions
C
si nucleolin 37°C
80S
OD 254 nm
40S
60S
Polysomes
8 12 14 16 18 20 22 24 26 28 30 32
Fractions
D
si nucleolin 42°C
80S
OD 254 nm
40S
60S
Polysomes
8 12 14 16 18 20 22 24 26 28 30 32
Fractions
E
PF4 mRNA relative level
2.5
2
1.5
1
0.5
0
*
37°C
42°C
37°C
42°C
Total mRNA
Polysomal mRNA

Figure S7

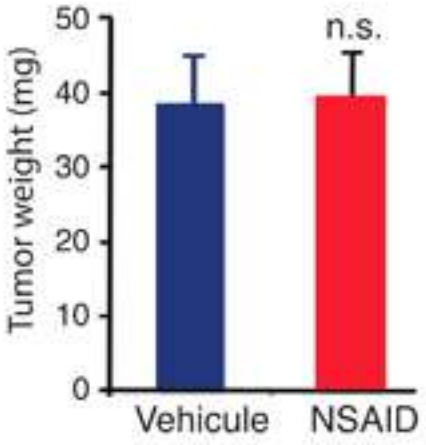

Figure S8

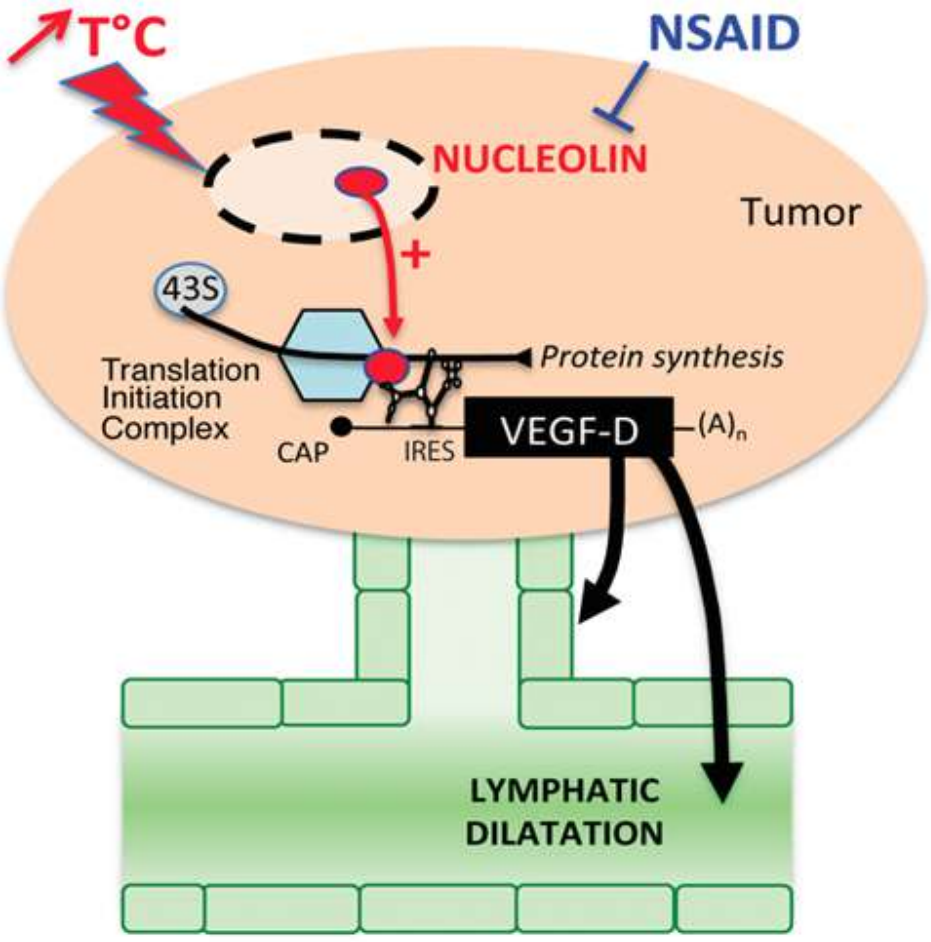

SUPPLEMENTAL INFORMATIONS

Figure S1. Method to quantify lymphatic vessels diameter

Staining for lyve-1 (green) to quantify lymphatic vessels diameter using 5 measures (white arrow) per vessel.

Figure S2. Expression of endogenous VEGF-D in mice tissues

(**A**) VEGF-D mRNA was detected in all mice tissues using RT-PCR analysis. (**B**) VEGF-D protein analysis using western blots shows an ubiquitous expression in mice tissues except for organ that do not contain lymphatic vessels (brain) or are poorly vascularized with lymphatic vessels (muscle).

Figure S3. Podoplanin staining of lymphatic vessels

Staining for lyve-1 (green), Podoplanin (red) and dapi (blue) demonstrated a colocalization of the lymphatic markers (Merge, white arrows) in 4T1 and 67NR tumors. Bar:50μm

Figure S4. Lymphangiogenesis and tumor gowth are not affected by 4T1 or 67NR lentiviral transduction.

(A) Lymph node lymphangiogenesis in 4T1 and 67NR draining (inguinal) lymph nodes was measured using Lyve-1 positive pixels densitometry analysis. (B,C) VEGF-D IRES-dependent Firefly luciferase immunodetection in 4T1 (B) and 67NR (C) tumors. (D,E) Lentiviral transduction of 4T1 (A) and 67NR (B) cell lines do not affect tumor growth. Bar:50μm

Figure S5. VEGF-D 5'UTR mRNA exhibits two structural forms that allow the binding of different proteins.

(A) Two RNA forms can be observed on a native 5% acrylamide gel (in TB 1X with 2 mM MgCl2) in all the different conditions used to fold in vitro the 5'UTR of VEGF-D mRNA. The lanes represent the following conditions: 1): RNA in water at 20°C; 2): RNA in SBC buffer at 20°C; 3): RNA thermally unfolded and then refolded at 20°C in water; 4): RNA thermally unfolded and then refolded at 20°C in 10 mM MgCl2; 5): RNA thermally unfolded and then refolded at 37°C in water; 6): RNA thermally unfolded and then refolded at 37°C in 10 mM MgCl2; 7): RNA thermally unfolded and then refolded at 20°C in SBC buffer. (B) Biomolecular interaction analysis (BIA) uses a surface plasmon resonance phenomenon to characterize macromolecular interactions and has been recently been optimized to enable the recovery and identification of interacting molecules by coupling BIA with mass spectrometry (MS). BIA-MS has proven successful in the identification of the partners in protein-protein interactions as it provides a high sensitivity compared to classical affinity chromatography approaches and permits identification from small quantities of bound ligands. This novel technology was selected in the present study to search for proteins bound to the VEGF-D IRES during heat shock stress and compared to EMCV viral IRES.

Figure S6. Polysome profiling of 4T1 cells

(A-D) Polysome profiling on 4T1 cells transfected with scrambled (A,B) or siRNA against nucleolin (C,D) incubated in physiological (37°C)(A,C) or heated (42°C)(B,D) temperature. (E) Quantitative PF4 RT-PCR on total mRNA and polysomal mRNA from 4T1 cells incubated in physiological (37°C) or heated (42°C).

Figure S7. Tumor growth after NSAID treatment

4T1-bearing mice treated with NSAID exhibits no tumor growth difference after 14 days with vehicule-treated mice.

Figure S8. Schematic representation of VEGF-D synthesis in tumor cells.

Increased temperature induces nucleolin export from the nuclei to cytoplasm. Cytoplasmic nucleolin can bind VEGF-D IRES to recruit translation initiation complex. In that context, secreted VEGF-D promotes lymphatic vessel dilatation. Non-steroidal anti-inflammatory drugs (NSAID) inhibit nucleolin export to the cytoplasm and reduce VEGF-D synthesis and subsequent lymphatic dilatation.

Chapitre 3

Les IRES sont des régulons traductionnels qui gouvernent l'induction séquentielle des facteurs de croissance (lymph)angiogéniques dans les cardiomyocytes en hypoxie

L'hypoxie est un acteur majeur de l'induction de l'angiogenèse et de la lymphangiogenèse qui affecte l'expression génique au niveau transcriptionnel et traductionnel. Ce stress inhibe la traduction globale dans la cellule. Malgré cette inhibition, la synthèse de certaines protéines dont les transcrits contiennent des IRES est maintenue voire activée.

Des études précédentes de l'équipe ont montré que les IRES de des ARNm de facteurs (lymph)angiogéniques comme le FGF2, le VEGFA et le VEGFC sont activés par l'hypoxie dans des cellules tumorales (VEGFA, VEGFC) ainsi que dans l'ischémie cutanée ou du membre (FGF2, VEGFA). J'ai contribué à l'étude sur le VEGFC qui est jointe en annexe.

Ce volet de mon travail de thèse est focalisé sur l'hypoxie non tumorale, qui survient lors de l'ischémie cardiaque. Je me suis intéressée au contrôle de l'expression génique dans des cardiomyocytes HL-1. Pour cela, une approche globale de qPCR à haut débit a été réalisée en utilisant une puce Fluidigm de 96 gènes "lymph"angiogéniques.

L'analyse du transcriptome et du traductome montre que peu de gènes sont induits au niveau du transcriptome alors que la plupart sont recrutés dans les polysomes en réponse à l'hypoxie, suggérant une induction traductionnelle. De plus certains gènes sont induits précocement et d'autres plus tardivement. De manière intéressante, tous les ARNm connus pour posséder un IRES ont été retrouvés dans les polysomes des cardiomyocytes hypoxiques.

Pour aller plus loin dans le mécanisme d'activation des gènes angiogéniques et lymphangiogéniques, nous avons étudié la régulation de l'activité d'une série d'IRES à différents temps d'hypoxie, après transduction des cardiomyocytes avec des lentivecteurs bicistroniques. Nous montrons que tous les IRES sont activés, mais à différents temps d'hypoxie. Les résultats font apparaître trois vagues d'activation : les IRES des FGF sont activés très précocement à 4h, ceux des VEGF un peu moins précocement à 8h, alors que les IRES de c-myc et d'EMCV, non liés à l'angiogenèse, sont activés en phase tardive à 24h d'hypoxie.

L'utilisation de la BIA-MS a été utilisée pour rechercher des ITAF "hypoxiques" dans les cardiomyocytes, ce qui a permis d'identifier pour l'instant un nouvel ITAF: la vasohibine-1 (VASH-1), qui paraît réguler spécifiquement l'IRES du FGF1 en hypoxie. L'identification d'autres ITAF spécifiques de chaque vague d'activation d'IRES est en cours. Ces résultats démontrent d'ores et déjà que le mécanisme IRES-dépendant est crucial pour contrôler l'expression des facteurs (lymph)angiogéniques dans le cœur. Ils suggèrent aussi que différents ITAF sont impliqués pour permettre ces différentes vagues d'induction traductionnelle, qui sont probablement requises pour permettre la formation de vaisseaux fonctionnels dans le cœur ischémique.

IRESs as translational regulons for sequential induction of (lymph)angiogenic growth factors in hypoxic cardiomyocytes

Fransky Hantelys[1], Edith Renaud-Gabardos[1], Anne-Claire Godet[1], Françoise Pujol[1], Isabelle Ader[2], Letitia Ligat[3], Anthony Henras[4], Angelo Parini[1], Barbara Garmy-Susini[1], and Anne-Catherine Prats[1§]

[1]UMR 1048-I2MC, Inserm, FHU IMPACT, UPS, F-31432 Toulouse, France.

[2]UMR 5273-STROMALAB, CNRS, Inserm, UPS, F-31432 Toulouse, France.

[3]UMR 1037-CRCT, Inserm, UPS, F-31432 Toulouse, France.

[4]UMR 5099-LBME, CNRS, UPS, F-31062 Toulouse, France.

[§]Corresponding author.

Contact information : Anne-Catherine Prats, Institut des Maladies Métaboliques et Cardiovasculaires, 1, Avenue Jean Poulhes, BP 84225, 31432 Toulouse cedex 4, France (e-mail: Anne-Catherine.Prats@inserm.fr)

Running title: IRESs as translational regulons in hypoxic cardiomyocytes

Key words: translation/ IRES/ FGF/ VEGF/ vasohibin/ hypoxia/ ischemic heart disease

ABSTRACT

Hypoxia, a major inducer of angiogenesis, is known to trigger major changes of gene expression, including transcription activation by hypoxia-induced factor (HIF) associated to a strong blockade of mRNA translation. Internal ribosome entry site (IRES)-dependent translation however allows expression of a few mRNAs during hypoxia. Here we performed gene expression profiling in hypoxic HL-1 cardiomyocytes from mouse ischemic heart, using a Fluidigm deltagene qPCR array dedicated to (lymph)angiogenesis genes. Total or polysomal RNAs were analyzed to obtain transcriptome or translatome signature, respectively. Data show that only a few genes, including the targets of HIF-1, are induced in the transcriptome, whereas most of them are recruited into polysomes during hypoxia, suggesting a wide translational induction. All the known IRES-containing mRNAs were found associated to polysomes of hypoxic cells. IRES-activities were measured at different times of hypoxia, after cardiomyocyte transduction with bicistronic lentivectors, revealing a sequential activation during hypoxia. Fibroblast growth factor IRESs were activated at 4 hours, vascular endothelial growth factor IRESs at 8 hours, whereas IRESs of non angiogenic mRNAs were activated at 24h only. Biomolecular analysis coupled to mass spectrometry and knock-down experiments led us to identification of vasohibin1 (VASH1) as a new IRES trans-acting factor (ITAF) active in cardiomyocytes in the first step of early hypoxia. These data suggest that IRESs constitute regulons under the control of specific ITAFs, leading to sequential translational induction of (lymph)angiogenic factors whose expression is required to form new functional vessels in ischemic heart.

INTRODUCTION

Hypoxia constitutes a major stress in different pathologies, including cancer where the center of solid tumors lacks oxygen, as well as ischemic pathologies where artery occlusion leads to hypoxic conditions due to a poor or absent tissue perfusion. In all these pathologies, hypoxia induces a cell response that stimulates angiogenesis in order to feed the starved cells with oxygen and nutriments (Pouyssegur et al., 2006). More recently it has been shown that formation of lymphatic vessels, lymphangiogenesis, is also induced by hypoxia (Morfoisse et al., 2014a). Hypoxia-induced (lymph)angiogenesis is mediated by a strong modification of gene expression at both transcriptional and post-transcriptional levels (Holcik & Sonenberg, 2005, Pouyssegur et al., 2006). A major way of gene expression regulation is mediated at the transcriptional level by the hypoxia induced factor 1 (HIF1), a transcription factor stabilized by oxygen deprivation, that activates transcription from promoters containing hypoxia responsive elements (HRE). One of the well-described HIF1 targets is vascular endothelial growth factor A (VEGFA), a major angiogenic factor (Forsythe et al., 1996, Pages & Pouyssegur, 2005). However, two other major angiogenic or lymphangiogenic growth factors, fibroblast growth factor 2 (FGF2) and VEGF-C, respectively, are induced by hypoxia in a HIF-independent manner by a translational mechanism, indicating the importance of the post-transcriptional regulation of gene expression in this process (Conte et al., 2008, Morfoisse et al., 2014a).

Translational control of gene expression plays a crucial role in the stress response. In particular, translation of most mRNAs, occuring by the classical cap-dependent mechanism, is silenced whereas alternative translational mechanisms allow enhanced expression of a small group of messengers involved in the control of cell survival (Baird et al., 2006, Holcik & Sonenberg, 2005, Spriggs et al., 2008). One of the major alternative mechanisms able to overcome this global inhibition of translation by stress depends on internal ribosome entry sites (IRESs) that correspond to RNA structural elements allowing internal ribosome recruitment on mRNA. As regards the molecular mechanisms of IRES activation by stress, several studies have reported the involvement of RNA binding proteins, called IRES trans-acting factors (ITAFs), able to stabilize the adequate RNA conformation allowing ribosome recruitment (Faye & Holcik, 2015, Lewis & Holcik, 2008, Liberman et al., 2015, Mitchell et al., 2003, Morfoisse et al., 2016). However, ITAFs involved in the hypoxic response remain a challenging question to address.

Interestingly, IRESs are present in the mRNAs of several (lymph)angiogenic growth factors in the FGF and VEGF families, suggesting that the IRES-dependent mechanism might be a major way to activate angiogenesis and lymphangiogenesis during stress (Huez et al., 1998, Martineau et al., 2004, Morfoisse et al., 2014a, Morfoisse et al., 2016, Stein et al., 1998, Vagner et al., 1995). However, most studies of the role of hypoxia in gene expression regulation have been performed in tumoral hypoxia, while it has been reported that tumoral angiogenesis leads to formation of abnormal vessels that are non functional, which strongly differs from

non tumoral angiogenesis that induces formation of functional vessels (Jain, 2005). This suggests that gene expression regulation in response to hypoxia may be different in cancer versus ischemic pathologies. In particular, the role of IRESs in the control of gene expression in ischemic heart, the most frequent ischemic pathology, remains to be elucidated.

Here we analyzed the transcriptome and the translatome of (lymph)angiogenic growth factors in hypoxic cardiomyocytes, and studied regulation of IRES activities in early and late hypoxia. Data show that in cardiomyocyte, most (lymph)angiogenic growth factor are mostly regulated at the translational level. Interestingly FGF and VEGF mRNA IRESs are activated at different times of early hypoxia in contrast to IRESs of non angiogenic messengers. We also looked for ITAFs governing IRES activation in hypoxia and identified Vasohibin 1 (VASH1) as a new ITAF expressed in hypoxic cardiomyocytes.

RESULTS

Few (lymph)angiogenic genes are induced in the transcriptome of hypoxic cardiomyocytes.

In order to analyze expression of angiogenic and lymphangiogenic growth factors in hypoxic cardiomyocytes, the HL-1 cell line was chosen: although immortalized, it has kept the beating phenotype specific to cardiomyocyte (Claycomb et al., 1998). HL-1 cells were submitted to increasing times of hypoxia, from 5 minutes to 24

hours, then cDNA was prepared from cell extracts and analyzed using a Fluidigm Deltagene PCR array targeting 96 genes of angiogenesis, lymphangiogenesis and/or stress (Fig. 1 and Table S1). Data showed that three known HIF1 targets VEGFA, PAI-1 and apelin are induced at 8h of hypoxia (Forsythe et al., 1996, Kietzmann et al., 1999, Ronkainen et al., 2007). Unexpectedly, only a few genes were significantly induced, whereas several genes of major angio- or lymphangiogenic factors, such as FGF2 and VEGFC, were strongly repressed at the mRNA level after 4h or 8h of hypoxia. These data indicate that the transcriptional response to hypoxia in cardiomyocytes is not the major mechanism controlling gene expression, suggesting that post-transcriptional mechanisms are probably involved.

mRNAs of most (lymph)angiogenic genes are recruited into polysomes in hypoxic cardiomyocytes.

The recruitment of mRNAs into polysomes was then analyzed to test the hypothesis of translational induction. This experiment was performed in early hypoxia (4 h). The polysome profile showed, as expected, a strong decrease of global translation (Fig. 2A). In contrast, most genes of the (lymph)angiogenic array were more efficiently recruited into polysomes in hypoxic conditions (Fig. 2B, Table S2). This translational induction not only targets major angiogenic factors and their receptors (VEGFA, FGF1, PDGFA, FGFR3, KDR,...), but genes involved in cardiomyocyte survival in ischemic heart (IGF1, IGF1R) or in inflammation (BAI1, TGFb). These data suggest that in cardiomyocytes, the main response to early hypoxia is not transcriptional, but translational.

All IRES-containing mRNAs are more efficiently associated to polysomes in hypoxic conditions.

IRES-dependent translation has been reported to drive translation of several mRNAs in stress conditions (Conte et al., 2008, Holcik & Sonenberg, 2005, Morfoisse et al., 2014a, Morfoisse et al., 2014b). Thus we focused onto the regulation of the different IRES-containing mRNAs present the Fluidigm array (Fig. 3). Interestingly, the only IRES-containing mRNA to be induced at the transcriptional level by hypoxia was VEGFA, up to ten times at 24 h of hypoxia (Fig. 3A). Expression of the apelin-receptor (aplnnr), presumably devoid of IRES, is also shown for comparison.

Polysome recruitment of these IRES-containing mRNAs is shown in figure 3B. Clearly, FGF1, VEGFA, VEGFD, HIF1α , IGF1R and Cyr61 mRNAs were recruited into polysomes in hypoxia 2 to 4 times more than in normoxia, which means an important induction in terms of protein synthesis. In contrast, the aplnnr mRNA present in polysomes decreases about three times. The data are not available for FGF2 and VEGFC mRNAs, which were under the threshold of detection. These results indicate that hypoxia in cardiomyocytes, although blocking global cap-dependent translation, is able to induce translation of all detectable IRES-containing angiogenic factor mRNAs. This mechanism occurs as soon as after 4 hours of oxygen deprivation, thus corresponding to an early event in the hypoxic response process.

IRESs of (lymph)angiogenic factor mRNAs are activated at different times of early hypoxia.

To check that the polysome recruitment of IRES-containing mRNAs actually corresponds to a stimulation of IRES-dependent translation, IRESs from FGF and VEGF mRNAs were introduced into a bicistronic dual luciferase gene expression cassette (Fig. 4A). As controls, two IRESs from non angiogenic mRNAs, c-myc and EMCV IRESs, were used in the experiment. The IRES-containing cassettes were subcloned into a lentivector plasmid, as HL-1 cells are not efficiently transfected by plasmids but can be easily transduced by lentivectors with an efficiency of more than 80% (not shown). The bicistronic vector strategy, previously validated by us and others, allows to measure IRES activity revealed by expression of the second cistron, LucF (Creancier et al., 2000, Morfoisse et al., 2014a). HL-1 cardiomyocytes were transduced by the different lentivectors, then submitted to increasing times of hypoxia. Luciferase activities were measured from cell extracts and IRES activities shown as the ratio LucF/LucR. Data showed different behaviors, depending on the IRES (Fig. 4B-D). Clearly, the FGF IRESs were induced early, after 4 hours of oxygen deprivation (Fig. 4B). The FGF1 IRES showed a peak at 4 hours, while the FGF2 IRES continued to be activated at 8 hours. The four VEGF IRESs all peaked after 8 hours of hypoxia (Fig. 4C). However the VEGFA IRES activities decreased at 4 hours whereas that of the VEGFC and -D IRESs did not. Finally, the c-myc and EMCV IRESs were activated only in late hypoxia after 24 hours (Fig. 4D). These data provide two important

informations: first, IRESs from (lymph)angiogenic growth factor mRNAs are activated during early hypoxia, in contrast to other IRESs. Second, these "angiogenic" IRESs are sequentially activated in two waves during early hypoxia. The earliest wave concerns the FGF IRESs, especially FGF1 IRES, whereas a second wave of activation concerns the VEGF IRESs.

Identification of IRES-bound proteins in hypoxic cardiomyocytes reveals the presence of vasohibin-1.

The two waves of activation of the angiogenic factor IRESs in early hypoxia suggested that different ITAFs may be involved at 4 hours and at 8 hours. In an attempt to identify such ITAFs, we used the technology of biomolecular analysis coupled to mass spectrometry (BIA-MS), validated for ITAF identification in two previous studies (Ainaoui et al., 2015, Morfoisse et al., 2016). Biotinylated RNAs corresponding to FGF1, VEGFA (a) and EMCV IRESs were used as probes for BIA-MS, then bound proteins from normoxic and hypoxic HL-1 cells were recovered and identified (Fig. 5A-B, Table S3). Surprisingly, except for nucleolin bound to the VEGFA IRES in normoxia, no known ITAF was identified as bound to these IRESs in normoxia or in hypoxia. Thus we considered potential interesting features of other candidates and were interested by the presence of vasohibin-1 (VASH1), a protein described as an endothelial cell-produced angiogenesis inhibitor, but also for its role in stress tolerance and cell survival (Sato, 2012, Sato,

2015). Interestingly, VASH1 was bound to the FGF1 IRES in hypoxia, but not in normoxia (Table S3). This protein was also bound to the EMCV IRES both in normoxia and hypoxia but not to the VEGFA IRES. VASH1 has been described as a secreted protein but never as an RNA-binding protein. However, the *in silico* analysis of VASH1 protein predicts an RNA-binding domain with the highest level of confidence, suggesting that it could bind directly to the IRES (Fig. 5C).

Vasohibin 1 is a new ITAF selectively active in early hypoxia.

VASH1 has been previously described for its expression in endothelial cells but never in cardiomyocytes (Sato, 2012). Our BIA-MS study provides evidence that it is expressed in HL-1 cardiomyocytes (Table S3). We analyzed the regulation of VASH1 expression at the mRNA level during hypoxia, obtained from the Fluidigm array (Fig 1, Table S1): VASH1 mRNA expression strongly decreases after 4 hours of hypoxia whereas it is slightly upregulated at 8 hours (Fig. 6A). However we have previously observed, in the case of FGF2 and VEGFC, that a decrease of mRNA accumulation in response to hypoxia may be accompanied by an increase of protein expression (Conte et al., 2008, Morfoisse et al., 2014a). Indeed, analysis of VASH1 mRNA level in polysomes showed a strong increase (almost 7 times) indicating that VASH1 expression is induced at the translational level after 4h of hypoxia (Fig. 6B).

The putative ITAF function of VASH1 was assessed by a knock-down approach using an siRNA smartpool (siVASH1). Transfection of HL-1 cardiomyocytes with siVASH1 was able to knock down VASH1 mRNA with an efficiency of 73% (Fig. 6C). The effect of VASH1 knock-down was analyzed in HL-1 cells transduced with the different IRES-containing bicistronic lentivectors used in Figure 4. The results showed that the FGF1 IRES activity decreases by 80% upon VASH1 knock-down, whereas the other IRESs are not down-regulated (Fig. 6D). Strikingly, the VEGFA (a) IRES activity is enhanced in the absence of VASH1. These data suggest that VASH1 is an ITAF active in early hypoxia (4 hours), able to up-regulate the FGF1 IRES, whereas it could act as a repressor of the VEGFAa IRES.

Vasohibin 1 knock-down affects the translation of (lymph)-angiogenic factor mRNAs .

In order to detect a possible effect of VASH1 on the translation of other mRNAs, polysomal RNAs were purified from HL-1 cells transfected by the VASH1 siRNA smartPool or by the control siRNA. RNA recruitment into polysomes was analyzed with the Fluidigm array as above. The data showed the VASH1 knock-down generates a decrease of polysome recruitment for numerous mRNAs, while another set of mRNAs are more efficiently recruited (Fig. 7 and Table S2). Interestingly, the presence of FGF1 and IGF1R mRNAs in polysomes decreased, whereas that of VEGFA and -D mRNAs increased. This was consistent with the data of Fig. 6D, at least for FGF1 and VEGFA. These results suggest that VASH1 could be widely involved, directly or indirectly, in translational control of (lymph)angiogenic factor

expression. Furthermore, it seems to be involved in mechanisms of translational activation or repression of subsets of mRNAs.

DISCUSSION

The present study highlights the crucial role of translational control in the cardiomyocyte response to hypoxia. Up to now, although a few genes had been described for their translational regulation by hypoxia, it was thought that most genes are transcriptionally regulated. Here we show that translational control, revealed by mRNA recruitment in polysomes during hypoxia, concerns the majority of the genes involved in angiogenesis and lymphangiogenesis. IRES-dependent translation appears as a key mechanism in this process, as we show that all the mRNAs known to contain an IRES are up-regulated. Furthermore, our data reveal that IRESs of angiogenic factor mRNAs are sequentially activated during early hypoxia, and could constitute translational regulons in the (lymph)angiogenic response to hypoxia. These waves of IRES activation indicate the involvement of different ITAFs, specific of these steps of early hypoxia. We have identified one of these ITAFs, vasohibin-1, responsible for activation of the FGF1 IRES in the first wave of IRES activation. VASH1 seems to influence widely the translation of (lymph)angiogenic factor mRNAs and may have a pivotal role in the translational response to hypoxia in cardiomyocytes.

Translational control in tumoral versus non tumoral hypoxia.

Most studies of gene expression in response to stress have been performed at the transcriptome level in tumoral cells of different origins, whereas the present study is focused on cardiomyocytes. HL-1 cardiomyocytes are immortalized but still exhibit the beating phenotype (Claycomb et al., 1998). This indicates that this cell model, although not perfectly mimicking the cardiomyocyte behavior in vivo, is still closer to a physiological state. The strong translational response to hypoxia revealed by our data, that differs from the transcriptional response usually observed in tumor cells, may reflect mechanisms occuring in cells that are non (or at least not too far) engaged into the cell transformation process leading to cancer. This hypothesis is supported by the observation that most tumor cell lines become resistant to hypoxia. Indeed, HL-1 cells respond to hypoxia very early, whereas various murine or human tumor cell lines described in other reports require a longer time of hypoxia for IRES-dependent translation to be stimulated. In human breast cancer BT474 cells, VEGFA, HIF and EMCV IRESs are all activated after 24h of hypoxia (Braunstein et al., 2007). In murine 4T1 and LLC cells (breast and lung tumor, respectively) as well as in human CAPAN-1 pancreatic adenocarcinoma, the VEGFA and VEGFC IRESs are activated after 24 hours of hypoxia whereas the EMCV IRES is not activated (Morfoisse et al., 2014a). The same observation of late activation in 4T1 cells has been made for the FGF1 IRES, while this IRES is activated after 4 hours in HL-1 cardiomyocytes (Godet AC, unpublished data) (Fig. 4). Also, VEGFD IRES is differently regulated in HL-1 cardiomyocytes compared to 4T1 tumor cells: only heat shock, but not hypoxia, is able to activate this IRES in 4T1 cells, whereas it is

activated after 8 hours of hypoxia in HL-1 cardiomyocytes (Morfoisse et al., 2016) (Fig. 4). These observations suggest that many tumoral cell lines have developed resistance to hypoxia are not able to govern subtle regulations of gene expression such as the waves of IRES regulation observed in HL-1 cells.

VASH1, an early hypoxic ITAF.

We also consider the hypothesis that the important process of translational regulation observed in our study may cardiomyocyte-specific. In such a case IRES-dependent translation would depend on cell type specific ITAFs as well as the early response to hypoxia. In agreement with this hypothesis, VASH1 expression is cell-type specific: described up to now as endothelial-specific, this protein is not expressed in tumoral cells (Sato, 2012). In the present study we show that this cell-type specificity extends to cardiomyocytes. Consistent with our data, this protein has been described as a key actor of striated muscle angio-adaptation (Kishlyansky et al., 2010). VASH1 may thus have a role in the early hypoxic response in a limited number of cell types. The role of VASH1 suggested by our data is meaningful if one considers the function of VASH1 in angiogenesis and stress tolerance (Sato, 2015). Furthermore, it has been reported that VASH1 is induced after 3 hours of cell stress at the protein level but not at the transcriptional level in endothelial cells (Miyashita et al., 2012). This is in agreement with our observation in cardiomyocytes where VASH1, although downregulated in the transcriptome at 4 hours of hypoxia, is more efficiently recruited in polysomes at the same time (Fig. 6).

It noteworthy that VASH1 itself seems to be induced translationally by stress (Miyashita et al., 2012) (Fig. 6). In endothelial cells, Myashita et al report that the protein HuR upregulates VASH1 by binding to its mRNA. HuR may bind to an AU-rich element present in the 3' untranslated region of the VASH1 mRNA. However, in other studies, HuR has also been described as an ITAF, thus it is possible that VASH1 itself may be induced by the IRES-dependent mechanism (Durie et al., 2011, Galban et al., 2008).

The anti-angiogenic function of VASH1 may appear inconsistent with its ability to activate the IRES of an angiogenic factor. However, VASH is described for its unique double feature of inhibiting angiogenesis and promoting endothelial cell survival (Miyashita et al., 2012, Sato, 2015). This could be due to the existence of five different isoforms of VASH1, and only two of them are able to inhibit endothelial cell growth (Kern et al., 2008, Kishlyansky et al., 2010). In the case of cardiomyocytes, the VASH1 function of cell survival promoter is probably involved. The translation activation or inhibition of subsets of genes, observed after VASH1 knock-down in the present study, also suggests that the VASH1 function in translation is not limited to the activation of the FGF1 IRES, and that VASH1 more widely acts on the angiogenic balance.

IRESs as cis-acting regulons in the hypoxic response.

The different waves of IRES activation observed in the present study suggest that different subsets of IRESs function as cis-acting regulons during hypoxia. The

concept of translational regulon has been revealed for the Hox gene family, whose mRNAs all contain IRESs that are regulated by ribosomal protein RPL38 (Xue et al., 2015).

Our data indicate that VASH1 participates in an IRESome able to activate the FGF-1 IRES whereas the data from the Fluidigm with the siRNA VASH1 suggest that additional IRES-containing mRNAs may be translationally induced by VASH1. We hypothesize that FGF1 might belong to a regulon of very early IRESs whereas the VEGF IRESs would constitute a regulon of mid-early IRESs. One must notice that the FGF2 IRES behaves differently from the FGF1 IRES, as it remains activated at 8 hours, in contrast to the FGF1 IRES. This indicates that the FGF2 is probably not regulated by the same IRESome complex as the FGF1 IRES.

Strikingly, VASH1 seems to inhibit the VEGFAa IRES activity, and the Fluidigm data indicate that VASH1 might regulate negatively a subset of other mRNAs. This raises the possibility that an ITAF may be either an activator or a repressor, depending on the IRES. Such a double role for an ITAF has been already described for the protein HuR, able to activate the XIAP and HIF-1α IRESs, whereas it down-regulates the IGF1R, BCL_{xl} and thrombomodulin IRESs (Durie et al., 2013, Durie et al., 2011, Galban et al., 2008, Meng et al., 2005, Yeh et al., 2008). Further study is required to determine the mechanism of action of VASH1. VASH1, itself regulated by HuR, could interact (directly or indirectly) with this protein in its function of translational regulator. Finally, the second wave of IRESs activated in mid-early hypoxia probably requires other ITAFs that remain to be discovered.

MATERIALS & METHODS

Lentivector construction and production

Bicistronic lentivectors coding for the *renilla* luciferase (LucR) and the stabilized firefly luciferase Luc+ (called LucF in the text) were constructed from the dual luciferase lentivectors described previously, which contained Luc2CP (Morfoisse et al., 2014a, Morfoisse et al., 2016). The cDNA sequences of the human FGF1, -2, VEGFA, -C, -D, c-myc and EMCV IRESs were introduced between the first (LucR) and the second cistron (LucF) (Nanbru et al., 1997, Prats et al., 2013, Vagner et al., 1995). The two IRESs of the VEGFA have been used and are called VEGFAa and VEGFAb, respectively (Huez et al., 1998). The expression cassettes were inserted into the SIN lentivector pTRIP-DU3-CMV-MCS vector described previously (Prats et al., 2013). All cassettes are under the control of the cytomegalovirus (CMV) promoter.

Lentivector particles were produced using the $CaCl_2$ method-based by tri-transfection with the plasmids pLvPack and pLvVSVg, $CaCl_2$ and Hepes Buffered Saline (Sigma-Aldrich, Saint-Quentin-Fallavier, France), into HEK-293FT cells. Viral supernatants were harvested 48 hours after transfection, passed through 0.45-µm filters PVDF filters (Dominique Dutscher SAS, Brumath, France) and stored in aliquots at -80C until use. Viral production titers were assessed on HT1080 cells

with serial dilutions and scored for GFP expression by flow cytometry analysis on a BD FACSVerse (BD Biosciences, Le Pont de Claix, France).

Cell culture, transfection and transduction

HEK-293FT cells and HT1080 cellswere cultured in DMEM-GlutaMAX + Pyruvate (Life Technologies SAS, Saint-Aubin, France), supplemented with 10% fetal bovine serum (FBS), and MEM essential and non-essential amino acids (Sigma-Aldrich).

Mouse atrial HL-1 cardiomyocytes were a kind gift from Dr. William Claycomb (Department of Biochemistry & Molecular Biology, School of Medicine, New Orleans) (Claycomb et al., 1998). HL-1 cells were cultured in Claycomb medium containing 10% FBS, Penicillin/Streptomycin (100U/mL-100μg/mL), 0.1mM norepinephrine, and 2mM L-Glutamine. Cell culture flasks were pre-coated with a solution of 0.5% fibronectin and 0.02% gelatin 1h at 37C (Sigma-Aldrich). To keep HL-1 phenotype, cell culture was maintained as previously described (Claycomb et al., 1998).

For hypoxia, cells were incubated at 37C at 1%O_2 and 5%CO_2.

HL-1 cardiomyocytes were transfected by siRNAs as follows: One day after being plated, cells were transfected with 10nM of small interference RNAs from Dharmacon Acell SMARTpool targeting VASH1 (siVASH1) or non-targeting siRNA control (siControl), using Lipofectamine RNAiMax (Invitrogen) according

to the manufacter's recommendations, in a media without penillin-streptomycin and norepinephrine. Cells are incubated 72h at 37C with siRNA (siRNA sequences are provided in Table S5).

For lentivector transduction, 6.10^4 HL-1 cells were plated into each well of a 6-well plate and transduced overnight in 1 mL of transduction medium (OptiMEM-GlutaMAX, Life Technologies SAS) containing 5μg/mL protamine sulfate in the presence of lentivectors (MOI 2). GFP-positive cells were quantified by flow cytometry analysis on a BD FACSVerse (BD Biosciences). HL-1 cells were transduced with a 80% efficiency.

Reporter activity assay

For reporter lentivectors, luciferase activities *in vitro* and *in vivo* were performed using Dual-Luciferase Reporter Assay (Promega, Charbonnières-les-Bains,France). Briefly, proteins from HL-1 cells were extracted with Passive Lysis Buffer (Promega France) and proteins from mice heart using PLB and a Precellys® homogenizer (Ozyme, Montigny-le-Bretonneux, France). Quantification of bioluminescence was performed with a luminometer (Centro LB960, Berthold, Thoiry, France).

RNA purification and RT-qPCR

Total RNA extraction from ischemic and healthy areas was performed using TRIzol reagent according to the manufacturer's instructions (Gibco BRL, Life Technologies, NY, USA). RNA quality and quantification were assessed by a Xpose spectrophotometer (Trinean, Gentbrugge, Belgium) and an automated electrophoresis system (Fragment Analyzer, Advanced Analytical Technologies, Paris, France).

500 ng RNA was used to synthesize cDNA using a High-Capacity cDNA Reverse Transcription Kit (Applied Biosystems, Villebon-sur-Yvette, France).

Gene expression was investigated using HotPol Evagreen Super qPCR Mix Plus (Euromedex, France) and performed on a StepOne sequence detection system (Applied Biosystems). 18S rRNA was used as a reference gene and all data were normalized based on 18S rRNA level. Relative gene expression was calculated using the $2^{-\Delta dCT}$method. The oligonucleotide primers used are detailed in Table S4.

qPCR array

The DELTAgene Assay™ was designed by Fluidigm Corporation (San Francisco, USA). The qPCR-array was performed on BioMark with the Fluidigm 96.96 Dynamic Array following the manufacturer's protocol (Real-Time PCR Analysis User Guide PN 68000088). The list of primers is provided in Table S4. A total of 1.25ng of cDNA was pre amplified using PreAmp Master Mix (Fluidigm, PN 100-5580, 100-5581, San Francisco, USA) in the plate thermal cycler at 95C for 2min,

10 cycles at 95C for 15sec and 60C for 4min. The preamplified cDNA was treated by endonuclease I (New England BioLabs, PN M0293L, Massachusetts, USA) **to remove unincorporated primers.**

The preamplified cDNA was mixed with 2x SsoFast EvaGreen Supermix (BioRad, PN 172-5211, California, USA), 50µM of mixed forward and reverse primers and sample Loading Reagent (Fluidigm, San Francisco, USA). The sample was loaded into the Dynamic Array 96.96 chip (Fluidigm San Francisco, USA). The RT-qPCR reactions were performed in the BioMark RT PCR system. Data was analyzed using the BioMark RT-PCR Analysis Software Version 2.0.

Polysomal RNA preparation

HL-1 cells were cultured in 150-mm dishes. 15 min prior to harversting, cells were treated by cycloheximide at 100µg/ml. Cells were washed three times in PBS cold containing 100 µg/mL cycloheximide and scraped in the PBS/cycloheximide. After centrifugation at 3,000 rpm for 2 min at 4C, cells were lysed by 450µl hypotonic lysis buffer (5 mM Tris-HCL, pH7.5 ; 2.5 mM $MgCl_2$; 1.5 mM KCl). Cell were centrifuged at 13,000 rpm for 5 min at 4C, the supernatants were collected and loaded onto a 10-50% sucrose gradient. The gradients were centrifuged in a Beckman SW40Ti rotor at 39,000 rpm for 2.5 h at 4C without brake. Fractions were collected using a Foxy JR ISCO collector and UV optical unit type 11. RNA was

purified from pooled heavy fractions containing polysomes, as well as from light fractions containing free RNA.

Preparation of biotinylated RNA

The FGF1, VEGFA or EMCV IRESs was cloned in pSCB-A-amp/kan plasmid (Agilent) downstream from the T7 sequence. The plasmid were linearized and in vitro transcription was performed with MEGAscript T7 kit (Ambion), according to the manufacturer's protocol, in the presence of Biotin-16-UTP at 1 mM (Roche), as previously described (Ainaoui et al., 2015). The synthesized RNA was purified using RNeasy kit (Qiagen).

BIA-MS experiments

BIA-MS studies based on surface plasmonic resonance (SPR) technology were performed on BIAcore T200 optical biosensor instrument (GE Healthcare), as described previously (Ainaoui et al., 2015, Morfoisse et al., 2016). Immobilization of biotinylated IRES RNAs was performed on a streptavidin-coated (SA) sensorchip in HBS-EP buffer (10mM Hepes pH 7.4, 150mM NaCl, 3mM EDTA, 0.005% surfactant P20) (GE Healthcare). All immobilization steps were performed at a flow rate of 2 μl/min with a final concentration of 100μg/ml.

Binding analyzes were performed with normoxic or hypoxic cell protein extracts at 100 μg/ml over the immobilized IRES RNAs surface for 7 minutes at a flow rate of 30 μl/min.

The channel (Fc1) was used as a reference surface for non-specific binding measurements.

The recovery wizard was used to recover selected proteins from cell protein extracts. This step was carried out with 0.1% SDS. Five recovery procedures were performed to get enough amounts of proteins for MS identification.

LC-MS/MS analyses were performed on Bruker Amazon ETD mass spectrometer.

Statistical analysis

All statistical analyzes were performed using a two-tailed Student's t-test or one-way ANOVA and are expressed as mean +- standard error of the mean, *p<0.05, **p<0.01, ***<0.001, ****<0.0001.

ACKNOWLEDGMENTS

Our thanks go to J.J. Maoret and F. Martin from the Inserm UMR1048 GeT-TQ plateau of the GeT plateform Genotoul (Toulouse), J. Iacovoni from the Inserm UMR 1048 bioinformatics plateau, as well asL.vandenBerghe and C. SegurafromtheInsermUMR1037vectorologyplateau (Toulouse).We alsothank W. Claycomb for providing HL-1 cells.

ThisworkwassupportedbyRégionMidi-Pyrénées, AssociationFrançaisecontrelesMyopathies (AFM-Téléthon),Association pour la Recherche sur leCancer (ARC),Europeanfunding (REFBIO).F.H. had fellowships from the Région Midi-Pyrénées and from the Ligue Nationale Contre le Cancer (LNCC). E.R.G.hadafellowshipfromAFM-Telethon. A.C. Godet had a fellowship from LNCC.

SUPPLEMENTARY MATERIAL

Tables S1, S2, S3, S4, S5

REFERENCES

Ainaoui N, Hantelys F, Renaud-Gabardos E, Bunel M, Lopez F, Pujol F, Planes R, Bahraoui E, Pichereaux C, Burlet-Schiltz O, Parini A, Garmy-Susini B, Prats AC (2015) Promoter-Dependent Translation Controlled by p54nrb and hnRNPM during Myoblast Differentiation. *PLoS One* 10: e0136466

Baird SD, Turcotte M, Korneluk RG, Holcik M (2006) Searching for IRES.*RNA* 12: 1755-1785

Braunstein S, Karpisheva K, Pola C, Goldberg J, Hochman T, Yee H, Cangiarella J, Arju R, Formenti SC, Schneider RJ(2007) A hypoxia-controlled cap-dependent to cap-independent translation switch in breast cancer. *Mol Cell* 28: 501-512

Claycomb WC, Lanson NA, Jr., Stallworth BS, Egeland DB, Delcarpio JB, Bahinski A, Izzo NJ, Jr. (1998) HL-1 cells: a cardiac muscle cell line that contracts and retains phenotypic characteristics of the adult cardiomyocyte. *Proc Natl Acad Sci U S A* 95: 2979-2984

Conte C, Riant E, Toutain C, Pujol F, Arnal JF, Lenfant F, Prats AC(2008) FGF2 translationally induced by hypoxia is involved in negative and positive feedback loops with HIF-1alpha. *PLoS One* 3: e3078

Creancier L, Morello D, Mercier P, Prats AC (2000) Fibroblast growth factor 2 internal ribosome entry site (IRES) activity ex vivo and in transgenic mice reveals a stringent tissue-specific regulation. *J Cell Biol* 150: 275-281

Durie D, Hatzoglou M, Chakraborty P, Holcik M (2013) HuR controls

mitochondrial morphology through the regulation of BclxL translation. *Translation (Austin)* 1

Durie D, Lewis SM, Liwak U, Kisilewicz M, Gorospe M, Holcik M (2011) RNA-binding protein HuR mediates cytoprotection through stimulation of XIAP translation. *Oncogene* 30: 1460-1469

Faye MD, Holcik M (2015) The role of IRES trans-acting factors in carcinogenesis. *Biochim Biophys Acta* 1849: 887-897

Forsythe JA, Jiang BH, Iyer NV, Agani F, Leung SW, Koos RD, Semenza GL (1996) Activation of vascular endothelial growth factor gene transcription by hypoxia-inducible factor 1. *Mol Cell Biol* 16: 4604-4613

Galban S, Kuwano Y, Pullmann R, Jr., Martindale JL, Kim HH, Lal A, Abdelmohsen K, Yang X, Dang Y, Liu JO, Lewis SM, Holcik M, Gorospe M (2008) RNA-binding proteins HuR and PTB promote the translation of hypoxia-inducible factor 1alpha. *Mol Cell Biol* 28: 93-107

Holcik M, Sonenberg N (2005) Translational control in stress and apoptosis. *Nat Rev Mol Cell Biol* 6: 318-327

Huez I, Creancier L, Audigier S, Gensac MC, Prats AC, Prats H (1998) Two independent internal ribosome entry sites are involved in translation initiation of vascular endothelial growth factor mRNA. *Mol Cell Biol* 18: 6178-6190

Jain RK (2005) Normalization of tumor vasculature: an emerging concept in antiangiogenic therapy. *Science* 307: 58-62

Kern J, Bauer M, Rychli K, Wojta J, Ritsch A, Gastl G, Gunsilius E,

Untergasser G (2008) Alternative splicing of vasohibin-1 generates an inhibitor of endothelial cell proliferation, migration, and capillary tube formation. *Arterioscler Thromb Vasc Biol* 28: 478-484

Kietzmann T, Roth U, Jungermann K (1999) Induction of the plasminogen activator inhibitor-1 gene expression by mild hypoxia via a hypoxia response element binding the hypoxia-inducible factor-1 in rat hepatocytes. *Blood* 94: 4177-4185

Kishlyansky M, Vojnovic J, Roudier E, Gineste C, Decary S, Forn P, Bergeron R, Desplanches D, Birot O (2010) Striated muscle angio-adaptation requires changes in Vasohibin-1 expression pattern. *Biochem Biophys Res Commun* 399: 359-364

Lewis SM, Holcik M (2008) For IRES trans-acting factors, it is all about location. *Oncogene* 27: 1033-1035

Liberman N, Gandin V, Svitkin YV, David M, Virgili G, Jaramillo M, Holcik M, Nagar B, Kimchi A, Sonenberg N (2015) DAP5 associates with eIF2beta and eIF4AI to promote Internal Ribosome Entry Site driven translation. *Nucleic Acids Res* 43: 3764-3775

Martineau Y, Le Bec C, Monbrun L, Allo V, Chiu IM, Danos O, Moine H, PratsH, Prats AC (2004) Internal ribosome entry site structural motifs conserved among mammalian fibroblast growth factor 1 alternatively spliced mRNAs. *Mol Cell Biol* 24: 7622-7635

Meng Z, King PH, Nabors LB, Jackson NL, Chen CY, Emanuel PD, Blume SW (2005) The ELAV RNA-stability factor HuR binds the 5'-untranslated region of the human IGF-IR transcript and differentially represses cap-dependent and IRES-mediated translation. *Nucleic Acids Res* 33: 2962-2979

Mitchell SA, Spriggs KA, Coldwell MJ, Jackson RJ, Willis AE (2003) The Apaf-1 internal ribosome entry segment attains the correct structural conformation for function via interactions with PTB and unr. *Mol Cell* 11: 757-771

Miyashita H, Watanabe T, Hayashi H, Suzuki Y, Nakamura T, Ito S, Ono M, Hoshikawa Y, Okada Y, Kondo T, Sato Y (2012) Angiogenesis inhibitor vasohibin-1 enhances stress resistance of endothelial cells via induction of SOD2 and SIRT1. *PLoS One* 7: e46459

Morfoisse F, Kuchnio A, Frainay C, Gomez-Brouchet A, Delisle MB, Marzi S, Helfer AC, Hantelys F, Pujol F, Guillermet-Guibert J, Bousquet C, Dewerchin M, Pyronnet S, Prats AC, Carmeliet P, Garmy-Susini B (2014) Hypoxia induces VEGF-C expression in metastatic tumor cells via a HIF-1alpha-independent translation-mediated mechanism. *Cell Rep* 6: 155-167

Morfoisse F, Renaud E, Hantelys F, Prats AC, Garmy-Susini B (2014) Role of hypoxia and vascular endothelial growth factors in lymphangiogenesis. *Mol Cell Oncol* 1: e29907

Morfoisse F, Tatin F, Hantelys F, Adoue A, Helfer AC, Cassant-Sourdy S, Pujol F, Gomez-Brouchet A, Ligat L, Lopez F, Pyronnet S, Courty J, Guillermet-Guibert J, Marzi S, Schneider RJ, Prats AC, Garmy-Susini BH (2016) Nucleolin Promotes Heat Shock-Associated Translation of VEGF-D to Promote Tumor Lymphangiogenesis. *Cancer Res* 76: 4394-4405

Nanbru C, Lafon I, Audigier S, Gensac MC, Vagner S, Huez G, Prats AC (1997) Alternative translation of the proto-oncogene c-myc by an internal ribosome entry site. *J Biol Chem* 272: 32061-32066

Pages G, Pouyssegur J (2005) Transcriptional regulation of the Vascular

Endothelial Growth Factor gene--a concert of activating factors. *Cardiovasc Res* 65: 564-573

Pouyssegur J, Dayan F, Mazure NM (2006) Hypoxia signalling in cancer and approaches to enforce tumour regression. *Nature* 441: 437-443

Prats AC, Van den Berghe L, Rayssac A, Ainaoui N, Morfoisse F, Pujol F, Legonidec S, Bikfalvi A, Prats H, Pyronnet S, Garmy-Susini B (2013) CXCL4L1-fibstatin cooperation inhibits tumor angiogenesis, lymphangiogenesis and metastasis. *Microvasc Res* 89: 25-33

Ronkainen VP, Ronkainen JJ, Hanninen SL, Leskinen H, Ruas JL, Pereira T, Poellinger L, Vuolteenaho O, Tavi P (2007) Hypoxia inducible factor regulates the cardiac expression and secretion of apelin. *FASEB J* 21: 1821-1830

Sato Y (2012) The vasohibin family: Novel regulators of angiogenesis. *Vascul Pharmacol* 56: 262-266

Sato Y (2015) Novel Link between Inhibition of Angiogenesis and Tolerance to Vascular Stress.*J Atheroscler Thromb* 22: 327-334

Spriggs KA, Stoneley M, Bushell M, Willis AE (2008) Re-programming of translation following cell stress allows IRES-mediated translation to predominate. *Biol Cell* 100: 27-38

Stein I, Itin A, Einat P, Skaliter R, Grossman Z, Keshet E (1998) Translation of vascular endothelial growth factor mRNA by internal ribosome entry: implications for translation under hypoxia. *Mol Cell Biol* 18: 3112-3119

Vagner S, Gensac MC, Maret A, Bayard F, Amalric F, Prats H, Prats AC (1995) Alternative translation of human fibroblast growth factor 2 mRNA occurs by internal entry of ribosomes. *Mol Cell Biol* 15: 35-44

Xue S, Tian S, Fujii K, Kladwang W, Das R, Barna M (2015) RNA regulons in Hox 5' UTRs confer ribosome specificity to gene regulation. *Nature* 517: 33-38

Yeh CH, Hung LY, Hsu C, Le SY, Lee PT, Liao WL, Lin YT, Chang WC, Tseng JT (2008) RNA-binding protein HuR interacts with thrombomodulin 5'untranslated region and represses internal ribosome entry site-mediated translation under IL-1 beta treatment. *Mol Biol Cell* 19: 3812-3822

FIGURE LEGENDS

Figure 1. Transcriptome of (lymph)angiogenic factors in hypoxic cardiomyocytes.

Total RNA was purified from HL-1 cardiomyocytes submitted to increasing times from 5 min to 24 h of hypoxia at 1% O_2, as well as from normoxic cardiomyocytes as a control. cDNA was synthesized and used for a Fluidigm delta gene PCR array dedicated to genes related to (lymph)angiogenesis or stress (Table S4). mRNA levels are presented by histograms for the times of 4 h, 8 h and 24 h, as the fold-change of repression (on the left of the axis) or induction (on the right of the axis) normalized to normoxia. The detailed values for all the times of the kinetics are presented in Table S1.

Figure 2. Translatome of (lymph)angiogenic factors in hypoxic cardiomyocytes.

In order to isolate translated mRNAs, polysomes were purified on sucrose gradient from HL-1 cardiomyocytes in normoxia or after 4 h of hypoxia at 1% O_2, as described in Materials and Methods. RNA was purified from polysome-bound and free RNA. cDNA and PCR array was performed as in Figure 1.

(A) Polysomes profiles obtained for normoxic and hypoxic cardiomyocytes. **(B)**mRNA levels (polysomal RNA/free RNA) expressed by histograms as fold-change of repression (on the left of the axis) or induction (on the right of the axis)

in hypoxia normalized to normoxia. The detailed values with all the times of the kinetics are presented in Table S2.

Figure 3. Transcriptome and translatome of IRES-containing genes during hypoxia.

mRNA level values for IRES-containing genes were selected from the transcriptome **(A)** and translatome **(B)** PCR array shown in Figure 1, Figure 2, Table S1 and Table S2. The gene Aplnnr (apelin receptor) was chosen as a control without an IRES. **(A)** Total mRNA expression of IRES-containing genes during the hypoxia kinetics from 5 min to 24 h (presented with different grey levels). As in Figure 1, mRNA expression is shown by histograms as fold-change of repression (on the left of the axis) or induction (on the right of the axis) during hypoxia normalized to normoxia. **(B)** Polysome recruitment of IRES-containing mRNAs during early hypoxia (4h). VEGFC and FGF2 mRNAs, repressed in the transcriptome, were under the detection threshold in polysomes.

Figure 4. IRES activities at different times of hypoxia.

To measure IRES-dependent translation during hypoxia, HL-1 cardiomyocytes were transduced with bicistronic dual luciferase lentivectors containing different IRESs cloned between the genes of renilla (LucR) and firefly (LucF) luciferase (A). Bicistronic vectors have been validated to measure IRES activities: the first cistron LucR is cap-dependent whereas the second cistron LucF is IRES-dependent

(Creancier et al., 2000). Lentivectors constitute a powerful tool to obtain efficient gene transfer when cells, such as HL-1 cardiomyocytes, are not efficiently transfected with plasmid DNA. Bicistronic lentivectors have been successfully used to analyze IRES activities in tumor cells (Morfoisse et al., 2014a, Morfoisse et al., 2016)... (B-D) Transduced cardiomyocytes were submitted to 4h, 8h or 24h of hypoxia and luciferase activities measured. IRES activities during hypoxia, expressed as LucF/LucF, are normalized to normoxia: (B) FGF IRESs, (C) VEGF IRESs, (D) non angiogenic IRESs.

Figure 5. BIA-MS analysis of IRES-bound proteins in hypoxic cardiomyocytes.

Biotinylated IRES RNAs were transcribed in vitro and immobilized on the sensorchip of the BIAcore T200 optical biosensor device **(A)**. Total cell extracts from normoxic or hypoxic HL-1 cardiomyocytes were injected. **(B)** Bound proteinswere recovered as described in Mat. & Meth. and identified by mass spectrometry (LC-MS/MS) after tryptic digestion (Table S3). **(C)** The ability of vasohibin-1 (VASH1), identified in Table S3, to bind RNA was assessed *in silico* using the BindN software (http://bioinfo.ggc.org/bindn/). Binding residues are labeled with "+" ans in red, non-binding residues labeled with "-" and in green. The confidence level is indicated from level 0 (lowest) to 9 (highest).

Figure 6. Regulation of VASH1 expression in cardiomyocytes and role in the control of the IRES activities.

VASH1 gene regulation was analyzed in HL-1 cardiomyocytes in response to hypoxia at the transcriptome (A) and translatome (B) levels. (A) Total RNAs were purified from cardiomyocytes in normoxia, or submitted to 4 h, 8 h or 24 h of hypoxia. (B) Polysomal RNA was purified from cardiomyocytes in normoxia of after 4 h of hypoxia. In (A) and (B),VASH1 mRNA level was measured by RT qPCR.

(C) VASH1 knock-down was perfomed in HL-1 cardiomyocytes using an siRNA Smartpool (siVASH1), compared to a control siRNA (sicontrol). VASH1 mRNA level was measured by RT qPCR.

(D) The knock-down experiment was performed on cardiomyocytes transduced by a set of IRES-containing lentivectors used in Fig. 4. After 4h of hypoxia, IRES activities (ratio LucF/LucR) were measured in cell extracts. The IRES activity values have been normalized to the control siRNA.

Figure 7. Effect of VASH1 knock-down on the translatome of hypoxic cardiomyocytes.

Study of the effect of VASH1 knock-down on the translatome. Polysomal RNA was purified from HL-1 cardiomyocytes treated with the VASH1 siRNA and mRNA levels were analyzed using the Fluidigm Deltagene PCR array described in Figures 1 to 3. The detailed values are shown in Table S2.

Transcriptome

Figure 1

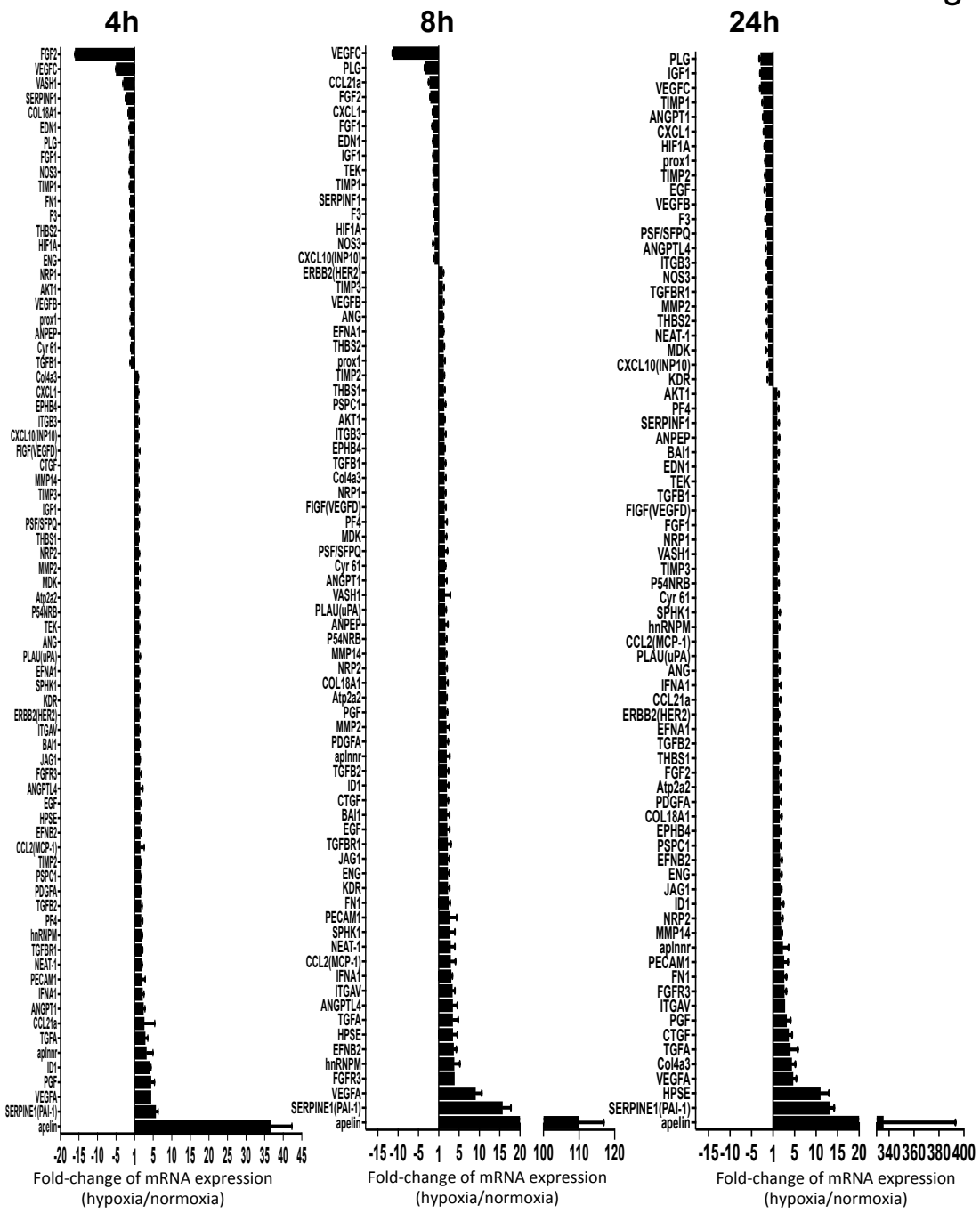

Figure 2

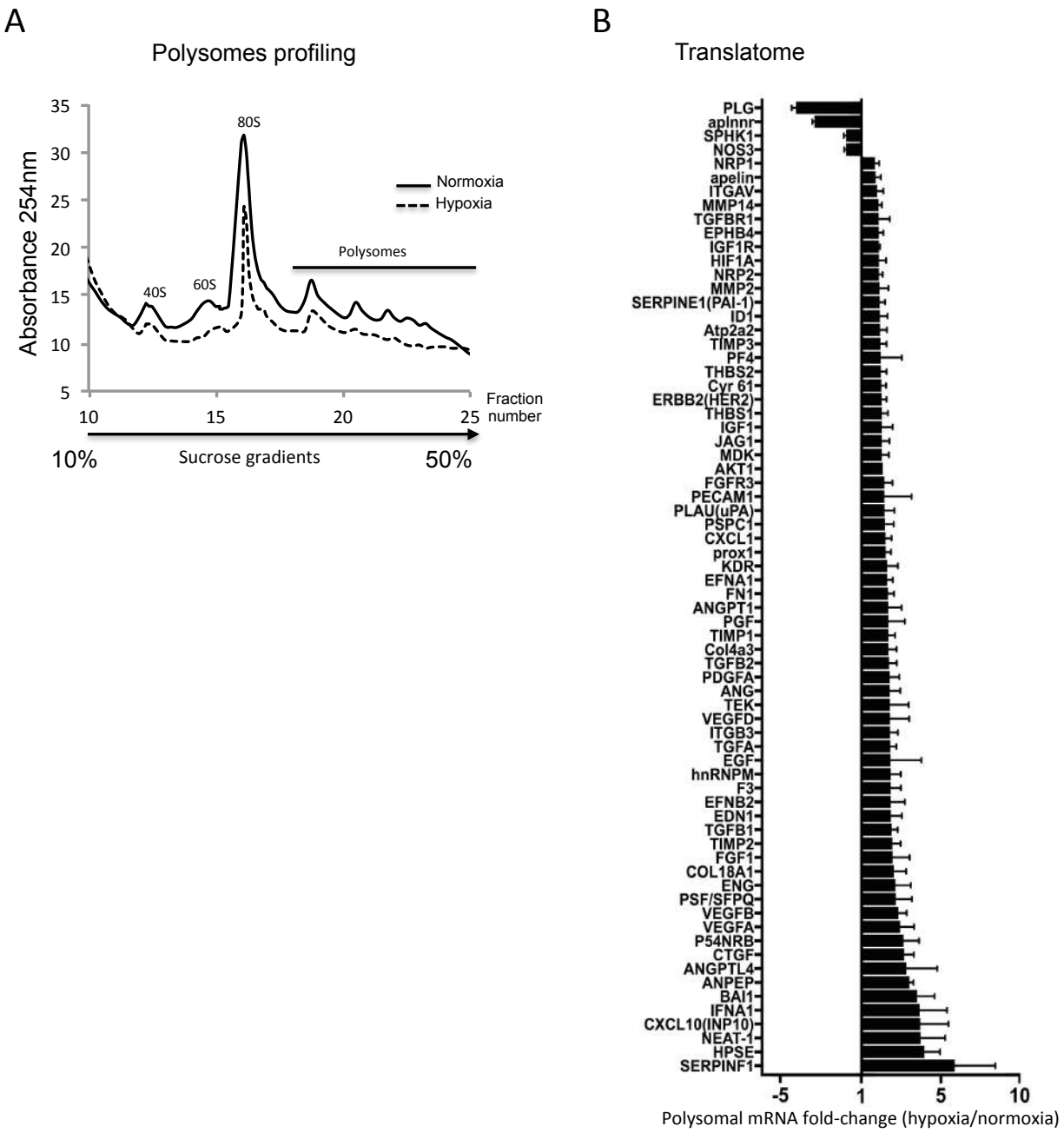
A
Polysomes profiling
Absorbance 254nm
35
30
25
20
15
10
5
80S
40S
60S
Polysomes
Normoxia
Hypoxia
10
15
20
25
Fraction number
10%
Sucrose gradients
50%
B
Translatome
PLG
aplnnr
SPHK1
NOS3
NRP1
apelin
ITGAV
MMP14
TGFBR1
EPHB4
IGF1R
HIF1A
NRP2
MMP2
SERPINE1(PAI-1)
ID1
Atp2a2
TIMP3
PF4
THBS2
Cyr 61
ERBB2(HER2)
THBS1
IGF1
JAG1
MDK
AKT1
FGFR3
PECAM1
PLAU(uPA)
PSPC1
CXCL1
prox1
KDR
EFNA1
FN1
ANGPT1
PGF
TIMP1
Col4a3
TGFB2
PDGFA
ANG
TEK
VEGFD
ITGB3
TGFA
EGF
hnRNPM
F3
EFNB2
EDN1
TGFB1
TIMP2
FGF1
COL18A1
ENG
PSF/SFPQ
VEGFB
VEGFA
P54NRB
CTGF
ANGPTL4
ANPEP
BAI1
IFNA1
CXCL10(INP10)
NEAT-1
HPSE
SERPINF1
-5
1
5
10
Polysomal mRNA fold-change (hypoxia/normoxia)

Figure 3

A Transcriptome

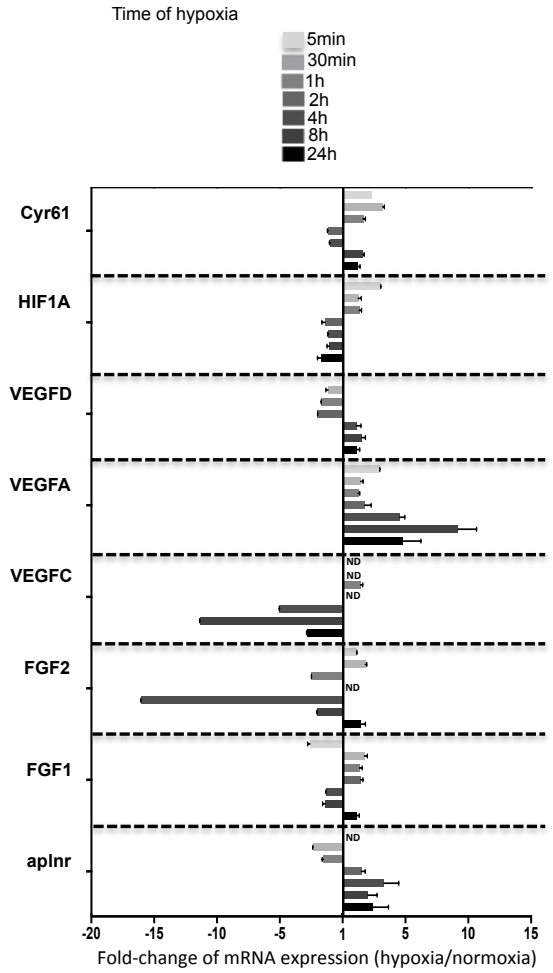

B Translatome

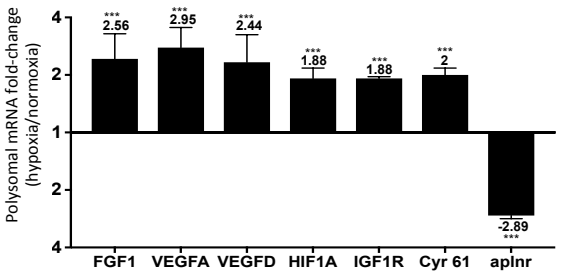

aplnr: no IRES

Figure 4

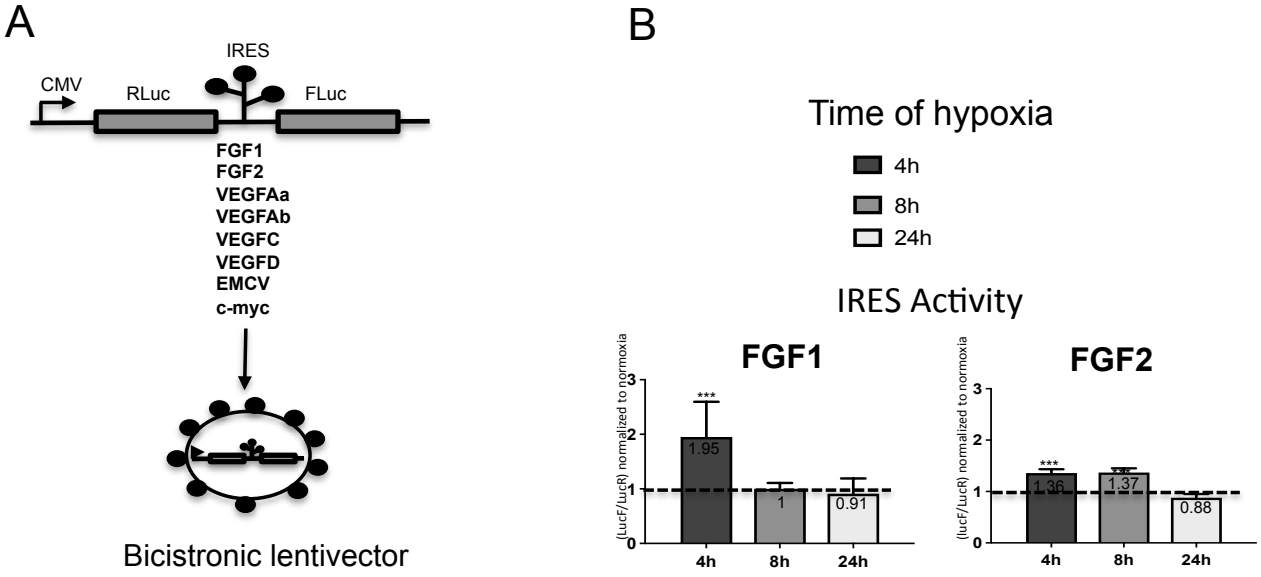
A
IRES
CMV
RLuc
FLuc
FGF1
FGF2
VEGFAa
VEGFAb
VEGFC
VEGFD
EMCV
c-myc
Bicistronic lentivector
B
Time of hypoxia
4h
8h
24h
IRES Activity
FGF1
FGF2
(LucF/LucR) normalized to normoxia
1.95
1
0.91
1.36
1.37
0.88
4h
8h
24h

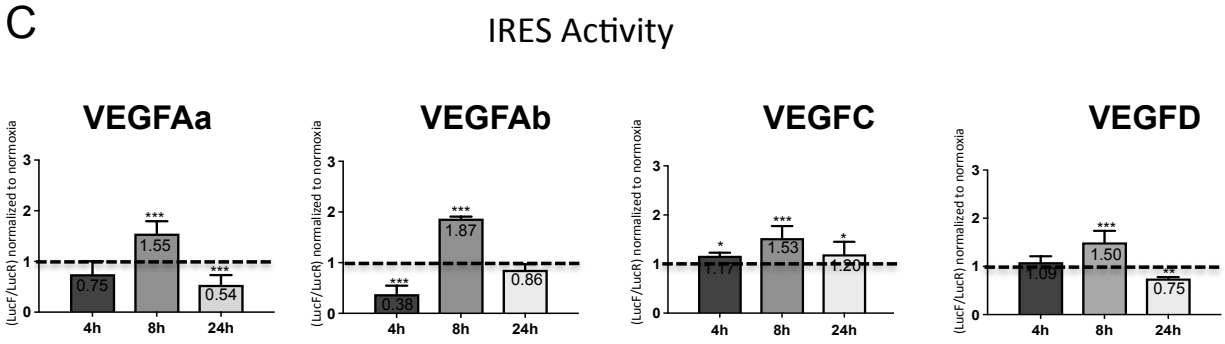
C
IRES Activity
VEGFAa
VEGFAb
VEGFC
VEGFD
(LucF/LucR) normalized to normoxia
0.75
1.55
0.54
0.38
1.87
0.86
1.17
1.53
1.20
1.09
1.50
0.75
4h
8h
24h

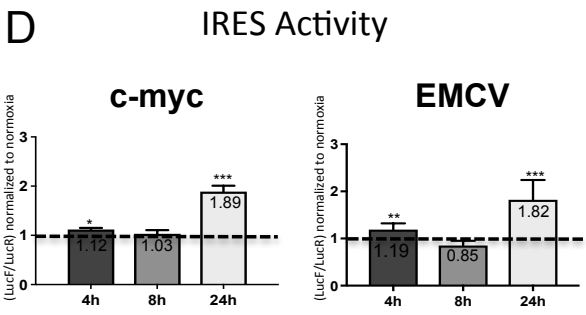
D
IRES Activity
c-myc
EMCV
(LucF/LucR) normalized to normoxia
1.12
1.03
1.89
1.19
0.85
1.82
4h
8h
24h

Figure 5

A

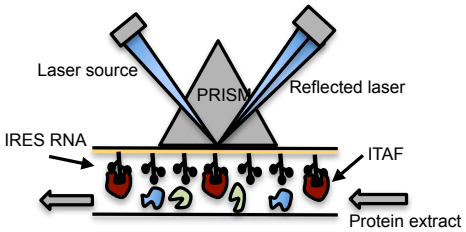
Laser source
PRISM
Reflected laser
IRES RNA
ITAF
Protein extract

B

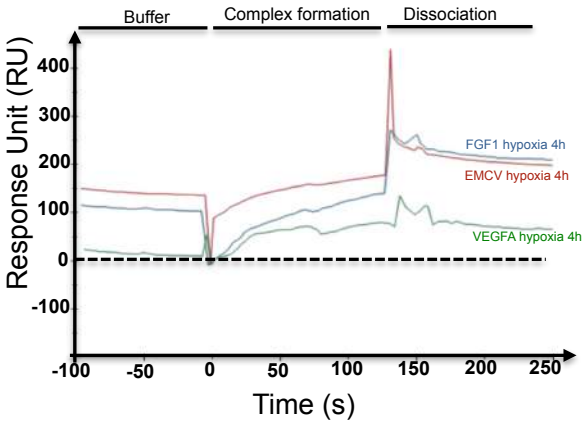
Buffer
Complex formation
Dissociation
Response Unit (RU)
400
300
200
100
0
-100
-100
-50
0
50
100
150
200
250
Time (s)
FGF1 hypoxia 4h
EMCV hypoxia 4h
VEGFA hypoxia 4h

C


VASH1
Sequence:
Prediction:
Confidence:

Figure 6

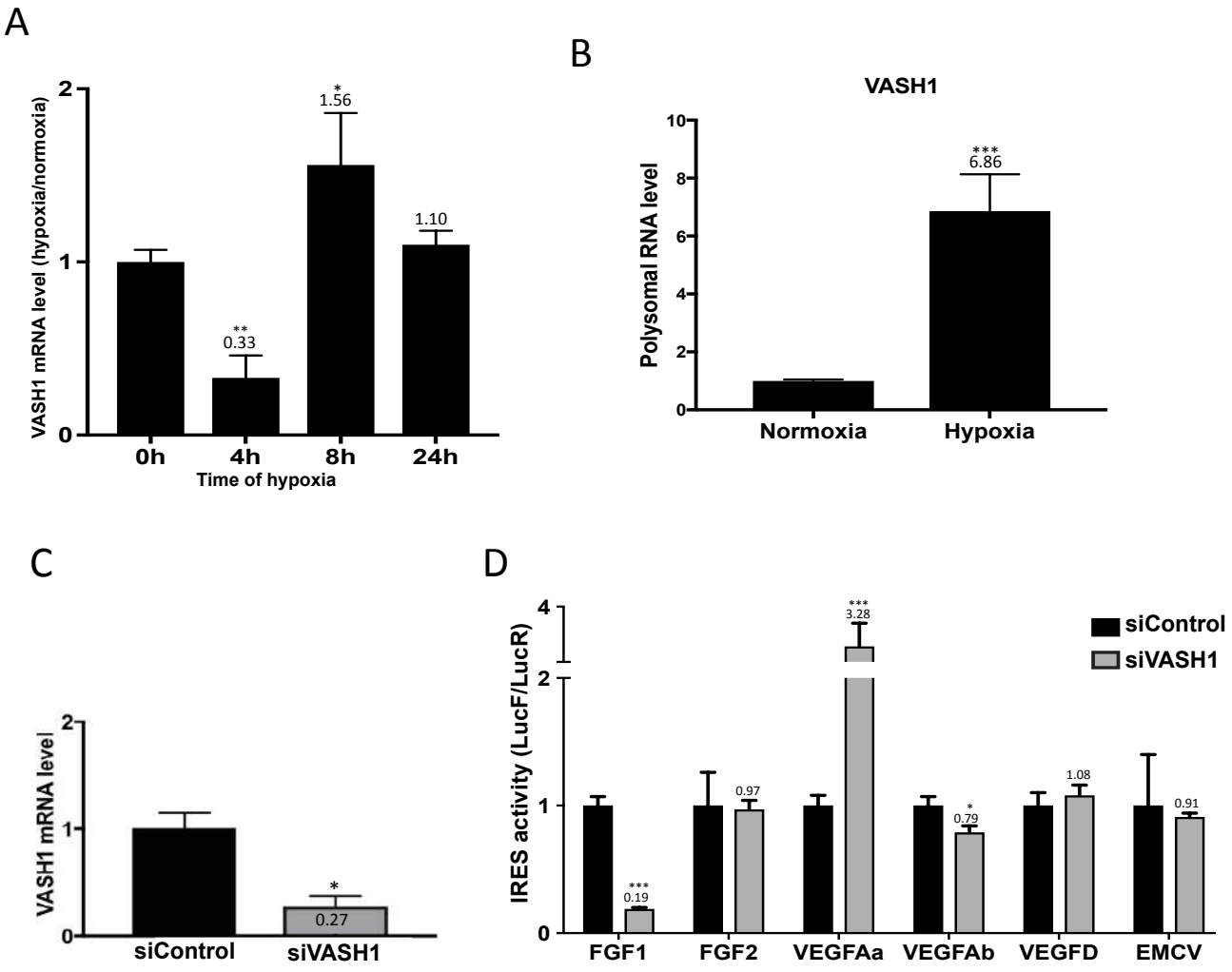
A
VASH1 mRNA level (hypoxia/normoxia)
2
1
0
*
1.56
**
0.33
1.10
0h
4h
8h
24h
Time of hypoxia
B
VASH1
Polysomal RNA level
10
8
6
4
2
0
***
6.86
Normoxia
Hypoxia
C
VASH1 mRNA level
2
1
0
*
0.27
siControl
siVASH1
D
IRES activity (LucF/LucR)
4
2
1
0
***
3.28
***
0.19
0.97
*
0.79
1.08
0.91
siControl
siVASH1
FGF1
FGF2
VEGFAa
VEGFAb
VEGFD
EMCV

Figure 7

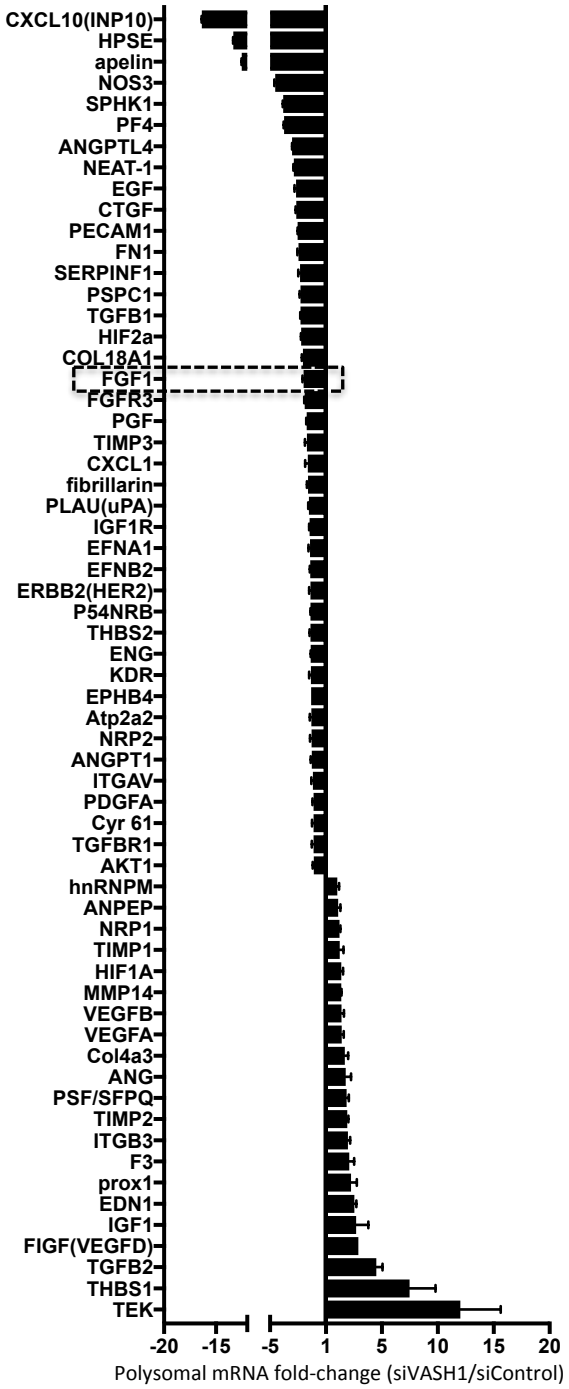
CXCL10(INP10)
HPSE
apelin
NOS3
SPHK1
PF4
ANGPTL4
NEAT-1
EGF
CTGF
PECAM1
FN1
SERPINF1
PSPC1
TGFB1
HIF2a
COL18A1
FGF1
FGFR3
PGF
TIMP3
CXCL1
fibrillarin
PLAU(uPA)
IGF1R
EFNA1
EFNB2
ERBB2(HER2)
P54NRB
THBS2
ENG
KDR
EPHB4
Atp2a2
NRP2
ANGPT1
ITGAV
PDGFA
Cyr 61
TGFBR1
AKT1
hnRNPM
ANPEP
NRP1
TIMP1
HIF1A
MMP14
VEGFB
VEGFA
Col4a3
ANG
PSF/SFPQ
TIMP2
ITGB3
F3
prox1
EDN1
IGF1
FIGF(VEGFD)
TGFB2
THBS1
TEK
-20
-15
-5
1
5
10
15
20
Polysomal mRNA fold-change (siVASH1/siControl)

Table S1

Time of hypoxia	5min		30min		1h		2h		4h		8h		24h	
Gene name	**RQ***	**ST DEV**	**RQ***	**ST DEV**	**RQ***	**ST DEV**	**RQ***	**ST DEV**	**RQ***	**ST DEV**	**RQ***	**ST DEV**	**RQ***	**ST DEV**
AKT1	1.60	0.13	1.30	0.06	1.20	0.15	1.36	0.25	-1.10	0.09	1.40	0.13	1.00	0.32
ANG	2.65	0.25	1.23	0.36	-1.04	0.12	1.24	0.04	1.24	0.12	1.09	0.08	1.26	0.28
ANGPT1	5.51	0.17	1.20	0.30	1.19	0.07	1.90	0.49	2.43	0.36	1.56	0.43	-2.27	0.06
ANGPTL4	1.03	0.02	-3.14	0.09	1.65	0.54	1.60	0.46	1.56	0.67	3.50	1.07	-1.37	0.35
ANPEP	ND	ND	-3.26	0.29	1.65	0.01	-8.05	0.06	-1.04	0.14	1.62	0.62	1.03	0.43
apelin	2.11		-19,21	0.01	-6.17	0.05	-29.04	0.01	36.77	5.59	109.98	6.98	335.72	57.52
aplnnr	ND	ND	-2.36	0.03	-1.57	0.10	1.44	0.32	3.25	1.70	1.98	0.72	2.31	1.29
Atp2a2	1.46	0.08	1.21	0.13	1.26	0.14	1.50	0.01	1.20	0.06	1.84	0.18	1.48	0.32
BAI1	-1.52	0.19	2.90	0.91	1.17	0.06	1.65	0.52	1.36	0.13	2.05	0.60	1.04	0.30
CCL2(MCP-1)	ND	ND	-1.09	0.49	1.76	0.46	-2.76	0.16	1.57	1.01	2.99	1.13	1.23	
CCL21a	ND	ND	-32.39	0.01	2.97	0.85	-1.90	0.03	2.65	2.78	-2.27	0.21	1.32	0.39
COL18A1	1.66	0.71	1.58	0.39	1.14	0.14	1.45	0.04	-1.69	0.09	1.82	0.43	1.57	0.43
Col4a3	19.64	0.07	1.52	0.19	1.20	0.21	1.31	0.04	1.00	0.03	1.45	0.30	4.40	0.80
CTGF	1.29	0.09	1.67	0.26	1.16	0.06	1.30	0.13	1.06	0.13	2.05	0.30	3.66	0.76
CXCL1	1.32	0.64	1.11	0.27	1.67	0.19	1.58	0.12	1.01	0.09	-1.43	0.08	-2.04	0.13
CXCL10(INP10)	1.37	0.86	1.36	0.29	1.11	0.14	1.33	0.25	1.05	0.09	-1.02	0.13	-1.08	0.23
Cyr 61	2.30	0.18	3.14	0.14	1.59	0.18	-1.18	0.07	-1.03	0.06	1.56	0.12	1.15	0.21
EDN1	-2.43	0.28	2.93	0.31	1.72	0.32	-1.4	0.24	-1.39	0.06	-1.33	0.09	1.04	0.26
EFNA1	2.08	0.15	1.23	0.10	-1.52	0.12	-1.16	0.19	1.25	0.09	1.17	0.05	1.35	0.33
EFNB2	1.74	0.14	1.55	0.25	1.14	0.23	-1.03	0.18	1.57	0.18	3.71	0.61	1.65	0.42
EGF	ND	ND	1.35	0.14	1.32	0.30	1.56	0.44	1.56	0.11	2.14	0.53	-1.61	0.35
ENG	2.96	0.94	1.55	0.39	1.18	0.19	-1.02	0.14	-1.11	0.15	2.27	0.33	1.65	0.34
EPHB4	2.22	0.13	1.67	0.16	-1.03	0.14	1.10	0.13	1.01	0.12	1.45	0.09	1.57	0.21
ERBB2(HER2)	1.87	0.19	1.85	0.26	-1.01	0.18	1.16	0.18	1.32	0.11	1.00	0.18	1.34	0.09
F3	1.12	0.94	1.45	0.18	1.28	0.11	-1.57	0.23	-1.23	0.07	-1.09	0.10	-1.56	0.21
FGF1	-2.63	0.18	1.69	0.23	1.29	0.22	1.37	0.21	-1.32	0.05	-1.43	0.20	1.08	0.20
FGF2	1.06	0.04	1.76	0.13	-2.5	0.03	ND	ND	-16.05	0.02	-2.05	0.07	1.43	0.35
FGFR3	1.41	0.07	1.34	0.27	-1.08	0.12	1.38	0.31	1.47	0.27	3.93	0.55	2.69	0.39
FIGF(VEGFD)	ND	ND	-1.19	0.17	-1.73	0.22	-1.99	0.23	1.05	0.37	1.48	0.29	1.08	0.24
FN1	3.30	0.07	1.70	0.15	-1.02	0.17	1.16	0.01	-1.25	0.06	2.45	0.36	2.61	0.49
HIF1A	2.97	0.03	1.20	0.24	1.28	0.18	-1.42	0.26	-1.15	0.08	-1.06	0.21	-1.75	0.22
hnRNPM	1.55	0.18	1.17	0.18	1.54	0.15	2.26	0.20	1.86	0.25	3.86	1.33	1.23	0.26
HPSE	ND	ND	3.23	1.07	1.25	0.34	1.64	0.16	1.56	0.14	3.52	1.07	11.04	1.95
ID1	-1.61	1.12	1.58	0.18	2.63	0.50	3.01	1.27	4.23	0.19	2.01	0.40	1.79	0.64
IFNA1	ND	ND	1.72	0.17	-1.09	0.06	1.73	0.07	2.19	0.33	3.11	0.25	1.31	0.49
IGF1	10.07	0.59	1.54	0.22	1.42	0.15	1.06	0.04	1.10	0.22	-1.25	0.14	-2.86	0.14
IGF1R	ND	ND	ND	ND	ND	ND	ND	ND	ND	ND	ND	ND	ND	ND
ITGAV	ND	ND	1.19	0.11	-1.36	0.14	1.33	0.29	1.33	0.12	3.41	0.56	2.82	0.64
ITGB3	-4.33	0.30	1.34	0.19	-1.35	0.02	1.04	0.20	1.03	0.20	1.42	0.34	-1.37	0.10
JAG1	2.13	0.09	1.80	0.24	1.03	0.13	1.66	0.46	1.46	0.06	2.26	0.37	1.76	0.21
KDR	-2.05	0.05	1.25	0.13	1.07	0.04	1.43	0.21	1.31	0.10	2.29	0.38	-1.01	0.30
MDK	1.14	0.21	2.45	0.17	-1.07	0.17	-1.27	0.00	1.16	0.32	1.52	0.38	-1.16	0.46
MMP14	-1.77	0.03	1.30	0.22	1.02	0.06	-1.16	0.17	1.06	0.11	1.70	0.24	1.95	0.15
MMP2	1.46	0.18	1.96	0.50	1.20	0.05	1.68	0.44	1.14	0.33	1.94	0.66	-1.23	0.37

NEAT-1	4.03	0.48	-1.17	0.23	-1.59	0.05	2.65	0.00	1.89	0.15	2.96	1.02	-1.16	0.29
NOS3	9.29		-4.01	0.10	2.00	0.54	-2.58	0.26	-1.30	0.14	-1.02	0.40	-1.32	0.19
NRP1	2.46	0.06	1.32	0.17	1.04	0.15	-1.25	0.25	-1.10	0.07	1.47	0.25	1.10	0.16
NRP2	2.50	0.07	1.55	0.05	1.02	0.12	1.02	0.12	1.14	0.19	1.72	0.32	1.83	0.39
P54NRB	2.96	0.09	1.58	0.42	1.21	0.20	1.42	0.29	1.22	0.13	1.66	0.30	1.11	0.23
PDGFA	3.65	0.43	1.45	0.18	1.29	0.26	1.59	0.36	1.71	0.11	1.97	0.35	1.54	0.34
PECAM1	1.48		-11.55	0.02	-1.09	0.24	2.86	1.08	2.09	0.77	2.70	1.72	2.60	0.86
PF4	ND	ND	-39.36	0.02	-1.79	0.33	-2.20	0.18	1.80	0.40	1.48	0.55	1.01	0.28
PGF	ND	ND	2.17	0.14	-1.36	0.19	-7.89	0.09	4.47	0.89	1.85	0.29	3.22	0.85
PLAU(uPA)	1.13	0.29	-1.04	0.24	-1.36	0.16	-1.31	0.13	1.25	0.30	1.58	0.26	1.24	0.24
PLG	ND	ND	-2.71	0.26	-1.05		2.45	0.63	-1.35	0.19	-3.33	0.16	-2.94	0.25
prox1	7.13	0.20	1.48	0.23	1.26	0.14	-1.13	0.14	-1.08	0.13	1.27	0.29	-1.72	0.07
PSF/SFPQ	1.45	0.17	1.37	0.09	1.30	0.19	1.22	0.08	1.10	0.15	1.55	0.59	-1.43	0.16
PSPC1	1.00	0.80	1.34	0.11	1.50	0.01	1.64	0.58	1.67	0.19	1.37	0.31	1.59	0.23
SERPINE1(PAI-1)	-1.73	0.12	2.18	0.54	1.46	0.15	1.74	0.65	5.75	0.57	15.76	2.01	13.18	1.02
SERPINF1	ND	ND	-31.89	0.02	-9.09	0.01	-1.91	0.33	-2.38	0.11	-1.14	0.17	1.02	0.37
SPHK1	ND	ND	1.91	0.80	1.70	0.04	-1.51	0.19	1.30	0.11	2.78	1.20	1.17	0.43
TEK	1.97	1.55	1.98	0.23	1.55	0.41	1.48	0.20	1.24	0.14	-1.25	0.09	1.04	0.13
TGFA	ND	ND	-2.01	0.13	-7.94	0.05	-6.9	0.03	2.91	0.63	3.50	1.29	4.05	1.71
TGFB1	-5.26	0.02	1.22	0.23	-1.45	0.14	1.03	0.10	-1.02	0.22	1.45	0.24	1.05	0.25
TGFB2	-2.45	0.08	1.50	0.31	1.22	0.07	1.37	0.12	1.78	0.24	2.00	0.39	1.43	0.40
TGFBR1	-2.03	0.57	1.33	0.16	1.28	0.25	1.48	0.14	1.86	0.34	2.23	0.77	-1.27	0.16
THBS1	2.65	0.09	1.88	0.12	1.19	0.09	1.47	0.33	1.12	0.07	1.30	0.22	1.44	0.08
THBS2	2.15	0.12	1.52	0.10	1.03	0.16	1.20	0.18	-1.20	0.01	1.21	0.15	-1.22	0.21
TIMP1	-2.20	0.04	1.13	0.27	-1.32	0.29	-1.96	0.17	-1.28	0.12	-1.22	0.11	-2.33	0.19
TIMP2	2.21	0.04	1.46	0.22	1.14	0.01	1.13	0.09	1.67	0.13	1.28	0.12	-1.69	0.15
TIMP3	ND	ND	2.70	0.43	1.40	0.23	1.98	0.46	1.09	0.16	1.04	0.29	1.11	0.17
VASH1	ND	ND	ND	ND	ND	ND	ND	ND	-3.01	0.14	1.56	1.30	1.10	0.08
VEGFA	2.90	0.02	1.40	0.18	1.20	0.12	1.72	0.50	4.48	0.43	9.12	1.48	4.71	0.69
VEGFB	1.38	0.04	1.33	0.10	-1.2	0.11	1.02	0.04	-1.09	0.07	1.04	0.22	-1.59	0.10
VEGFC	ND	ND	ND	ND	1.38	0.18	ND	ND	-5.03	0.05	-11.37	0.03	-2.86	0.16

* RQ<1 were replaced by -1/RQ

Table S2

	Polysomes in hypoxia		SiVASH1 polysomes in normoxia	
Gene name	**RQ***	ST DEV	**RQ***	ST DEV
AKT1	2.07	0.07	-1.08	0.10
ANG	2.42	0.53	1.77	0.47
ANGPT1	2.35	0.67	-1.27	0.10
ANGPTL4	3.26	1.56	-3.02	0.01
ANPEP	3.41	0.21	1.10	0.20
apelin	1.71	0.27	-12.53	0.01
aplnnr	-2.89	0.11	ND	ND
Atp2a2	1.94	0.34	-1.30	0.15
BAI1	3.80	0.89	ND	ND
CCL2(MCP-1)	ND	ND	ND	ND
CCL21a	ND	ND	ND	ND
COL18A1	2.64	0.61	-2.05	0.11
Col4a3	2.36	0.41	1.70	0.29
CTGF	3.15	0.49	-2.66	0.05
CXCL1	2.21	0.30	-1.61	0.25
CXCL10(INP10)	3.96	1.43	-16.36	0.02
Cyr 61	2.00	0.24	-1.11	0.14
EDN1	2.49	0.55	2.54	0.19
EFNA1	2.29	0.29	-1.42	0.14
EFNB2	2.48	0.71	-1.41	0.03
EGF	2.46	1.56	-2.68	0.12
ENG	2.71	0.78	-1.36	0.01
EPHB4	1.87	0.23	-1.33	0.00
ERBB2(HER2)	2.02	0.24	-1.39	0.11
F3	2.48	0.51	2.09	0.44
FGF1	2.56	0.87	-1.99	0.11
FGF2	ND	ND	ND	ND
FGFR3	2.15	0.41	-1.89	0.05
fibrillarin	ND	ND	-1.60	0.10
FIGF(VEGFD)	2.44	0.96	2.90	0.39
FN1	2.34	0.30	-2.46	0.10
HIF1A	1.88	0.36	1.38	0.16
HIF2a	ND	ND	-2.21	0.03
hnRNPM	2.48	0.50	1.01	0.17
HPSE	4.17	0.79	-13.33	0.02
ID1	1.93	0.38	ND	ND
IFNA1	3.93	1.38	ND	ND
IGF1	2.03	0.54	2.71	1.08

IGF1R	1.88	0.06	-1.47	0.04
ITGAV	1.79	0.31	-1.17	0.13
ITGB3	2.44	0.40	1.96	0.20
JAG1	2.03	0.38	ND	ND
KDR	2.29	0.55	-1.35	0.15
MDK	2.03	0.35	ND	ND
MMP14	1.85	0.18	1.38	0.02
MMP2	1.91	0.44	ND	ND
NEAT-1	3.98	1.24	-2.86	0.05
NOS3	-1.29	0.10	-4.54	0.08
NRP1	1.67	0.22	1.21	0.09
NRP2	1.88	0.18	-1.28	0.14
P54NRB	3.12	0.78	-1.38	0.01
PDGFA	2.42	0.48	-1.11	0.10
PECAM1	2.15	1.37	-2.53	0.01
PF4	1.97	1.07	-3.75	0.03
PGF	2.36	0.83	-1.71	0.04
PLAU(uPA)	2.16	0.50	-1.53	0.05
PLG	-3.83	0.21	ND	ND
prox1	2.22	0.27	2.24	0.52
PSF/SFPQ	2.74	0.80	1.85	0.20
PSPC1	2.19	0.43	-2.27	0.08
SERPINE1(PAI-1)	1.92	0.27	ND	ND
SERPINF1	5.70	2.05	-2.32	0.15
SPHK1	-1.29	0.12	-3.82	0.04
TEK	2.43	0.95	12.03	3.59
TGFA	2.45	0.31	ND	ND
TGFB1	2.52	0.31	-2.27	0.03
TGFB2	2.39	0.39	4.51	0.55
TGFBR1	1.86	0.57	-1.10	0.17
THBS1	2.03	0.30	7.48	2.32
THBS2	1.98	0.28	-1.38	0.08
TIMP1	2.36	0.34	1.24	0.34
TIMP2	2.55	0.42	1.91	0.10
TIMP3	1.95	0.31	-1.70	0.17
VASH1	6.86	1.27	ND	ND
VEGFA	2.95	0.70	1.41	0.19
VEGFB	2.85	0.43	1.40	0.21
VEGFC	ND	ND	ND	ND

* RQ<1 were replaced by -1/RQ

Table S3

A: BIA-MS data: total HL-1 extract proteins bound to the EMCV IRES RNA

	Normoxia		
ID	**Description**	**Score**	**Peptides**
LOX15_MOUSE	Arachidonate 15-lipoxygenase	23	1
ASAP2_MOUSE	Arf-GAP with SH3 domain, ANK repeat and PH domain-containing protein 2	88	1
KCTD9_MOUSE	BTB/POZ domain-containing protein KCTD9	23	1
BRCC3_MOUSE	Lys-63-specific deubiquitinase BRCC36	27	1
PCLO_MOUSE	Protein piccolo	24	1
RPAP1_MOUSE	RNA polymerase II-associated protein 1	23	1
ALBU_MOUSE	Serum albumin	73	1
GUF1_MOUSE	Translation factor Guf1, mitochondrial	24	1

	4h hypoxia		
ID	**Description**	**Score**	**Peptides**
ASAP2_MOUSE	Arf-GAP with SH3 domain, ANK repeat and PH domain-containing protein 2	81	1
KCTD9_MOUSE	BTB/POZ domain-containing protein KCTD9	23	1
NUDC2_MOUSE	NudC domain-containing protein 2	20	1
PLPL1_MOUSE	Patatin-like phospholipase domain-containing protein 1	24	1
TAM41_MOUSE	Phosphatidate cytidylyltransferase, mitochondrial	21	1
VASH1_MOUSE	Vasohibin-1	22	1

	8h hypoxia		
ID	**Description**	**Score**	**Peptides**
ASAP2_MOUSE	Arf-GAP with SH3 domain, ANK repeat and PH domain-containing protein 2	36	1
EMAL6_MOUSE	Echinoderm microtubule-associated protein-like 6	30	1
BRCC3_MOUSE	Lys-63-specific deubiquitinase BRCC36	24	1
RPAP1_MOUSE	RNA polymerase II-associated protein 1	23	1
VASH1_MOUSE	Vasohibin-1	26	1

B: BIA-MS data: total HL-1 extract proteins bound to the VEGFA(a) IRES RNA

	Normoxia		
ID	**Description**	**Score**	**Peptides**
ATPA_MOUSE	ATP synthase subunit alpha, mitochondrial	912	16
ATPO_MOUSE	ATP synthase subunit O, mitochondrial	374	7
ATPB_MOUSE	ATP synthase subunit beta, mitochondrial	372	8
ADT2_MOUSE	ADP/ATP translocase 2	364	5
HNRPU_MOUSE	Heterogeneous nuclear ribonucleoprotein	348	9
ACTA_MOUSE	Actin, aortic smooth muscle	147	1
ECHA_MOUSE	Trifunctional enzyme subunit alpha, mitochondrial	134	8
ACTB_MOUSE	Actin, cytoplasmic 1	119	1
ALBU_MOUSE	Serum albumin	100	1
NX SUCA_MOUSE	Succinyl-CoA ligase [ADP/GDP-forming] subunit alpha, mitochondrial	86	1
ATPG_MOUSE	ATP synthase subunit gamma, mitochondrial	78	1
THIM_MOUSE	3-ketoacyl-CoA thiolase, mitochondrial	57	1
SERPH_MOUSE	Serpin H1	54	1
ASAP2_MOUSE	Arf-GAP with SH3 domain, ANK repeat and PH domain-containing protein 2	52	1
PTRF_MOUSE	Polymerase I and transcript release factor	51	1
AT2A2_MOUSE	Sarcoplasmic/endoplasmic reticulum calcium ATPase 2	4	1
ILF2_MOUSE	Interleukin enhancer-binding factor 2	43	2
MOCS3_MOUSE	Adenylyltransferase and sulfurtransferase MOCS3	39	1
MYOG_MOUSE	Myogenin	33	1
TAGAP_MOUSE	T-cell activation Rho GTPase-activating protein	27	1
CH60_MOUSE	60 kDa heat shock protein, mitochondrial	26	1
C2C2L_MOUSE	C2 domain-containing protein 2-like	25	1
EFC14_MOUSE	EF-hand calcium-binding domain-containing protein 14	24	1
SPIR1_MOUSE	Protein spire homolog 1	24	1
ATAD3_MOUSE	ATPase family AAA domain-containing protein 3	20	1

	4h hypoxia		
ID	**Description**	**Score**	**Peptides**
ATPA_MOUSE	ATP synthase subunit alpha, mitochondrial	42	1
ASAP2_MOUSE	Arf-GAP with SH3 domain, ANK repeat and PH domain-containing protein 2	38	1
RN181_MOUSE	E3 ubiquitin-protein ligase RNF181	30	1
DOC10_MOUSE	Dedicator of cytokinesis protein 10	26	1
NID2_MOUSE	Nidogen-2	26	1
C2C2L_MOUSE	C2 domain-containing protein 2-like	25	1
PLCL1_MOUSE	Inactive phospholipase C-like protein 1	21	1

	8h hypoxia		
ID	**Description**	**Score**	**Peptides**
SPTC2_MOUSE	Serine palmitoyltransferase 2	20	1
CCD66_MOUSE	Coiled-coil domain-containing protein 66	28	1
ASAP2_MOUSE	Arf-GAP with SH3 domain, ANK repeat and PH domain-containing protein 2	35	1
ATPA_MOUSE	ATP synthase subunit alpha, mitochondrial	60	1
PHRF1_MOUSE	PHD and RING finger domain-containing protein 1	41	1
OXR1_MOUSE	Oxidation resistance protein 1	26	1
KCTD9_MOUSE	BTB/POZ domain-containing protein KCTD9	24	1
BIK_MOUSE	Bcl-2-interacting killer	21	1

C: BIA-MS data: total HL-1 extract proteins bound to the FGF1 IRES RNA

	Normoxia		
ID	**Description**	**Score**	**Peptides**
ASAP2_MOUSE	Arf-GAP with SH3 domain, ANK repeat and PH domain-containing protein 2	48	1
EMAL6_MOUSE	Echinoderm microtubule-associated protein-like 6	43	1
FXL14_MOUSE	F-box/LRR-repeat protein 14	15	1
BRCC3_MOUSE	Lys-63-specific deubiquitinase BRCC36	20	1
MYBA_MOUSE	Myb-related protein A	26	1
NUDC2_MOUSE	NudC domain-containing protein 2	17	1
GUF1_MOUSE	Translation factor Guf1, mitochondrial	25	1
TMPSD_MOUSE	Transmembrane protease serine 13	15	1

	4h hypoxia		
ID	**Description**	**Score**	**Peptides**
ASAP2_MOUSE	Arf-GAP with SH3 domain, ANK repeat and PH domain-containing protein 2	51	2
ATPA_MOUSE	ATP synthase subunit alpha, mitochondrial	52	2
C2C2L_MOUSE	C2 domain-containing protein 2-like	25	2
PDE8B_MOUSE	High affinity cAMP-specific and IBMX-insensitive 3~,5~-cyclic phosphodiesterase 8B	23	1
GVIN1_MOUSE	Interferon-induced very large GTPase 1	29	1
ACOX1_MOUSE	Peroxisomal acyl-coenzyme A oxidase 1	23	1
TAM41_MOUSE	Phosphatidate cytidylyltransferase, mitochondrial	23	1
ALBU_MOUSE	Serum albumin	35	1
TCPG_MOUSE	T-complex protein 1 subunit gamma	28	1
VASH1_MOUSE	Vasohibin-1	26	1

	8h hypoxia		
ID	**Description**	**Score**	**Peptides**
ACTA_MOUSE	Actin, aortic smooth muscle	36	1
ADT1_MOUSE	ADP/ATP translocase 1	32	1
ASAP2_MOUSE	Arf-GAP with SH3 domain, ANK repeat and PH domain-containing protein 2	51	2
C2C2L_MOUSE	C2 domain-containing protein 2-like	32	1
CSPRS_MOUSE	Component of Sp100-rs	23	1
MCM8_MOUSE	DNA helicase MCM8	25	1
EMAL6_MOUSE	Echinoderm microtubule-associated protein-like 6	34	1
GKAP1_MOUSE G	kinase-anchoring protein 1	26	1
H1T_MOUSE	Histone H1t	41	1
ALBU_MOUSE	Serum albumin	41	1
SPE39_MOUSE	Spermatogenesis-defective protein 39 homolog	20	1
GUF1_MOUSE	Translation factor Guf1, mitochondrial	22	1
VASH1_MOUSE	Vasohibin-1	28	1

Table S4

Target	Foward primer 5' to 3'	Reverse primer 5' to 3'
AKT1	AGAACTCTAGGCATCCCTTCC	CGTTGGCATACTCCATGACA
ANG	TCCTGACTCAGCACCATGAC	ACATCTTTGCAGGGTGAGGTTA
ANGPT1	ACAACACCGGGAAGATGGAA	TTCACCAGAGGGATTCCCAAAA
ANGPT2	GAACCAGACAGCAGCACAAA	TCGAGTCTTGTCGTCTGGTTTA
ANGPTL4	CTTGGGACCAAGACCATGAC	TGGCTACAGGTACCAAACCA
ANPEP	TGGGACTTTGTCCGAAGCA	TCCCTGGATGAGATTGGCAAA
apelin	GCAGGAGGAAATTTCGCAGAC	ACTTGGCGAGCCCTTCAA
aplnnr	TTGACTGGCCTTTTGGAACC	GCAAAAGACACTGGCGTACA
Atp2a2	CGGTCCAAGAGTCTCCTTCTA	GCACAATCCACTCCATCGAA
BAI1	GGTCCTGAGAAGCAAACCAA	GACCATTCGTTCCAGTTTCCA
CCL11(Eotaxin)	CAACAACAGATGCACCCTGAA	CACAGATCTCTTTGCCCAACC
CCL2(MCP-1)	AGCAGCAGGTGTCCCAAA	TTCTTGGGGTCAGCACAGAC
CCL21a	GTCAGGACTGCTGCCTTAAGTA	GCTTCCTATAGCCTCGGACAA
CDH5	AACGAGGACAGCAACTTCAC	TGGCATGCTCCCGATTAAAC
COL18A1	CAGGACCAAAGGGTGACAAA	TTCCAGGTGGAAGAGGTCAA
Col4a3	GCTGGTACAAAGGGCAACAA	TAAGCCTGGCAATCCATCCA
CTGF	AAGCTGACCTGGAGGAAAACA	TGCAGCCAGAAAGCTCAAAC
CXCL1	CCTGAAGCTCCCTTGGTTCA	TTCTCCGTTACTTGGGGACAC
CXCL10(INP10)	ATCCGGAATCTAAGACCATCAAGAA	GCTCTCTGCTGTCCATCCA
IL8	GGCTACTGTTGGCCCAATTAC	GCTTCATTGCCGGTGGAAA
CXCL5(ENA78/LIX)	GGCATTTCTGTTGCTGTTCAC	TGCGGCTATGACTGAGGAA
CXCL9	AGCCCCAATTGCAACAAAAC	TCTTCACATTTGCCGAGTCC
Cyr 61	CCACACCAAGGGGTTGGAA	CACAGGGTCTGCCTTCTGAC
EDN1	CCTGGACATCATCTGGGTCAA	AACGCTTGGACCTGGAAGAA
EFNA1	TGGGCAAGGAGTTCAAGGAA	GCACTGGGATTCCTGATGGTA
EFNB2	TGCCAGACAAGAGCCATGAA	GTCTTGTTGGACCGTGATTCC
EGF	GGAGAGACTGCTGAGTGTCA	AGCCAGCACACACTCATCTA
ENG	AGGCATCCAACACCATCGAA	TCTAGCTGGACTGTGACCTCA
EPHB4	CCTCACGGAATTCATGGAGAAC	ACCAGCTGGATGACTGTGAA
ERBB2(HER2)	ATTCTCAGACGCCGGTTCA	TTGGCCCCAAAGGTCATCA
F3	ACCCAAACCCACCAACTATACC	GTGTCTGTGGTCGAGAAGCA
FGF1	TGGACACCGAAGGGCTTTTA	GCATGCTTCTTGGAGGTGTAA
FGF2(bFGF)	TCTTCCTGCGCATCCATCC	GCACACACTCCCTTGATAGACA
FGFR3	AGGATTTAGACCGCATCCTCAC	CCTGGCGAGTACTGCTCAAA
FIGF(VEGFD)	TCCATTCAGACCCCAGAAGAA	GTGTTATCCCACAGCATGTCA
FLT1	TTGCACGGGAGAGACTGAAA	GCCAAATGCAGAGGCTTGAA
VEGFR3	CTCGCTCGGGACATCTACAAA	GGGCCATCCATTTCAGAGGAA
FN1	CGTCATTGCCCTGAAGAACA	AAGGGTAACCAGTTGGGGAA
HGF	CATCAAATGCCAGCCTTGGAA	TCTTTACCGCGATAGCTCGAA
HIF1A	TCGACACAGCCTCGATATGAA	TTCCGGCTCATAACCCATCA

hnRNPM	GATGCCAACCATCTGAGCAAA	CCAAATCCTATGCCTTCCATTCC
HPSE	GCCTCGAGGGAAGACAGTTAAA	TGCCATGTAAGAGAGTCGATCAC
ID1	ACCCTGAACGGCGAGATCA	GATCGTCGGCTGGAACACA
IFNA1	TCCACCAGCAGCTCAATGAC	TCTTCCTGGGTCAGGGGAAA
IFNG	GGCACAGTCATTGAAAGCCTA	GCCAGTTCCTCCAGATATCCA
IGF1	GAGCTGGTGGATGCTCTTCA	CTCCGAATGCTGGAGCCATA
IL1B	TGGCAACTGTTCCTGAACTCA	GGGTCCGTCAACTTCAAAGAAC
IL6	CCAGAAACCGCTATGAAGTTCC	GTTGTCACCAGCATCAGTCC
ITGAV	AAAGGCAGATGGCAAGGGAA	GGCTCCCTTCTGCTTGAGTTTA
ITGB3	CCCACCACAGGCAATCAAAA	GCGTCAGCACGTGTTTGTA
JAG1	TCCCAAGCATGGGTCTTGTA	GATGCACTTGTCGCAGTACA
KDR	ATTTCACCTGGCACTCTCCA	TCCCAGGAAAGGGTTTCACA
LECT1	CCTGCCGATTTTCTGGCTTA	AGAGGGAGCACTGTTTCTCA
LEP	AGACCATTGTCACCAGGATCA	ATGAAGTCCAAGCCAGTGAC
MDK	TTGCCCTCTTGGTGGTCAC	CCAGGTCCACTCCGAACAC
MMP14	CAAGGCTGATTTGGCAACCA	GCCTTGATCTCAGTCCCAAAC
MMP2	CGAGGACTATGACCGGGATA	GGGCACCTTCTGAATTTCCA
MMP9	TCCCCAAAGACCTGAAAACC	GGGTGTAACCATAGCGGTAC
NEAT-1	GGGAAGCTGATTGCCAAGAA	ATGGTTTCAGAGCCCACAAC
P54NRB	TGGTACTCCAGCTCCTCCA	CAGCTTGGCCAAAACGTTCA
NOS3	GGGATTCTGGCAAGACAGACTA	GCAGCCAAACACCAAAGTCA
NOTCH4	ACCTGCTTGCAACCTTCCA	GGTGCACTCATTGACCTCCA
NRP1	CCTGTATCCTGGGAAACTGGTA	GCCCAACATTCCAGAGCAA
NRP2	GTGGATCAGCAGCGCTAAC	GCCATCACTCTGCAGTTTCAA
PDGFA	TGTAACACCAGCAGCGTCAA	GGCTTCTTCCTGACATACTCCA
PECAM1	GCACAGTGATGCTGAACAAC	GTCACCTTGGGCTTGGATAC
PF4	CCAGCCTGGAGGTGATCAA	GGCAAATTTTCCTCCCATTCTTCA
PGF	CCAATCGGGATCCACATTTCTA	GCCTTTGTCGTCTCCAGAATA
PLAU(uPA)	TAGCCTAGGCCTGGGGAAA	AGGCCAATCTGCACATAGCA
PLG	TGGAATTGCCCACAGTTTCC	CCGATAGTCTTTGCCATTCCC
PROK2	GGCTTGGCGTGTTTAAGGAC	GGGTCGCATTTCAAGTTCCTAC
prox1	GCCCTCAACATGCACTACAAC	CGTGATCTGCGCAACTTCC
PSPC1	TCCCCGTGGAGCAATAAACA	ATACCCATCATTGGAGGAGGAC
PTGS1	TATCACCTGCGGCTCTTCAA	GTTCCACGGAAGGTGGGTA
S1PR1	CGGTGTAGACCCAGAGTCC	GAGAGGCCTCCGAGAAACA
SERPINE1(PAI-1)	CAGACAATGGAAGGGCAACA	GAGGTCCACTTCAGTCTCCA
SERPINF1	AGAACCTCAAGAGTGCTTCCA	TTCTCCAGAGGGGCAACAAA
PSF/SFPQ	TGAAAAGCTGGCCCAGAAGAA	TGTGCCATGCTGAGCAAAAC
SPHK1	GGCAGCTTCTGTGAACCACTA	CAGCAGGTTCATGGGTGACA
TEK	GTTGGATGGCAATCGAATCAC	CCAGAGCAATACACCATAGGAC
TGFA	CCCTGGCTGTCCTCATTATCA	CAGTGTTTGCGGAGCTGAC
TGFB1	GCTGCGCTTGCAGAGATTAA	GTAACGCCAGGAATTGTTGCTA

TGFB2	GCCCATATCTATGGAGTTCAGACA	AGCGGAAGCTTCGGGATTTA
TGFBR1	AATTGCTCGACGCTGTTCTA	ACCGATGGATCAGAAGGTACA
THBS1	CCCCAGAAGACATTCTCAGGAA	CGTTCACCACGTTGTTGTCA
THBS2	GACTGCACGTCATGGTGAAC	CCCAATGAGCTCCAAAAGGAAC
TIE1	CCTTTGCTCAGATCGCACTA	CTCAAACAGCGACATGTTCAC
TIMP1	TCCCCAGAAATCAACGAGACC	CATTTCCCACAGCCTTGAATCC
TIMP2	GAAGAGCCTGAACCACAGGTA	TCATCCGGGGAGGAGATGTA
TIMP3	CCCTTTGGCACTCTGGTCTA	ACGTGGGGCATCTTACTGAA
TNF	CAAATGGCCTCCCTCTCATCA	TGGGCTACAGGCTTGTCAC
TYMP	GGCACACTGGATAAGCTGGAA	CAGCAGCCGACTTCCTCAA
VASH1	GGCTGCCAAGTTGGGGTGTGTT	AAACCAGGGCGTGGCTCCTGTA
VEGFA	CCAGCACATAGGAGAGATGAG	CTGGCTTTGTTCTGTCTTTCTT
VEGFB	GAGATGTCCCTGGAAGAACACA	TGGCTTCACAGCACTCTCC
VEGFC	AGACGTTCTCTGCCAGCAA	AGGCATCGGCACATGTAGTTA
18S	CAACTAAGAACGGCCATGCA	AGCCTGCGGCTTAATTTGAC

Table S5

siControl 5’ → 3’	siVASH1 5’ → 3’
ACCAAAUGUACAGCUGAUU	GACACUAGGACCCUUAAAU
ACCAAAUGUACAAAAGACU	CGAAGUUCUGGAUAAAGAG
ACCAAAUGUACAAAAGGAU	CCCUCCUGGACUACAUGUU
ACCAAAUGUACAACACACU	CAUGUUAGUGUGUCCCUGU

Discussion

Discussion

Les résultats de cette thèse démontrent que la régulation de la traduction est un processus complexe et fondamental de l'expression des gènes. La traduction alternative par le mécanisme à IRES est régulée par les acteurs majeurs qui sont les ITAF. Plusieurs paramètres sont essentiels dans cette traduction : le type cellulaire et le stimulus.

Un ITAF serait-il stress-dépendant ?

Le premier chapitre sur l'étude sur l'activité de l'IRES du FGF1 durant la différenciation myoblastique révèle une activité IRES-dépendante du promoteur qui est orchestrée par les ITAF p54^{nrb}/NONO et hnRNPM. Dans le troisième chapitre l'IRES de FGF1 est activé par l'ITAF VASH1 en réponse à une hypoxie précoce dans les cardiomyocytes. Ces données suggèrent que l'activation de l'IRES de FGF1 recrute un ITAF spécifique selon le stimulus perçu.

Dans le deuxième chapitre, l'IRES du VEGFD est activé par l'ITAF nucléoline lors du choc thermique. En revanche, la nucléoline n'a pas était identifié en hypoxie. La nucléoline serait-elle l'ITAF des autres VEGF à 8h en hypoxie ?

Un ITAF serait-il stimulus-dépendant ? Pour cela, il faut étudier l'effet de p54nrb/NONO et hnRNPM dans les cardiomyocytes en hypoxie et inversement, étudier si VASH1 active l'IRES de FGF1 durant la différenciation myoblastique. Il faut également étudier l'effet de la nucléoline sur les VEGF à 8h en hypoxie dans les cardiomyocytes.

Les paraspeckles ont-ils un lien avec les IRES ?

Cependant, l'interaction de p54nrb/NONO et hnRNPM a été déjà montréeen 2010 par Marko et ses collègues. Ces auteurs ont montré également la localisation de ces protéines dans le noyau en liaison avec une autre protéine PSF, composant de corps nucléaires appelés "paraspeckles" dans les cellules cancéreuses (Marko*et al*, 2009). Ces paraspeckles se forment dans des situations pathologiques comme lors

de la différenciation cellulaire et lors du stress, le cancer aété identifié plus tard (Fox *et al*, 2002, Imamura *et al*, 2014, Choudhry *et al*, 2015, Chen and Carmichael, 2009). Le long non-codant Neat1, est un marqueur de stress essentiel à la formation de ces paraspeckles. Les conditions de formation des paraspeckles sont similaires aux conditions d'activation des IRES. Nous avons identifié une corrélation entre la formation des paraspeckles et l'activation des IRES lors de la différenciation myoblastique et lors du stress hypoxique à 4h dans les cariomyocytes et à 24h dans les cellules tumorales (Godet *et al*, non publié). De plus dans le noyau, les paraspeckles sont localisés près des espaces interchromatiniens et enrichis en facteurs d'épissage (Fox *et al* 2002). Ces données corrèlent avec l'implication de $p54^{nrb}$/NONO et hnRNPM quant à leur fonction facteur de transcription du promoteur du gène FGF1. Nos résultats montre que Neat1 est surexprimé en hypoxie et retrouvé dans les polysomes. Le long ARN non-codant Neat1 serait-il un ITAF, impliqué dans l'activation de l'IRES de FGF1 ?

En effet, il a été rapporté qu'il interagit avec p54nrb/NONO, elle-même identifiée an tant qu'ITAF. Neat-1 pourrait intervenir dans la formation de l'IRESsome. La localisation de Neat-1 dans les polysomes (alors qu'il est décrit comme étant uniquement nucléaire) suggère aussi son implication dans la régulation de la traduction.

Il faut vérifier l'implication de ce long ARN non-codant dans l'activation de l'IRES de FGF1 en hypoxie.

Y aurait-il des ITAF responsablesde chaque vague d'activation ?

Dans les cardiomyocytes, les résultats de l'activation des IRES (lymph)angiogéniques montrent deux vagues d'activation. Les IRES de la famille des FGF sont activés à 4h et ceux de la famille des VEGF sont activés à 8h. Ces vagues d'activation semblent fonctionner comme des régulons. Ce concept de régulon traductionnel a déjà été démontré dans la famille les gènes Hox dans le développement. Les ARNm des gènes hox possèdent un IRES qui est activé par RPL18 (Xue *et al*, 2015).

Il serait intéressant de déterminer les ITAF responsables des vagues d'activation des IRES en réponse à l'hypoxie précoce dans les cardiomyocytes.

La vasohibine 1 active spécifiquement l'IRES de FGF1 mais n'agit pas sur l'IRES de FGF2 à 4h en hypoxie. Curieusement, l'activation de l'IRES de FGF2 est maintenue jusqu'à 8h.

L'IRES de FGF2 serait-il activé par d'autres ITAF ?

Nos résultats sur la qPCR à haut-débit avec l'invalidation de VASH1 montre un effet de VASH1 sur de nombreux gènes. Les données suggèrent que VASH1 activerait également d'autres IRES.

La double fonction de VASH1

De façon surprenante, l'invalidation de VASH1 augmente l'activation de l'IRES de VEGFAa. VASH1 serait un ITAF répresseur de VEGFAa. VASH1 serait un ITAF à double rôle : activateur de l'IRES de FGF1 et inhibiteur de l'IRES de VEGFAa en hypoxie dans les cardiomyocytes. La littérature a montré que la protéine HuR est un ITAF activateur de l'IRES de XIAP et de HIF-1A mais également un répresseur de l'IRES de IGF1R et BCL_x (Meng *et al*, 2005, Durieu *et al*, 2011, 2013 Galban *et al*, 2008). Ces deux fonctions peuvent être expliquées par l'existence de deux isoformes de VASH1. Il serait intéressant de déterminer l'isoforme responsable de l'activation de l'IRES de FGF1 et l'inhibition de l'IRES de VEGFAa en réponse à l'hypoxie dans les cardiomyocytes.

VASH1 aurait-elle un IRES régulé par HuR ?

VASH1 est connu commun gène anti-angiogenique (Watanabe *et al,* 2004, Sonoda *et al,* 2006). Ce qui corrobore avec son rôle en qu'ITAF répresseur de VEGFAa dans les cardiomyocytes en hypoxie. En revanche, il pourrait être un activateur comme dans le cas de FGF1 ; ces différentes fonctions seraient liées à son expression en fonction du tissu. En effet VASH1 n'est pas exprimée dans les cellules cancéreuses mais nos résultats révèlent qu'elle est fortement exprimée dans les cardiomyocytes en hypoxie (Watanabe *et al,* 2004). Outre sa fonction anti-angiogénique, Miyashita et ses collègues ont montré que VASH1 est impliquée dans la tolérance au stress. VASH1 améliore la tolérance au stress des cellules endothéliales en induisant l'expression de SOD2 et SIRT1 (Miyashita *et al*, 2012). De plus sa synthèse protéique est activée par HuR en réponse au stress en se fixant sur sa région 3'UTR dans les cellules endothéliales (Miyashita *et al,* 2012) avec une

expression transcriptionnelle inchangée. Ces résultats sont retrouvés dans les cardiomycocytes en réponse à l'hypoxie, VASH1 est induite au niveau de la traduction mais pas au niveau de la transcription en réponse à l'hypoxie.

L'ARNm deVASH1 possèderait-il un IRES régulé par HuR ? De plus, dans la littérature, HuR a été décrit comme un ITAF (Yeh *et al,* 2008, Galban *et al*, 2008, Durie *et al*, 2011).

L'importance des partenaires protéiques

L'étude sur l'activité de l'IRES du FGF1 durant la différenciation myoblastique révèle une activité IRES-dépendante du promoteur qui est orchestrée par les ITAF p54^{nrb}/NONO et hnRNPM. Concernant la fonction de ces ITAF, hnRNPM est impliqué dans l'épissage et p54^{nrb}/NONO a un rôle dans le couplage transcription-épissage (Hovhannisyan and Carstens 2007, Pandit *et al*, 2008). De plus, p54nrb/NONO a été déjà décrit comme ITAF des IRES c-, L-, et N-myc et APAF-1 (Cobbold *et al,* 2008). Dans ce travail l'interaction de p54^{nrb}/NONO et hnRNPM leur confère un nouveau rôle dans la stimulation de la différenciation myoblastique par l'activation de l'IRES du FGF1 dépendant du promoteur. Ces protéines sont multifonctionnelles. Ces données révèlent l'importance du partenaire protéique pour définir leur fonction.

L'importance de l'évènement nucléaire

Ce travail rejoint de nombreuses publications montrant l'importance de l'évènement nucléaire. Nos résultats sur l'activation de l'IRES de VEGFD montrent que la nucléoline est exportée dans le cytoplasme pour activer l'IRES de VEGFD en réponse au choc thermique. Deux mécanismes sont alors émis : **(i)** les ITAF servent à retenir les ARNm dans le noyau avant leur relargage dans le cytoplasme en réponse à un stimulus spécifique, **(ii)** les ITAF sont séparés des IRES dans le noyau en attendant le signal d'un stress pour être relargués dans le cytoplasme afin d'activer l'IRES. Il serait important d'élucider ces mécanismes en suivant la localisation de l'ITAF avec l'activation de l'IRES cible.

Modèle non-tumoral pour l'étude de l'angiogenèse en hypoxie

Les cardiomyocytes HL1 sont de bons modèles pour étudier la réponse au stress et l'expression de facteurs de croissance angiogéniques. Les cardiomyocytes HL1 présentent le même phénotype que les cardiomyocytes adultes avec les mêmes propriétés morphologiques, électrophysiologiques et biochimiques (Claycomb *et al*, 1998). En ce qui concerne le stress hypoxique, les cellules cancéreuses sont résistantes par conséquent les IRES sont activés plus tardivement (Braunstein *et al*, 2007, Morfoisse *et al,* 2014). Les cardiomyocytes sont donc de bons modèles pour étudier la régulation de la traduction par le mécanisme à IRES en réponse à une hypoxie précoce. De plus, les cardiomyocytes HL-1 sont facilement transduits par les lentivecteurs pour un bon suivi de l'expression des transgènes à long terme.

L'importance de l'étude des ITAF dans la thérapie génique et comme nouvelles cibles thérapeutiques

La régulation de la traduction IRES-dépendante est très complexe et nécessite encore beaucoup d'investigations pour être élucidée. Les ITAF sont des acteurs importants pour réguler finement cette traduction. Comme je l'ai mentionné dans l'introduction, actuellement la thérapie combinée s'avère indispensable. Dans ce contexte l'IRES est un outil prometteur pour l'expression de transgènes. Par conséquent, les résultats cette thèse rappellent l'importance du rôle des ITAF en fonction du type de stress et du type cellulaire. Ils fournissent des données importantes pour la vectorologie, car le choix des IRES à utiliser pour créer des vecteurs de transfert de gène pour la thérapie génique de l'ischémie cardiaque.

Il a aussi été montré que les IRES sont responsables de l'activation de l'expression génique dans des situations pathologiques, notamment dans les cellules cancéreuses (Marcel *et al*, 2013). Avec le concept de régulon traductionnel qui est apparu pour les IRES, les ITAF identifiés constituent donc de nouvelles cibles potentielles pour bloquer (ou activer) de manière concertée l'expression de familles de gènes.

Bibliographie

Bibliographie

Alam, K. Y., A. Frostholm, K. V. Hackshaw, J. E. Evans, A. Rotter and I. M. Chiu (1996). "Characterization of the 1B promoter of fibroblast growth factor 1 and its expression in the adult and developing mouse brain." J Biol Chem**271** (47): 30263-30271.

Allera-Moreau, C., P. Chomarat, V. Audinot, F. Coge, M. Gillard, Y. Martineau, J. A. Boutin and A. C. Prats (2006). "The use of IRES-based bicistronic vectors allows the stable expression of recombinant G-protein coupled receptors such as NPY5 and histamine 4." Biochimie**88** (6): 737-746.

Allera-Moreau, C., A. Delluc-Clavieres, C. Castano, L. Van den Berghe, M. Golzio, M. Moreau, J. Teissie, J. F. Arnal and A. C. Prats (2007). "Long term expression of bicistronic vector driven by the FGF-1 IRES in mouse muscle." BMC Biotechnol**7**: 74.

Allouche, M. and A. Bikfalvi (1995). "The role of fibroblast growth factor-2 (FGF-2) in hematopoiesis." Prog Growth Factor Res**6** (1): 35-48.

Arcondeguy, T., E. Lacazette, S. Millevoi, H. Prats and C. Touriol (2013). "VEGF-A mRNA processing, stability and translation: a paradigm for intricate regulation of gene expression at the post-transcriptional level." Nucleic Acids Res**41** (17): 7997-8010.

Arnaud, E., C. Touriol, C. Boutonnet, M. C. Gensac, S. Vagner, H. Prats and A. C. Prats (1999). "A new 34-kilodalton isoform of human fibroblast growth factor 2 is cap dependently synthesized by using a non-AUG start codon and behaves as a survival factor." Mol Cell Biol**19** (1): 505-514.

Audigier, S., J. Guiramand, L. Prado-Lourenco, C. Conte, I. G. Gonzalez-Herrera, C. Cohen-Solal, M. Recasens and A. C. Prats (2008). "Potent activation of FGF-2 IRES-dependent mechanism of translation during brain development." RNA**14** (9): 1852-1864.

Bah, A., R. M. Vernon, Z. Siddiqui, M. Krzeminski, R. Muhandiram, C. Zhao, N. Sonenberg, L. E. Kay and J. D. Forman-Kay (2015). "Folding of an intrinsically disordered protein by phosphorylation as a regulatory switch." Nature**519** (7541): 106-109.

Bal, N. V., D. Susorov, E. Chesnokova, A. Kasianov, T. Mikhailova, E. Alkalaeva, P. M. Balaban and P. Kolosov (2016). "Upstream Open

Reading Frames Located in the Leader of Protein Kinase Mzeta mRNA Regulate Its Translation." Front Mol Neurosci**9**: 103.

Barouki, M. G. a. R. (2002). "Le stress du réticulum endoplasmique : adaptation et toxicité." Medecine/Sciences**18**: 585-594.

Basilico, C. and D. Moscatelli (1992). "The FGF family of growth factors and oncogenes." Adv Cancer Res**59**: 115-165.

Bastide, A., Z. Karaa, S. Bornes, C. Hieblot, E. Lacazette, H. Prats and C. Touriol (2008). "An upstream open reading frame within an IRES controls expression of a specific VEGF-A isoform." Nucleic Acids Res**36** (7): 2434-2445.

Baumgartner, I., A. Pieczek, O. Manor, R. Blair, M. Kearney, K. Walsh and J. M. Isner (1998). "Constitutive expression of phVEGF165 after intramuscular gene transfer promotes collateral vessel development in patients with critical limb ischemia." Circulation**97** (12): 1114-1123.

Belsham, G. J. and N. Sonenberg (1996). "RNA-protein interactions in regulation of picornavirus RNA translation." Microbiol Rev**60** (3): 499-511.

Beretta, L., A. C. Gingras, Y. V. Svitkin, M. N. Hall and N. Sonenberg (1996). "Rapamycin blocks the phosphorylation of 4E-BP1 and inhibits cap-dependent initiation of translation." EMBO J**15** (3): 658-664.

Bernstein, J., O. Sella, S. Y. Le and O. Elroy-Stein (1997). "PDGF2/c-sis mRNA leader contains a differentiation-linked internal ribosomal entry site (D-IRES)." J Biol Chem**272** (14): 9356-9362.

Bonnal, S., F. Pileur, C. Orsini, F. Parker, F. Pujol, A. C. Prats and S. Vagner (2005). "Heterogeneous nuclear ribonucleoprotein A1 is a novel internal ribosome entry site trans-acting factor that modulates alternative initiation of translation of the fibroblast growth factor 2 mRNA." J Biol Chem**280** (6): 4144-4153.

Bonnal, S., C. Schaeffer, L. Creancier, S. Clamens, H. Moine, A. C. Prats and S. Vagner (2003). "A single internal ribosome entry site containing a G quartet RNA structure drives fibroblast growth factor 2 gene expression at four alternative translation initiation codons." J Biol Chem**278** (41): 39330-39336.

Bonnet-Magnaval, F., C. Philippe, L. Van Den Berghe, H. Prats, C. Touriol and E. Lacazette (2016). "Hypoxia and ER stress promote Staufen1

expression through an alternative translation mechanism." Biochem Biophys Res Commun**479** (2): 365-371.

Boren, J., M. Gustafsson, K. Skalen, C. Flood and T. L. Innerarity (2000). "Role of extracellular retention of low density lipoproteins in atherosclerosis." Curr Opin Lipidol**11** (5): 451-456.

Borman, A. M. and K. M. Kean (1997). "Intact eukaryotic initiation factor 4G is required for hepatitis A virus internal initiation of translation." Virology**237** (1): 129-136.

Bornes, S., M. Boulard, C. Hieblot, C. Zanibellato, J. S. Iacovoni, H. Prats and C. Touriol (2004). "Control of the vascular endothelial growth factor internal ribosome entry site (IRES) activity and translation initiation by alternatively spliced coding sequences." J Biol Chem**279** (18): 18717-18726.

Bornes, S., L. Prado-Lourenco, A. Bastide, C. Zanibellato, J. S. Iacovoni, E. Lacazette, A. C. Prats, C. Touriol and H. Prats (2007). "Translational induction of VEGF internal ribosome entry site elements during the early response to ischemic stress." Circ Res**100** (3): 305-308.

Bosch-Marce, M., H. Okuyama, J. B. Wesley, K. Sarkar, H. Kimura, Y. V. Liu, H. Zhang, M. Strazza, S. Rey, L. Savino, Y. F. Zhou, K. R. McDonald, Y. Na, S. Vandiver, A. Rabi, Y. Shaked, R. Kerbel, T. Lavallee and G. L. Semenza (2007). "Effects of aging and hypoxia-inducible factor-1 activity on angiogenic cell mobilization and recovery of perfusion after limb ischemia." Circ Res**101** (12): 1310-1318.

Brahimi-Horn, C. and J. Pouyssegur (2005). "When hypoxia signalling meets the ubiquitin-proteasomal pathway, new targets for cancer therapy." Crit Rev Oncol Hematol**53** (2): 115-123.

Brahimi-Horn, M. C., J. Chiche and J. Pouyssegur (2007). "Hypoxia and cancer." J Mol Med (Berl)**85** (12): 1301-1307.

Brahimi-Horn, M. C. and J. Pouyssegur (2007). "Harnessing the hypoxia-inducible factor in cancer and ischemic disease." Biochem Pharmacol**73** (3): 450-457.

Braunschweig, U., S. Gueroussov, A. M. Plocik, B. R. Graveley and B. J. Blencowe (2013). "Dynamic integration of splicing within gene regulatory pathways." Cell**152** (6): 1252-1269.

Bregman, A., M. Avraham-Kelbert, O. Barkai, L. Duek, A. Guterman and M. Choder (2011). "Promoter elements regulate cytoplasmic mRNA decay." Cell**147** (7): 1473-1483.

Braunstein, S., K. Karpisheva, C. Pola, J. Golberg, T. Hochman, H. Yee, J. Cangiiarella, R. Arju, S. C. Formenti, R. J. Shneider (2007). "A hypoxia-controlled cap-dependent to cap-independent translation switch in breast cancer." Mol Cell **28** (3): 501-512.

Brunn, G. J., P. Fadden, T. A. Haystead and J. C. Lawrence, Jr. (1997). "The mammalian target of rapamycin phosphorylates sites having a (Ser/Thr)-Pro motif and is activated by antibodies to a region near its COOH terminus." J Biol Chem**272** (51): 32547-32550.

Buchler, P., H. A. Reber, M. Buchler, S. Shrinkante, M. W. Buchler, H. Friess, G. L. Semenza and O. J. Hines (2003). "Hypoxia-inducible factor 1 regulates vascular endothelial growth factor expression in human pancreatic cancer." Pancreas**26** (1): 56-64.

Buehler, A., A. Martire, C. Strohm, S. Wolfram, B. Fernandez, M. Palmen, X. H. Wehrens, P. A. Doevendans, W. M. Franz, W. Schaper and R. Zimmermann (2002). "Angiogenesis-independent cardioprotection in FGF-1 transgenic mice." Cardiovasc Res**55** (4): 768-777.

Buschmann, I. and W. Schaper (1999). "Arteriogenesis Versus Angiogenesis: Two Mechanisms of Vessel Growth." News Physiol Sci**14**: 121-125.

Buttgereit, F. and M. D. Brand (1995). "A hierarchy of ATP-consuming processes in mammalian cells." Biochem J**312 (Pt 1)**: 163-167.

Canaani, D., M. Revel and Y. Groner (1976). "Translational discrimination of 'capped' and 'non-capped' mRNAS: inhibition of a series of chemical analogs of m7GpppX." FEBS Lett**64** (2): 326-331.

Cao, R., E. Brakenhielm, R. Pawliuk, D. Wariaro, M. J. Post, E. Wahlberg, P. Leboulch and Y. Cao (2003). "Angiogenic synergism, vascular stability and improvement of hind-limb ischemia by a combination of PDGF-BB and FGF-2." Nat Med**9** (5): 604-613.

Carew, T. E., R. C. Pittman, E. R. Marchand and D. Steinberg (1984). "Measurement in vivo of irreversible degradation of low density lipoprotein in the rabbit aorta. Predominance of intimal degradation." Arteriosclerosis**4** (3): 214-224.

Carmeliet, P. and R. K. Jain (2000). "Angiogenesis in cancer and other diseases." Nature**407** (6801): 249-257.

Casanova, C. M., P. Sehr, K. Putzker, M. W. Hentze, B. Neumann, K. E. Duncan and C. Thoma (2012). "Automated high-throughput RNAi screening in human cells combined with reporter mRNA transfection to identify novel regulators of translation." PLoS One**7** (9): e45943.

Chae, J. K., I. Kim, S. T. Lim, M. J. Chung, W. H. Kim, H. G. Kim, J. K. Ko and G. Y. Koh (2000). "Coadministration of angiopoietin-1 and vascular endothelial growth factor enhances collateral vascularization." Arterioscler Thromb Vasc Biol**20** (12): 2573-2578.

Chan, D. A. and A. J. Giaccia (2007). "Hypoxia, gene expression, and metastasis." Cancer Metastasis Rev**26** (2): 333-339.

Chen, L-L., G. G. Carmichael (2009). " Aletred nuclear retention of mRNAs containing inverted repeats in human embryonic stem cells: functional role of a nuclear noncoding RNA."Mol. Cell **35** (4): 476-478.

Cho, E. J., T. Takagi, C. R. Moore and S. Buratowski (1997). "mRNA capping enzyme is recruited to the transcription complex by phosphorylation of the RNA polymerase II carboxy-terminal domain." Genes Dev**11** (24): 3319-3326.

Cho, P. F., F. Poulin, Y. A. Cho-Park, I. B. Cho-Park, J. D. Chicoine, P. Lasko and N. Sonenberg (2005). "A new paradigm for translational control: inhibition via 5'-3' mRNA tethering by Bicoid and the eIF4E cognate 4EHP." Cell**121** (3): 411-423.

Chotani, M. A. and I. M. Chiu (1997). "Differential regulation of human fibroblast growth factor 1 transcripts provides a distinct mechanism of cell-specific growth factor expression." Cell Growth Differ**8** (9): 999-1013.

Chotani, M. A., R. A. Payson, J. A. Winkles and I. M. Chiu (1995). "Human fibroblast growth factor 1 gene expression in vascular smooth muscle cells is modulated via an alternate promoter in response to serum and phorbol ester." Nucleic Acids Res**23** (3): 434-441.

Chotani, M. A., K. Touhalisky and I. M. Chiu (2000). "The small GTPases Ras, Rac, and Cdc42 transcriptionally regulate expression of human fibroblast growth factor 1." J Biol Chem**275** (39): 30432-30438.

Choudhry, H., A. Albukhari, M. Morotti, S. Haider, D. Moralli, J. Smythies, J. Schodel, C. M. Green, C. Camps, F. Buffa, P. Ratcliffe, J. Ragoussis, A. L. Harris and D. R. Mole (2015). "Tumor hypoxia induces nuclear

paraspeckle formation through HIF-2alpha dependent transcriptional activation of NEAT1 leading to cancer cell survival." Oncogene**34** (34): 4482-4490.

Christmann, J. L. and M. E. Dahmus (1981). "Monoclonal antibody specific for calf thymus RNA polymerases IIO and IIA." J Biol Chem**256** (22): 11798-11803.

Cobbold, L. C., K. A. Spriggs, S. J. Haines, H. C. Dobbyn, C. Hayes, C. H. de Moor, K. S. Lilley, M. Bushell and A. E. Willis (2008). "Identification of internal ribosome entry segment (IRES)-trans-acting factors for the Myc family of IRESs." Mol Cell Biol**28** (1): 40-49.

Claycomb W. C., N. A. Jr Lanson, B. S. Stallworth, D. B. Egeland, J. B. Delcarpio, A. Bahinski, N. J Jr Izzo (1998). "HL-1 cells: a cardiac muscle cell line that contracts and retains phenotypic characteristics of the adult cardiomyocyte." Proc Natl Acad Sci USA**95** (6): 2979-2984.

Cohen, B., Y. Addadi, S. Sapoznik, G. Meir, V. Kalchenko, A. Harmelin, S. Ben-Dor and M. Neeman (2009). "Transcriptional regulation of vascular endothelial growth factor C by oxidative and thermal stress is mediated by lens epithelium-derived growth factor/p75." Neoplasia**11** (9): 921-933.

Coldwell, M. J., M. L. deSchoolmeester, G. A. Fraser, B. M. Pickering, G. Packham and A. E. Willis (2001). "The p36 isoform of BAG-1 is translated by internal ribosome entry following heat shock." Oncogene**20** (30): 4095-4100.

Coldwell, M. J., S. A. Mitchell, M. Stoneley, M. MacFarlane and A. E. Willis (2000). "Initiation of Apaf-1 translation by internal ribosome entry." Oncogene**19** (7): 899-905.

Conte, C., N. Ainaoui, A. Delluc-Clavieres, M. P. Khoury, R. Azar, F. Pujol, Y. Martineau, S. Pyronnet and A. C. Prats (2009). "Fibroblast growth factor 1 induced during myogenesis by a transcription-translation coupling mechanism." Nucleic Acids Res**37** (16): 5267-5278.

Conte, C., E. Riant, C. Toutain, F. Pujol, J. F. Arnal, F. Lenfant and A. C. Prats (2008). "FGF2 translationally induced by hypoxia is involved in negative and positive feedback loops with HIF-1alpha." PLoS One**3** (8): e3078.

Cobbold L. LC., K. A. Spriggs, S. J. Haines, H. C. Dobbyn, C. Hayes, C. H. de Moore, K. S. Lilley, M. Bushell, AE Willis (2008). "Identification of

internal ribosome entry segment (IRES)-trans-acting factors for the Myc family of IRESs." Mol Cell Biol**28** (1): 40-49.

Creancier, L., P. Mercier, A. C. Prats and D. Morello (2001). "c-myc Internal ribosome entry site activity is developmentally controlled and subjected to a strong translational repression in adult transgenic mice." Mol Cell Biol**21** (5): 1833-1840.

Creancier, L., D. Morello, P. Mercier and A. C. Prats (2000). "Fibroblast growth factor 2 internal ribosome entry site (IRES) activity ex vivo and in transgenic mice reveals a stringent tissue-specific regulation." J Cell Biol**150** (1): 275-281.

Cross, M. J. and L. Claesson-Welsh (2001). "FGF and VEGF function in angiogenesis: signalling pathways, biological responses and therapeutic inhibition." Trends Pharmacol Sci**22** (4): 201-207.

Cuevas, P., D. Reimers, F. Carceller, V. Martinez-Coso, M. Redondo-Horcajo, I. Saenz de Tejada and G. Gimenez-Gallego (1997). "Fibroblast growth factor-1 prevents myocardial apoptosis triggered by ischemia reperfusion injury." Eur J Med Res**2** (11): 465-468.

Cursiefen, C., L. Chen, L. P. Borges, D. Jackson, J. Cao, C. Radziejewski, P. A. D'Amore, M. R. Dana, S. J. Wiegand and J. W. Streilein (2004). "VEGF-A stimulates lymphangiogenesis and hemangiogenesis in inflammatory neovascularization via macrophage recruitment." J Clin Invest**113** (7): 1040-1050.

Dahmus, M. E. (1996). "Reversible phosphorylation of the C-terminal domain of RNA polymerase II." J Biol Chem**271** (32): 19009-19012.

David, C. J., A. R. Boyne, S. R. Millhouse and J. L. Manley (2011). "The RNA polymerase II C-terminal domain promotes splicing activation through recruitment of a U2AF65-Prp19 complex." Genes Dev**25** (9): 972-983.

De Felipe, P., G. A. Luke, L. E. Hughes, D. Gani, C. Halpin and M. D. Ryan (2006). "E unum pluribus: multiple proteins from a self-processing polyprotein." Trends Biotechnol**24** (2): 68-75.

Debinski, W., B. Slagle-Webb, M. G. Achen, S. A. Stacker, E. Tulchinsky, G. Y. Gillespie and D. M. Gibo (2001). "VEGF-D is an X-linked/AP-1 regulated putative onco-angiogen in human glioblastoma multiforme." Mol Med**7** (9): 598-608.

Dejean, E., M. H. Renalier, M. Foisseau, X. Agirre, N. Joseph, G. R. de Paiva, T. Al Saati, J. Soulier, C. Desjobert, L. Lamant, F. Prosper, D. W. Felsher, J. Cavaille, H. Prats, G. Delsol, S. Giuriato and F. Meggetto (2011). "Hypoxia-microRNA-16 downregulation induces VEGF expression in anaplastic lymphoma kinase (ALK)-positive anaplastic large-cell lymphomas." Leukemia**25** (12): 1882-1890.

Dellinger, M. T. and R. A. Brekken (2011). "Phosphorylation of Akt and ERK1/2 is required for VEGF-A/VEGFR2-induced proliferation and migration of lymphatic endothelium." PLoS One**6** (12): e28947.

Dellinger, M. T., S. M. Meadows, K. Wynne, O. Cleaver and R. A. Brekken (2013). "Vascular endothelial growth factor receptor-2 promotes the development of the lymphatic vasculature." PLoS One**8** (9): e74686.

Deng, J., J. Cui, N. Jiang, R. Zhang, L. Zhang, X. Hao and H. Liang (2014). "STAT3 regulation the expression of VEGF-D in HGC-27 gastric cancer cell." Am J Transl Res**6** (6): 756-767.

Dholakia, J. N. and A. J. Wahba (1989). "Mechanism of the nucleotide exchange reaction in eukaryotic polypeptide chain initiation. Characterization of the guanine nucleotide exchange factor as a GTP-binding protein." J Biol Chem**264** (1): 546-550.

Du, Q., L. Jiang, X. Wang, M. Wang, F. She and Y. Chen (2014). "Tumor necrosis factor-alpha promotes the lymphangiogenesis of gallbladder carcinoma through nuclear factor-kappaB-mediated upregulation of vascular endothelial growth factor-C." Cancer Sci**105** (10): 1261-1271.

Eguchi, H., T. Ikuta, T. Tachibana, Y. Yoneda and K. Kawajiri (1997). "A nuclear localization signal of human aryl hydrocarbon receptor nuclear translocator/hypoxia-inducible factor 1beta is a novel bipartite type recognized by the two components of nuclear pore-targeting complex." J Biol Chem**272** (28): 17640-17647.

Durie, D., M. Hatzoglou, P. Chakraborty, M. Holcik (2013). " HuR controls mitochondrial morphology through the regulation of BclxL translation." Translation**1** (1): e23980

Durie, D., S. M. Lewis, U. Liwak, M. Kisilewicz, M Gorospe, M Holcik (2011). " RNA-binding protein HuR mediates cytoprotection through stimulation of XIAP translation." Oncogene**30** (12): 1460-1469.

Emerson, B. M. (2002). "Specificity of gene regulation." Cell**109** (3): 267-270.

Evans, J. R., S. A. Mitchell, K. A. Spriggs, J. Ostrowski, K. Bomsztyk, D. Ostarek and A. E. Willis (2003). "Members of the poly (rC) binding protein family stimulate the activity of the c-myc internal ribosome entry segment in vitro and in vivo." Oncogene**22** (39): 8012-8020.

Fan, D., A. Takawale, M. Shen, W. Wang, X. Wang, R. Basu, G. Y. Oudit and Z. Kassiri (2015). "Cardiomyocyte A Disintegrin And Metalloproteinase 17 (ADAM17) Is Essential in Post-Myocardial Infarction Repair by Regulating Angiogenesis." Circ Heart Fail**8** (5): 970-979.

Fernandez, J., I. Yaman, C. Huang, H. Liu, A. B. Lopez, A. A. Komar, M. G. Caprara, W. C. Merrick, M. D. Snider, R. J. Kaufman, W. H. Lamers and M. Hatzoglou (2005). "Ribosome stalling regulates IRES-mediated translation in eukaryotes, a parallel to prokaryotic attenuation." Mol Cell**17** (3): 405-416.

Ferrara, N. (2005). "The role of VEGF in the regulation of physiological and pathological angiogenesis." EXS (94): 209-231.

Ferrara, N. and T. Davis-Smyth (1997). "The biology of vascular endothelial growth factor." Endocr Rev**18** (1): 4-25.

Ferrara, N. and R. S. Kerbel (2005). "Angiogenesis as a therapeutic target." Nature**438** (7070): 967-974.

Flynn, A. and G. Proud (1996). "Insulin-stimulated phosphorylation of initiation factor 4E is mediated by the MAP kinase pathway." FEBS Lett**389** (2): 162-166.

Forsdyke, D. R. (1994). "The heat-shock response and the molecular basis of genetic dominance." J Theor Biol**167** (1): 1-5.

Forsythe, J. A., B. H. Jiang, N. V. Iyer, F. Agani, S. W. Leung, R. D. Koos and G. L. Semenza (1996). "Activation of vascular endothelial growth factor gene transcription by hypoxia-inducible factor 1." Mol Cell Biol**16** (9): 4604-4613.

Fox, H., Y. W. Lam, A. K.L. Leung, C. E. Lyon, J. Andersen, M. Mann, A. I. Lamond (2002). "Paraspeckles: a novel nuclear domain." Curr. Biol. **12** (1): 13-25

Furic, L., L. Rong, O. Larsson, I. H. Koumakpayi, K. Yoshida, A. Brueschke, E. Petroulakis, N. Robichaud, M. Pollak, L. A. Gaboury, P. P. Pandolfi, F. Saad and N. Sonenberg (2010). "eIF4E phosphorylation

promotes tumorigenesis and is associated with prostate cancer progression." Proc Natl Acad Sci U S A**107** (32): 14134-14139.

Furuichi, Y., A. LaFiandra and A. J. Shatkin (1977). "5'-Terminal structure and mRNA stability." Nature**266** (5599): 235-239.

Gaccioli, F., C. C. Huang, C. Wang, E. Bevilacqua, R. Franchi-Gazzola, G. C. Gazzola, O. Bussolati, M. D. Snider and M. Hatzoglou (2006). "Amino acid starvation induces the SNAT2 neutral amino acid transporter by a mechanism that involves eukaryotic initiation factor 2alpha phosphorylation and cap-independent translation." J Biol Chem**281** (26): 17929-17940.

Galbán, S., Y. Kuwano, R. Jr Pullmann, J. L. Martindale, H. H. Kim, A. Lal,, K. Abdelmohsen, X Yang, Y. Dang, J. O. Liu, S. M. Lewis, M. Holcik, M. Gorospe (2008). " RNA-binding proteins HuR and PTB promote the translation of hypoxia-inducible factor 1alpha." Mol. Cell. Biol. (1): 93-107

Garneau, N. L., J. Wilusz and C. J. Wilusz (2007). "The highways and byways of mRNA decay." Nat Rev Mol Cell Biol**8** (2): 113-126.

Gavin, A. C. and S. Schorderet-Slatkine (1997). "Ribosomal S6 kinase p90rsk and mRNA cap-binding protein eIF4E phosphorylations correlate with MAP kinase activation during meiotic reinitiation of mouse oocytes." Mol Reprod Dev**46** (3): 383-391.

Gerald, D., E. Berra, Y. M. Frapart, D. A. Chan, A. J. Giaccia, D. Mansuy, J. Pouyssegur, M. Yaniv and F. Mechta-Grigoriou (2004). "JunD reduces tumor angiogenesis by protecting cells from oxidative stress." Cell**118** (6): 781-794.

Gerhardt, H. and C. Betsholtz (2005). "How do endothelial cells orientate?" EXS (94): 3-15.

Germain, S., C. Monnot, L. Muller and A. Eichmann (2010). "Hypoxia-driven angiogenesis: role of tip cells and extracellular matrix scaffolding." Curr Opin Hematol**17** (3): 245-251.

Gill, G. (2001). "Regulation of the initiation of eukaryotic transcription." Essays Biochem**37**: 33-43.

Gingras, A. C., Y. Svitkin, G. J. Belsham, A. Pause and N. Sonenberg (1996). "Activation of the translational suppressor 4E-BP1 following infection with encephalomyocarditis virus and poliovirus." Proc Natl Acad Sci U S A**93** (11): 5578-5583.

Giraud, S., A. Greco, M. Brink, J. J. Diaz and P. Delafontaine (2001). "Translation initiation of the insulin-like growth factor I receptor mRNA is mediated by an internal ribosome entry site." J Biol Chem**276** (8): 5668-5675.

Gonzalez-Herrera, I. G., L. Prado-Lourenco, F. Pileur, C. Conte, A. Morin, F. Cabon, H. Prats, S. Vagner, F. Bayard, S. Audigier and A. C. Prats (2006). "Testosterone regulates FGF-2 expression during testis maturation by an IRES-dependent translational mechanism." FASEB J**20** (3): 476-478.

Gordan, J. D., C. B. Thompson and M. C. Simon (2007). "HIF and c-Myc: sibling rivals for control of cancer cell metabolism and proliferation." Cancer Cell**12** (2): 108-113.

Griseri, P. and G. Pages (2014). "Regulation of the mRNA half-life in breast cancer." World J Clin Oncol**5** (3): 323-334.

Gygi, S. P., Y. Rochon, B. R. Franza and R. Aebersold (1999). "Correlation between protein and mRNA abundance in yeast." Mol Cell Biol**19** (3): 1720-1730.

Haiko, P., T. Makinen, S. Keskitalo, J. Taipale, M. J. Karkkainen, M. E. Baldwin, S. A. Stacker, M. G. Achen and K. Alitalo (2008). "Deletion of vascular endothelial growth factor C (VEGF-C) and VEGF-D is not equivalent to VEGF receptor 3 deletion in mouse embryos." Mol Cell Biol**28** (15): 4843-4850.

Hashimoto, T., L. Chen, H. Kimura, A. Endler, H. Koyama, T. Miyata, F. Shibasaki and T. Watanabe (2016). "Silencing of eIF3e promotes blood perfusion recovery after limb ischemia through stabilization of hypoxia-inducible factor 2alpha activity." J Vasc Surg**64** (1): 219-226 e213.

Heim, C., W. Bernhardt, S. Jalilova, Z. Wang, B. Motsch, M. Ramsperger-Gleixner, N. Burzlaff, M. Weyand, K. U. Eckardt and S. M. Ensminger (2016). "Prolyl-hydroxylase inhibitor activating hypoxia-inducible transcription factors reduce levels of transplant arteriosclerosis in a murine aortic allograft model." Interact Cardiovasc Thorac Surg**22** (5): 561-570.

Hinnebusch, A. G. (1997). "Translational regulation of yeast GCN4. A window on factors that control initiator-trna binding to the ribosome." J Biol Chem**272** (35): 21661-21664.

Hirose, Y., R. Tacke and J. L. Manley (1999). "Phosphorylated RNA polymerase II stimulates pre-mRNA splicing." Genes Dev**13** (10): 1234-1239.

Holcik, M., C. Lefebvre, C. Yeh, T. Chow and R. G. Korneluk (1999). "A new internal-ribosome-entry-site motif potentiates XIAP-mediated cytoprotection." Nat Cell Biol**1** (3): 190-192.

Holcik, M. and N. Sonenberg (2005). "Translational control in stress and apoptosis." Nat Rev Mol Cell Biol**6** (4): 318-327.

Hornstein, E., H. Harel, G. Levy and O. Meyuhas (1999). "Overexpression of poly (A)-binding protein down-regulates the translation or the abundance of its own mRNA." FEBS Lett**457** (2): 209-213.

Hovhannisyan, R. H., R. P. Carstens (2007). " Heterogeneous ribonucleoprotein m is a splicing regulatory protein that can enhance or silence splicing of alternatively spliced exons." J Bio Chem**282** (50): 36265-74

Hsin, J. P. and J. L. Manley (2012). "The RNA polymerase II CTD coordinates transcription and RNA processing." Genes Dev**26** (19): 2119-2137.

Hsu, Y. C., W. C. Liao, C. Y. Kao and I. M. Chiu (2010). "Regulation of FGF1 gene promoter through transcription factor RFX1." J Biol Chem**285** (18): 13885-13895.

Htun, P., W. D. Ito, I. E. Hoefer, J. Schaper and W. Schaper (1998). "Intramyocardial infusion of FGF-1 mimics ischemic preconditioning in pig myocardium." J Mol Cell Cardiol**30** (4): 867-877.

Hu, C., S. Pang, X. Kong, M. Velleca and J. C. Lawrence, Jr. (1994). "Molecular cloning and tissue distribution of PHAS-I, an intracellular target for insulin and growth factors." Proc Natl Acad Sci U S A**91** (9): 3730-3734.

Huez, I., L. Creancier, S. Audigier, M. C. Gensac, A. C. Prats and H. Prats (1998). "Two independent internal ribosome entry sites are involved in translation initiation of vascular endothelial growth factor mRNA." Mol Cell Biol**18** (11): 6178-6190.

Hussey, G. S., A. Chaudhury, A. E. Dawson, D. J. Lindner, C. R. Knudsen, M. C. Wilce, W. C. Merrick and P. H. Howe (2011). "Identification of an mRNP complex regulating tumorigenesis at the translational elongation step." Mol Cell**41** (4): 419-431.

Ichise, T., N. Yoshida and H. Ichise (2010). "H-, N- and Kras cooperatively regulate lymphatic vessel growth by modulating VEGFR3 expression in lymphatic endothelial cells in mice." Development**137** (6): 1003-1013.

Isner, J. M., A. Pieczek, R. Schainfeld, R. Blair, L. Haley, T. Asahara, K. Rosenfield, S. Razvi, K. Walsh and J. F. Symes (1996). "Clinical evidence of angiogenesis after arterial gene transfer of phVEGF165 in patient with ischaemic limb." Lancet**348** (9024): 370-374.

Immamura, K., N. Imamachi,G. Akizuki, M. Kumakura, A. Kawaguchi, K. Nagata, A. Kato, Y. Kawaguchi, H. Sato, M. Yoneda, C. Kai, T. Yada, Y. Suzuki, T. Yamada, T. Ozawa, K. Kaneki, T. Inoue, M. Kobayashi, T. Kodama, Y. Wada, K. Sekimizu, N. Akimitsu (2014). "Long non-coding RNA NEAT1-dependent SFPQ relocation from promoter region to paraspeckle mediates IL8 expression upon immune stimuli." Mol. Cell**53** (3): 393-406.

Jackson, A., S. Friedman, X. Zhan, K. A. Engleka, R. Forough and T. Maciag (1992). "Heat shock induces the release of fibroblast growth factor 1 from NIH 3T3 cells." Proc Natl Acad Sci U S A**89** (22): 10691-10695.

Jackson, R. J. (1988). "RNA translation. Picornaviruses break the rules." Nature**334** (6180): 292-293.

Jang, S. K., H. G. Krausslich, M. J. Nicklin, G. M. Duke, A. C. Palmenberg and E. Wimmer (1988). "A segment of the 5' nontranslated region of encephalomyocarditis virus RNA directs internal entry of ribosomes during in vitro translation." J Virol**62** (8): 2636-2643.

Jazwa, A., M. Tomczyk, H. M. Taha, E. Hytonen, M. Stoszko, L. Zentilin, M. Giacca, S. Yla-Herttuala, C. Emanueli, A. Jozkowicz and J. Dulak (2013). "Arteriogenic therapy based on simultaneous delivery of VEGF-A and FGF4 genes improves the recovery from acute limb ischemia." Vasc Cell**5**: 13.

Jego, G., A. Hazoume, R. Seigneuric and C. Garrido (2013). "Targeting heat shock proteins in cancer." Cancer Lett**332** (2): 275-285.

Jewell, U. R., I. Kvietikova, A. Scheid, C. Bauer, R. H. Wenger and M. Gassmann (2001). "Induction of HIF-1alpha in response to hypoxia is instantaneous." FASEB J**15** (7): 1312-1314.

Jiang, Y., A. Dai, Q. Li and R. Hu (2007). "Hypoxia induces transforming growth factor-beta1 gene expression in the pulmonary artery of rats via hypoxia-inducible factor-1alpha." Acta Biochim Biophys Sin (Shanghai)**39** (1): 73-80.

Johannes, G., M. S. Carter, M. B. Eisen, P. O. Brown and P. Sarnow (1999). "Identification of eukaryotic mRNAs that are translated at reduced cap

binding complex eIF4F concentrations using a cDNA microarray." Proc Natl Acad Sci U S A**96** (23): 13118-13123.

Jopling, C. L., K. A. Spriggs, S. A. Mitchell, M. Stoneley and A. E. Willis (2004). "L-Myc protein synthesis is initiated by internal ribosome entry." RNA**10** (2): 287-298.

Joshi, B., A. Cameron and R. Jagus (2004). "Characterization of mammalian eIF4E-family members." Eur J Biochem**271** (11): 2189-2203.

Joshi-Barve, S., W. Rychlik and R. E. Rhoads (1990). "Alteration of the major phosphorylation site of eukaryotic protein synthesis initiation factor 4E prevents its association with the 48 S initiation complex." J Biol Chem**265** (5): 2979-2983.

Kahvejian, A., G. Roy and N. Sonenberg (2001). "The mRNA closed-loop model: the function of PABP and PABP-interacting proteins in mRNA translation." Cold Spring Harb Symp Quant Biol**66**: 293-300.

Karaa, Z. S., J. S. Iacovoni, A. Bastide, E. Lacazette, C. Touriol and H. Prats (2009). "The VEGF IRESes are differentially susceptible to translation inhibition by miR-16." RNA**15** (2): 249-254.

Karkkainen, M. J., P. Haiko, K. Sainio, J. Partanen, J. Taipale, T. V. Petrova, M. Jeltsch, D. G. Jackson, M. Talikka, H. Rauvala, C. Betsholtz and K. Alitalo (2004). "Vascular endothelial growth factor C is required for sprouting of the first lymphatic vessels from embryonic veins." Nat Immunol**5** (1): 74-80.

Karpanen, T. and K. Alitalo (2001). "Lymphatic vessels as targets of tumor therapy?" J Exp Med**194** (6): F37-42.

Kieft, J. S. (2008). "Viral IRES RNA structures and ribosome interactions." Trends Biochem Sci**33** (6): 274-283.

Kieft, J. S. (2009). "Comparing the three-dimensional structures of Dicistroviridae IGR IRES RNAs with other viral RNA structures." Virus Res**139** (2): 148-156.

Kim, Y. K. and S. K. Jang (2002). "Continuous heat shock enhances translational initiation directed by internal ribosomal entry site." Biochem Biophys Res Commun**297** (2): 224-231.

Kimball, S. R., J. R. Fabian, G. D. Pavitt, A. G. Hinnebusch and L. S. Jefferson (1998). "Regulation of guanine nucleotide exchange through

phosphorylation of eukaryotic initiation factor eIF2alpha. Role of the alpha- and delta-subunits of eiF2b." J Biol Chem**273** (21): 12841-12845.

King, H. A., L. C. Cobbold and A. E. Willis (2010). "The role of IRES trans-acting factors in regulating translation initiation." Biochem Soc Trans**38** (6): 1581-1586.

Koromilas, A. E., A. Lazaris-Karatzas and N. Sonenberg (1992). "mRNAs containing extensive secondary structure in their 5' non-coding region translate efficiently in cells overexpressing initiation factor eIF-4E." EMBO J**11** (11): 4153-4158.

Kozak, M. (1987). "Effects of intercistronic length on the efficiency of reinitiation by eucaryotic ribosomes." Mol Cell Biol**7** (10): 3438-3445.

Kroon, M. E., P. Koolwijk, B. van der Vecht and V. W. van Hinsbergh (2000). "Urokinase receptor expression on human microvascular endothelial cells is increased by hypoxia: implications for capillary-like tube formation in a fibrin matrix." Blood**96** (8): 2775-2783.

Kupatt, C., R. Hinkel, A. Pfosser, C. El-Aouni, A. Wuchrer, A. Fritz, F. Globisch, M. Thormann, J. Horstkotte, C. Lebherz, E. Thein, A. Banfi and P. Boekstegers (2010). "Cotransfection of vascular endothelial growth factor-A and platelet-derived growth factor-B via recombinant adeno-associated virus resolves chronic ischemic malperfusion role of vessel maturation." J Am Coll Cardiol**56** (5): 414-422.

Kwek, K. Y., S. Murphy, A. Furger, B. Thomas, W. O'Gorman, H. Kimura, N. J. Proudfoot and A. Akoulitchev (2002). "U1 snRNA associates with TFIIH and regulates transcriptional initiation." Nat Struct Biol**9** (11): 800-805.

LaGrandeur, T. E. and R. Parker (1996). "mRNA decapping activities and their biological roles." Biochimie**78** (11-12): 1049-1055.

Lagrange, T., A. N. Kapanidis, H. Tang, D. Reinberg and R. H. Ebright (1998). "New core promoter element in RNA polymerase II-dependent transcription: sequence-specific DNA binding by transcription factor IIB." Genes Dev**12** (1): 34-44.

Lang, K. J., A. Kappel and G. J. Goodall (2002). "Hypoxia-inducible factor-1alpha mRNA contains an internal ribosome entry site that allows efficient translation during normoxia and hypoxia." Mol Biol Cell**13** (5): 1792-1801.

Lanneau, D., M. Brunet, E. Frisan, E. Solary, M. Fontenay and C. Garrido (2008). "Heat shock proteins: essential proteins for apoptosis regulation." J Cell Mol Med**12** (3): 743-761.

Layman, H., M. Sacasa, A. E. Murphy, A. M. Murphy, S. M. Pham and F. M. Andreopoulos (2009). "Co-delivery of FGF-2 and G-CSF from gelatin-based hydrogels as angiogenic therapy in a murine critical limb ischemic model." Acta Biomater**5** (1): 230-239.

Le Quesne, J. P., M. Stoneley, G. A. Fraser and A. E. Willis (2001). "Derivation of a structural model for the c-myc IRES." J Mol Biol**310** (1): 111-126.

Lee, A. H., N. N. Iwakoshi and L. H. Glimcher (2003). "XBP-1 regulates a subset of endoplasmic reticulum resident chaperone genes in the unfolded protein response." Mol Cell Biol**23** (21): 7448-7459.

Lee, J. S., J. M. Kim, K. L. Kim, H. S. Jang, I. S. Shin, E. S. Jeon, W. Suh, J. Byun and D. K. Kim (2007). "Combined administration of naked DNA vectors encoding VEGF and bFGF enhances tissue perfusion and arteriogenesis in ischemic hindlimb." Biochem Biophys Res Commun**360** (4): 752-758.

Levy, N. S., S. Chung, H. Furneaux and A. P. Levy (1998). "Hypoxic stabilization of vascular endothelial growth factor mRNA by the RNA-binding protein HuR." J Biol Chem**273** (11): 6417-6423.

Liu, Y., S. R. Cox, T. Morita and S. Kourembanas (1995). "Hypoxia regulates vascular endothelial growth factor gene expression in endothelial cells. Identification of a 5' enhancer." Circ Res**77** (3): 638-643.

Long, J. C. and J. F. Caceres (2009). "The SR protein family of splicing factors: master regulators of gene expression." Biochem J**417** (1): 15-27.

Lu, P. D., C. Jousse, S. J. Marciniak, Y. Zhang, I. Novoa, D. Scheuner, R. J. Kaufman, D. Ron and H. P. Harding (2004). "Cytoprotection by pre-emptive conditional phosphorylation of translation initiation factor 2." EMBO J**23** (1): 169-179.

Luo, Z., M. Diaco, T. Murohara, N. Ferrara, J. M. Isner and J. F. Symes (1997). "Vascular endothelial growth factor attenuates myocardial ischemia-reperfusion injury." Ann Thorac Surg**64** (4): 993-998.

M. J. Clemens (1996). "Protein kinases that phosphorylate eIF2 and eIF2B, and their role in eukaryotic cell translational control." In Translational Control,

edited by J. W. B. Hershey, M. B. Mathews and N. Sonenberg. Cold Spring Harbor Laboratory Press, Cold Spring Harbor, NY.: pp. 139–172.

Macejak, D. G. and P. Sarnow (1991). "Internal initiation of translation mediated by the 5' leader of a cellular mRNA." Nature**353** (6339): 90-94.

Makinen, T., T. Veikkola, S. Mustjoki, T. Karpanen, B. Catimel, E. C. Nice, L. Wise, A. Mercer, H. Kowalski, D. Kerjaschki, S. A. Stacker, M. G. Achen and K. Alitalo (2001). "Isolated lymphatic endothelial cells transduce growth, survival and migratory signals via the VEGF-C/D receptor VEGFR-3." EMBO J**20** (17): 4762-4773.

Marcel, V., S. E. Ghayad, S. Belin, G. Therizols, A-P. More, E. Solano-Gonzalez, J. A Vendrell, S. Hacot, H. C. Mertani, M. A. Albaret, J-C Bourdon, L. Jordan, A. Thompson, Y. Tafer, R. Cong, P. Bouvet, J-C. Saurin, F. Catez, A-C Prats, A. Puisieux, J-J Diaz (2013). "p53 acts as a safeguard of translational control by regulating fibrillarin and rRNA methylation in cancer." Cancer Cell **24** (3): 318-330.

Marko , M., M. Leichter , M.Patrinou-Georgoula, A. Guilis (2009). " hnRNP M interacts with PSF and p54^{nrb} and co-localizes within defined nuclear structures." Exp Cell Res**316** (3): 390-400.

Martineau, Y., C. Le Bec, L. Monbrun, V. Allo, I. M. Chiu, O. Danos, H. Moine, H. Prats and A. C. Prats (2004). "Internal ribosome entry site structural motifs conserved among mammalian fibroblast growth factor 1 alternatively spliced mRNAs." Mol Cell Biol**24** (17): 7622-7635.

Martinez-Sanchez, G. and A. Giuliani (2007). "Cellular redox status regulates hypoxia inducible factor-1 activity. Role in tumour development." J Exp Clin Cancer Res**26** (1): 39-50.

Masson, N. and P. J. Ratcliffe (2014). "Hypoxia signaling pathways in cancer metabolism: the importance of co-selecting interconnected physiological pathways." Cancer Metab**2** (1): 3.

Mathis, D. J. and P. Chambon (1981). "The SV40 early region TATA box is required for accurate in vitro initiation of transcription." Nature**290** (5804): 310-315.

Mathison, M., V. P. Singh, R. P. Gersch, M. O. Ramirez, A. Cooney, S. M. Kaminsky, M. J. Chiuchiolo, A. Nasser, J. Yang, R. G. Crystal and T. K. Rosengart (2014). ""Triplet" polycistronic vectors encoding Gata4, Mef2c, and Tbx5 enhances postinfarct ventricular functional improvement compared with singlet vectors." J Thorac Cardiovasc Surg**148** (4): 1656-1664 e1652.

Matsunaga, H. and H. Ueda (2006). "Evidence for serum-deprivation-induced co-release of FGF-1 and S100A13 from astrocytes." Neurochem Int**49** (3): 294-303.

McAvoy, J. W., C. G. Chamberlain, R. U. de Iongh, N. A. Richardson and F. J. Lovicu (1991). "The role of fibroblast growth factor in eye lens development." Ann N Y Acad Sci**638**: 256-274.

McCracken, S., N. Fong, K. Yankulov, S. Ballantyne, G. Pan, J. Greenblatt, S. D. Patterson, M. Wickens and D. L. Bentley (1997). "The C-terminal domain of RNA polymerase II couples mRNA processing to transcription." Nature**385** (6614): 357-361.

Meadows, K. N., P. Bryant and K. Pumiglia (2001). "Vascular endothelial growth factor induction of the angiogenic phenotype requires Ras activation." J Biol Chem**276** (52): 49289-49298.

Meng, Z., P. H. King, L. B.Nabors, N. L. Jackson, C. Y. Chen, P. D. Emanuel, S. W. Blume (2005). "The ELAV RNA-stability factor HuR binds the 5'-untranslated region of the human IGF-IR transcript and differentially represses cap-dependent and IRES-mediated translation." Nucleic Acids Res. **33** (9): 2962-79.

Merrick, W. C. (1992). "Mechanism and regulation of eukaryotic protein synthesis." Microbiol Rev**56** (2): 291-315.

Mihailescu, R. (2015). "Gene expression regulation: lessons from noncoding RNAs." RNA**21** (4): 695-696.

Milanini, J., F. Vinals, J. Pouyssegur and G. Pages (1998). "p42/p44 MAP kinase module plays a key role in the transcriptional regulation of the vascular endothelial growth factor gene in fibroblasts." J Biol Chem**273** (29): 18165-18172.

Miller, M. A. and W. M. Olivas (2011). "Roles of Puf proteins in mRNA degradation and translation." Wiley Interdiscip Rev RNA**2** (4): 471-492.

Min, Y., S. Ghose, K. Boelte, J. Li, L. Yang and P. C. Lin (2011). "C/EBP-delta regulates VEGF-C autocrine signaling in lymphangiogenesis and metastasis of lung cancer through HIF-1alpha." Oncogene**30** (49): 4901-4909.

Minet, E., G. Michel, D. Mottet, J. P. Piret, A. Barbieux, M. Raes and C. Michiels (2001). "c-JUN gene induction and AP-1 activity is regulated by a JNK-dependent pathway in hypoxic HepG2 cells." Exp Cell Res**265** (1): 114-124.

Ming, J., Q. Zhang, X. Qiu and E. Wang (2009). "Interleukin 7/interleukin 7 receptor induce c-Fos/c-Jun-dependent vascular endothelial growth factor-D up-regulation: a mechanism of lymphangiogenesis in lung cancer." Eur J Cancer**45** (5): 866-873.

Mitchell, S. A., E. C. Brown, M. J. Coldwell, R. J. Jackson and A. E. Willis (2001). "Protein factor requirements of the Apaf-1 internal ribosome entry segment: roles of polypyrimidine tract binding protein and upstream of N-ras." Mol Cell Biol**21** (10): 3364-3374.

Mitchell, S. A., K. A. Spriggs, M. J. Coldwell, R. J. Jackson and A. E. Willis (2003). "The Apaf-1 internal ribosome entry segment attains the correct structural conformation for function via interactions with PTB and unr." Mol Cell**11** (3): 757-771.

Miyagi, Y., A. Sugiyama, A. Asai, T. Okazaki, Y. Kuchino and S. J. Kerr (1995). "Elevated levels of eukaryotic translation initiation factor eIF-4E, mRNA in a broad spectrum of transformed cell lines." Cancer Lett**91** (2): 247-252.

Miyashita, H., T. Watanabe, H. Hayashi, Y. Suzuki, T. Nakamura, S. Ito, M. Ono, Y. Hoshikawa, T. Kondo, Y. Sato (2012). " Angiogenesis inhibitor casohibin-1 enhances stress resistance of endothelial cells via induction of SOD2 and SIRT1." PloS One 7 (10): e46459

Moore, D. F., H. Li, N. Jeffries, V. Wright, R. A. Cooper, Jr., A. Elkahloun, M. P. Gelderman, E. Zudaire, G. Blevins, H. Yu, E. Goldin and A. E. Baird (2005). "Using peripheral blood mononuclear cells to determine a gene expression profile of acute ischemic stroke: a pilot investigation." Circulation**111** (2): 212-221.

Morfoisse, F., A. Kuchnio, C. Frainay, A. Gomez-Brouchet, M. B. Delisle, S. Marzi, A. C. Helfer, F. Hantelys, F. Pujol, J. Guillermet-Guibert, C. Bousquet, M. Dewerchin, S. Pyronnet, A. C. Prats, P. Carmeliet and B. Garmy-Susini (2014). "Hypoxia induces VEGF-C expression in metastatic tumor cells via a HIF-1alpha-independent translation-mediated mechanism." Cell Rep**6** (1): 155-167.

Morita, M., L. W. Ler, M. R. Fabian, N. Siddiqui, M. Mullin, V. C. Henderson, T. Alain, B. D. Fonseca, G. Karashchuk, C. F. Bennett, T. Kabuta, S. Higashi, O. Larsson, I. Topisirovic, R. J. Smith, A. C. Gingras and N. Sonenberg (2012). "A novel 4EHP-GIGYF2 translational repressor complex is essential for mammalian development." Mol Cell Biol**32** (17): 3585-3593.

Morley, S. J. (1997). "Intracellular signalling pathways regulating initiation factor eIF4E phosphorylation during the activation of cell growth." Biochem Soc Trans**25** (2): 503-509.

Morley, S. J. and V. M. Pain (1995). "Hormone-induced meiotic maturation in Xenopus oocytes occurs independently of p70s6k activation and is associated with enhanced initiation factor (eIF)-4F phosphorylation and complex formation." J Cell Sci**108 (Pt 4)**: 1751-1760.

Mouta Carreira, C., M. Landriscina, S. Bellum, I. Prudovsky and T. Maciag (2001). "The comparative release of FGF1 by hypoxia and temperature stress." Growth Factors**18** (4): 277-285.

Mouta Carreira, C., T. M. LaVallee, F. Tarantini, A. Jackson, J. T. Lathrop, B. Hampton, W. H. Burgess and T. Maciag (1998). "S100A13 is involved in the regulation of fibroblast growth factor-1 and p40 synaptotagmin-1 release in vitro." J Biol Chem**273** (35): 22224-22231.

Mudo, G., A. Bonomo, V. Di Liberto, M. Frinchi, K. Fuxe and N. Belluardo (2009). "The FGF-2/FGFRs neurotrophic system promotes neurogenesis in the adult brain." J Neural Transm (Vienna)**116** (8): 995-1005.

Myers, R. L., M. Chedid, S. R. Tronick and I. M. Chiu (1995). "Different fibroblast growth factor 1 (FGF-1) transcripts in neural tissues, glioblastomas and kidney carcinoma cell lines." Oncogene**11** (4): 785-789.

Myers, R. L., R. A. Payson, M. A. Chotani, L. L. Deaven and I. M. Chiu (1993). "Gene structure and differential expression of acidic fibroblast growth factor mRNA: identification and distribution of four different transcripts." Oncogene**8** (2): 341-349.

Nagy, J. A., E. Vasile, D. Feng, C. Sundberg, L. F. Brown, E. J. Manseau, A. M. Dvorak and H. F. Dvorak (2002). "VEGF-A induces angiogenesis, arteriogenesis, lymphangiogenesis, and vascular malformations." Cold Spring Harb Symp Quant Biol**67**: 227-237.

Nakagawa, T., H. Zhu, N. Morishima, E. Li, J. Xu, B. A. Yankner and J. Yuan (2000). "Caspase-12 mediates endoplasmic-reticulum-specific apoptosis and cytotoxicity by amyloid-beta." Nature**403** (6765): 98-103.

Nanbru, C., I. Lafon, S. Audigier, M. C. Gensac, S. Vagner, G. Huez and A. C. Prats (1997). "Alternative translation of the proto-oncogene c-myc by an internal ribosome entry site." J Biol Chem**272** (51): 32061-32066.

Nikol, S., I. Baumgartner, E. Van Belle, C. Diehm, A. Visona, M. C. Capogrossi, N. Ferreira-Maldent, A. Gallino, M. G. Wyatt, L. D. Wijesinghe, M. Fusari, D. Stephan, J. Emmerich, G. Pompilio, F. Vermassen, E. Pham, V. Grek, M. Coleman, F. Meyer and T. investigators (2008). "Therapeutic angiogenesis with intramuscular NV1FGF improves amputation-free survival in patients with critical limb ischemia." Mol Ther**16** (5): 972-978.

Oh, S. K. and P. Sarnow (1993). "Gene regulation: translational initiation by internal ribosome binding." Curr Opin Genet Dev**3** (2): 295-300.

Okada, T., H. Yoshida, R. Akazawa, M. Negishi and K. Mori (2002). "Distinct roles of activating transcription factor 6 (ATF6) and double-stranded RNA-activated protein kinase-like endoplasmic reticulum kinase (PERK) in transcription during the mammalian unfolded protein response." Biochem J**366** (Pt 2): 585-594.

Okamoto, T., S. Yamamoto, Y. Watanabe, T. Ohta, F. Hanaoka, R. G. Roeder and Y. Ohkuma (1998). "Analysis of the role of TFIIE in transcriptional regulation through structure-function studies of the TFIIEbeta subunit." J Biol Chem**273** (31): 19866-19876.

Orphanides, G. and D. Reinberg (2002). "A unified theory of gene expression." Cell**108** (4): 439-451.

Pages, G. and J. Pouyssegur (2005). "Transcriptional regulation of the Vascular Endothelial Growth Factor gene--a concert of activating factors." Cardiovasc Res**65** (3): 564-573.

Palmen, M., M. J. Daemen, L. J. De Windt, J. Willems, W. R. Dassen, S. Heeneman, R. Zimmermann, M. Van Bilsen and P. A. Doevendans (2004). "Fibroblast growth factor-1 improves cardiac functional recovery and enhances cell survival after ischemia and reperfusion: a fibroblast growth factor receptor, protein kinase C, and tyrosine kinase-dependent mechanism." J Am Coll Cardiol**44** (5): 1113-1123.

Pandit, S., D. Wang, X. D. Fu (2008). "Functional integration of transcriptional and RNA processing machineries." Curr Opin Cell Biol (3): 260-265.

Park, Y. S., G. Kim, Y. M. Jin, J. Y. Lee, J. W. Shin and I. Jo (2016). "Expression of angiopoietin-1 in hypoxic pericytes: Regulation by hypoxia-inducible factor-2alpha and participation in endothelial cell migration and tube formation." Biochem Biophys Res Commun**469** (2): 263-269.

Passmore, L. A., T. M. Schmeing, D. Maag, D. J. Applefield, M. G. Acker, M. A. Algire, J. R. Lorsch and V. Ramakrishnan (2007). "The eukaryotic translation initiation factors eIF1 and eIF1A induce an open conformation of the 40S ribosome." Mol Cell**26** (1): 41-50.

Payson, R. A., M. A. Chotani and I. M. Chiu (1998). "Regulation of a promoter of the fibroblast growth factor 1 gene in prostate and breast cancer cells." J Steroid Biochem Mol Biol**66** (3): 93-103.

Pelletier, J. and N. Sonenberg (1987). "The involvement of mRNA secondary structure in protein synthesis." Biochem Cell Biol**65** (6): 576-581.

Pelletier, J. and N. Sonenberg (1988). "Internal initiation of translation of eukaryotic mRNA directed by a sequence derived from poliovirus RNA." Nature**334** (6180): 320-325.

Pestova, T. V., C. U. Hellen and I. N. Shatsky (1996). "Canonical eukaryotic initiation factors determine initiation of translation by internal ribosomal entry." Mol Cell Biol**16** (12): 6859-6869.

Philippe, C., A. Dubrac, C. Quelen, A. Desquesnes, L. Van Den Berghe, C. Segura, T. Filleron, S. Pyronnet, H. Prats, P. Brousset and C. Touriol (2016). "PERK mediates the IRES-dependent translational activation of mRNAs encoding angiogenic growth factors after ischemic stress." Sci Signal**9** (426): ra44.

Pickering, B. M., S. A. Mitchell, K. A. Spriggs, M. Stoneley and A. E. Willis (2004). "Bag-1 internal ribosome entry segment activity is promoted by structural changes mediated by poly (rC) binding protein 1 and recruitment of polypyrimidine tract binding protein 1." Mol Cell Biol**24** (12): 5595-5605.

Pierre Gourdy, F. o. B., Jean-François Arnal (2005). "Oestrogènes et risque cardiovasculaire." Sang Thrombose Vaisseaux 2005**17** (3): 155-161.

Pollenz, R. S., C. A. Sattler and A. Poland (1994). "The aryl hydrocarbon receptor and aryl hydrocarbon receptor nuclear translocator protein show distinct subcellular localizations in Hepa 1c1c7 cells by immunofluorescence microscopy." Mol Pharmacol**45** (3): 428-438.

Poulin, F., A. C. Gingras, H. Olsen, S. Chevalier and N. Sonenberg (1998). "4E-BP3, a new member of the eukaryotic initiation factor 4E-binding protein family." J Biol Chem**273** (22): 14002-14007.

Prats, A. C., S. Vagner, H. Prats and F. Amalric (1992). "cis-acting elements involved in the alternative translation initiation process of human basic fibroblast growth factor mRNA." Mol Cell Biol**12** (10): 4796-4805.

Prats, H., M. Kaghad, A. C. Prats, M. Klagsbrun, J. M. Lelias, P. Liauzun, P. Chalon, J. P. Tauber, F. Amalric, J. A. Smith (1989). "High molecular mass forms of basic fibroblast growth factor are initiated by alternative CUG codons." Proc Natl Acad Sci U S A**86** (6): 1836-1840.

Proudfoot, N. J., A. Furger and M. J. Dye (2002). "Integrating mRNA processing with transcription." Cell**108** (4): 501-512.

Pyronnet, S., H. Imataka, A. C. Gingras, R. Fukunaga, T. Hunter and N. Sonenberg (1999). "Human eukaryotic translation initiation factor 4G (eIF4G) recruits mnk1 to phosphorylate eIF4E." EMBO J**18** (1): 270-279.

Quarto, N., F. P. Finger and D. B. Rifkin (1991). "The NH2-terminal extension of high molecular weight bFGF is a nuclear targeting signal." J Cell Physiol**147** (2): 311-318.

Quarto, N., D. Talarico, R. Florkiewicz and D. B. Rifkin (1991). "Selective expression of high molecular weight basic fibroblast growth factor confers a unique phenotype to NIH 3T3 cells." Cell Regul**2** (9): 699-708.

Ray, P. S., R. Grover and S. Das (2006). "Two internal ribosome entry sites mediate the translation of p53 isoforms." EMBO Rep**7** (4): 404-410.

Rayssac, A., C. Neveu, M. Pucelle, L. Van den Berghe, L. Prado-Lourenco, J. F. Arnal, X. Chaufour and A. C. Prats (2009). "IRES-based vector coexpressing FGF2 and Cyr61 provides synergistic and safe therapeutics of lower limb ischemia." Mol Ther**17** (12): 2010-2019.

Renaud-Gabardos, E. Thèse de doctorat (Décémbre 2016).

Renaud-Gabardos, E., F. Hantelys, F. Morfoisse, X. Chaufour, B. Garmy-Susini and A. C. Prats (2015). "Internal ribosome entry site-based vectors for combined gene therapy." World J Exp Med**5** (1): 11-20.

Renko, M., N. Quarto, T. Morimoto and D. B. Rifkin (1990). "Nuclear and cytoplasmic localization of different basic fibroblast growth factor species." J Cell Physiol**144** (1): 108-114.

Rogers, G. W., Jr., N. J. Richter, W. F. Lima and W. C. Merrick (2001). "Modulation of the helicase activity of eIF4A by eIF4B, eIF4H, and eIF4F." J Biol Chem**276** (33): 30914-30922.

Romero-Ramirez, L., H. Cao, D. Nelson, E. Hammond, A. H. Lee, H. Yoshida, K. Mori, L. H. Glimcher, N. C. Denko, A. J. Giaccia, Q. T. Le and A. C. Koong (2004). "XBP1 is essential for survival under hypoxic conditions and is required for tumor growth." Cancer Res**64** (17): 5943-5947.

Rosonina, E., J. Y. Ip, J. A. Calarco, M. A. Bakowski, A. Emili, S. McCracken, P. Tucker, C. J. Ingles and B. J. Blencowe (2005). "Role for PSF in mediating transcriptional activator-dependent stimulation of pre-mRNA processing in vivo." Mol Cell Biol**25** (15): 6734-6746.

Rouault, T. and R. Klausner (1997). "Regulation of iron metabolism in eukaryotes." Curr Top Cell Regul**35**: 1-19.

Rowlands, A. G., K. S. Montine, E. C. Henshaw and R. Panniers (1988). "Physiological stresses inhibit guanine-nucleotide-exchange factor in Ehrlich cells." Eur J Biochem**175** (1): 93-99.

Rubanyi, G. M. (2013). "Mechanistic, technical, and clinical perspectives in therapeutic stimulation of coronary collateral development by angiogenic growth factors." Mol Ther**21** (4): 725-738.

Saed, G. M., K. L. Collins and M. P. Diamond (2002). "Transforming growth factors beta1, beta2 and beta3 and their receptors are differentially expressed in human peritoneal fibroblasts in response to hypoxia." Am J Reprod Immunol**48** (6): 387-393.

Salceda, S. and J. Caro (1997). "Hypoxia-inducible factor 1alpha (HIF-1alpha) protein is rapidly degraded by the ubiquitin-proteasome system under normoxic conditions. Its stabilization by hypoxia depends on redox-induced changes." J Biol Chem**272** (36): 22642-22647.

Sarnow, P. (2003). "Viral internal ribosome entry site elements: novel ribosome-RNA complexes and roles in viral pathogenesis." J Virol**77** (5): 2801-2806.

Schafer, G., C. Wissmann, J. Hertel, V. Lunyak and M. Hocker (2008). "Regulation of vascular endothelial growth factor D by orphan receptors hepatocyte nuclear factor-4 alpha and chicken ovalbumin upstream promoter transcription factors 1 and 2." Cancer Res**68** (2): 457-466.

Schwanhausser, B., D. Busse, N. Li, G. Dittmar, J. Schuchhardt, J. Wolf, W. Chen and M. Selbach (2011). "Global quantification of mammalian gene expression control." Nature**473** (7347): 337-342.

Schwartz, S. M. and L. Liaw (1993). "Growth control and morphogenesis in the development and pathology of arteries." J Cardiovasc Pharmacol**21 Suppl 1**: S31-49.

Seghezzi, G., S. Patel, C. J. Ren, A. Gualandris, G. Pintucci, E. S. Robbins, R. L. Shapiro, A. C. Galloway, D. B. Rifkin and P. Mignatti (1998). "Fibroblast growth factor-2 (FGF-2) induces vascular endothelial growth factor (VEGF) expression in the endothelial cells of forming capillaries: an autocrine mechanism contributing to angiogenesis." J Cell Biol**141** (7): 1659-1673.

Sella, O., G. Gerlitz, S. Y. Le and O. Elroy-Stein (1999). "Differentiation-induced internal translation of c-sis mRNA: analysis of the cis elements and their differentiation-linked binding to the hnRNP C protein." Mol Cell Biol**19** (8): 5429-5440.

Semenza, G. L., S. T. Koury, M. K. Nejfelt, J. D. Gearhart and S. E. Antonarakis (1991). "Cell-type-specific and hypoxia-inducible expression of the human erythropoietin gene in transgenic mice." Proc Natl Acad Sci U S A**88** (19): 8725-8729.

Sevin, M., F. Girodon, C. Garrido and A. de Thonel (2015). "HSP90 and HSP70: Implication in Inflammation Processes and Therapeutic Approaches for Myeloproliferative Neoplasms." Mediators Inflamm**2015**: 970242.

Shi, Y., D. C. Di Giammartino, D. Taylor, A. Sarkeshik, W. J. Rice, J. R. Yates, 3rd, J. Frank and J. L. Manley (2009). "Molecular architecture of the human pre-mRNA 3' processing complex." Mol Cell**33** (3): 365-376.

Shi, Y., Y. Yang, B. Hoang, C. Bardeleben, B. Holmes, J. Gera and A. Lichtenstein (2016). "Therapeutic potential of targeting IRES-dependent c-myc translation in multiple myeloma cells during ER stress." Oncogene**35** (8): 1015-1024.

Shimoda, L. A., M. Fallon, S. Pisarcik, J. Wang and G. L. Semenza (2006). "HIF-1 regulates hypoxic induction of NHE1 expression and alkalinization of intracellular pH in pulmonary arterial myocytes." Am J Physiol Lung Cell Mol Physiol**291** (5): L941-949.

Shin, J. T., S. R. Opalenik, J. N. Wehby, V. K. Mahesh, A. Jackson, F. Tarantini, T. Maciag and J. A. Thompson (1996). "Serum-starvation induces the extracellular appearance of FGF-1." Biochim Biophys Acta**1312** (1): 27-38.

Skobe, M., T. Hawighorst, D. G. Jackson, R. Prevo, L. Janes, P. Velasco, L. Riccardi, K. Alitalo, K. Claffey and M. Detmar (2001). "Induction of tumor lymphangiogenesis by VEGF-C promotes breast cancer metastasis." Nat Med**7** (2): 192-198.

Smih, F., F. Desmoulin, M. Berry, A. Turkieh, R. Harmancey, J. Iacovoni, C. Trouillet, C. Delmas, A. Pathak, O. Lairez, F. Koukoui, P. Massabuau, J. Ferrieres, M. Galinier and P. Rouet (2011). "Blood signature of pre-heart failure: a microarrays study." PLoS One**6** (6): e20414.

Sonenberg, N. (1996). In: Translational control. Cold Spring Harbor Laboratory Press**:** pp. 245–269.

Sonenberg, N. and A. C. Gingras (1998). "The mRNA 5' cap-binding protein eIF4E and control of cell growth." Curr Opin Cell Biol**10** (2): 268-275.

Sonenberg, N., M. A. Morgan, W. C. Merrick and A. J. Shatkin (1978). "A polypeptide in eukaryotic initiation factors that crosslinks specifically to the 5'-terminal cap in mRNA." Proc Natl Acad Sci U S A**75** (10): 4843-4847.

Sonenberg, N., K. M. Rupprecht, S. M. Hecht and A. J. Shatkin (1979). "Eukaryotic mRNA cap binding protein: purification by affinity chromatography on sepharose-coupled m7GDP." Proc Natl Acad Sci U S A**76** (9): 4345-4349.

Sonoda, H., H. Ohta, K. Watanabe, H. Yamashita, H. Kimura, Y. Sato (2006). "Multiple processing forms and their biological activities of a novel angiogenesis inhibitor." Biochem Biophys Res Commun**342** (2): 640-6

Sood, R., A. C. Porter, D. A. Olsen, D. R. Cavener and R. C. Wek (2000). "A mammalian homologue of GCN2 protein kinase important for translational control by phosphorylation of eukaryotic initiation factor-2alpha." Genetics**154** (2): 787-801.

Stein, I., A. Itin, P. Einat, R. Skaliter, Z. Grossman and E. Keshet (1998). "Translation of vascular endothelial growth factor mRNA by internal ribosome entry: implications for translation under hypoxia." Mol Cell Biol**18** (6): 3112-3119.

Sternfeld, M. D., J. E. Hendrickson, W. W. Keeble, J. T. Rosenbaum, J. E. Robertson, M. R. Pittelkow and G. D. Shipley (1988). "Differential expression of mRNA coding for heparin-binding growth factor type 2 in human cells." J Cell Physiol**136** (2): 297-304.

Stoneley, M., F. E. Paulin, J. P. Le Quesne, S. A. Chappell and A. E. Willis (1998). "C-Myc 5' untranslated region contains an internal ribosome entry segment." Oncogene**16** (3): 423-428.

Stoneley, M., T. Subkhankulova, J. P. Le Quesne, M. J. Coldwell, C. L. Jopling, G. J. Belsham and A. E. Willis (2000). "Analysis of the c-myc IRES; a potential role for cell-type specific trans-acting factors and the nuclear compartment." Nucleic Acids Res**28** (3): 687-694.

Stoneley, M. and A. E. Willis (2004). "Cellular internal ribosome entry segments: structures, trans-acting factors and regulation of gene expression." Oncogene**23** (18): 3200-3207.

Su, J. L., C. J. Yen, P. S. Chen, S. E. Chuang, C. C. Hong, I. H. Kuo, H. Y. Chen, M. C. Hung and M. L. Kuo (2007). "The role of the VEGF-C/VEGFR-3 axis in cancer progression." Br J Cancer**96** (4): 541-545.

Sullivan, R. and C. H. Graham (2007). "Hypoxia-driven selection of the metastatic phenotype." Cancer Metastasis Rev**26** (2): 319-331.

Tang, Y., E. Pacary, T. Freret, D. Divoux, E. Petit, P. Schumann-Bard and M. Bernaudin (2006). "Effect of hypoxic preconditioning on brain genomic response before and following ischemia in the adult mouse: identification of potential neuroprotective candidates for stroke." Neurobiol Dis**21** (1): 18-28.

Tanguay, R. M., Y. Wu and E. W. Khandjian (1993). "Tissue-specific expression of heat shock proteins of the mouse in the absence of stress." Dev Genet**14** (2): 112-118.

Teshima-Kondo, S., K. Kondo, L. Prado-Lourenco, I. G. Gonzalez-Herrera, K. Rokutan, F. Bayard, J. F. Arnal and A. C. Prats (2004). "Hyperglycemia upregulates translation of the fibroblast growth factor 2 mRNA in mouse aorta via internal ribosome entry site." FASEB J**18** (13): 1583-1585.

Thomas, M. C. and C. M. Chiang (2006). "The general transcription machinery and general cofactors." Crit Rev Biochem Mol Biol**41** (3): 105-178.

Tissieres, A., H. K. Mitchell and U. M. Tracy (1974). "Protein synthesis in salivary glands of Drosophila melanogaster: relation to chromosome puffs." J Mol Biol**84** (3): 389-398.

Touriol, C., A. Morillon, M. C. Gensac, H. Prats and A. C. Prats (1999). "Expression of human fibroblast growth factor 2 mRNA is post-transcriptionally controlled by a unique destabilizing element present in the 3'-

untranslated region between alternative polyadenylation sites." J Biol Chem**274** (30): 21402-21408.

Touriol, C., M. Roussigne, M. C. Gensac, H. Prats and A. C. Prats (2000). "Alternative translation initiation of human fibroblast growth factor 2 mRNA controlled by its 3'-untranslated region involves a Poly (A) switch and a translational enhancer." J Biol Chem**275** (25): 19361-19367.

Trcek, T., D. R. Larson, A. Moldon, C. C. Query and R. H. Singer (2011). "Single-molecule mRNA decay measurements reveal promoter- regulated mRNA stability in yeast." Cell**147** (7): 1484-1497.

Tsukiyama-Kohara, K., F. Poulin, M. Kohara, C. T. DeMaria, A. Cheng, Z. Wu, A. C. Gingras, A. Katsume, M. Elchebly, B. M. Spiegelman, M. E. Harper, M. L. Tremblay and N. Sonenberg (2001). "Adipose tissue reduction in mice lacking the translational inhibitor 4E-BP1." Nat Med**7** (10): 1128-1132.

Tsukiyama-Kohara, K., S. M. Vidal, A. C. Gingras, T. W. Glover, S. M. Hanash, H. Heng and N. Sonenberg (1996). "Tissue distribution, genomic structure, and chromosome mapping of mouse and human eukaryotic initiation factor 4E-binding proteins 1 and 2." Genomics**38** (3): 353-363.

Uniacke, J., C. E. Holterman, G. Lachance, A. Franovic, M. D. Jacob, M. R. Fabian, J. Payette, M. Holcik, A. Pause and S. Lee (2012). "An oxygen-regulated switch in the protein synthesis machinery." Nature**486** (7401): 126-129.

Uriel, S., E. M. Brey and H. P. Greisler (2006). "Sustained low levels of fibroblast growth factor-1 promote persistent microvascular network formation." Am J Surg**192** (5): 604-609.

Vagner, S., M. C. Gensac, A. Maret, F. Bayard, F. Amalric, H. Prats and A. C. Prats (1995). "Alternative translation of human fibroblast growth factor 2 mRNA occurs by internal entry of ribosomes." Mol Cell Biol**15** (1): 35-44.

Vagner, S., C. Touriol, B. Galy, S. Audigier, M. C. Gensac, F. Amalric, F. Bayard, H. Prats and A. C. Prats (1996). "Translation of CUG- but not AUG-initiated forms of human fibroblast growth factor 2 is activated in transformed and stressed cells." J Cell Biol**135** (5): 1391-1402.

Virmani, R., F. D. Kolodgie, A. P. Burke, A. Farb and S. M. Schwartz (2000). "Lessons from sudden coronary death: a comprehensive morphological classification scheme for atherosclerotic lesions." Arterioscler Thromb Vasc Biol**20** (5): 1262-1275.

Wang, X., M. Chen, J. Zhou and X. Zhang (2014). "HSP27, 70 and 90, anti-apoptotic proteins, in clinical cancer therapy (Review)." Int J Oncol**45** (1): 18-30.

Wang, X. and A. Schneider (2010). "HIF-2alpha-mediated activation of the epidermal growth factor receptor potentiates head and neck cancer cell migration in response to hypoxia." Carcinogenesis**31** (7): 1202-1210.

Watanabe, K., Y. Hasegawa, H. Yamashita, K. Shimizu, Y. Ding, M. Abe, H. Ohta, K. Imagawa, K. Hojo, H. Sonoda, Y. Sato (2004). " Vasohibin as an endothelium-derived negative feedback regulator of angiogenesis." J. Clin. Invest.**114** (7): 898-907.

Webb, T. E., A. Hughes, D. S. Smalley and K. A. Spriggs (2015). "An internal ribosome entry site in the 5' untranslated region of epidermal growth factor receptor allows hypoxic expression." Oncogenesis**4**: e134.

Werner, E. D., J. L. Brodsky and A. A. McCracken (1996). "Proteasome-dependent endoplasmic reticulum-associated protein degradation: an unconventional route to a familiar fate." Proc Natl Acad Sci U S A**93** (24): 13797-13801.

Wickner, S., M. R. Maurizi and S. Gottesman (1999). "Posttranslational quality control: folding, refolding, and degrading proteins." Science**286** (5446): 1888-1893.

Wu, C. (1995). "Heat shock transcription factors: structure and regulation." Annu Rev Cell Dev Biol**11**: 441-469.

Wuest, T. R. and D. J. Carr (2010). "VEGF-A expression by HSV-1-infected cells drives corneal lymphangiogenesis." J Exp Med**207** (1): 101-115.

Xu, Z., J. N. Dholakia and M. B. Hille (1993). "Maturation hormone induced an increase in the translational activity of starfish oocytes coincident with the phosphorylation of the mRNA cap binding protein, eIF-4E, and the activation of several kinases." Dev Genet**14** (6): 424-439.

Xue, S., S. Tian, K. Fujii, W. Kladwang, R. Das, M. Barna (2015). " RNA regulons in *Hox* 5′ UTRs confer ribosome specificity to gene regulation."Nature 517 (7532): 33-38

Ye, X., P. Fong, N. Iizuka, D. Choate and D. R. Cavener (1997). "Ultrabithorax and Antennapedia 5' untranslated regions promote developmentally regulated internal translation initiation." Mol Cell Biol**17** (3): 1714-1721.

Yeh, C.H., L.Y.Hung, C. Hsu, S.Y. Le, P. T. Lee, W.L. Liao, Y. T. Lin, W. C. Chang, J. T. Tseng (2008). " RNA-binding Protein HuR Interacts with Thrombomodulin 5′Untranslated Region and Represses Internal Ribosome Entry Site–mediated Translation under IL-1β Treatment." Mol Biol Cell**19** (9): 3812-3822.

Yin, Z., J. Haynie, X. Yang, B. Han, S. Kiatchoosakun, J. Restivo, S. Yuan, N. R. Prabhakar, K. Herrup, R. A. Conlon, B. D. Hoit, M. Watanabe and Y. C. Yang (2002). "The essential role of Cited2, a negative regulator for HIF-1alpha, in heart development and neurulation." Proc Natl Acad Sci U S A**99** (16): 10488-10493.

Yost, H. J. and S. Lindquist (1986). "RNA splicing is interrupted by heat shock and is rescued by heat shock protein synthesis." Cell**45** (2): 185-193.

Zachary, I. and G. Gliki (2001). "Signaling transduction mechanisms mediating biological actions of the vascular endothelial growth factor family." Cardiovasc Res**49** (3): 568-581.

Zeng, C. and S. M. Berget (2000). "Participation of the C-terminal domain of RNA polymerase II in exon definition during pre-mRNA splicing." Mol Cell Biol**20** (21): 8290-8301.

Zhang, C., K. Z. Wang, H. Qiang, Y. L. Tang, Q. Li, M. Li and X. Q. Dang (2010). "Angiopoiesis and bone regeneration via co-expression of the hVEGF and hBMP genes from an adeno-associated viral vector in vitro and in vivo." Acta Pharmacol Sin**31** (7): 821-830.

Zhang, K. and R. J. Kaufman (2004). "Signaling the unfolded protein response from the endoplasmic reticulum." J Biol Chem**279** (25): 25935-25938.

Zhang, X., O. A. Ibrahimi, S. K. Olsen, H. Umemori, M. Mohammadi and D. M. Ornitz (2006). "Receptor specificity of the fibroblast growth factor family. The complete mammalian FGF family." J Biol Chem**281** (23): 15694-15700.

Liste des figures

Figure 1 : Régulation de l'expression génique 11

Figure 2 : Initiation de la transcription 15

Figure 3 : Régulation de la transcription 16

Figure 4 : Epissage 18

Figure 5 : Illustration du couplage entre transcription et épissage 20

Figure 6 : Initiation de la traduction chez les eucaryotes 23

Figure 7 : Comparaison de la traduction dépendante de la coiffe et des 4 types d'IRES 27

Figure 8 : Activation de l'IRES Bag-1 par les ITAF PCBP1 et PTB 34

Figure 9 : Les principales étapes de la régulation de l'expression génique en réponse à des stimuli externes et internes 35

Figure 10: Schéma de la régulation de HIF par la concentration en oxygène 37

Figure 11 : Tumeur mammaire durant une inflammation 40

Figure 12 : Mécanisme de régulation de la traduction par 4E-BP 42

Figure 13 : Régulation de l'initiation de la traduction par phosphorylation d'eIF2α 43

Figure 14 : Illustration de la formation de l'atherosclérose 50

Figure 15 : Le concept du vecteur multicistronique basé sur les IRES 54

Annexe

Annexe

Cell Reports
Article

Hypoxia Induces VEGF-C Expression in Metastatic Tumor Cells via a HIF-1α-Independent Translation-Mediated Mechanism

Florent Morfoisse,[1,2] Anna Kuchnio,[3] Clement Frainay,[1,2] Anne Gomez-Brouchet,[1,2] Marie-Bernadette Delisle,[1,2] Stefano Marzi,[4] Anne-Catherine Helfer,[4] Fransky Hantelys,[5] Francoise Pujol,[5] Julie Guillermet-Guibert,[1,2] Corinne Bousquet,[1,2] Mieke Dewerchin,[3] Stephane Pyronnet,[1,2] Anne-Catherine Prats,[5,6] Peter Carmeliet,[3,6] and Barbara Garmy-Susini[1,2,*]

[1]Inserm, U1037, 31432 Toulouse, France
[2]Université de Toulouse, UPS, Cancer Research Center of Toulouse, Equipe Labellisee Ligue Contre le Cancer and Laboratoire d'Excellence Toulouse Cancer, 31432 Toulouse, France
[3]Vesalius Research Center, VIB, University of Leuven, 3000 Leuven, Belgium
[4]UPR 9002 CNRS-ARN, Université De Strasbourg, IBMC, 67084 Strasbourg, France
[5]Université de Toulouse, UPS, TRADGENE, EA4554, 31432 Toulouse, France
[6]These authors contributed equally to this work
*Correspondence: barbara.garmy-susini@inserm.fr
http://dx.doi.org/10.1016/j.celrep.2013.12.011

SUMMARY

Various tumors metastasize via lymph vessels and lymph nodes to distant organs. Even though tumors are hypoxic, the mechanisms of how hypoxia regulates lymphangiogenesis remain poorly characterized. Here, we show that hypoxia reduced vascular endothelial growth factor C (VEGF-C) transcription and cap-dependent translation via the upregulation of hypophosphorylated 4E-binding protein 1 (4E-BP1). However, initiation of VEGF-C translation was induced by hypoxia through an internal ribosome entry site (IRES)-dependent mechanism. IRES-dependent VEGF-C translation was independent of hypoxia-inducible factor 1α (HIF-1α) signaling. Notably, the VEGF-C IRES activity was higher in metastasizing tumor cells in lymph nodes than in primary tumors, most likely because lymph vessels in these lymph nodes were severely hypoxic. Overall, this transcription-independent but translation-dependent upregulation of VEGF-C in hypoxia stimulates lymphangiogenesis in tumors and lymph nodes and may contribute to lymphatic metastasis.

INTRODUCTION

The lymphatic vasculature consists of a network of lymph vessels that drain interstitial fluid from tissues and return it to the blood. It is also essential for immune surveillance. However, increased lymphangiogenesis also contributes to tumor metastasis and various inflammatory diseases, while insufficient lymph vessel growth or dysfunction causes lymphedema (Albrecht and Christofori, 2011; Alitalo, 2011; Bonnal et al., 2003; Christiansen and Detmar, 2011; Martinez-Corral and Makinen, 2013). Blocking lymphangiogenesis may offer therapeutic benefit to limit tumor spread.

Hypoxia promotes the growth of blood vessels (angiogenesis), but only limited data are available on whether and how hypoxia regulates lymphangiogenesis. Nevertheless, lymph vessels are often located in remote areas away from oxygen-carrying blood vessels and do not contain oxygen-carrying red blood cells; they are thus exposed to a milieu with very low oxygen levels (Guzy et al., 2008; Ivanovic, 2009). Some correlative studies suggest a link among tumor hypoxia, the hypoxia-inducible transcription factor HIF-1α, and lymphangiogenesis (Schoppmann et al., 2006; Tao et al., 2005). Another study reported that HIF-1α promotes lymphatic metastasis by transcriptional activation of the lymphangiogenic factor platelet derived growth factor B (Schito et al., 2012). HIF-1α also stimulates transcription of Prox-1, another lymph-angiogenic factor (Zhou et al., 2013). However, whether hypoxia signaling (and in particular HIF-1α) regulates the expression of vascular endothelial growth factor C (VEGF-C), one of the key lymphangiogenic factors (Alitalo and Detmar, 2012), remains unknown. Only a single report documented an associative correlation between HIF-1α and VEGF-C in cancer (Liang et al., 2008). It is also unknown whether VEGF-C expression in hypoxic conditions relies on transcriptional or translational mechanisms.

When cells are exposed to low oxygen levels, they suppress general protein synthesis in order to save energy (Kaelin and Ratcliffe, 2008; Majmundar et al., 2010; Maxwell, 2005; Semenza, 2012). Hypoxia inhibits mRNA translation by affecting the activity of two kinases, mTOR and PERK (Larsson et al., 2013; Silvera and Schneider, 2009). Inactivation

Cell PRESS
Open ACCESS

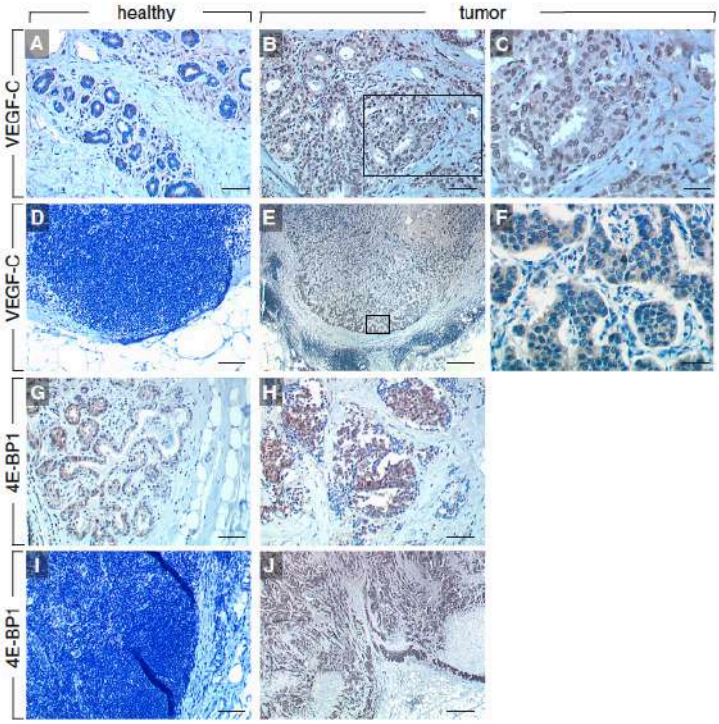

Figure 1. Expression Levels of VEGF-C and 4E-BP1 in Breast Tumor Specimens

(A–F) Immunostaining of VEGF-C in human specimens of healthy breast tissue (A), invasive breast cancer (B and C), and in healthy (D) and metastasized (E and F) lymph nodes. (C) and (F) show larger magnification of the framed area of (B) and (E), respectively.

(G–J) Immunostaining of 4E-BP1 in human healthy breast epithelium (G), invasive breast cancer (H), and normal (I) and metastasized (J) lymph nodes. Scale bar represents 50 μm (A, B, G, and H), 25 μm (C and F), and 250 μm (D, E, I, and J).

of mTOR results in hypophosphorylation of eIF4E-binding proteins (4E-BP), which promotes the sequestering of eIF4E, a factor necessary for cap-dependent translation (Martineau et al., 2013; Richter and Sonenberg, 2005). Hypoxic activation of PERK is mediated by the unfolded protein response and inhibits translation by phosphorylating the translation initiation factor eIF2-α (Koumenis and Wouters, 2006).

Other mRNAs are translated in hypoxic conditions by an alternative mechanism, mediated by internal ribosome entry sites (IRESs) located in their 5′ UTRs, which allows the ribosome to be recruited to a site that is at a considerable distance from the cap structure, most frequently in the presence of *trans*-acting factors (Spriggs et al., 2008; Vagner et al., 2001). Many cellular mRNAs have now been documented to contain IRESs. The majority of identified IRESs are found in mRNAs of proteins that are associated with the control of cell growth and death, including growth factors, proto-oncogenes and proteins required for apoptosis (Bushell et al., 2004). IRES elements have also been identified in VEGF-A and fibroblast growth factor 2 mRNA sequences and are activated by hypoxia to stimulate angiogenesis (Bornes et al., 2007). However, since it is unknown if IRES-dependent expression of VEGF-C in hypoxic conditions regulates lymphangiogenesis, we characterized IRES-dependent induction of VEGF-C in hypoxic tumors and lymph nodes.

RESULTS

Coexpression of VEGF-C and 4E-BP1 in Tumor Cells

We examined by immunohistochemistry (IHC) the expression levels of VEGF-C in human healthy breast specimens, tumor biopsies of invasive ductal carcinomas, and draining metastatic lymph nodes. Fifteen tumor biopsy specimens and their sentinel nodes were analyzed. Immunoreactive VEGF-C levels were moderate in healthy tissues but elevated in tumor samples (Figures 1A–1C). VEGF-C was undetectable in healthy lymph nodes but upregulated in metastatic tumor cells in lymph nodes (Figures 1D–1F).

Notably, 4E-BP1, a negative regulator of cap-dependent mRNA translation, was overexpressed in tumors and metastatic lymph nodes as compared to healthy epithelium and noninvaded lymph nodes (Figures 1G–1J). Since overexpression of 4E-BP1 inhibits cap-dependent translation induced by hypoxia in tumors (Braunstein et al., 2007), these findings raised the question whether VEGF-C translation in tumors and metastatic lymph nodes relied on a cap-independent regulation of VEGF-C translation.

VEGF-C mRNA Is Reduced while VEGF-C Protein Is Increased in Tumors

We used three different mouse tumor models known to induce lymphangiogenesis and to metastasize via lymph vessels: Capan-1, a xenograft of human pancreatic adenocarcinoma; 4T1, an orthotopic syngeneic mouse model of metastatic breast cancer; and a syngeneic subcutaneous model of Lewis lung carcinoma (LLC) (Deer et al., 2010; Garmy-Susini et al., 2010; Pulaski and Ostrand-Rosenberg, 2001). When studying the expression of VEGF-C in primary tumor extracts during tumor progression, we found that VEGF-C mRNA levels were decreased (Figures 2A–2C), while human VEGF-C protein levels were increased in the three tumor cell types, as observed by a human VEGF-C-specific ELISA (Figure 2D) and by immunoblotting (Figures 2E and 2F). These data suggested that induction of VEGF-C expression occurred via a posttranscriptional

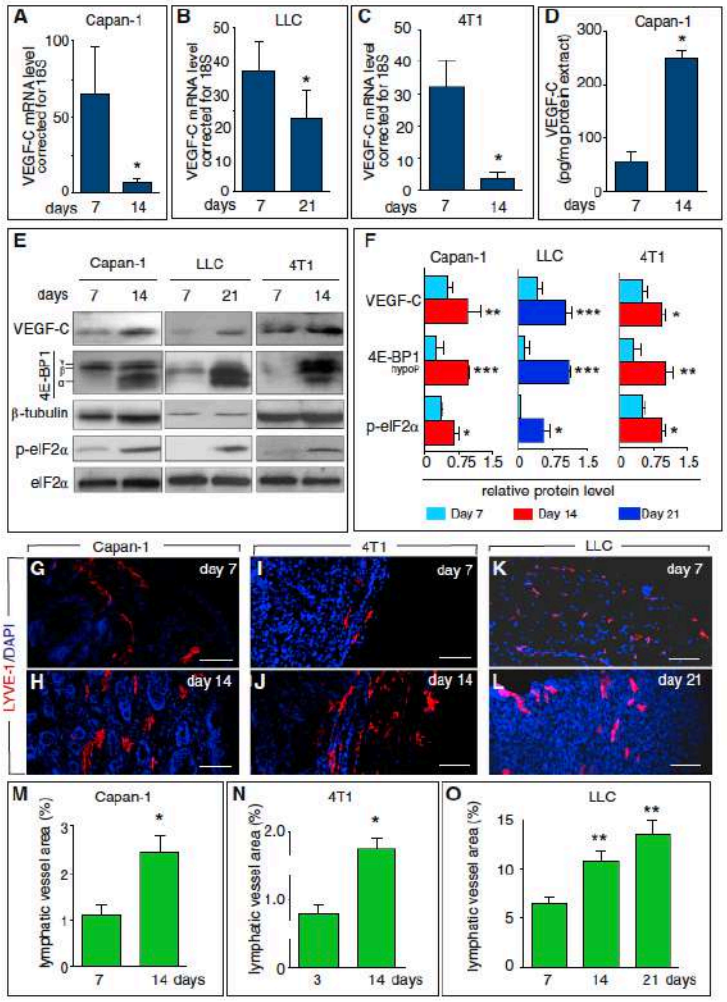

Figure 2. Tumor Lymphangiogenesis Correlates with Posttranscriptional Induction of VEGF-C In Vivo

(A–C) Quantitative RT-PCR (qRT-PCR) of VEGF-C mRNA in Capan-1 pancreatic (A), LLC (B), and 4T1 breast (C) tumors shows a decrease of VEGF-C transcript levels during tumor growth (mean ± SEM; n = 8–10; *p < 0.001).

(D), ELISA analysis showing increased VEGF-C protein levels during Capan-1 tumor growth (mean ± SEM; n = 5, *p < 0.001).

(E and F) Immunoblot of VEGF-C, 4E-BP1, and eIF2α and phosphorylated eIF2α (p-eIF2α) in Capan-1 pancreatic, LLC, and 4T1 breast tumors, showing an increase in VEGF-C protein levels, associated with increased expression and dephosphorylation of 4E-BP1 and with increased phosphorylation of eIF2α when comparing day 14 (Capan-1, 4T1) or day 21 (LLC) with day 7 tumor protein extracts. Quantification by densitometry is shown in (F). Relative levels are normalized to β-tubulin (VEGF-C, hypophosphorylated 4E-BP1) or to eIF2α (p-eIF2α) (mean ± SEM; n = 8–10; *p < 0.05 **p < 0.01, ***p < 0.001).

(G–L) Immunostaining for LYVE-1 (red) demonstrating increased lymphangiogenesis during Capan-1 pancreatic (G and H), 4T1 breast (I and J), and LLC (K and L) growth. Nuclei are visualized by DAPI staining (blue).

(M–O) Morphometric quantification of tumor lymphatic vessel area (% of tumor area) in Capan-1 (M), 4T1 (N), and LLC (O) tumors (mean ± SEM; n = 8–10; *p < 0.01).

Scale bar represents 50 μm (G–L). See also Figure S1.

mechanism. Use of murine VEGF-C-specific primers in the human Capan-1 tumor model revealed that stromal cells did not compensate for the reduced human VEGF-C mRNA levels by upregulating murine VEGF-C transcript levels (Figure S1). Staining for the lymphatic endothelial cell marker LYVE-1 complemented with quantification of lymph vessel area showed that lymphangiogenesis increased during tumor progression (Figures 2G–2O), in agreement with the enhanced VEGF-C protein levels.

We studied the phosphorylation status of 4E-BP1 by immunoblotting. 4E-BP1 can be hypophosphorylated (designated α-form) or hyperphosphorylated (designated β and γ forms). In its hypophosphorylated state, 4E-BP1 inhibits cap-dependent translation initiation by sequestering eIF-4E (Martineau et al., 2013; Richter and Sonenberg, 2005). During tumor progression, total 4E-BP1 protein levels increased and 4E-BP1 became increasingly hypophosphorylated, as evidenced by the shift to a lower molecular weight (Figures 2E and 2F). We also analyzed eIF2α phosphorylation using antibodies recognizing phosphorylated and total eIF2α, as eIF2α phosphorylation downregulates protein synthesis in various stress conditions, including hypoxia (Koumenis and Wouters, 2006). Notably, phosphorylated eIF2α (p-eIF2α) levels increased during tumor progression (Figures 2E and 2F). Thus, decreased VEGF-C mRNA and increased VEGF-C protein levels, together with the decrease of global translation initiation in tumors mediated by 4E-BP and eIF2α, suggested a stress-specific mechanism of regulation of VEGF-C translation, such as an IRES-dependent translation process.

Structure Probing of the 5′ UTR mRNA of VEGF-C

We therefore explored if VEGF-C might be translated via IRES-dependent regulation. In order to analyze if the 5′ UTRs of the human and murine VEGF-C contained conserved structural features, the secondary structures of both RNAs were studied by using "selective 2′-hydroxyl acylation analyzed by primer extension" (SHAPE) analysis to obtain information on the RNA

Cell PRESS
Open ACCESS

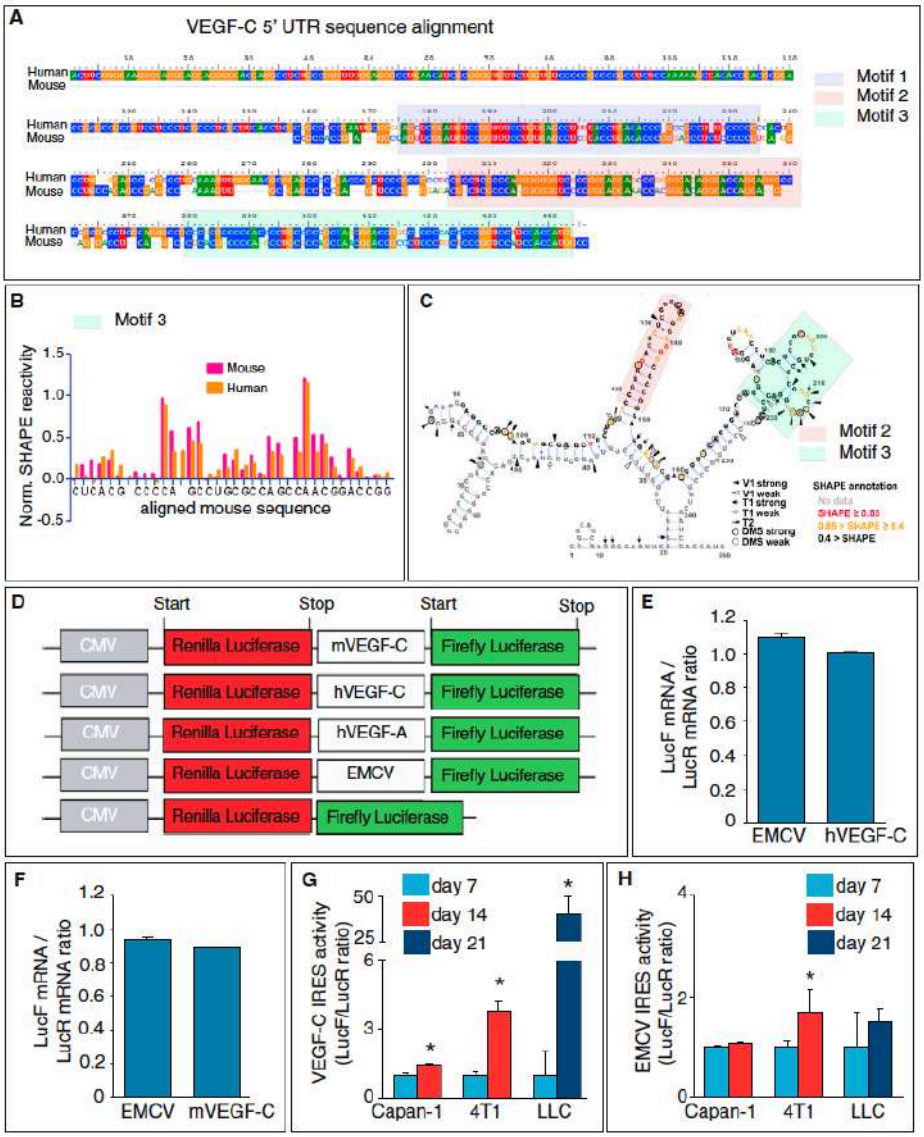

Figure 3. VEGF-C mRNA Contains an IRES Element Activated during Tumor Growth

(A) Sequence alignment of the murine and human VEGF-C 5′ UTR sequences. A color code is used for each nucleotide: guanine (orange), adenine (green), uridine (red), and cytosine (blue). Three stretches of nucleotides are highly conserved between the two RNA sequences: motif 1 (light blue), motif 2 (light orange), and motif 3 (light green).

(B) Quantification of the SHAPE analysis (see the Experimental Procedures) is shown for the conserved nucleotides of motif 3 of the human (orange) and murine (red) 5′ UTRs, showing very similar reactivity patterns.

(C) Putative secondary structure of the murine 5′ UTR of VEGF-C mRNA, as predicted on the basis of the ribose reactivities toward SHAPE and the reactivities of adenines at N1 and cytosines at N3 toward DMS. For each nucleotide, the level of reactivity toward SHAPE is indicated in red, yellow, or black font character for strong, medium, or weak reactivity, respectively. The cleavage sites induced by ribonucleases V1, T1, or T2 are indicated by arrows. Motifs 2 and 3 are color-coded as in (A).

(legend continued on next page)

Cell PRESS
Open ACCESS

secondary structure at single nucleotide resolution. SHAPE takes advantage of the fact that only flexible nucleotides are reactive toward hydroxyl-selective electrophiles, whereas constrained nucleotides are unreactive. We used as chemical probing reagents benzoyl cyanide in order to provide information on the flexibility of each ribose (Mortimer and Weeks, 2009) and dimethyl sulfate (DMS), which methylates single-stranded cytosines at N3 and adenines at N1 (Figure S2A). To footprint and probe the RNA structure, we also took advantage of the enzymatic cleavage by RNase T1 (which cleaves single-stranded RNA after unpaired guanines residues), RNase T2 (cleaving single-stranded RNA after unpaired nucleotides with a preference for adenines), and RNase V1 (cleaving base-paired nucleotide residues in a non-sequence-specific manner) (Figure S2A).

This analysis revealed that the 5′ UTRs were highly structured because of a high GC content (Figures 3A and 3B; Figures S2A and S2B). However, the concomitant presence of RNase V1 cleavages and of single-strand specific cuts, together with the sensitivity to modifications by DMS in the SHAPE analysis, suggested that these RNAs do not fold into a unique fixed structure but are able to adopt alternative conformations at equilibrium. Nevertheless, based on the quantification of the DMS and SHAPE reactivities, the most representative of the putative secondary structures of the murine 5′ UTR is shown in Figure 3C. Using sequence alignment, we observed three highly conserved regions between the human and murine 5′ UTRs (Figure 3A). Interestingly, SHAPE analysis revealed that two of these motifs adopted the same structure, since the reactivity pattern of the conserved residues was nearly identical (Figure 3B; Figure S2B). These motifs, located at the same distance from the initiation codon in human and murine RNAs, might be appropriate for binding of *trans*-acting factor(s) necessary to activate IRES-dependent translation.

The 5′ UTR of VEGF-C Exhibits IRES Activity

We then explored if the putative IRES sequences in the human and murine 5′ UTR of the VEGF-C mRNAs were translationally active and cloned these sequences in a double luciferase bicistronic vector (Figure 3D) (Créancier et al., 2000). In this vector, the first *Renilla* luciferase (LucR) cistron is translated by a cap-dependent mechanism, while the second firefly luciferase (LucF) cistron can be translated only if an IRES is present between the two cistrons. We used bicistronic vectors containing the encephalomyocarditis virus (EMCV) IRES sequence since it is not or only minimally regulated in mammalian cells, and we also used the VEGF-A IRES since it is activated by hypoxia (Bornes et al., 2007) (the VEGF-A data are discussed below). An empty control bicistronic vector, containing a sequence without IRES activity between the two cistrons, was inactive (Figure 3D; Figure S2C). Control RT-PCR analysis showed that both proteins were translated from a single mRNA transcript, since comparable amounts of LucR and LucF mRNA were measured (Figures 3E and 3F), indicating that a cryptic promoter or splicing event did not influence the results (Martineau et al., 2004).

To quantify the IRES activity in human and murine VEGF-C 5′ UTR sequences in vivo, Capan-1, 4T1, and LLC tumor cells were transduced with the bicistronic lentiviral vectors and injected subcutaneously (Capan-1, LLC) or orthotopically in the mammary fat pad (4T1). We used the human VEGF-C 5′ UTR for the human cell line (Capan-1) and the murine VEGF-C 5′ UTR for the murine cell lines (4T1, LLC). Transduction of the bicistronic vector did not affect tumor growth (Figures S2D and S2E). The VEGF-C IRES activity was quantified by measuring the LucF/LucR ratio as a parameter of the relative contribution of IRES-dependent versus cap-dependent translation after 7, 14, and 21 days. The IRES activity levels at day 14 and 21 were expressed relative to the IRES activity at day 7. These experiments revealed an IRES activity for both human and murine VEGF-C 5′ UTRs (Figures 3G and 3H). Furthermore, this IRES activity increased during tumor progression, especially in breast and lung tumors, while the EMCV IRES activity changed only minimally in 4T1 tumors (1.68-fold), e.g., less than the VEGF-C IRES activity in these tumors (3.75-fold).

The VEGF-C IRES Activity Is Higher in Metastatic Lymph Nodes

Analysis of the LYVE-1-positive lymphatic area in Capan-1, 4T1, and LLC tumors showed that lymphangiogenesis in lymph nodes was minimal at 3 days after inoculation but progressively increased from 7 days onward (Figures 4A–4J). This raised the question whether VEGF-C protein synthesis was increased in metastatic lymph nodes. However, substantial numbers of metastatic cytokeratin-positive tumor cells were detected in draining lymph nodes of Capan-1 and 4T1 tumors only from 14 days onward and of LLC tumors only from 21 days onward, i.e., later than the first signs of increased lymphangiogenesis in metastatic lymph nodes (Figures 4K–4N). Previous reports already documented that lymph node lymphangiogenesis precedes lymph node metastasis, presumably because primary tumors release VEGF-C in the lymph fluid of efferent lymphatics (Hirakawa, 2009).

We also explored whether tumor cells might upregulate VEGF-C production to higher levels, once they had intravasated and traveled through lymph vessels to the lymph node, and therefore analyzed the VEGF-C IRES activity in draining lymph nodes to which tumor cells metastasized. In order to compare the IRES activity in tumors and metastatic lymph nodes, the firefly/*Renilla* luciferase ratio in each tumor type was normalized

(D) Schematic representation of the bicistronic expression cassettes subcloned in lentivectors, encoding two luciferase reporters that are translated by cap-dependent translation (*Renilla* luciferase) or by IRES-dependent translation (firefly luciferase). IRESs used are the murine and human VEGF-C 5′ UTR, the human VEGF-A IRES, as well as the viral EMCV IRES (EMCV) and a short sequence devoid of IRES as positive and negative controls, respectively.
(E and F) mRNA expression analysis of firefly luciferase (LucF) and *Renilla* luciferase (LucR) by qRT-PCR on cells transduced with the bicistronic lentivector containing human (E) or murine (F) VEGF-C 5′ UTR, revealing comparable expression of LucR and LucF mRNA, suggesting transcription of a single mRNA (mean ± SEM; n = 6; p = NS).
(G and H) In vivo VEGF-C (G) and EMCV (H) IRES activity in Capan-1, 4T1, and LLC tumors (values are relative to day 7; mean ± SEM; n = 8–10; *p < 0.01).
See also Figure S2.

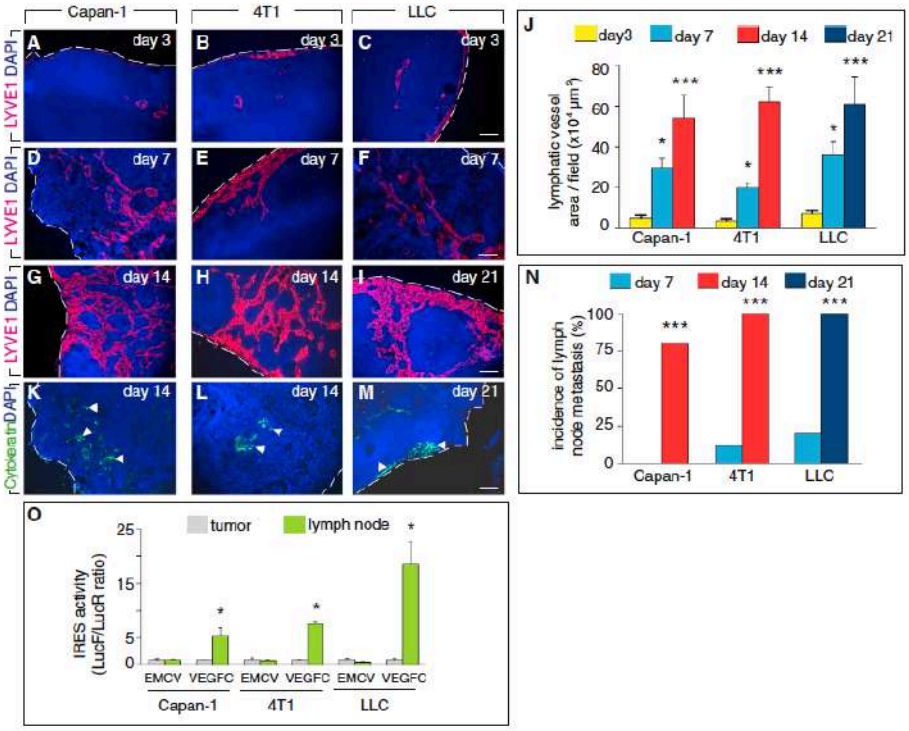

Figure 4. VEGF-C IRES Activity Is Higher in Metastatic Tumor Cells in the Lymph Node

(A–I) Staining for LYVE-1 (red) and nuclei (DAPI, blue) at day 3 (A–C), 7 (D–F) and 14 (G and H) or 21 (I) revealed that lymphangiogenesis progressively increased in tumor-draining lymph nodes in Capan-1, 4T1, and LLC tumors. Dashed lines denote the border of the tissue.

(J) Quantification of lymphatic vessel area in lymph node (mean ± SEM; n = 8–10; *p < 0.05, ***p < 0.001).

(K–M) Staining for cytokeratin (green, see arrowheads) and nuclei (DAPI, blue) revealed metastatic dissemination to lymph node of Capan-1, 4T1 and LLC tumors. Dashed lines denote the border of the tissue.

(N) Quantification of metastasis positive lymph nodes (mean ± SEM; n = 8–10; ***p < 0.001).

(O) In vivo VEGF-C- and EMCV-IRES activity in metastatic lymph nodes of Capan-1, 4T1, and LLC tumors at 14, 14, and 21 days, respectively (values are expressed relative to the respective value in the tumor; mean ± SEM; n = 8–10; *p < 0.01).

Scale bar represents 50 µm (all).

to the value of 1, both for the EMCV and VEGF-C IRES, and the IRES activities in the lymph nodes were expressed as a fold induction over the IRES activity in the tumor. This analysis revealed that compared to primary tumors, the VEGF-C IRES activity in metastatic lymph nodes was 5-, 7-, and 18-fold higher in the Capan-1, 4T1, and LLC tumor models at 14, 14, and 21 days after tumor inoculation, respectively, while the EMCV IRES activity was not affected (Figure 4O). These findings suggested that the lymphatic milieu influenced VEGF-C translation in tumor cells.

Lymph Vessels Are Hypoxic and Develop Nearby Hypoxic Tumor Cells

We then sought to determine why the lymphatic milieu enhanced the VEGF-C IRES activity in metastatic tumor cells. Since lymphatics are known to be hypoxic (Guzy et al., 2008; Ivanovic, 2009) and IRES elements are activated in cellular stress conditions such as hypoxia (Braunstein et al., 2007; Komar and Hatzoglou, 2011; Pestova et al., 2001; Sachs, 2000; Silvera and Schneider, 2009; Spriggs et al., 2010; Vagner et al., 2001), we explored whether hypoxia affected IRES-dependent initiation of translation of VEGF-C. We first explored a possible link between hypoxia and lymphatic development and therefore double stained tumors for the hypoxyprobe pimonidazole and the lymphatic markers LYVE-1 or podoplanin. Already at an early stage of tumor development (in <5 mm^3 tumors), the pancreas, breast, and lung cancer models contained hypoxic regions, which became more widespread and stained more strongly after 2 weeks (Figures 5A–5C). Immunoblotting for HIF-1α confirmed activation of this hypoxia-inducible transcription factor (Figure 5D). In all cancer models, lymph vessels developed in proximity of hypoxic tumor cell clusters (Figures 5E–5G). Unlike blood

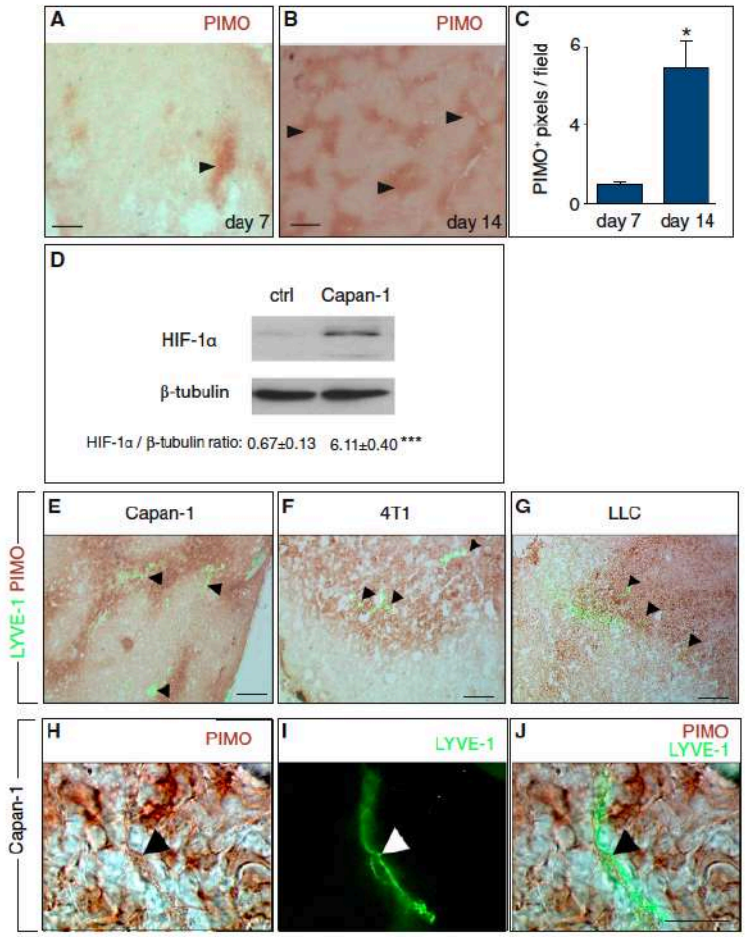

Figure 5. Tumor VEGF-C Levels Are Increased in Hypoxic Zones

(A–C) Immunodetection of hypoxic areas (hypoxyprobe, brown) in Capan-1 tumors revealed few small hypoxic areas at early time points (A, day 7), which became more abundant by 14 days after injection (B). Arrowheads indicate pimonidazole adduct (PIMO)-positive hypoxic areas. Quantification of PIMO$^+$ area is shown in (C) (mean ± SEM; n = 10; $^*p < 0.001$).

(D) Immunoblot for HIF-1α in Capan-1 tumors showing stabilization of the protein in vivo. Normal healthy skin was used as control. Densitometric quantification is shown (mean ± SEM; n = 6; $^{***}p < 0.001$). ctrl, control.

(E–G) Staining for LYVE-1 (green, see arrowheads) revealing the presence of lymphatic vessels close to hypoxic areas (hypoxyprobe [PIMO], brown) in Capan-1 (E), 4T1 (F), and LLC (G) tumors.

(H–J) Staining of Capan-1 tumor for LYVE-1 (green, arrowhead) and hypoxyprobe (PIMO, brown) revealed hypoxic lymph vessels. Merged image is shown in (J).

Scale bar represents 50 μm (Aand B), 50 μm (E–G), 25 μm H–J). See also Figure S3.

endothelial cells, lymphatic endothelial cells also stained positively for pimonidazole, indicating that lymph vessels are hypoxic (Figures 5H–5J; Figures S3A–S3F).

Hypoxia Induces VEGF-C Expression by a Nontranscriptional Mechanism

We then studied the regulation of IRES-dependent VEGF-C translation by hypoxia. Immunostaining revealed that VEGF-C and LucF were expressed predominantly in pimonidazole-positive hypoxic tumor areas in vivo (Figures 6A–6F). To study the effect of hypoxia on VEGF-C expression in vitro, we exposed LLC, Capan-1, or 4T1 tumor cells to 1% oxygen or to cobalt chloride ($CoCl_2$), known to activate hypoxia signaling. Hypoxia reduced VEGF-C mRNA levels in LLC and 4T1 cells while not affecting its levels in Capan-1 cells (Figures 6G–6I). In LLC and 4T1 cells, hypoxia increased the protein levels of VEGF-C and of hypophosphorylated 4E-BP1, suggesting increased VEGF-C production despite a decrease in cap-dependent initiation of translation (Figures 6J and 6K). In Capan-1 cells, VEGF-C protein levels were comparable in hypoxic conditions, though 4E-BP1 dephosphorylation was increased, suggesting that the reduced cap-dependent initiation of VEGF-C translation was balanced off by an increase in IRES-dependent initiation of VEGF-C translation (Figures 6J and 6K). In each cell line, eIF2α phosphorylation was increased by hypoxia, suggesting that hypoxia downregulated global mRNA translation (Figures 6J and 6K). Since hypoxia increased the VEGF-C IRES activity in all human and murine tumor lines (also in the Capan-1 cells, in which VEGF-C levels did not increase) (Figures 6L–6N), hypoxia thus induced a switch from cap-dependent to IRES-dependent initiation of VEGF-C translation. Similar results were obtained when we used $CoCl_2$ (Figure 6O). Phosphorylation of eIF2α inhibits the EMCV IRES activity (Sanz et al., 2013) and the increased eIF2α phosphorylation levels might thus be responsible for the inhibition of the EMCV IRES activity in hypoxia, while the variable EMCV IRES activity in hypoxia in distinct tumor cell lines likely reflects cell-type-dependent regulation of this IRES activity, which has been recognized previously (Pilipenko et al., 2000).

The VEGF-C IRES Activity Is Reduced in More Oxygenated Tumors

We then explored whether tumor oxygen levels in vivo influenced the switch between cap-dependent VEGF-C translation (in oxygenated conditions) versus IRES-dependent VEGF-C translation (in hypoxic conditions). We therefore used prolyl

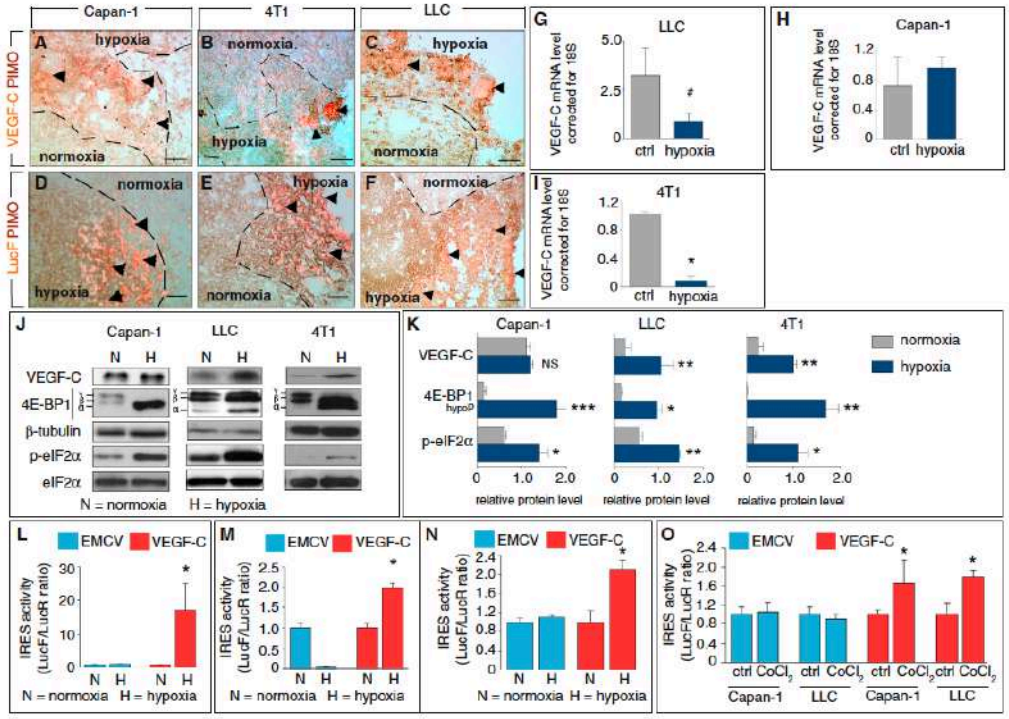

Figure 6. Hypoxia Induces VEGF-C-IRES Activity In Vitro

(A–C) Staining for VEGF-C (red) and hypoxyprobe (PIMO, brown) revealed VEGF-C colocalization (arrows) in hypoxic areas in Capan-1 (A), 4T1 (B), and LLC (C) tumors. Dashed lines denote more hypoxic from more normoxic zones.

(D–F) Staining for firefly luciferase (LucF, red) and hypoxyprobe (PIMO, brown) revealed IRES-dependent luciferase translation (arrows) primarily in hypoxic areas in Capan-1 (D), 4T1 (E), and LLC (F) tumors. Dashed lines denote more hypoxic from more normoxic zones.

(G–I) qRT-PCR for VEGF-C showing reduced mRNA levels in hypoxic conditions in LLC (G) and 4T1 (I) tumor cells, but not in Capan-1 tumor cells (H) (mean ± SEM; n = 9, *$p < 0.001$ in I; #$p = 0.059$ in G; p = NS in H).

(J and K) Immunoblot of VEGF-C, 4E-BP1, eIF2α, and phosphorylated eIF2α (p-eIF2α) in Capan-1, LLC, or 4T1 tumor cells, cultured in normoxia or hypoxia (1% O_2). Quantification by densitometry is shown in (K). Relative levels are normalized to β-tubulin (VEGF-C, hypophosphorylated 4E-BP1) or to eIF2α (p-eIF2α) (mean ± SEM; n = 3–6; *$p < 0.05$, **$p < 0.01$).

(L–N) VEGF-C- and EMCV IRES activity under normoxic and hypoxic conditions (1% O_2) in Capan-1 (L), 4T1 (M), and LLC (N) tumor cells in vitro (values are expressed relative to the respective normoxia condition; mean ± SEM; n = 6; *$p < 0.01$ versus normoxia).

(O) VEGF-C- and EMCV IRES activity in control and $CoCl_2$ conditions in Capan-1 and LLC cells in vitro (values are expressed relative to the respective controls; mean ± SEM; n = 5; *$p < 0.01$).

Scale bar represents 50 μm (A–F). ctrl, control.

hydroxylase domain protein-2 $(PHD2)^{+/-}$ mice, in which tumor hypoxia is reduced because of normalization of tumor blood vessels and improved tumor vessel perfusion (Mazzone et al., 2009), hypothesizing that the VEGF-C IRES activity would be reduced in these mice. We thus implanted bicistronic luciferase vector-transduced LCC tumor cells in wild-type (WT) and $PHD2^{+/-}$ mice. Tumor growth of cancer cells, transduced with VEGF-C- or EMCV-IRES vectors, was comparable in WT and $PHD2^{+/-}$ mice (Figure S4A), consistent with reports that PHD2 haplodeficiency did not affect tumor growth (Mazzone et al., 2009). Also, staining for the hypoxia marker pimonidazole demonstrated that hypoxia levels were lower in EMCV IRES- and VEGF-C IRES-expressing tumors in $PHD2^{+/-}$ mice than in WT mice (Figures 7A, 7D, and 7G).

Compared to tumors in WT mice, tumors in $PHD2^{+/-}$ mice had similar VEGF-C immunoreactive protein levels, which colocalized in part with the pimonidazole-positive hypoxic regions, showing that both normoxic and hypoxic tumor cells produced VEGF-C (Figures 7B, 7C, 7E, 7F, and 7H). Immunoblotting confirmed these findings (Figure S4B). However, a reduced fraction of

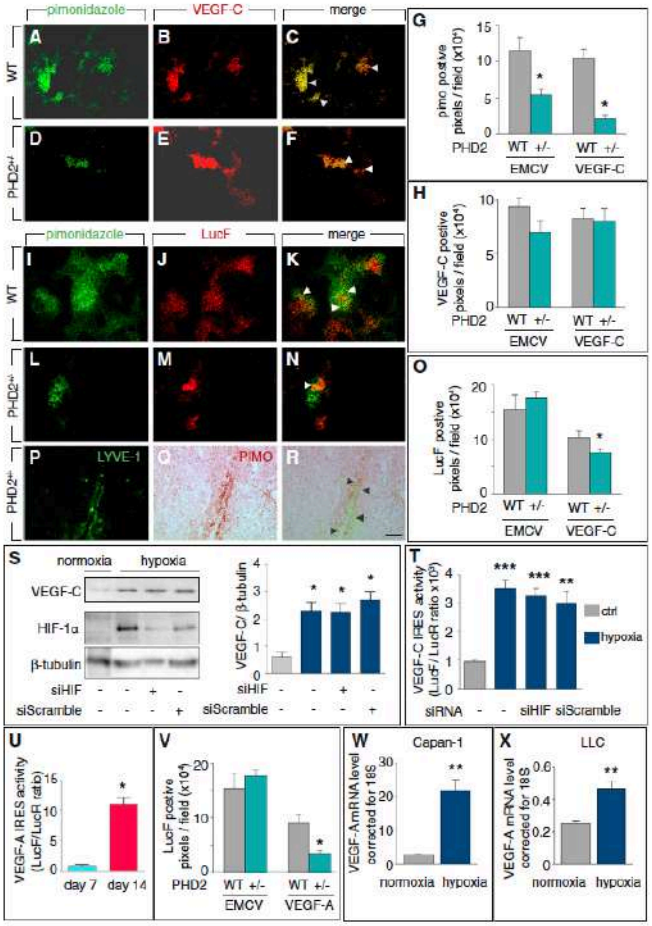

Figure 7. VEGF-C Induction by Hypoxia Is Translationally Regulated but HIF-1α Independent

(A–F) Immunostaining for hypoxyprobe (pimonidazole, green) and VEGF-C (red) in LLC tumors in wild-type (WT) (A–C) and PHD2$^{+/-}$ mice (D–F).

(G) Quantification of pimonidazole-positive pixel density in tumors transduced with EMCV- or VEGF-C IRES luciferase constructs showed a decrease in hypoxia in PHD2$^{+/-}$ mice (mean ± SEM; n = 6; *p < 0.05).

(H) Quantification of VEGF-C-positive pixel density in tumors transduced with EMCV- or VEGF-C IRES luciferase lentivector constructs revealing no differences (mean ± SEM; n = 8–10; p = NS).

(I–O) Staining for firefly luciferase (LucF, red) and hypoxyprobe (pimonidazole, green) revealed reduced VEGF-C IRES-dependent translation in LLC-bearing PHD2$^{+/-}$ mice (L–N) as compared to WT mice (I–K). Quantification of LucF-positive pixel density is shown in (O) confirming the decrease in luciferase signal for VEGF-C-IRES, which was not seen with the EMCV control IRES (mean ± SEM; n = 8–10; *p < 0.01).

(P–R) Micrographs of LLC tumor sections in PHD2$^{+/-}$ mice, stained for LYVE-1 (green) and hypoxyprobe (PIMO, brown), revealing that lymph vessels were hypoxic in this model.

(S) Immunoblot of VEGF-C or HIF-1α in lysates of Capan-1 cells incubated in normoxia or hypoxia and treated with or without siRNA against HIF-1α (siHIF) or a scrambled siRNA control (siScramble). Densitometric quantification is shown in the graph (right) (mean ± SEM; n = 4; *p < 0.01).

(T) VEGF-C IRES activity in Capan-1 cell lines in vitro incubated under normoxia or hypoxia and treated with or without siRNA against HIF-1α or a scrambled siRNA control (mean ± SEM; n = 5; ***p < 0.001).

(U) VEGF-A IRES activity in Capan-1 tumors in vivo revealing increased IRES activity with tumor progression (mean ± SEM; n = 8–10; *p < 0.005).

(V) Quantification of staining for firefly luciferase (LucF) revealed that VEGF-A IRES activity was lower in LLC tumors in PHD2$^{+/-}$ mice than in WT mice. The activity of EMCV IRES was not affected (mean ± SEM; n = 6; *p < 0.01). Note: since the data shown in Figure 7V and Figure 7O were generated in the same experiments, the EMCV control data are the same.

(W and X) qRT-PCR for VEGF-A showing increased mRNA levels in hypoxic conditions in Capan-1 (C) and LLC (D) tumor cells in vitro (mean ± SEM; n = 6; *p < 0.05).

Scale bar represents 50 μm (all). See also Figure S4.

VEGF-C was translated via IRES-dependent mechanisms in the more oxygenated tumors of PHD2$^{+/-}$ mice. Indeed, when double staining for pimonidazole and firefly luciferase (LucF), VEGF-C IRES-expressing tumors in PHD2$^{+/-}$ mice had reduced LucF but increased LucR levels (Figures 7I–7O; Figures S4C and S4D), indicating that the VEGF-C IRES activity was reduced while cap-dependent translation initiation was increased. VEGF-C IRES-dependent translation of LucF was only detected in the residual hypoxic tumor zones in PHD2$^{+/-}$ mice (Figures 7L–7N). Interestingly, even though overall tumor oxygenation in PHD2$^{+/-}$ mice was improved because of blood vessel normalization, lymph vessels remained immunoreactive for the hypoxyprobe pimonidazole in tumors of PHD2$^{+/-}$ mice (Figures 7P–7R). Thus, IRES-dependent VEGF-C translation was reduced in more oxygenated tumors of PHD2$^{+/-}$ mice, confirming the regulation of the translational switch (cap versus IRES dependence) by oxygen levels in vivo. That VEGF-C protein levels were not lower in tumors of PHD2$^{+/-}$ mice than in WT mice, despite overall improved oxygenation, may be due to the fact that the oxygenation conditions in tumors of PHD2$^{+/-}$ mice were still not sufficiently improved to completely abrogate IRES-dependent VEGF-C translation. In addition, even though HIF-1α levels are

Cell PRESS
Open ACCESS

reduced in more oxygenated tumors of PHD2$^{+/-}$ mice (Mazzone et al., 2009), the residual HIF-1α levels may still promote cap-dependent translation, since HIF-1α induces the transcription of the cap-binding factor eIF-4E (Yi et al., 2013).

HIF-1α-Independent Hypoxic Induction of VEGF-C Synthesis

To explore if VEGF-C protein production in hypoxic conditions was HIF dependent, we used a small interfering RNA (siRNA) against human HIF-1α (siHIF) to silence HIF-1α expression, which reduced HIF-1α protein levels to nearly undetectable levels in hypoxic Capan-1 tumor cells (Figure 7S). Silencing of HIF-1α also reduced the expression levels of VEGF-A, phosphoglycerate kinase (PGK), hexokinase-2, and the glucose transporter GLUT-1, all known HIF-1α target genes (Figure S4E). Despite the strong decrease of the HIF-1α levels in hypoxic Capan-1 tumor cells transfected with siHIF (Figure 7S), VEGF-C protein levels were maintained in hypoxic conditions (Figure 7S), whereas the VEGF-C IRES activity was not affected by HIF-1α silencing (Figure 7T). Thus, these data suggest that the posttranscriptional induction of VEGF-C via IRES was independent of HIF-1α.

Regulation of VEGF-A Expression by Hypoxia

For reasons of comparison, we also studied the relative importance of the cap-dependent versus IRES-dependent translation of VEGF-A in hypoxia. Previous in vitro studies documented that VEGF-A translation relies on cap-dependent mechanisms in normoxia and on IRES-dependent mechanisms in hypoxia (Bornes et al., 2004). Transgenic mouse lines, expressing reporter genes under the control of IRESs, also revealed that VEGF-A translation in ischemic muscle partly depends on the IRES activity (Bornes et al., 2007). However, it is unknown whether IRES-dependent translation of VEGF-A can also occur in tumors or metastatic lymph nodes. When tumor cells, stably transduced with a bicistronic lentiviral vector containing the VEGF-A IRES sequence, were injected in vivo, the VEGF-A IRES activity levels were detectable and increased during tumor progression (Figure 7U). The VEGF-A IRES activity was sensitive to oxygen levels in tumors in vivo, since tumors (transduced with lentiviral bicistronic vectors containing VEGF-A IRES) had lower VEGF-A IRES activity levels in PHD2$^{+/-}$ mice, as revealed by staining for firefly luciferase (Figure 7V). This was not influenced by the tumor size, since tumor growth was not affected by the PHD2 genotype or type of bicistronic vector (VEGF-A- or EMCV-IRES) (Figure S4F).

However, different from VEGF-C, regulation of VEGF-A expression also relied on transcriptional upregulation in hypoxic conditions. Indeed, VEGF-A mRNA levels were increased in tumor cells in hypoxia (Figures 7W and 7X) and also increased during tumor progression in vivo, both at the protein and mRNA levels (Figures S4G–S4J). Thus, unlike VEGF-A, the expression of which is upregulated in hypoxia at the transcriptional and translational level, the expression of VEGF-C in hypoxia is regulated by translational, but not by transcriptional, mechanisms.

DISCUSSION

We identified a translational regulation of VEGF-C production in hypoxic conditions, both in primary tumors and in (pre)-metastatic lymph nodes, that is distinct from previously identified mechanisms of how hypoxia stimulates lymphangiogenesis.

Tumor Cells Metastasizing via Hypoxic Lymphatics Induce VEGF-C

For tumor cells to spread to distant organs via lymphatics, they induce lymphangiogenesis. However, since tumors are often deprived of oxygen and lymphatics are extremely hypoxic (Guzy et al., 2008; Ivanovic, 2009), tumor cells must have mechanisms to stimulate lymph vessel growth in hypoxic conditions. Our findings demonstrate that tumor cells can upregulate VEGF-C protein levels in hypoxic conditions in vitro and in vivo and that lymph vessels grew in and around hypoxic tumor areas, where VEGF-C was produced. While hypoxia often upregulates protein levels via HIF-1α-dependent gene transcription, this study shows that hypoxia augments VEGF-C protein levels via a HIF-1α-independent effect on VEGF-C IRES-dependent initiation of translation.

Hypoxia Regulates VEGF-C Protein Levels via an IRES-Dependent Activity

We demonstrate that murine and human VEGF-C mRNAs are translated by IRES-dependent initiation of translation in hypoxic tumor areas during tumor development in vivo. Sequence alignment revealed that murine and human VEGF-C 5′ UTRs share three highly conserved motifs. Interestingly, probing the RNA secondary structures by SHAPE analysis showed that two of these motifs adopt the same two-dimensional structure, since the reactivity pattern of the conserved residues was nearly identical. These motifs, located at the same distance from the initiation codon, might be appropriate for binding of specific *trans*-acting factor(s), necessary to activate IRES-dependent translation. Use of a bicistronic vector provided functional evidence that the 5′ UTR of murine and human VEGF-C mRNA indeed functioned as IRES sequences to initiate cap-independent translation of the VEGF-C mRNA. Thus, translation of the VEGF-C mRNA in normoxia occurs via cap- and/or IRES-dependent mechanisms. In hypoxia, when global translation is suppressed through dephosphorylation of 4E-BP1 and increased phosphorylation of eIF2α, IRES-mediated mRNA translation is activated, leading to an overall increase in VEGF-C protein levels.

VEGF-C IRES Activity Is Higher in Lymph Nodes

Previous studies reported that expression of VEGF-C by cancer cells promotes tumor and lymph node lymphangiogenesis as well as metastasis (Hirakawa et al., 2005, 2007). Even before metastatic tumor cells reach the sentinel lymph nodes, VEGF-C, released by malignant cells of the primary tumor into the lymphatic circulation, stimulates lymphangiogenesis in lymph nodes at a distance (Hirakawa et al., 2005, 2007). Using luciferase reporters of posttranscriptional VEGF-C regulation, we observed that the VEGF-C IRES firefly luciferase activity was increased in lymph nodes at the time when they were colonized by metastatic tumor cells. Notably, however, the induction of the VEGF-C IRES activity was higher in tumor cells that had metastasized to the lymph nodes than in tumor cells that were present in the primary tumors. Lymphangiogenesis was also

more extensive in metastatic lymph nodes than in primary tumors. These data indicate that the lymph node milieu stimulates VEGF-C expression. Since lymphatics are highly hypoxic, the hypoxic milieu seems to be of key importance to activate IRES-dependent VEGF-C translation.

HIF-1α-Independent Regulation of VEGF-C Translation in Hypoxia

Hypoxia signaling is well known to stimulate angiogenesis, in part by promoting HIF-1α dependent transcription of VEGF-A as well as by stimulating IRES-dependent VEGF-A translation (Bornes et al., 2007; Huez et al., 2001). In contrast, VEGF-C transcript levels were reduced, yet VEGF-C protein levels were increased, in hypoxia by switching from cap-dependent to IRES-dependent VEGF-C translation. Notably, this regulation seemed to be independent of HIF-1α, since near-complete silencing of HIF-1α to levels sufficient to lower HIF-1α target gene transcription did not abrogate the hypoxia-induced post-transcriptional IRES-activated translation of VEGF-C mRNA and production of VEGF-C protein. Different molecular mechanisms thus evolved to ensure production of VEGF-A and VEGF-C, two closely related and homologous members of the VEGF family.

Hypoxic Lymph Vessels Ensure Lymphangiogenesis in Cancer

Our findings may also be relevant to understand how tumor cells have developed mechanisms to ensure spreading via lymphatics in oxygen-deprived conditions. Lymph vessels are severely hypoxic, not only because they lack oxygen-carrying red blood cells, but also because they reside in very hypoxic regions in tissues and tumors (Guzy et al., 2008; Ivanovic, 2009). Such a hypoxic milieu suppresses cap-dependent mRNA translation of VEGF-C in tumor cells, traveling inside lymphatics to the lymph nodes. However, by switching to IRES-dependent initiation of translation of VEGF-C, tumor cells can upregulate the production of this key lymphangiogenic factor in hypoxia and thereby ensure increased growth of lymph vessels via which they metastasize. Hence, tumor cells have adopted mechanisms to stimulate lymphangiogenesis when metastasizing through hypoxic lymph vessels and lymph nodes.

EXPERIMENTAL PROCEDURES

All human tissue was used under approval from the Human Subjects Institutional Review Board of the University of Toulouse III. More detailed procedures are described in Supplemental Experimental Procedures.

Tissue Specimens

In total, 15 primary human breast cancer specimens and their associated lymph nodes were collected from pretreatment surgical resections (Rangueil Hospital, Toulouse, France). Sample collection was approved by the INSERM Institutional Review Board (DC-2008-463) and Research State Department (Ministère de la Recherche, ARS, CPP2, authorization AC-2008-820).

Cell Culture

Cell culture of Capan-1 pancreatic carcinoma cells, 4T1 breast carcinoma, and LLC cells under normoxia or hypoxia (1% O_2 or 300 μM $CoCl_2$) was as described in the Supplemental Experimental Procedures.

Tumor Studies and Immunohistochemical Phenotyping

Animal experiments were conducted in accordance with recommendations of the European Convention for the Protection of Vertebrate Animals used for experimentation and according to the INSERM IACUC (France) and the KU Leuven (Belgium) guidelines for laboratory animal husbandry. All animal experiments were approved by the local branch Inserm Rangueil-Purpan of the Midi-Pyrénées ethics committee, France (protocol 091037615), or by the Institutional Animal Care and Research Advisory Committee of the KU Leuven, Leuven, Belgium (protocol P166/2011). The LLC syngenic tumor model in C57Bl6 mice, Capan-1 xenograft model in NMRI nude mice, syngenic orthotopic 4T1 breast carcinoma model in Balb/c mice, and the collection and immunohistological analysis of tumor and lymph nodes was performed as detailed in the Supplemental Experimental Procedures.

RNA and Protein Analysis

SHAPE Analysis

In-vitro-transcribed RNA was prepared and subjected to SHAPE analysis as previously described (Helfer et al., 2013) (Mortimer and Weeks, 2009) and further detailed in the Supplemental Experimental Procedures.

RNA Analysis

Expression of human and murine VEGF-C, VEGF-A, hexokinase II, Glut1, PGK, LucR, and LucF was by SYBR green quantitative RT-PCR (Table S1) as described in the Supplemental Experimental Procedures.

Protein Analysis

VEGF-C protein levels in Capan-1 tumor extracts were measured by ELISA (R&D Systems).

Lentivector Construction and Luciferase Reporter Gene Assay

Cloning of the cDNAs coding human and murine VEGF-C 5′ UTR, VEGF-A 5′ UTR, and EMCV 5′ UTR into the bicistronic lentivectors expressing *Renilla* luciferase under the cytomegalovirus promoter and firefly luciferase under the control of the respective 5′ UTR IRES, and cell transduction was as described in the Supplemental Experimental Procedures. In vitro or ex vivo luciferase assays on cell or tissue lysates were performed using the Dual-Luciferase Assay System kit (Promega).

siRNA and Cell Transfection

siRNA-mediated silencing of human HIF1α was done using a pool of siRNAs as listed in the Supplemental Experimental Procedures. Transfection of Capan-1 cells and verification of silencing by immunoblotting was as described in the Supplemental Experimental Procedures.

Statistical Analysis

All statistical analyses were performed with a two-tailed Student's t test or one-way ANOVA. All experiments were performed three times, with one exception, where the incidence of metastasis is reported as the average ± SEM of three separate animal experiments. All other data presented are of one representative experiment.

SUPPLEMENTAL INFORMATION

Supplemental Information includes Supplemental Experimental Procedures, four figures, and one table and can be found with this article online at http://dx.doi.org/10.1016/j.celrep.2013.12.011.

ACKNOWLEDGMENTS

This study was supported by the Ligue Régionale Contre le Cancer, Fondation pour la Recherche Médicale and Association Française contre les Myopathies, Association pour la Recherche sur le Cancer, and Conseil Régional Midi-Pyrénées (France). We thank the Biological Resources Center and G. Escourrou and I. Rouquette from the Pathology and Histology Department of Rangueil Hospital in Toulouse for providing human tissue samples. We thank J.J. Maoret (GeT Genotoul Platform), Y. Barreira (ANEXPLO Genotoul Platform), A. Delluc-Clavières, and L. Van den Berghe for technical assistance and F. Lenfant, H. Prats, and P. Romby for scientific support. A.K. is funded

by a fellowship of the Belgian Science Fund—Flanders; F.H. is funded by the Conseil Régional Midi-Pyrénées (France). The work of P.C. is funded by Long-term Structural Funding Methusalem by the Flemish Government, the Interuniversitary Actraction Poles (P7/03), the Belgian Government, and Leducq Transatlantic Network—Artemis.

Received: May 24, 2013
Revised: October 28, 2013
Accepted: December 6, 2013
Published: January 2, 2014

REFERENCES

Albrecht, I., and Christofori, G. (2011). Molecular mechanisms of lymphangiogenesis in development and cancer. Int. J. Dev. Biol. *55*, 483–494.

Alitalo, K. (2011). The lymphatic vasculature in disease. Nat. Med. *17*, 1371–1380.

Alitalo, A., and Detmar, M. (2012). Interaction of tumor cells and lymphatic vessels in cancer progression. Oncogene *31*, 4499–4508.

Bonnal, S., Schaeffer, C., Créancier, L., Clamens, S., Moine, H., Prats, A.C., and Vagner, S. (2003). A single internal ribosome entry site containing a G quartet RNA structure drives fibroblast growth factor 2 gene expression at four alternative translation initiation codons. J. Biol. Chem. *278*, 39330–39336.

Bornes, S., Boulard, M., Hieblot, C., Zanibellato, C., Iacovoni, J.S., Prats, H., and Touriol, C. (2004). Control of the vascular endothelial growth factor internal ribosome entry site (IRES) activity and translation initiation by alternatively spliced coding sequences. J. Biol. Chem. *279*, 18717–18726.

Bornes, S., Prado-Lourenco, L., Bastide, A., Zanibellato, C., Iacovoni, J.S., Lacazette, E., Prats, A.C., Touriol, C., and Prats, H. (2007). Translational induction of VEGF internal ribosome entry site elements during the early response to ischemic stress. Circ. Res. *100*, 305–308.

Braunstein, S., Karpisheva, K., Pola, C., Goldberg, J., Hochman, T., Yee, H., Cangiarella, J., Arju, R., Formenti, S.C., and Schneider, R.J. (2007). A hypoxia-controlled cap-dependent to cap-independent translation switch in breast cancer. Mol. Cell *28*, 501–512.

Bushell, M., Stoneley, M., Sarnow, P., and Willis, A.E. (2004). Translation inhibition during the induction of apoptosis: RNA or protein degradation? Biochem. Soc. Trans. *32*, 606–610.

Christiansen, A., and Detmar, M. (2011). Lymphangiogenesis and cancer. Genes Cancer *2*, 1146–1158.

Créancier, L., Morello, D., Mercier, P., and Prats, A.C. (2000). Fibroblast growth factor 2 internal ribosome entry site (IRES) activity ex vivo and in transgenic mice reveals a stringent tissue-specific regulation. J. Cell Biol. *150*, 275–281.

Deer, E.L., González-Hernández, J., Coursen, J.D., Shea, J.E., Ngatia, J., Scaife, C.L., Firpo, M.A., and Mulvihill, S.J. (2010). Phenotype and genotype of pancreatic cancer cell lines. Pancreas *39*, 425–435.

Garmy-Susini, B., Avraamides, C.J., Schmid, M.C., Foubert, P., Ellies, L.G., Barnes, L., Feral, C., Papayannopoulou, T., Lowy, A., Blair, S.L., et al. (2010). Integrin alpha4beta1 signaling is required for lymphangiogenesis and tumor metastasis. Cancer Res. *70*, 3042–3051.

Guzy, R.D., Sharma, B., Bell, E., Chandel, N.S., and Schumacker, P.T. (2008). Loss of the SdhB, but Not the SdhA, subunit of complex II triggers reactive oxygen species-dependent hypoxia-inducible factor activation and tumorigenesis. Mol. Cell. Biol. *28*, 718–731.

Helfer, A.C., Romilly, C., Chevalier, C., Lioliou, E., Marzi, S., and Romby, P. (2013). Probing RNA Structure. In Vitro with Enzymes and Chemicals, *Volume 2*, Second Edition (Weinheim: Wiley-VCH Verlag).

Hirakawa, S. (2009). From tumor lymphangiogenesis to lymphvascular niche. Cancer Sci. *100*, 983–989.

Hirakawa, S., Kodama, S., Kunstfeld, R., Kajiya, K., Brown, L.F., and Detmar, M. (2005). VEGF-A induces tumor and sentinel lymph node lymphangiogenesis and promotes lymphatic metastasis. J. Exp. Med. *201*, 1089–1099.

Hirakawa, S., Brown, L.F., Kodama, S., Paavonen, K., Alitalo, K., and Detmar, M. (2007). VEGF-C-induced lymphangiogenesis in sentinel lymph nodes promotes tumor metastasis to distant sites. Blood *109*, 1010–1017.

Huez, I., Bornes, S., Bresson, D., Créancier, L., and Prats, H. (2001). New vascular endothelial growth factor isoform generated by internal ribosome entry site-driven CUG translation initiation. Mol. Endocrinol. *15*, 2197–2210.

Ivanovic, Z. (2009). Physiological, ex vivo cell oxygenation is necessary for a true insight into cytokine biology. Eur. Cytokine Netw. *20*, 7–9.

Kaelin, W.G., Jr., and Ratcliffe, P.J. (2008). Oxygen sensing by metazoans: the central role of the HIF hydroxylase pathway. Mol. Cell *30*, 393–402.

Komar, A.A., and Hatzoglou, M. (2011). Cellular IRES-mediated translation: the war of ITAFs in pathophysiological states. Cell Cycle *10*, 229–240.

Koumenis, C., and Wouters, B.G. (2006). "Translating" tumor hypoxia: unfolded protein response (UPR)-dependent and UPR-independent pathways. Mol. Cancer Res. *4*, 423–436.

Larsson, O., Tian, B., and Sonenberg, N. (2013). Toward a genome-wide landscape of translational control. Cold Spring Harb. Perspect. Biol. *5*, a012302.

Liang, X., Yang, D., Hu, J., Hao, X., Gao, J., and Mao, Z. (2008). Hypoxia inducible factor-alpha expression correlates with vascular endothelial growth factor-C expression and lymphangiogenesis/angiogenesis in oral squamous cell carcinoma. Anticancer Res. *28* (3A), 1659–1666.

Majmundar, A.J., Wong, W.J., and Simon, M.C. (2010). Hypoxia-inducible factors and the response to hypoxic stress. Mol. Cell *40*, 294–309.

Martineau, Y., Le Bec, C., Monbrun, L., Allo, V., Chiu, I.M., Danos, O., Moine, H., Prats, H., and Prats, A.C. (2004). Internal ribosome entry site structural motifs conserved among mammalian fibroblast growth factor 1 alternatively spliced mRNAs. Mol. Cell. Biol. *24*, 7622–7635.

Martineau, Y., Azar, R., Bousquet, C., and Pyronnet, S. (2013). Anti-oncogenic potential of the eIF4E-binding proteins. Oncogene *32*, 671–677.

Martinez-Corral, I., and Makinen, T. (2013). Regulation of lymphatic vascular morphogenesis: Implications for pathological (tumor) lymphangiogenesis. Exp. Cell Res. http://dx.doi.org/10.1016/j.yexcr.2013.01.016

Maxwell, P.H. (2005). The HIF pathway in cancer. Semin. Cell Dev. Biol. *16*, 523–530.

Mazzone, M., Dettori, D., Leite de Oliveira, R., Loges, S., Schmidt, T., Jonckx, B., Tian, Y.M., Lanahan, A.A., Pollard, P., Ruiz de Almodovar, C., et al. (2009). Heterozygous deficiency of PHD2 restores tumor oxygenation and inhibits metastasis via endothelial normalization. Cell *136*, 839–851.

Mortimer, S.A., and Weeks, K.M. (2009). Time-resolved RNA SHAPE chemistry: quantitative RNA structure analysis in one-second snapshots and at single-nucleotide resolution. Nat. Protoc. *4*, 1413–1421.

Pestova, T.V., Kolupaeva, V.G., Lomakin, I.B., Pilipenko, E.V., Shatsky, I.N., Agol, V.I., and Hellen, C.U. (2001). Molecular mechanisms of translation initiation in eukaryotes. Proc. Natl. Acad. Sci. USA *98*, 7029–7036.

Pilipenko, E.V., Pestova, T.V., Kolupaeva, V.G., Khitrina, E.V., Poperechnaya, A.N., Agol, V.I., and Hellen, C.U. (2000). A cell cycle-dependent protein serves as a template-specific translation initiation factor. Genes Dev. *14*, 2028–2045.

Pulaski, B.A., and Ostrand-Rosenberg, S. (2001). Mouse 4T1 breast tumor model. Curr. Protoc. Immunol. *Chapter 20*, Unit 20.2.

Richter, J.D., and Sonenberg, N. (2005). Regulation of cap-dependent translation by eIF4E inhibitory proteins. Nature *433*, 477–480.

Sachs, A.B. (2000). Cell cycle-dependent translation initiation: IRES elements prevail. Cell *101*, 243–245.

Sanz, M.A., Redondo, N., García-Moreno, M., and Carrasco, L. (2013). Phosphorylation of eIF2α is responsible for the failure of the picornavirus internal ribosome entry site to direct translation from Sindbis virus replicons. J. Gen. Virol. *94*, 796–806.Phosphorylation of eIF2α is responsible for the failure of the picornavirus internal ribosome entry site to direct translation from Sindbis virus replicons.

Schito, L., Rey, S., Tafani, M., Zhang, H., Wong, C.C., Russo, A., Russo, M.A., and Semenza, G.L. (2012). Hypoxia-inducible factor 1-dependent expression

of platelet-derived growth factor B promotes lymphatic metastasis of hypoxic breast cancer cells. Proc. Natl. Acad. Sci. USA *109*, E2707–E2716.

Schoppmann, S.F., Fenzl, A., Schindl, M., Bachleitner-Hofmann, T., Nagy, K., Gnant, M., Horvat, R., Jakesz, R., and Birner, P. (2006). Hypoxia inducible factor-1alpha correlates with VEGF-C expression and lymphangiogenesis in breast cancer. Breast Cancer Res. Treat. *99*, 135–141.

Semenza, G.L. (2012). Hypoxia-inducible factors in physiology and medicine. Cell *148*, 399–408.

Silvera, D., and Schneider, R.J. (2009). Inflammatory breast cancer cells are constitutively adapted to hypoxia. Cell Cycle *8*, 3091–3096.

Spriggs, K.A., Stoneley, M., Bushell, M., and Willis, A.E. (2008). Re-programming of translation following cell stress allows IRES-mediated translation to predominate. Biol. Cell *100*, 27–38.

Spriggs, K.A., Bushell, M., and Willis, A.E. (2010). Translational regulation of gene expression during conditions of cell stress. Mol. Cell *40*, 228–237.

Tao, J., Li, T., Li, K., Xiong, J., Yang, Z., Wu, H., and Wang, C. (2006). Effect of HIF-1alpha on VEGF-C induced lymphangiogenesis and lymph nodes metastases of pancreatic cancer. J. Huazhong Univ. Sci. Technolog. Med. Sci. *26*, 562–564.

Vagner, S., Galy, B., and Pyronnet, S. (2001). Irresistible IRES. Attracting the translation machinery to internal ribosome entry sites. EMBO Rep. *2*, 893–898.

Yi, T., Papadopoulos, E., Hagner, P.R., and Wagner, G. (2013). Hypoxia-inducible factor-1α (HIF-1α) promotes cap-dependent translation of selective mRNAs through up-regulating initiation factor eIF4E1 in breast cancer cells under hypoxia conditions. J. Biol. Chem. *288*, 18732–18742.

Zhou, B., Si, W., Su, Z., Deng, W., Tu, X., and Wang, Q. (2013). Transcriptional activation of the Prox1 gene by HIF-1α and HIF-2α in response to hypoxia. FEBS Lett. *587*, 724–731.